BIOFABRICATION OF A HEART WALL SECTION USING THE FRESH BIOPRINTING METHOD

VICTORIA BIANCA HORVATH

A DISSERTATION SUBMITTED TO THE FACULTY OF GRADUATE STUDIES IN PARTIAL FULFILLMENT OF THE REQUIREMENTS FOR THE DEGREE OF MASTER OF APPLIED SCIENCE

GRADUATE PROGRAM IN MECHANICAL ENGINEERING

YORK UNIVERSITY

TORONTO, ONTARIO

April 2024

Abstract

This dissertation addresses the challenge of bioprinting cardiac wall tissues. It focuses on three different aspects. The first is around materials that mimic the different cardiac wall tissue layers by testing the different materials pre- and post-crosslinked for their characteristics and behaviour. Secondly, it explores the adaptation of a 3D printer for bioprinting using the FRESH bioprinting method, which utilizes a single extrusion point for multi-material printing. This printer came with a unique printhead design, allowing multiple materials to enter the chamber to print continuously. Lastly, it explores the 3D printing of hybrid tissue and the optimization of the printing process. The hybrid tissue creation started with two materials before moving to three materials for the cardiac wall.

The outcomes of this study The outcomes of the study such as the bioprinter that can print multiple material without leaving the print site and the materials which work as the anatomical heart wall layers, represent a significant step forward in the field of tissue and organ engineering, offering promising new directions for personalized medical treatments and advances for organ transplants by bridging the research gap between hybrid tissue bioprinting with specialized materials and a unique bioprinter that specializes in multi-material printing with better precision and material structure. This research lays the foundation for future advancements in the field of regenerative medicine.

To,

Monika Horvath and Erik Steiger-Horvath

Acknowledgments

I would like to express my gratitude to my supervisor, Prof. Aleksander Czekanski, as well as my lab mates, who have been supportive and helpful throughout my Master's journey. Especially Roger, Salman, Daphene, Rooz, and Usman, who helped me troubleshoot items that did not work as expected. Without my lab mates and my professor, this work would not have been possible. I really enjoyed our collaboration and the collective idea generation. It has been amazing to have people around who are as excited as you are when things go the way you planned. My lab mates really made the continuous experiments enjoyable and informative. I would also like to thank my committee member, Prof. Sachlos, for their time and willingness to help.

I am also grateful to my friends and family for their constant support throughout my journey. I am grateful to my close friend Tayler and Adonai, who spent hours with me in the lab watching me work just so they could spend some time with me. Most importantly, this research would not have been possible without my mother, who has continuously helped me when needed so that I can dedicate more time to my work. I also want to give a special thank you to my son Erik; without him, I would never have embarked on such a journey. I hope to inspire him one day to follow his passions and interests and never to give up.

Table of Contents

List of Tables

List of Figures

Chapter 1 Introduction

Summary: In this introductory chapter, the foundational framework for the dissertation is laid out. It outlines the motivation for the research by explaining the reason behind the push for 3D organ bioprinting, as well as introducing the heart wall, which is the main focus of the research. Furthermore, the research objectives are outlined in this section, and an introduction to all the chapters is provided. This introductory chapter lays the groundwork for the following chapters.

1.1 What are Cardiovascular Disease and Heart Failure?

Cardiac failure, otherwise known as heart failure, is a condition where the heart is unable to pump a sufficient amount of blood to meet the body's needs [1]. This complex syndrome currently does not have a clear diagnostic path. The diagnosis of cardiac failure typically involves a combination of physical examinations, looking at the medical history and diagnostic tests such as echocardiography and cardiac catheterization [2]. There are two main types of heart failure - systolic and diastolic. Systolic heart failure is when the heart cannot pump enough blood to the body. Diastolic heart failure is when the heart cannot receive and fill up with enough blood to function and then circulate to the rest of the body [3]. Several causes can contribute to these heart conditions, including coronary artery disease, hypertension, and valve disease [4, 5].

The main reason for blood delivery restriction is a partial arterial blockage, as seen in Figure 1.1. Cardiomyocyte and endothelial cell death occur fast due to blood delivery restrictions to a specific group of cells. In addition, cell death causes an inflammatory response and, as a result, cytokine release. The following phase involves spreading cell death and starting a mild natural heart regeneration effort. The final stage that leads to heart failure is the creation of scar tissue, which causes excessive stiffness of cardiac tissue and left ventricular dilatation [6]. Figure 1.2 depicts the stages of cardiac failure.

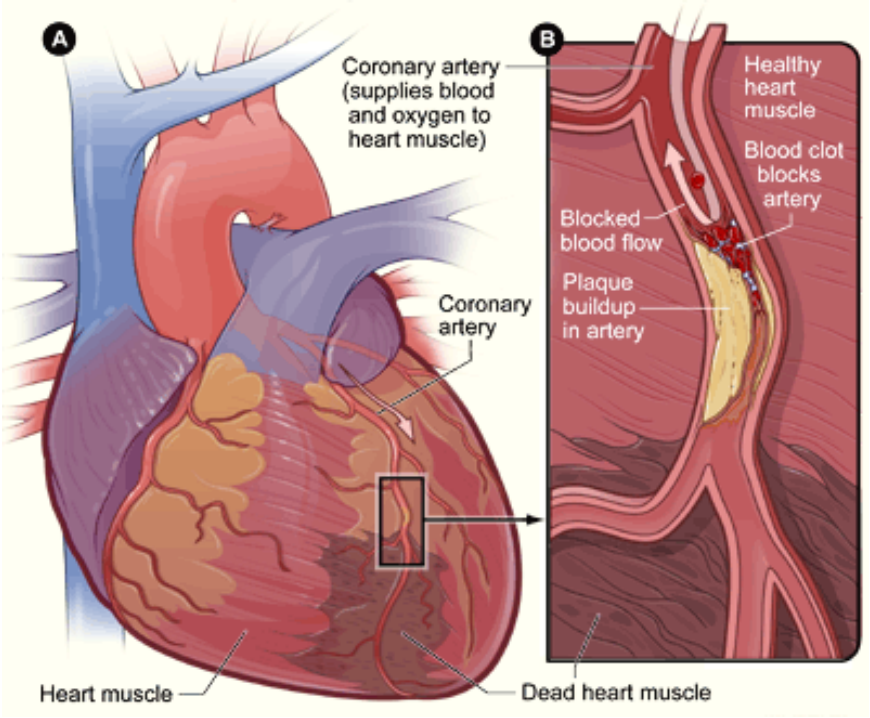

Figure 1.1 (a) Deceased cardiac tissue due to a heart attack, (b) blocked artery restricting blood flow and thus oxygen delivered its caption to the tissue [7].

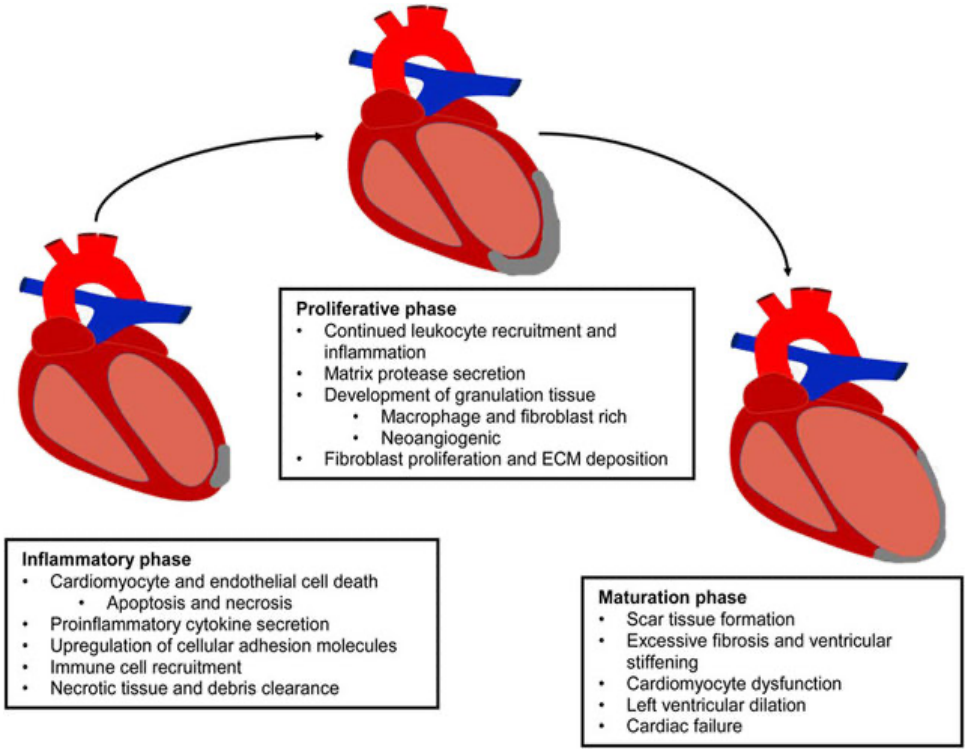

Figure 1.2 Three phases of myocardial infarction: the three phases may be summarized as inflammatory phases, proliferative phases, and maturation phases [6].

Heart muscle is distinct from the rest of the skeletal muscles in the body. While typical skeletal muscle regenerates to some extent, cardiac muscle regenerates at a much slower rate [8, 9]. It was discovered that the pace of cellular regeneration of the heart muscle is inadequate to accomplish complete recovery [1]. Scientists have begun looking into new approaches to battle heart disease, one of them being tissue engineering. One of the approaches in tissue engineering is to create tissue using 3D bioprinting.

1.2 Cardiac Failure Impact

Cardiovascular disease is a significant health problem which affects a vast percentage of the population worldwide. The number of individuals affected is estimated at 26 million individuals [10]. The prevalence of heart failure varies depending on factors such as age, gender and geographical location. Heart failure is the leading cause of death in North America [11]. According to the American Heart Association, an estimated 6.2 million adults in the United States suffer from heart failure, and this number is expected to increase to more than 8 million by 2030. Heart disease is responsible for one out of every four deaths in the United States, amounting to 655,000 deaths every year [12]. This burden of heart failure is set to rise due to factors such as obesity, diabetes, and the aging population.

Cardiac failure has a significant impact on a person's health and quality of life. Not only can patients experience a wide range of symptoms which vary according to severity, but it can also cause psychological impacts, especially if the patients cannot participate in activities they once enjoyed. Heart condition doesn't stop there; it can also increase a patient's risk of complications in terms of kidney disease, stroke, and death. It also economically impacts the individuals due to the cost of medication, treatments, hospitalization, or simply extended time off of work.

Since heart disease impacts so many people and affects the quality of life largely, there have been many solutions brought forward by medical professionals and/or researchers. One of the solutions is medicines that offer improved quality of life in varied degrees. However, many patients continue to require hospitalization [13], especially for individuals over the age of 65. Several research studies have been conducted to investigate the effect of exercise on heart failure patients, and it has been concluded that anaerobic exercise must be adjusted to the individuals, complicating the recovery process [14]. Furthermore, because of diminished movement functions, older demographic patients often have difficulty exercising [13].

On the other hand, heart failure costs healthcare an estimated $108 billion globally each year, accounting for 1-2% of the global healthcare budget. While spending is unevenly distributed globally, 28% happens in the United States, 7% in Europe, and the other 65% throughout the rest of the globe [13]. Heart failure is the main cause of hospitalization in both North America and Europe, accounting for one million admissions. Individuals admitted with a preliminary diagnosis of heart failure account for 1-2% of all hospitalizations. In contrast, early post-discharge mortality and readmission rates have remained unchanged [15].

1.3 Introduction of the Heart

The human heart is a complex organ which plays a vital role in survival. The heart is responsible for the circulation of blood throughout the body. The heart varies in size depending on age, gender, demographic, and their respective

physical and medical condition [16]. The heart size is 12cm in length, 8.5 cm in width and 6cm in thickness. It also weighs 280 – 340 grams for males and 230 – 280 grams for females [17].

The heart's internal cavity comprises four chambers: right atrium, right ventricle, left atrium, and left ventricle. The atria chambers are thin-walled chambers that receive the blood from the body through the veins. The right atrium in the heart receives the deoxygenated blood from the systemic veins, and the left atrium receives oxygenated blood through the pulmonary veins. The two ventricles are thick-walled chambers that pump the blood from the heart to the rest of the body. The difference in thicknesses comes from the amount of myocardium present in the chamber walls, which reflects the force required by each chamber to operate.

The heart also has two types of valves that maintain the correct direction of blood flow. Cuspid valves, also known as atrioventricular valves, are found between the atria and ventricles. The vessels which leave the base of larger vessels are called semilunar valves. The valve on the right atrioventricular valve is called the tricuspid valve, while the one on the left is called the bicuspid or mitral valve. Then, there is also a valve found between the right ventricle and the pulmonary trunk, which is called the pulmonary semilunar valve. The last valve is the semilunar valve, which is found between the left ventricle and the aorta. When the heart contracts, the valves contract as well, and the atrioventricular valves close to prevent the blood flow back into the atria. Then, when the heart relaxes to prevent blood from flowing back to the ventricles, the semilunar valves close [18].

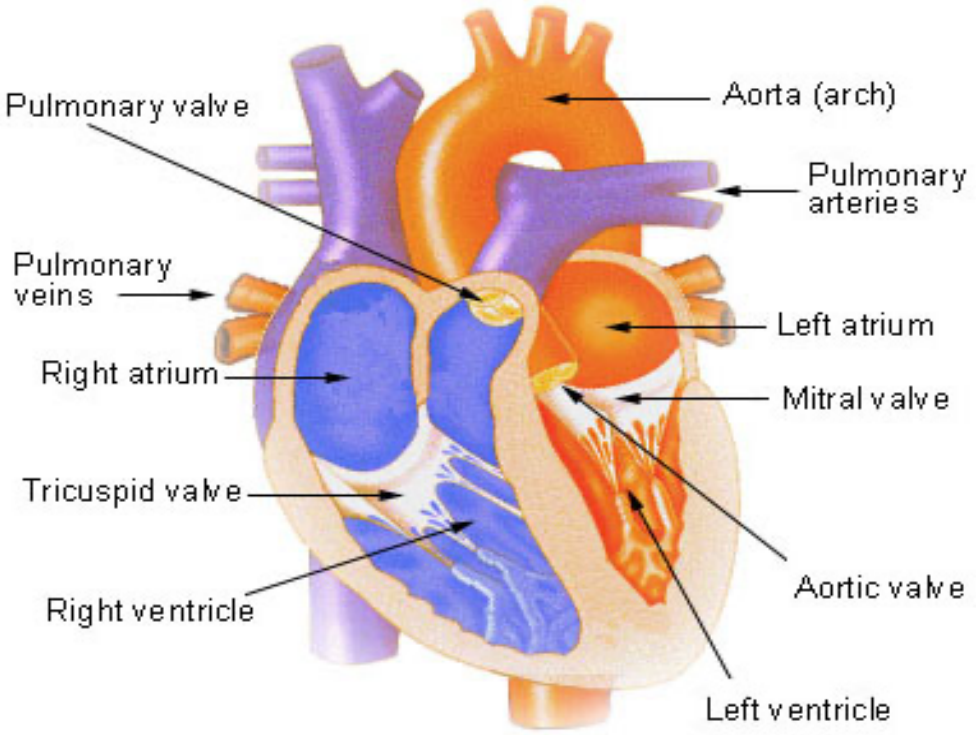

Figure 1.3 Internal view of the heart with labels of all the components [18].

The heart is enclosed in a pericardial sac. This sack is lined with the parietal layers of a serous membrane. The serosa is the outer lining of several organs and cavities in the abdomen and chest. This also includes the stomach. The visceral layer of this serous membrane creates the epicardium layer in the heart.

1.3.1 Heart Wall

The heart wall is made of three layers of tissue. These layers are the epicardium, myocardium and the endocardium. The thicknesses for the layers are less than 1 mm for the endocardium and epicardium, while the myocardium thickness is 8 – 10 mm. Those numbers are the mean thicknesses of the layer as the thicknesses vary from the left to right side of the heart. Each of these layers has unique characteristics and functions, which are essential for the heart to function properly.

1.3.1.1 Epicardium

The epicardium layer is the outermost layer of the heart wall. It is a conserved layer of mesothelium cells that covers the outermost cell layer of the vertebrate heart. It is usually referred to as the protective latter. The epicardium has many functions besides protection. It provides the signals for the heart for proper formation and maturation while in the embryo. This heart layer is the progenitor source during fetal development. It contributes to multipotent cells, which produce cardiac mesenchyme [19]. It also provides signals for secreting factors, which are important for the survival and proliferation of cardiomyocytes, which are the cells that make up the heart muscle layer. Furthermore, the cells derived from the epicardium also perform as cardiac cell progenitors. These are cells that can develop into different cell types. Lastly, the epicardium plays a major role in the heart's injury response to heart disease or heart attacks and subsequently to heart regeneration with its epicardial signals [20].

1.3.1.2 Myocardium

The myocardium layer is the muscle layer of the heart wall. It is made up of fibrous tissue which contracts to create movement. The cardiac muscle is the most organized muscle in the body, it containing muscle cells and non-myocytes such as endothelial cells, fibroblasts, pericytes, neurons, stem cells, and immune cells [21]. These cells play vital roles in maintaining the heart's structure and function. The function of this muscle layer is to circulate the blood in the body by pumping the heart. This layer has pacemaker-like cells that expand and contract according to the electrical impulses received from the nervous system. These cells also control the heart rate, determining how fast the heart pumps blood. This muscle layer acquires its strength and flexibility from the interconnectedness of the cells and fibres found in this wall layer. These fibres are held together by desmosomes, which are membrane domains that mediate the adhesion and contact between cells [22]. The cardiac muscle cells contain mitochondria, which are organelles that transform oxygen and glucose into energy in the form of adenosine triphosphate. This is the energy used to contract the heart [23].

1.3.1.3 Endocardium

The endocardium is the interior portion of the heart's wall. It comprises endothelial cells that line blood vessels and the heart valves. The function of the endocardium is to keep the blood flowing through the heart separately from the myocardium. It controls myocardial functions such as contractility. Endocardial endothelium acts as a barrier between

the heart and the blood, thus controlling the ionic composition of the extracellular fluid. This is an important function as it is the fluid the cardiomyocytes found in the muscle later bathe in. The development of the heart in the embryo and as an adult is controlled by the cardiac endothelium in both the endocardial and the myocardial capillaries. An example of when this function would be needed as an adult is during hypertrophy. Another function regulated by the cardiac endothelium is the contractility and electrophysiological environment of the cardiomyocytes [24].

1.3.2 Characteristics of the Heart

It is important to understand the mechanical properties of the cardiac wall for functionality and disease response purposes. The mechanical properties vary from person to person, depending on demographics. The main mechanical properties are the heart wall, especially stiffness, viscoelasticity, anisotropy, and strain rate dependency. These properties can be found in various techniques, such as tensile testing, indentation testing, and ultrasound elastography. For best results, it is important to conduct tests in vivo. However, these are very invasive tests and are hard to conduct.

The heart wall stiffness exhibits non-linear, viscoelastic and anisotropic behaviour. The stiffness in the heart wall increases with age and due to pathological conditions, such as heart failure and hypertension. Heart stiffness was predicted and tested by many different researchers. Using an aortic magnetic resonance elastography (MRE), it was seen that patients who were hypertensive had a mean stiffness of 9.3 kPa, while the patients with normotensives had a mean stiffness of 3.7 kPA. The experiment was performed on a patient with abdominal aortic aneurysms, and the mean stiffness was 13.97 kPa [25]. Young's modulus is between 8 and 15 kPa of a diastolic adult human myocardium. This was found using an MRE and tensile testing [26].

The viscoelasticity of the heart wall exhibits both elastic and viscous behaviour as it stores or dissipates energy during deformation, such as contraction and expansion. The strain rate dependency of the heart wall affects the ability of the heart to function properly. At higher strain rates, the heart becomes stiffer, affecting its ability to function efficiently in terms of decreased blood flow. The heart tissue has the ability to expand up to 20% of its sedentary size throughout the contraction segment of the heart's functional rhythm. During this phase, the heart rate can reach up to 200 beats per minute [27].

Anisotropy means that the mechanical properties vary with direction. The mechanical properties will differ according to the orientation of the muscle fibres and their corresponding complex helical pattern. The tissues in the heart displayed a non-linear anisotropic mechanical response with a radial stretch that, on average, was 30.7% greater than the circumferential stretches. These properties were shown under equibiaxial physiological loading. Mechanical response of the tissue in the heart valve leaflets shown a consistent mechanical stiffening due to an increased loading rate and some temperature reaction. An anatomical study on chordae quantities shown that the porcine mitral had 30.5 ± 1.43 chords, and tricuspid valves had 35.3 ± 2.45 chords [28].

1.4 Research Objectives

This thesis aims to develop a way to 3D print a heart wall with similar mechanical properties for each wall layer. It unravels the question: How can we use the FRESH method for bioprinting to print a section of the cardiac wall

containing three sections of tissues and cells using a single needle fed by three syringes using a for a continuous stream? FRESH, which is otherwise known as Freeform Reversible Embedding of Suspended Hydrogels is a bioprinting method which allows for the printing of delicate and complex shapes. Further details on the printing method will be explored in Chapter 2. The research will focus on the three main layers of the heart wall: the epicardium, myocardium, and endocardium. The objective of the study is divided into three sections, which aim to (i) create an open-source bioprinter, (ii) characterize the materials for each layer and (iii) 3D print the heart wall using the FRESH printing method. The specific research objectives are:

i. Mechanical characterization of the materials used for bioprinting

The bioinks used to create the heart wall are characterized by their pre-printing and post-printed properties through rheology testing. Some of the tests include shear stress and tensile testing. The sacrificial materials that the biomaterials will be printed will be examined for their shear stress rheological properties and microparticles. The materials will also be combined with dead cells to examine cells' distribution and survival rate through the printing process. The materials will also be viewed before and after crosslinking with cells to see if the distribution changes. Additionally, due to the lack of available information on this material, these tests will be examined to find an ideal concentration that speeds up printing prep time by creating a larger volume in less time while not compromising the printing outcome.

ii. Creation of an open-source and low-cost bioprinter for using the FRESH printing method and multiple materials

An extrusion-based 3D printer that originally uses plastic as the extruded material is converted to a bioprinter with a custom printhead that allows for printing multiple materials out of a single needle. This printer is designed for the FRESH bioprinting method. It uses a sacrificial material that the biomaterial gets printed into, which is stored in a container, making it difficult to switch materials easily. It is also a low-cost option for printing structures with multiple materials.

iii. Optimizing the printing process of FRESH Bioprinting

The printing process is different for each bioprinting method and the associated printer used for printing. While current methods discuss the ideal process for the printing method, there are some challenges with printing. They are optimizing the printing process by examining different processes to speed up the printing and crosslinking time, as well as different cell safety procedures for more efficient printing.

iv. Bioprinting a section of the heart wall

The bioprinting of a section of the heart wall will first print two sections with their corresponding material. Different printing layouts will be tested for the material. Then, with the chosen layout, all three materials will be printed. The printed test The printed sections will be evaluated in terms of tension and compression.

1.5 Thesis Outline

Chapter 2 provides the literature review, which includes the types of bioprinting, its corresponding materials and the FRESH printing method. It also examines some printer modifications that exist under the umbrella of the FRESH printing method. Following the literature review, **Chapter 3** divides the study of the sacrificial material and the characteristics of the biomaterials. The results of studies focusing on the materials' mechanical characteristics are also discussed in this chapter. It also outlines the methodology for the conducted studies and the creation of materials used. **Chapter 4** examines the printer design for the modification to take a plastic 3D printer and allow it to be able to print multiple biomaterials out of a single needle. **Chapter 5** highlights the printing process for the designed printer. The following chapter, **Chapter 6,** discusses the results of creating hybrid tissue and its characteristics, the steps needed for cell addition, and the results of the tests conducted with the cells. Finally, **Chapter 7** contains the conclusions and future remarks for the study.

Chapter 2 Literature Review

Summary: This chapter provides a comprehensive literature review on the emerging field of bioprinting, focusing on a new bioprinting technique named FRESH bioprinting. The chapter first explores the different bioprinting methods and some new and unique methods in bioprinting. It then looks at the different biomaterials used for bioprinting and their different crosslinking possibilities. The chapter concludes with the different open-source 3D bioprinter adaptations for better-printed structures.

2.1 Introduction to 3D Printing

3D printing is a process of creating a three-dimensional and physical object from a digital design. The process involves laying down a successive layer of material, usually plastic or metal, to create the desired object. This process is also referred to as additive manufacturing due to the additions of layers rather than the subtraction of material, as is the case with traditional manufacturing methods, such as machining or casting. 3D printers are an essential technology as they can create a wide range of objects, from simple households to complex mechanical parts and even medical implants.

According to the ASTM Standard F2792 [29], the types of 3D printing have been categorized into seven groups, and these are binder jetting, sheet lamination, directed energy deposition, material jetting, material extrusion, powder bed fusion, and vat photopolymerization [30].

Like any manufacturing process, 3D printing requires a high-quality material to meet consistency when it comes to specifications for high-quality results. 3D printing technologies can use various materials, including polymers, metals, and ceramics, and their combinations in the form of composites and hybrids [31].

3D printing has the potential to revolutionize manufacturing by making it faster, cheaper, and more customizable. It can also be used to create objects that would be impossible or impractical to make using traditional manufacturing methods. From the basic 3D printing came bioprinting, which emerged as a disruptive technology in the medical research field.

2.2 Bioprinting

Over the last decade, biomaterial techniques in additive manufacturing have transformed from a research and development perspective in the form of a fast-prototyping tool to a viable tool for the medical field. This transformation came to be from the ability to manufacture precisely defined structures in three dimensions. It adjusts the properties of the print to the unique anatomical criteria based on imaging and medical data from Magnetic Resonance Imaging (MRI) and Computed Tomography (CT).

3D bioprinting has been increasingly utilized in tissue engineering and regenerative medicine in pharmaceuticals, cancer research, clinical transplantation and high-throughput screening (HTS). This increased use has increased the demand for bioprinters. In correspondence with the wide range of usage, there has been a development in a variety of

bioprinters. Most of these printers have been developed at research institutions and universities worldwide, and this has caught the attention of numerous companies that have raced to commercialize bioprinter technology advancement.

There are several bioprinters available on the market. Still, the main ones that are available are either too big, do not have the needed features or are just out of the budget, which is why there are multiple requirements that bioprinters need to possess for bioprinting, primarily focused on the need of researchers in a biomedical or bioengineering background.

For starters, bioprinters need to be affordable. The increasing usage of 3D printing in research fields requires reasonable prices for printers to be able to open the door for innovation. Another factor that needs to be considered for printers is workability. Highly integrated bioprinters are typically expensive and difficult to use for beginners. Workable bioprinting machines are modularized configurations that are as simple to operate as common household devices. One way to establish common usability for the printer is through modularization, which allows users to pick different modules based on their needs. The printers also need to be quantifiable. It is really important that there is consistency in printing outcomes, especially when it comes to precision and cell growth. The last requirement that a bioprinter needs is applicability. One of the most significant factors for bioprinters is the consideration of possible cell injuries, such as those that arise from mechanical damage during the printing process, as well as cell damage during the metastasis and digestion phases. These must be measured the printing process to ensure they do not affect the user's work [32].

With these printing requirements in mind, users can break down their printer choices based on their needs by considering the printing fabrications and desired materials.

2.3 Printing Fabrications

Additive manufacturing, otherwise referred to as 3D printing, is referred to as the reverse process of cutting up a potato and assembling the pieces to integrity by Ye and colleagues [33]. They mention that the classifications for cell-laden 3D bioprinting are extrusion-based, droplet-based and photocuring-based, which are in accordance with different printing principles. These categories are based on their printing technique, such as the extrusion-based extrudes hydrogel fibres to create 3D structures, the droplet-based creates droplets for bio fabrication, and the photocuring-based utilizes light-sensitive materials for 3D model stacking [32].

These different printing categories can be divided into the four main bioprinting techniques that are widely known: inkjet-based, pressure-assisted, laser-assisted, and stereolithography.

2.3.1 Inkjet-Based

Inkjet-based bioprinters are similar to traditional inkjet printers. It is a non-contact printing process that deposits precise droplets of biomaterial onto a hydrogel substrate. This printing style could be further broken down into two classification methods, thermal and piezoelectric, which are based on droplet actuation mechanisms [34]. In piezoelectric technology, the droplets are created by transient pressure provided by a piezoelectric actuator. The droplets from this technique remain directional and regular while maintaining a constant size throughout the printing

process. This is due to the fact that the piezoelectric method doesn't use heat, nor does it cause orifice clogging. This is a viable printing technique for ophthalmological applications as it provides versatility, high sensibility and accuracy [34]. The thermal technological application is a bit different. It uses heat to cause gasification to form bubbles, which force the ink to extrude out of a narrow nozzle and onto the printer's substrate [36].

2.3.2 Pressure-Assisted

Pressure-assisted, also called extrusion-based, is a bioprinting process that uses mechanical pressure to extrude thicker biomaterials in a continuous and controlled fashion through a microneedle or a microscale nozzle. A 3D structure is generated from this method by repeatedly stacking fibres layer-by-layer on a substrate. It is currently the most widely used bioprinting method due to its high range of suitable biocompatible materials and high precision production of chemically appropriate organs or tissues.

There are three subcategories for this type of bioprinting which are based on the material used to extrude the biomaterial, and these are air, piston and screw.

In the sense of materials, when it comes to printing, materials with higher viscosities provide a more supportive structure for maintaining the printing shape. However, materials with lower viscosities offer a better, more suitable printing environment for cell viability and functionality. Thus, acknowledging that while there is a wide range of possible printable material for this type of bioprinting with a wide range of viscosities, they all come with their unique setbacks and scenarios.

The printing process can be optimized for a particular hydrogel by adjusting the jet diameter. The jet diameter is usually set low for viscous hydrogels requiring high extrusion pressure. However, the high pressure for delivering the material also comes with a high extrusion pressure, which increases the shearing stress on the cells. Cells are not found in stress. It has been seen that cellular damage can occur when printing at higher stress rates. This damage can reduce the life cycle of the cells once printed. The pneumatic or air approach helps reduce cellular damage by lowering the shear stress needed during the printing procedure [37,38]. Scholars often lean towards a temperature-sensitive or a shear-thinning material that meets the requirements for printability. The materials shown to be compatible with extrusion-based bioprinters tend to have viscosities ranging from 30 to 6 x 10^7 mPa/s [39]. The resolution of extrusion-based printing is around 200 μm, which makes imitating natural tissue structures challenging and limits the possible applications.

Extrusion-based printing also allows for multi-material printing, which is a concept of utilizing two or more types of biomaterials in the printing process to create a 3D printed structure in collaboration. One of the reasons extrusion-based is preferred is that it allows for such a printing setup.

2.3.3 Laser-Assisted

Laser-assisted bioprinting, or LAB, uses a laser to deposit biomaterials onto a metal film. This technique uses three parts: a pulsed laser source, a biomaterial layer in the form of a ribbon coated with liquid-coated biological material, and the receiving substrate. Stereolithography (or SLA) is a nozzle-free bioprinting technique that uses ultraviolet

light or visible light to cure the biomaterial, which is in the form of a photosensitive polymer. The material is printed in a layer-by-layer fashion. Each of these techniques uses different bioprinting speeds and biomaterials. The table 2.1 below shows the possible biomaterials, printing speeds, and costs.

2.3.4 Comparison of the Main Methods

Each of these different bioprinting approaches has its own specific requirements in terms of biomaterial and has diverse characteristics for addressing various scenarios. To allow for a simplistic overview of the different technologies and their possible materials, printing speed and cost are covered under Table 1 [40].

Table 2.1 Different bioprinting technologies and their characteristics

Types of Bioprinting	Possible Biomaterials	Printing Speed	Cost
Inkjet-based	Low-viscosity suspension, live cells, biomolecules, growth factors	Fast (<10,000 droplets/s)	Low
Pressure-assisted	Hydrogels, ceramics, low – high viscosity	Slow	Medium
Laser-assisted	Hydrogels, cells, varying viscosity materials	Medium	High
Stereolithography	Light-sensitive polymer (acrylics, epoxies)	Fast (<40,000 μm/s)	Low

Based on the information above, the best bioprinter in terms of low cost, printing speed, and range of biomaterials would be inkjet-based bioprinting. However, there are some disadvantages to the technique that may make it unsuitable for all bioprinting processes. Making it simpler to assess the different bioprinting techniques for their advantages and disadvantages, the information is summarized in Table 2 [41 – 53].

Table 2.2 Summary of the advantages and disadvantages of different bioprinting techniques

Types of Bioprinting	Advantages	Disadvantages
Inkjet-based	Wide availability Low cost High resolution High printing speed Ability to add concentration gradients	Poor vertical structure Clogging Thermal stress to cells Mechanical stress to cells Limited material for printing Need to be liquid (low viscosity)
Pressure-assisted	Wide variety of materials Can set the print dimensions Mild conditions needed (such as room temperature) Can use cellular spheroids Direct incorporation of cells Homogenous distribution of cells	Limited mechanical stiffness Critical timing (gelation of material) Low resolution Low viability Specific use of densities of material and liquid medium Used to preserve printed shapes
Laser-assisted	Nozzle free A non-contact process High resolution High cell activity Control of ink droplets Precise delivery	High cost Time-consuming Requires a metal film Increase chances of contamination

Stereolithography	Wide availability Low cost High resolution High printing speed Ability to add concentration gradients Eliminates shear pressure forces	Poor vertical structure Clogging Thermal stress on cells Mechanical stress on cells Limited material for printing Need to be liquid (low viscosity)

When considering the information in Tables 2.1 and 2.2, it can be clearly seen that each bioprinter has its own challenges and advantages that must be considered when choosing a technique. Initially, the chosen bioprinter would have been inkjet due to its low cost and fast printing properties. However, after looking at the advantages and disadvantages, it can be seen that the preferred bioprinting style is pressure-assisted due to the large range of materials that it works with.

2.3.5 Other Methods

The first demonstration of the possibility of printing biologics was in 1988 by Klebe [54], which then carried forward to the process we call bioprinting, which encompasses the concept of printing cells and organs shown by Boland et al. back in 2003 [55,56]. Since then, bioprinting has been rapidly improving, and the number of methods is increasing. The above section mentioned the most popular types of bioprinting. However, there are a number of recent advances in the field that show promising outcomes. These recently emerged methods are coaxial bioprinting, embedded bioprinting, projection-based and 4D bioprinting.

Coaxial bioprinting is a type of extrusion-based bioprinting that was introduced to the tissue engineering field in 2015 [57]. This method has been used in blood vessel fabrication and vascularization due to its capability to create tubular structures. The process uses a coaxial printing process of using a sacrificial material on the inside of the print structure and a biocompatible material on the outside. This allows for the printing of hollow tubular structures as, under certain conditions, the core material can be eliminated, leaving only the desired material in a tube form. This method plays an increasing role in in-vitro structure creation [32].

Embedded bioprinting solves traditional bioprinters' limitations when constructing complex shapes that cannot be supported mechanically. It allows for anti-gravity bioprinting using freeform constructs in a support bath. This yields stress-supporting materials that allow for the printing of channels and additional harder-to-print mechanisms [58 - 60]. The only downside to this method is the narrow selection of biomaterials that can be used as printed and support materials. FRESH bioprinting falls under this category of printing methods.

Projection-based bioprinting uses photosensitive materials, such as GelMA, also known as gelatin methacryloyl hydrogel, to create a 3D structure by stacking the material layer-by-layer while exposing it to a certain wavelength for curation. This method has the advantage of time for printing since it does not matter how complicated the structure is; the printing time of the layers does not change. It also has a much better printing resolution and reproductivity when compared to the other printing methods [61]. It creates constructs using a much smoother method that can lead to an improvement when it comes to the standardization of mechanical properties and structural integrity. Since this method

does not extrude a material, it also has the advantage of not worrying about the nozzle plugging or cell viability due to stress.

Another recent bioprinting technique is the use of 3D to 4D. This style of bioprinting uses specialized materials that are 3D printed and then change shape or function over time in response to a stimulant [62]. This stimulant can be heat, moisture or some kind of external force. Some examples of this type of 3D printing are self-folding structures and objects that can expand or contract in response to changes in temperature or humidity. 4D printing is leading the way for intelligent materials and structures to adapt and change in response to their environment. Making it an interesting approach when looking for solutions for developing vascular systems.

The artificial development of organs and the vascular system, specifically the printing of the blood vessel network, is considered the holy grail of tissue engineering [63 - 65]. It is considered highly important because the blood vessels are the main components that produce organs such as the pancreas, heart, liver, and kidneys [66, 67]. The need for the vascular system comes from the fact that it is used to transport important needs of the body to function, such as nutrients, oxygen and waste products [63]. One of the ways to 3D print these vascular systems and organs is to use the FRESH Bioprinting method.

2.4 FRESH Bioprinting

The FREH bioprinting technique was developed as a method to give structures widespread, temporary support throughout the printing process. Essentially, integrated 3D printing can be seen as a bearing-material-filled building chamber into which biomaterials, cellular spheroids, hydrogels loaded with cells, and other materials are deposited using an extruder that is syringe-based [68]. Because of its low cost, excellent reproducibility, considerable control over macro/microarchitecture, and ability to handle a wide range of materials, multiple authors believe that free-forming extrusion is the most economical manufacturing method for producing scaffolds [69 - 70]. Specifically, the capacity to print new tissues from living cells makes FRESH 3D bioprinting an innovative technology that could quickly and effectively enhance medicine.

FRESH bioprinting differs from other forms of bioprinting and 3D printing techniques in its use of a support bath in the printing of structures. The bath eliminates the traditional support structures. FRESH stands for Freeform Reversible Embedding of Suspended Hydrogels, and it is a technique that uses a thermal reversible gelatin support bath as a sacrificial base material that materials and structures are printed into and washed away once they’re set. The support material is used to assist with the printing of complex and delicate shapes, such as the human heart, which needs a supportive material to hold the extruded biomaterial into the desired shape, or it would buckle under its own weight. FRESH is one of the unique methods used to print volumetric patterns with extrusion printing [71].

2.4.1 Principles of FRESH Bioprinting

FRESH is a method which is based on the principle of releasing liquid biomaterial from the reservoir syringe into a support bath, where it is required to polymerize quickly. Rapid crosslinking of the polymer molecules drives this polymerization process, and the specific type of 3D printed hydrogel determines the crosslinking mechanism [72].

FRESH employs a thermoreversible support bath, enabling the placement of hydrogels in 3D biological structures of the desired shape. This method offers the advantage of storing and positioning hydrogels or biomaterials, previously 3D printed in a secondary hydrogel support bath. This bath maintains the intended shape throughout the printing process, greatly enhancing print accuracy [73]. The support bath, along with the hydrogel, is placed in a container of the desired size, containing gelatin particles that act as Bingham plastic during printing. This means they behave like a solid body under low shear stresses but flow as a viscous fluid under higher shear stresses. As the needle nozzle moves through the bath, there is little mechanical resistance, allowing the hydrogel to be expelled from the nozzle and stored in the bath, where it remains in place. During this step, the gelatin suspension is kept at 22°C to maintain its rheological properties. This environment allows soft materials that would collapse if printed in the air to maintain their intended 3D geometry. The entire process occurs in a sterile, aqueous, buffered medium that is biocompatible with the cells being used [72]. After the complete 3D structure is printed using FRESH, the temperature is increased to a cell-friendly 37°C. This causes the gelatin support bath to melt, allowing the printed cells in the biomaterial to be released without damage. FRESH thus facilitates the direct 3D printing of biologically important hydrogel inks, such as alginate, fibrin, type I collagen, and Matrigel, within a support bath that can be removed afterward [58]. Gelatin is frequently chosen as the material for the supportive bath due to its biocompatibility. It cannot be entirely removed from the extruded structure, but this is not problematic as its origin in collagen allows it to bind to polysaccharides and other extracellular matrix (ECM) proteins. This residual amount of support bath does not negatively impact cell integration and may actually enhance cell adhesion.

2.4.2 Different Gelatin Slurry Baths for FRESH Bioprinting

Since the evolution of FRESH bioprinting, Lee and colleagues have developed a new advancement for this printing technique's resolution by creating a new and refined support bath. The key advancement between these baths is in the preparation [74]. FRESH v1.0 uses Calcium Chloride and gelatin to create a gelatin slurry by pulverizing large gelatin blocks using a consumer-grade blender. FRESH v2.0 uses a coacervation method to create a gelatin slurry by creating colloidal gelatin droplets from a reaction between gelatin and gum Arabic in an ethanol solution [58]. These reactions generated microparticles that were smaller in diameter. The average particle diameter for FRESH v1.0 is around 60 μm, while FRESH v2.0 is said to have particles around 25 μm, which are more spherical and uniform [68, 74]. These small changes create a difference in the print resolution and the printed shape's surface. Lee and colleagues were also able to print individual filaments of collagen as thin as 20 μm in diameter using FRESH v2.0 compared to FRESH v1.0, which had a limit of around 250 μm.

FRESH v2.0 has another advantage relative to other volumetric printing strategies: its possible biomaterial versatility. FRESH v2.0 can print with photo-cross-linkable materials, as well as unmodified natural extracellular matrix proteins (collagen and fibrinogen) [58]. Multi-material prints can be achieved using an orthogonal gelation mechanism and incorporating the different crosslinking agents into the FRESH support bath without the need for additional wash steps. However, the negative of extrusion printing is the lengthy fabrication times. These time frames are dependent on the printing size and volume, the needed resolution and the layer complexity. An example of this comes from Lee and colleagues, who printed a collagen scaffold for the human heart that ranged from 5cm in length without using cells.

The print took hours to complete, showcasing the extended printing time. When considering print scaling, these printing times pose a problem with cell viability and phenotype. When comparing extrusion that uses voxels or volume pixels serially with photo-crosslinking that prints millions of voxels in a step simultaneously and independently [75 - 78]. The approach also has the advantage of printing speed and maximum resolution when coming from a cellularized construct standpoint, as well as for the printing of entangled features such as airways (for the lung), blood vessels and bile ducts (for the liver) [75]. The discussion of the 'best method for printing' will be dependent on the application, as well as on the further advancement in the different printing modalities.

The push for a higher resolution in 3D bioprinting stems from the need to supply engineered tissue with a hierarchical network of blood vessels. The smallest capillary diameter is between 5 and 10 μm. Lee and colleagues were able to fabricate vascular structures that ranged from 100 μm to less in diameter and found the limitation in printing to pattern small-scale vascular tissue such as capillaries [74]. They, however, overcame these challenges by combining bioprinting methods such as incorporating pores of controlled size and growth factors such as VEGF. Adding these methods promotes cellular infiltration and vascularization in bioprinted tissue upon implementation [78, 79].

2.5 Bioprinting Materials

The materials used in bioprinting are important due to their determination of the final printed product's function and structure. The materials used in the printing process should be biocompatible. Biocompatible materials are materials that are non-toxic to humans, and they do not create an immune response when implemented in the body. It should also mimic the natural tissue, such as its extracellular matrix or organ while supporting cell attachment and growth.

Additionally, the materials need to maintain their structural integrity during the printing process to be able to form the desired shape. The material's mechanical properties will be based on the intended printed product. For example, when bioprinting a heart valve, the printed product needs to withstand the high pressures and stresses that the product would be subjected to in the body.

2.5.1 Materials for FRESH Bioprinting

FRESH bioprinting utilizes a hydrogel material to 3D print tissues and organs. Hydrogels are biomaterials and are hydrophilic polymers capable of holding large amounts of water while maintaining their desired structure. The stability of the structure is thanks to either a chemical or a physical crosslinking of the individual polymer chains. When holding a lot of water, the hydrogels show a high elasticity similar to the native tissue elasticity. Hydrogels were initially founded for contact lens development back in the 1950s [80].

Some of the materials that can be used for FRESH bioprinting are:

- Hydrogels possess many attractive properties which are suitable for the application of hydrogels as tissue scaffolds. For example, they are biocompatible and typically biodegradable, the majority having specific cell-bonding sites necessary to adhere, proliferate, grow and differentiate. Furthermore, some of these biomaterials may be cross-linked in modified forms [72].

- Biomaterials are solutions from biomaterials that contain encapsulated living cells and are the basis of bioprinting. Such materials contained in biomaterial solutions must protect cells from mechanical deformation during the printing process, provide them with nutrients and allow them to proliferate [81].
- Collagen is a significant building block found in mammalian cells, specifically in the extracellular matrix, making it an attractive material for biomedical engineering, tissue engineering and regenerative medicine applications. It has similar physicochemical properties to tissues. Due to its biocompatibility, it is widely used in both in vivo and in vitro applications. Type I collagen has been applied using the FRESH method and is the most common collagen type. It represents up to 90% of collagen in the skin, tendons, bones and elsewhere in organisms [80].
- Gelatin is produced by denaturing collagen, for example, from the bones, tendons or skin of animals by acidic or basic hydrolysis. Due to its properties, such as thermosensitivity and the ability to form a hydrogel at lower temperatures depending on the concentration, it is one of the most commonly used natural polymers. In addition to biocompatibility and biodegradability, the advantages of gelatin include low antigenicity, the absence of harmful by-products, easy processing and low costs. All these properties, particularly its cellular affinity, make it a universal material for applications in tissue engineering and bioprinting [80].
- Hyaluronic acid (HA) is a hydrophilic linear anionic polysaccharide composed of 1,3-β-D-glucuronic acid and 1,4-β-Nacetyl-D-glucosamine. It is a major component in the extracellular matrix (ECM), where it plays a crucial role in maintaining cartilage homeostasis by regulating cellular functions and the production and retention of matrix components. It is found in most tissue binders in all living organisms. HA is currently used as a lubricant and in healthcare to prevent postoperative adhesions. Because HA is naturally present in tissues, it can be used to encapsulate cells [73,82].
- Alginate is a natural polysaccharide - a natural anionic polysaccharide refined from brown seaweed and is similar to the glycosaminoglycans found in the native ECM of the human body [73].
- Chitosan has been studied in recent years for various tissue engineering applications due to its biocompatibility, biodegradability, low immunogenicity, and cationic nature. These properties make it a promising biomaterial for tissue engineering applications. The higher degree of deacetylation of the chitin chain promotes the biocompatibility of these hydrogels [81].

2.5.2 Cross-linking in Materials

In the field of biomaterial fabrication, a variety of crosslinking methodologies have been developed to enhance the properties of biopolymers. The choice of crosslinking method depends largely on the chemical nature of the biopolymer being used. Crosslinkers can be broadly classified into four categories: physical, chemical, enzymatic, and non-enzymatic crosslinking methodologies. Physical crosslinking involves the formation of reversible bonds, such as hydrogen bonds or hydrophobic interactions, which can be broken and reformed under certain conditions. Chemical crosslinking, on the other hand, involves the formation of covalent bonds between polymer chains, resulting in a more stable structure. Enzymatic crosslinking utilizes enzymes to catalyze the formation of bonds between polymer chains, while non-enzymatic crosslinking occurs through chemical reactions that do not involve enzymes. Each of these

crosslinking methodologies offers unique advantages and limitations, and the choice of method depends on the specific requirements of the biomaterial being fabricated.

2.5.2.1 Physical Crosslinking

Physical crosslinkers are a favoured choice among researchers due to their ability to reduce toxicity and enhance the biocompatibility of biological macromolecules. Among the various physical crosslinking techniques, two of the most commonly employed methods are dehydrothermal treatment (DHT) and ultraviolet (UV) treatment. Dehydrothermal treatment involves subjecting the material to elevated temperatures and reduced pressures, causing dehydration and the formation of physical crosslinks between polymer chains. This method is particularly useful for proteins and polysaccharides, as it can enhance their mechanical properties without the use of chemical crosslinkers. On the other hand, UV treatment involves exposing the material to ultraviolet radiation, which induces the formation of crosslinks through photochemical reactions. UV treatment is often used for its ability to create localized and controlled crosslinking, making it suitable for applications where precise control over crosslinking density is required. Both DHT and UV treatment offer advantages in terms of biocompatibility and ease of use, making them attractive options for researchers in biomaterials and tissue engineering [83].

Dehydrothermal Treatment

Dehydrothermal treatment, also known as DHT, is a physical crosslinking method that involves exposing the material to elevated temperatures under vacuum conditions. This process causes water molecules to evaporate, leading to the formation of intermolecular crosslinks through esterification or amide formation [84]. This simultaneous crosslinking and sterilization process results in the bonding of amine and carboxyl groups of the protein backbone when they are in close proximity. One of the advantages of this treatment method is that it sterilizes and crosslinks the material simultaneously, thereby reducing the immunogenic response and increasing cellular activity [85, 86]. Nitzsche et al. found that composite materials made from collagen and hydroxyapatite synthesized via DHT treatment exhibited highly biomimetic properties for repairing bone defects, with improved degradation kinetics [87]. In an interesting study, Tierney et al compared two different DHT conditions: 105°C for 24 hours and 150°C for 48 hours. The results shown that DHT crosslinking at 150°C for 48 hours enhanced the mechanical and biological properties of collagen-glycosaminoglycan (GAG) scaffolds, increasing pore size, permeability rate, and cellular metabolic activity [88]. An in vivo study by Kamakura et al. on rat cranial critical defect recovery using collagen-octacalcium phosphate composite material significantly influenced bone regeneration, with substantial evidence of radiological and histological improvements [89]. Wahl et al. reported that DHT treatment decreased the scaffold's resistance to collagenase enzyme in collagen-hydroxyapatite composites for bone tissue engineering applications [90].

Ultra-Violet Light

UV crosslinking is a straightforward and effective method that results in protein linkage by forming bonds between aromatic residues like tyrosine and phenylalanine. This method often creates bonds between polypeptide chains without affecting the acidic and basic side chains crucial for cell recognition sites [91]. A significant advantage of UV crosslinking is its strong sterilization capability; UV light at 254 nm can damage the nucleic acids of microorganisms, ensuring sterility of the material [92]. During UV exposure, two main processes occur: crosslinking and UV-induced

denaturation, and the balance between these processes affects the mechanical properties and degradation behaviour of the irradiated samples [93]. Poldervaat et al. demonstrated that UV treatment of methacrylated hyaluronic acid hydrogel increased its storage and elastic moduli, enhancing rigidity and osteogenicity [94]. Tsai et al. shown that UV-crosslinked chitosan with RGD peptides provided an osteoconductive environment for the proliferation and osteogenic differentiation of rat MSCs [95]. Shimogo et al. evaluated the osteogenic activity of UV-crosslinked alginate/demineralized bone matrix on a mice subcutaneous implantation model, finding reduced bone formation due to degradation of intrinsic growth factors but increased crosslinking density with favourable enzymatic resistivity [96]. George et al. demonstrated that UV-crosslinked honeycomb collagen structure was an effective substrate for the differentiation of rat MSCs into osteoblasts [97]. Lin et al. fabricated multifunctional gelatin scaffolds incorporating hydroxyapatite nanoparticles and crosslinked them with UV through an electrospinning process to enhance osteogenesis of human MSCs through BMP-2 coating [98]. Despite its usefulness, UV treatment is most effective for thin or transparent scaffolds as it is less efficient in penetrating solid 3D scaffolds [99].

2.5.2.2 Chemical Crosslinking

Chemical crosslinking is widely utilized in regenerative medicine due to its rapid capacity to chemically modify the polymeric backbone, leading to a higher degree of crosslinking. Glutaraldehyde, 1-ethyl-3-[3-dimethylaminopropyl] carbodiimide hydrochloride, and 1,4-Butanediol diglycidyl ether are among the most frequently used crosslinkers.

Glutaraldehyde

Glutaraldehyde, also known as GTA, is a bi-functional crosslinking agent that facilitates covalent bonding between the amine groups of lysine or hydroxylysine residues of polypeptide chains and the aldehyde group of GTA, collectively enhancing the degradability resistivity of the protein molecule. Despite being extensively investigated, the biocompatibility of GTA remains a concern. There is a substantial body of literature that supports and questions GTA as an ideal crosslinker. The advantages associated with GTA include its low cost, easy availability, quick reaction, and strong stabilization [100]. However, the local cytotoxicity of GTA is problematic as it can trigger an unwanted immune response in the host system [101]. Nevertheless, several studies have shown that the cytotoxicity of GTA is concentration-dependent, and concentrations up to 8% are considered safe and non-toxic [102]. Moreover, GTA toxicity can be reduced by washing the GTA-crosslinked scaffolds with a glycine solution to remove unbound free aldehyde groups, which are potent toxic stimulants. Analysis of the table reveals a wide variation in the concentration of GTA used to achieve stable crosslinks in all the reported studies, indicating a heterogeneous concentration. Regarding raw material choice, most studies used hydroxyapatite particles or nanophase additives to mimic native bone architecture. Scaffold fabrication primarily involved the freeze-drying technique, with relatively few articles focusing on electrospinning procedures. Cell-material interactions to assess GTA toxicity were validated in most studies, yielding predominantly positive results for GTA in terms of toxicity. Twenty articles reported using GTA as a crosslinker, with six studies conducting in vivo experiments supporting the beneficial role of GTA as a stable crosslinker even under biological conditions.

1,4-Butanediol diglycidyl ether

1,4-Butanediol diglycidyl ether, otherwise referred to as BDDGE, is a widely used crosslinker primarily employed to stabilize collagen dermal fillers. However, its use in developing bone-like scaffolds is relatively unexplored. The crosslinking mechanism of BDDGE with any polymer depends largely on the reactivity of the epoxide groups located at the ends of the molecules. Furthermore, the crosslinking reactivity is influenced by pH and temperature conditions. BDDGE forms functional covalent bridges with macromolecular substrates through hydroxyl group bonding. The crosslinking mechanism with the macromolecule involves secondary amide bonding via the opening of the epoxide ring by amine groups under basic pH conditions, forming a strong ether bond connection [103]. Bock et al. demonstrated that magnetic biomimetic scaffolds developed using iron-oxide nanoparticles in a collagen-hydroxyapatite matrix crosslinked with BDDGE attracted and supported the adhesion and proliferation of human mesenchymal stem cells [104]. Similarly, Tampieri et al. shown the feasibility of doping iron ions into a collagen-hydroxyapatite lattice crosslinked by BDDGE to produce magnetic composites with super-magnetic properties for improved biological performance [105]. Minardi et al. reported a method for synthesizing magnesium-doped hydroxyapatite collagen scaffolds crosslinked with BDDGE, which shown promising results in terms of enhanced osteoconductivity and improved control over the physical-chemical properties of a bioinspired scaffold [106]. Similarly, Calabrese et al. demonstrated the high osteogenic differentiation potential of human adipose-derived stem cells in magnesium-doped hydroxyapatite collagen scaffolds [107]. Bang et al. shown that sodium hyaluronate crosslinked with BDDGE using a micro-molding technique exhibited high proliferation of mouse osteoblast-like cells. Moreover, the pattern-gel-like scaffold shown good angiogenic and osteogenic responses [108].

Genipin

Genipin, a green crosslinker derived from gardenia fruits, can create permanent crosslinks between two protein macromolecules through intra- and intermolecular crosslinking reactions. The crosslinking mechanism between genipin and protein macromolecules involves a two-step process. Initially, genipin undergoes a nucleophilic attack at the C3 carbon atom to form an immediate intermediate aldehyde group. Subsequently, the aldehyde group reacts with a secondary amine to form a heterocyclic compound. The ester group on the protein backbone is then replaced through a secondary amide linkage, resulting in nucleophilic substitution [109]. The reaction of genipin with protein amine groups leads to the formation of a bluish-green colour due to the formation of a heterocyclic compound through oxygen-radical-induced polymerization of genipin [110]. Genipin has been widely used as a suitable crosslinker for human tissue engineering applications due to its natural origin and low immunogenicity. It has been extensively investigated as a promising crosslinker due to its non-toxic behaviour and potential safety [111]. However, similar to GTA, the cytotoxicity of genipin is a subject of debate in the literature, leading to discrepancies regarding its safety and toxicity. Many studies have reported that genipin toxicity is dose-dependent and acute but not time-dependent. Therefore, restricting the genipin dose to 0.5 mM is highly recommended for tissue applications without inducing any toxic responses [112,113]. Evaluating the results from different literatures shows a significant variation in the concentration of genipin used in all the analyzed studies, indicating a heterogeneous concentration similar to that reported for GTA crosslinker. This highlights the need for optimizing genipin concentration, especially for developing bone-like scaffolds [83]. Freeze-drying was the most commonly used method for scaffold fabrication, followed by

electrospinning and air drying. Regarding the choice of raw materials, chitosan and collagen derivatives were predominantly used in most studies. Except for one study, all other analyzed papers conducted in vitro cell studies using established cells to evaluate the biological performance of the proposed crosslinker. In vivo experiments were performed in four studies, mainly focusing on calvarial bone defects. Overall, the use of genipin as a crosslinker is still considered safe and effective if used in minimal dosages. However, concentration optimization is needed to eliminate any toxic and undesired responses.

1-ethyl-3-[3-dimethylaminopropyl] Carbodiimide Hydrochloride

Ethyl-3-[3-dimethylaminopropyl] carbodiimide hydrochloride and N-hydroxy-succinimide, which can be referred to as EDC and NHS, are commonly used zero-length crosslinking agents for conjugating carboxyl or phosphate groups to primary amines. EDC primarily forms an active O-urea when reacting with any biopolymer, which then binds to amino groups, forming an amide linkage and releasing iso-urea as a by-product [114]. The formed iso-urea is water-soluble and can be easily eliminated. EDC crosslinking is pH-dependent; under acidic conditions with buffers such as 4-morpholinoethanesulfonic acid (MES), the reactivity is stronger and more efficient [115]. Under basic conditions, the reaction can still occur but with lower efficiency. An important aspect of EDC crosslinking is the coupling with N-hydroxysuccinimide (NHS) to improve stability and efficiency. NHS or its analog Sulfo-NHS is water-soluble, enabling direct coupling to carboxyls to form NHS esters, which are more stable than O-acylisourea intermediates, aiding in efficient conjugation of primary amines at physiological pH [116]. Unlike GTA or genipin crosslinking, EDC is not part of the final product, reducing the chance of toxicity [117]. However, EDC uses primary amino groups and cell-reactive carboxylate anions for crosslinking, which may reduce the availability of essential cell binding motifs on collagen-like biomaterials [118]. There is a need to reduce EDC concentration to enhance scaffold cell reactivity without compromising surface chemistry and biomechanics. Studies have shown that a significant reduction in EDC concentration (10-fold reduction) leads to improved biological performance with enhanced mechanical integrity and stability against dissolution [119]. EDC/NHS has been commonly used as a crosslinker for developing bone-specific scaffolds using gelatin or collagen as raw materials in most analyzed papers [120 - 133]. EDC/NHS concentrations of 50 mM and 25 mM, respectively, were mostly employed, indicating that these concentrations are optimized and sufficient for inducing crosslinking between polymers. Similar to other crosslinkers, scaffold synthesis methods mainly involved freeze-drying, and all reported papers were conducted in vitro cell culture using bone-specific cells. In vivo studies were performed in three papers, with two studies on subcutaneous implantation and one study on mandibular defects.

2.5.2.3 Enzymatic Crosslinking

Transglutaminases (TG) are enzymes that require calcium and are distributed throughout the body, primarily functioning to stabilize tissue components by forming high molecular weight complexes through chemical crosslinking [134]. The TG reaction catalyzes the formation of amide crosslinks from γ-carboxamide and primary amine functionalities, with the reaction occurring between glutamine and lysine residues of collagen under in vivo conditions [135]. Protein modification using TG has garnered significant interest among material scientists due to its low toxicity and biological relevance. TG is found ubiquitously in all organisms, including vertebrates, invertebrates,

plants, and microorganisms, where they regulate various biological activities such as epidermal keratinization, blood coagulation, and regulation of erythrocyte membrane [136]. A non-mammalian source of TG was first isolated from the culture medium of the bacteria Streptoverticillium, which is a variant of Streptoverticillium mobaraense [137]. Microbial TG catalyzes protein crosslinking by forming isopeptide bonds through an acyl-transfer reaction between the γ-carboxamide groups of glutamine residues as acyl donors and the ε-amino groups of lysine residues or some naturally occurring primary amino groups as acyl acceptors [138]. Microbial TG offers several advantages, including Ca2+ independence, broader substrate specificity for acyl donors, smaller molecule size, and higher reaction rate, making them suitable for industrial applications [139]. Interest in these enzymes is further driven by their involvement in various human disease states, such as certain neurodegenerative diseases, autoimmune conditions like coeliac disease, cancer, and tissue fibrosis, representing a growing area of TG research [140]. Regarding bone tissue engineering, only two studies have utilized TG as a potential crosslinker to develop strong bone-like scaffolds. Oh et al. demonstrated that TG crosslinking of tilapia fish scale collagen scaffold enhanced the expression of osteoblastic differentiation, suggesting its potential in bone tissue engineering [141]. Ciardelli et al. reported that TG crosslinking of porous hydroxyapatite-collagen composites exhibited better mechanical and thermal stability, along with improved cell adhesion and proliferation of osteoblast and umbilical endothelial cells [142]. TG has also been extensively investigated for other tissue engineering applications, including wound healing, ocular implants, and cancer therapies. Additionally, other enzymatic crosslinkers, such as tyrosinase and horseradish peroxidase, are less explored and do not have significant beneficial roles.

2.5.2.4 Non-enzymatic Crosslinking

Non-enzymatic glycation of proteins plays a critical role in various metabolic disorders, including diabetes mellitus, aging, and bone diseases [143]. In biomedical applications, non-enzymatic crosslinking using sugar derivatives is a commonly employed technique. This method involves a simple, natural, and non-enzymatic reaction where a reducing sugar interacts with the amino group of proteins, leading to chemical alterations in their structure known as Schiff's base alteration. The Schiff's base then rearranges to form an Amadori product, facilitating protein-to-protein crosslinking and eventually leading to the formation of advanced glycation end products (AGEs) [144, 145]. AGEs contribute to increased matrix stiffness, decreased solubility, and high enzymatic resistivity of the crosslinked tissue. This glycation process is a normal biochemical reaction that occurs in living systems as a result of natural aging. Researchers are currently investigating the use of this glycation technique in vitro and in vivo to enhance tissue functionality in tissue engineering applications [146]. The rationale behind using the glycation reaction is to address challenges in scaffold processing, such as poor mechanical properties and high susceptibility to enzymatic degradation [147]. Recent studies have shown promising results using this technique. For example, Krishnakumar et al. demonstrated that ribose crosslinking of magnesium-substituted hydroxyapatite-collagen composites resulted in superior mechanical and degradation properties compared to non-crosslinked composites [148]. Lam et al. reported that a D-glucose-modified gelatin/collagen matrix shown excellent biocompatibility for drug delivery and therapeutic applications [149]. Baskin et al. found that collagen-apatite scaffolds crosslinked using ribose exhibited a dose-dependent response under in vivo conditions, affecting cellular infiltration and decreasing the biological response

[150]. Several studies have emphasized that a minimum concentration of ribose (30 mM) strongly accelerates cellular activities without any toxic response [148, 151, 152].

2.6 Bioprinting Process

As mentioned before, bioprinting is an innovative technology that involves the precise layer-by-layer deposition of biological materials to create three-dimensional structures. It is frequently used with the intention of creating functional organs or tissues. The 3D bioprinting process has multiple stages, from start to finalization. The process typically involves several key steps, which include a digital model, selection of a biomaterial, cell culturing, preparation of biomaterial, printing process, crosslinking and solidification, post-processing and maturation and lastly, quality control and assessment. This process is shown in Figure 5.5.

These steps can be classified into pre-printing and post-printing. The preprinting stage is crucial to guarantee that the right quality of cells is obtained. The bioprinting stage consists of the biomaterial, bioprinter, and bioprinting process, all of which are influenced by biological, physicochemical, and additional process-based factors [153]. Bioprinted materials are moved to bioreactors as a byproduct of the bioprinting process during the post-printing phase. At this point, stimulation should be used to induce tissue maturation, and biosensors can be used to track the functioning, stiffness, and stability of formed tissue or organs [154].

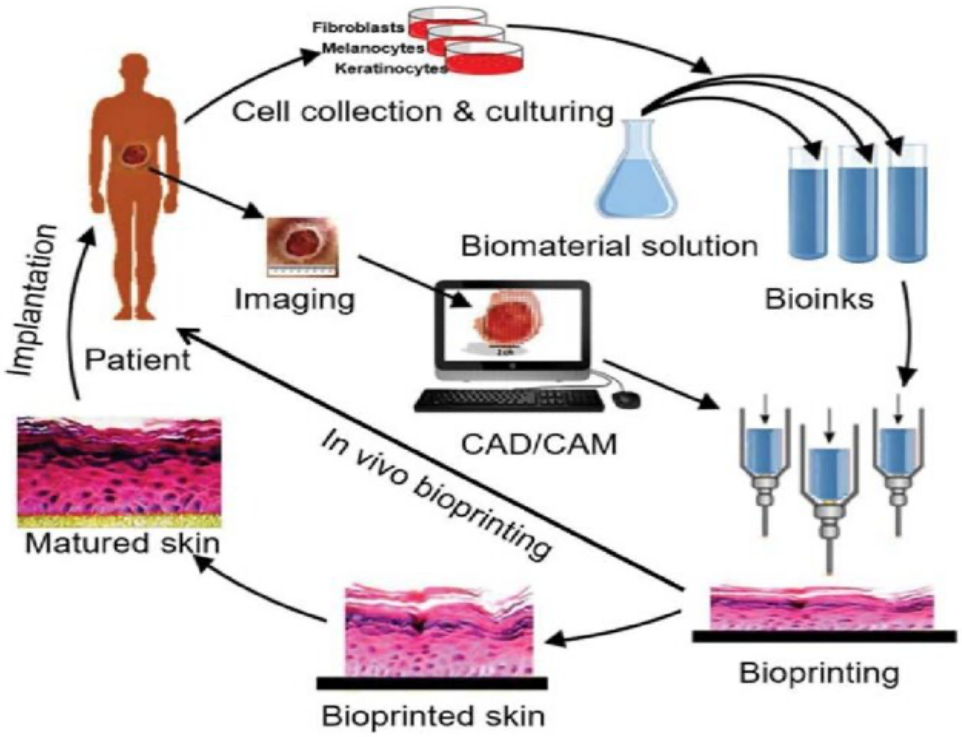

Figure 2.1 Shows the bioprinting process [153]

2.6.1.1 Digital model

The digital design process for bioprinting is a crucial step that involves creating a three-dimensional (3D) model of the target tissue or organ using computer-aided design (CAD) software. This digital model acts as a blueprint for the bioprinter, directing the exact and regulated deposition of biomaterial and bioinks.

High-Resolution Imaging

The planning of tissue constructs preceding bioprinting is a crucial step in the workflow, demanding adherence to injury-specific geometrical dimensions and alignment with tissue-specific extracellular matrix (ECM) attributes. The role of medical imaging, particularly 3D imaging, in tissue engineering has gained prominence in this context [155 – 157]. Accurate information on the geometry of vessel networks is imperative for addressing the critical bottleneck of cell viability within constructs, ensuring optimal nutrient transport for clinical application. To achieve optimal patient compliance, non-invasive imaging techniques with minimal radiation exposure, such as X-ray, MRI, and CT, are widely employed for designing anatomically accurate 3D implants, such as cardiovascular, orthopedic, and nervous tissues [158, 159]. MRI, renowned for soft tissue visualization, relies on the contrast in images based on the state of water molecules in tissues. Increasing the external magnetic field strength enhances resolution, with current machines operating in the range of 1.5 to 11.7 T. Despite MRI's non-ionizing radiation and relative safety, high magnetic field exposures may cause discomfort. Applying contrast agents, like superparamagnetic iron oxide nanoparticles, further improves resolutions [160]. While high-resolution MRI provides detailed insights into tissue-engineered constructs, challenges include prolonged scan times and potential signal distortions due to patient movements. CT imaging, offering higher resolution and faster scans than MRI, demands contrast agents and involves significant radiation exposure. Micro-computed tomography (μ-CT) delivers exceptionally high resolutions, such as 1–200 μm, but is limited in imaging larger volumes [156]. Ultrasound techniques offer a radiation-free and quick scanning alternative but with limited resolution. Similarly, 3D Photogrammetry provides high-resolution images with a short scan time but only applies to external tissues. The selection of an imaging method depends on the target tissue, considering factors like resolution, radiation exposure, and the need for contrast agents. For instance, MRI is preferred for meniscus imaging, while CT may be suitable for obtaining high-resolution bony structures like the femoral head. Echocardiography emerges as a non-invasive option for mitral valve imaging due to the associated challenges of radiation exposure and expense in CT and MRI usage [6]. Recent studies show the utilization of MRI imaging for bile duct regeneration and CT image processing for designing bioprinted heart valves, highlighting the evolving role of advanced imaging techniques in tissue engineering [45, 161]. Molecular imaging advancements also hold promise for combining functional information with tomographic imaging in future bioprinting applications [162].

Rapid Image Processing

3D printing is experiencing rapid growth in healthcare, finding applications in the fabrication of personalized prosthetics, implants, and tissues/organs. Accurate anatomical models are derived from various medical imaging modalities (as discussed in the previous sub-section) to design tissue constructs. Processing steps, including image segmentation and pattern recognition, are crucial [163, 164]. Image acquisition commonly employs digital formats like Analyze, Nifti, Minc, VPX, Interfile, and occasionally Digital Imaging and Communications in Medicine

(DICOM) [165]. Image processing involves pre-processing, scaling, noise removal, and brightness/contrast correction. Image registration precedes segmentation, identifying regions of interest through thresholding, edge detection, or cluster-based methods. Often supervised or unsupervised, segmentation adheres to deformable, parametric, or geometric models. Dedicated segmentation software aids in extracting surface structures from 3D images. Following segmentation, morphological and textural features are extracted, and spatial patterns are identified. Image processing not only reveals the architecture of the intended bioprinted construct but also optimizes stress distribution and oxygen perfusion for incorporated cells [166 – 168]. Design software, such as MIMICS, TSIM, Solidworks, 3D Slicer, MATLAB, and OsiriX, is essential for 3D modelling. Finite element analysis (FEA) has been utilized in stereolithography for tissue engineering constructs, emphasizing the importance of design software [169]. Mahmoud et al. demonstrated an automated scaffold design using the k-means clustering algorithm for 3D volume reconstruction of bone defects [170]. The Computer-Aided System for Tissue Scaffolds (CASTS) automatically designs 3D porous constructs based on a defined external geometry, meeting the demands of rapid scaffold design in bioprinting for clinical applications [171]. Computer-aided design (CAD) models are instrumental in designing scaffolds with gradient porosity for bioprinting [172]. Bücking et al. presented an optimized workflow using CT images for segmentation and subsequent conversion to numerical control (NC) coding for bioprinting [173].

Blueprint Modelling

To operate most bioprinters effectively, it is crucial to convert the CAD model of the defect site into an STL format or a 3D graphics format such as virtual reality modelling language [174, 175]. Following conversion, these models undergo analysis with finite element analysis (FEA) software, enabling the rapid evaluation of bioprinted construct properties in silico before physical bioprinting. Various CAD systems, including constructive solid geometry (CSG), spatial occupancy enumeration (SOE), and boundary-representation methods (B-rep), have been developed for generating models for bioprinting [176]. CSG and SOE involve combining primitives and cubic unit cells to construct models, a computationally expensive process. Alternatively, B-rep uses boundary elements, such as edges and vertices, to define closed objects. Negative geometry in CT-scanned models can be identified through image segmentation, and porous internal architectures can be created by subtracting the negative geometry. An extension of B-rep methods, incorporating iso-geometric analysis (IGA) with volumetric representation (V-rep) through trimmed B-spline trivariates, offers potential applications in precisely defining the interior architecture of heterogeneous scaffolds [177]. In a different approach, 3D images extracted from CT scans directly define the external contours of tissue constructs, which can be rapidly filled with unit cells to generate the bioprinting file. To overcome the uniform porosity limitation of CSG, a freeform systems approach partitions the whole structure into different sub-regions, each assigned different porosity and material properties. An example of this approach has been reported for wound device design using 3D images extrapolated from 2D scans processed in ImageJ software [178]. Additionally, the method allows the modelling of irregular and complex geometrical patterns, which traditional CAD designs struggle with. The use of implicit functions with periodic minimal surfaces, dividing the geometrical space into periodic interconnected domains, addresses this limitation. Designs of scaffolds with gyroid and diamond structures, as well as structures with heterogeneous porosity, have been illustrated using minimal surfaces [179 – 181]. Another significant limitation of traditional CAD designs is their incompatibility with most common extrusion-based bioprinters, which rely on

deposition in a 0/90° raster pattern. To address this challenge, toolpaths using space-filling curves, including lay-down angles of 0/45/90/135°, have been employed [175]. Hilbert curves, a continuous fractal plane-filling function, have also proven useful in this context [182, 183]. Open-source software availability is considered a crucial requirement for bioprinting development, allowing end-users to generate their toolpaths using G-codes [184 – 186].

2.6.1.2 Selection of a Biomaterial

Biomaterial, a pivotal component in the realm of bioprinting, encompasses a diverse array of biologics, such as cells, media, serum, genes, and proteins, constituting a print-friendly material for three-dimensional fabrication. This versatile substance can manifest as a combination of cells with hydrogel biomaterials or as cell aggregates and spheroids in scaffold-free bioprinting [187]. Achieving an ideal biomaterial formulation entails meticulous optimization of material properties, striking a balance between printability, degradation, and biocompatibility. The rheological characteristics of biomaterials, encompassing viscosity, gelation kinetics, shear thinning properties, yield stress and shear recovery, significantly influence print fidelity and mechanical strength. The intricate challenge lies in the interplay between these properties, making the design and selection of biomaterial formulations a crucial aspect of the bio-printing workflow [187]. Integrating cells into biomaterials introduces several complexities. To ensure effective bioprintability with hydrogel-based biomaterials, the concentrations of individual ingredients must be precisely optimized [188]. An exemplary biomaterial should prevent the need for pre- or post-printing processes, such as chemical, physical, or photo-crosslinking, to ensure cell-friendly attributes, homogeneous mixing, and reduced cell encapsulation time [189]. Challenges arise when cells are suspended in an aqueous precursor solution along with water-soluble constituents, affecting the stability and strength of the resulting hydrogel-based biomaterial. Volume variations in the suspension can influence critical properties like cross-linking time, swelling, mechanical strength, and gelation time [190, 191].

Scaffold-free cell bioprinting, exemplified by the work of Yu et al., offers an alternative approach where cells are bioprinted without encapsulation in support of hydrogel or media requirements on substrate surfaces [192]. However, this technique necessitates careful consideration of oxygen and nutrient availability for sustaining cell viability during bioprinting, urging the exploration of biomaterial solutions with ingredients from culture media or the incorporation of microspheres with oxygen-filled microenvironments to mitigate hypoxia-related issues [193].

Homogeneous cell suspension within biomaterial solutions, particularly when hydrogels are involved, poses another challenge, impacting subsequent biomaterial extrusion. Mechanical mixing systems have been employed to achieve uniform cell suspension in fibrous hydrogels, addressing issues with chain entanglements that hinder homogeneity. Careful encapsulation of cells within hydrogels is essential to minimize bubble formation, ensuring optimal bioprintability. However, the desirability of cell encapsulation within hydrogel-based biomaterial depends on various factors, including bioprinted constructs' stability, pH, biomaterial reagents' toxicity, and biocompatibility of hydrogels and their degradation products [194]. For instance, the use of thermo-reversible material, Pluronic F127, in hydrogel-based biomaterial warrants caution due to its rapid dissolution in aqueous media, impacting the stability of bioprinted constructs [195]. In such cases, alternative strategies like seeding cells on bioprinted constructs may be more favourable than encapsulating cells within the bioink [189, 196].

Biocompatibility

Undoubtedly, one of the most crucial factors to take into account while using bioprinting is process biocompatibility. Preserving viability and function is one of the critical goals of bioprinting. Furthermore, there must be no phenotypic or genotypic alterations brought about by the process. Different external stresses, such as mechanical in extrusion-based bioprinting, mechanical, acoustic, thermal, or electrical in droplet-based bioprinting, and optical or thermal in laser-based bioprinting, might cause cell morbidities depending on the modality. Murphy and Atala state typical viabilities are 40–80% for extrusion-based bioprinting, 85% for DBB, and 95% for laser-based bioprinting [197]. These lead to the conclusion that shear stress is the most harmful to cells [198]. Undoubtedly, one of the most crucial factors to take into account while using bioprinting is process biocompatibility. In addition to biomaterial compatibility, common stresses such as flow rate and bioprinting time are present for each modality and can lead to reduced cell viability. The biocompatibility of the laser-based bioprinting method is also determined by other parameters like the air gap between the collator and receiver plates and the duration of the laser pulse [199]. UV is often responsible for solidification, which could potentially have a further effect on viability. The use of stereolithography in bioprinting was first demonstrated by Boland and associates' studies. Using this technique of printing, a vat containing cells and photocurable hydrogen was placed on a table that allowed for vertical axis movement control. After that, UV radiation was applied to the biomaterial, which caused the biomaterial to polymerize as a result of the radical that photoinitiators produced. The toolpath was traced by UV light in accordance with the CAD file, curing the biomaterial at certain locations within the vat. In order to create the 3D constructions, which can range in size from a few hundred μm to a few millimetres, the procedure was repeated for every layer. Chinese hamster ovary cells were first bioprinted with over 90% viability in PEO and PEO-dimethacrylate (PEGDMA) hydrogels. Later, 3T3 fibroblasts within PEGDMA hydrogels were proven to be bioprinted in cylindrical constructions using SLA-based bioprinting technology. Trimethylolpropane triacrylate and acrylate polymers with urethane segments have also frequently been utilized in hydrogels for SLA bioprinting. In addition to photocurable polymers, a vital element of this modality for enhancing solidification is photoinitiators, such as Irgacure. As a result, it becomes imperative to optimize the photo-initiator concentration in a biomaterial composition. Furthermore, because the photo-initiator is hazardous, caution must be used in determining the optimal concentration [200, 201]. Lately, it has shown promise to sustain high cell viability to employ visible light-induced crosslinking of poly(ethylene glycol diacrylate), gelatin methacrylate, and eosin Y photo-initiator [202].

2.6.1.3 Cell Culturing

Cell culturing is a fundamental technique in modern biological research involving cells' propagation and maintenance outside their natural environment. This versatile methodology has become a cornerstone in various scientific disciplines, ranging from basic cell biology to advanced applications in biotechnology and medicine. Through the controlled conditions of cell culture, researchers can explore cellular behaviour, study molecular processes, and develop innovative approaches for therapeutic and regenerative purposes. The ability to manipulate and sustain cells in vitro not only facilitates a deeper understanding of fundamental biological phenomena but also plays a pivotal role in the production of biopharmaceuticals, tissue engineering, and disease modelling. As a critical tool in the hands of scientists, cell culturing continues to unlock new frontiers in scientific discovery and technological advancements.

Minimally Invasive Biopsy

Utilizing the patient's cells is preferred to minimize the risk of immune rejection in bioprinted tissues. While many research labs predominantly focus on material, process, and structure development using model cell lines, successful clinical translation in bioprinting requires prioritizing primary cells obtained from patients. A patient-lab-patient strategy is vital for success, recognizing cells' diverse survival, proliferation, and maturation kinetics with different phenotypes and genotypes. The acquisition of cells is crucial for bioprinting, and minimally invasive biopsy is gaining importance in obtaining cells for successful 3D bioprinting and regenerative approaches. Although biopsy has been the gold standard in medical diagnosis, routine screening needs have escalated, leading surgical oncology toward evolving minimally invasive biopsy methods [203]. For instance, special vacuum-assisted needle biopsy systems enable the collection of tiny skin samples with minimal deformation and rapid recovery. Emerging minimally invasive procedures, such as focused ultrasound and MRI-guided biopsy, facilitate early diagnosis and treatment without extensive surgical intervention. In bioprinting, harvesting volumetric tissue samples, such as adipose tissue, is gaining significance for creating decellularized ECM-based biomaterials. Minimally invasive biopsy is becoming popular for obtaining live tissues, addressing complications associated with traditional tissue harvesting methods. Researchers explore microbiopsy and nano biopsy techniques, with the latter demonstrating the potential for collecting extremely tiny samples, even isolating single cells, through a minimally invasive method using a nanopipette inserted through the cell membrane.

Stem Cell Differentiation and Expansion Protocol

In the realm of regenerative medicine, there is a growing interest in the application of bioprinting methods [204]. However, numerous biological challenges persist. Among these challenges, one significant hurdle is ensuring stem cells' viability and sustained functionality throughout sequential differentiation processes. Researchers continuously strive to identify optimal sources of stem cells and develop efficient protocols for their isolation and expansion through cost-effective and rapid methods. Various stem cell sources, including embryonic stem cells (ESCs) and human mesenchymal stem cells (hMSC) isolated from bone marrow and adipose tissue, have been explored for bioprinting [205 – 207]. ESCs possess the ability to differentiate into any cell type and form embryoid bodies (EBs) during early embryogenesis, establishing a microenvironment for lineage-specific differentiation of stem cells [208, 209]. However, ethical restrictions and concerns about uncontrollable cellular differentiation and potential immunogenicity limit the widespread application of ESCs. Induced pluripotent stem cells (iPSCs) present an ethical and immunogenicity-free alternative [210]. Undifferentiated stem cells exhibit greater immune tolerance, enabling successful implantation and reducing host rejection of grafts [64, 211 – 213]. Despite ongoing efforts to develop rapid and robust protocols for stem cell differentiation, most available methods are time-consuming and lack reproducibility [214]. Recent approaches involving forced expression of lineage-specific master regulators for direct reprogramming of somatic cells offer potential alternatives [215, 216]. Current forward programming methods use lentiviral transduction of human pluripotent stem cells (hPSCs), but concerns about random transgene insertion into the genome have led researchers to explore alternative safe harbour targeting strategies [217 – 219]. For neurogenic differentiation of ESCs or iPSCs, Lukovic et al. demonstrated a method without using animal factors, enhancing efficiency [220].

2.6.1.4 Preparation of Biomaterial

Preparing biomaterial and the printing material is the final step of the pre-printing process before the actual printing process begins. The preparation of biomaterial will depend on the material being made and if the cells are added prior to printing or after the printed structure is complete.

However, to successfully create functional tissues through bioprinting, there are a few essential procedures in the preparation of biomaterials. The first step is carefully choosing cells corresponding to the intended tissue or organ. In order to offer structural support and replicate the extracellular environment, the choice of a biomaterial matrix—such as hydrogels like alginate, collagen, or gelatin—is subsequently essential. Crosslinking chemicals, like calcium chloride or UV radiation, must be added in order to harden the biomaterial both before and after printing. Viscosity modifiers such as hyaluronic acid or pluronic acid are frequently used to ensure adequate flow through printer nozzles. In order to sustain biological function both during and after printing, additional elements are introduced to improve cell viability, such as growth factors and nutrition. Temperature regulation and pH modifications are considered to guarantee the stability of the biomaterial components. In addition to testing and optimizing the overall biomaterial formulation for printability, cell viability, and structural integrity, sterilization techniques are used to prevent contamination. Customization of the biomaterial formulation is done based on the desired tissue properties and the particular bioprinting technique used. It is notable that in order to expand the potential of bioprinting for uses in regenerative medicine, researchers are constantly investigating and improving biomaterial formulations.

2.6.1.5 Printing Process

Physical bioprinting becomes important after choosing the suitable biomaterial formulation and bioprinter technology. This is because the process parameters include a variety of selections that need to be optimized on a case-by-case basis in order to produce the intended constructions. Process automation is required at this point to produce constructions for clinical applications quickly. The bioprinting procedure should likewise be performed in strictly regulated and managed settings, with adequate controls to enable repeatable outcomes.

Reprintability

For clinical usage, tissue-engineered constructions must adhere to precise and quantifiable safety and performance standards [221, 222]. Standardization is more challenging with bioprinted constructions since they are more intricate and personalized than regular constructs. In this regard, it has been noted that reproducible bioprinting is made possible by using tissue strands as biomaterials instead of liquid media or moulds [192]. The three main factors used to estimate the repeatability of bioprinted objects for standardization are mechanical attributes, cell survival, and print fidelity. It should be remembered that certain characteristics, including mechanical strength, are dynamic and will alter over time as individual cells deposit their own extracellular matrix. Standardized procedures must be dynamic as a result (i.e. analysis at numerous time points). Numerous automated techniques have been developed for measuring tissue in situ's mechanical properties and cell viability [223]. One example is label-free cell viability measurement using a microscope, which should be used more frequently [224 – 226]. Process reproducibility in droplet-based bioprinting modalities is higher than in Laser-based or extrusion-based bioprinting modalities. Extrusion-based bioprinting frequently experiences erratic process pauses as a result of hydrogel expansion or contraction [227]. The nozzle-free

nature of laser-based bioprinting ensures that repeatability is unaffected by clogging issues; however, the mechanical strengths of the printed construct are restricted by the viscosity range that can be handled. The processes in laser-based bioprinting are highly complex, with nonlinear physical relationships between factors, making the procedure difficult to duplicate.

Resolution

The resolution of a bioprinting process, signifying the minor achievable pattern, deviates from the instrumental resolution of a bioprinter due to the rheological properties and non-instantaneous solidification nature of most hydrogels. Typically, LBB, DBB, and EBB processes achieve bioprinting resolutions of around 5, 50, and 100 μm, respectively [35, 228 – 230]. Transitioning from hydrogel to cell aggregates, such as tissue spheroids or strands, tends to degrade resolution. Quick crosslinking is an effective method to enhance resolution, but it often leads to nozzle clogging and the nozzle adhering to bioprinted layers. Reducing nozzle diameter is not a viable solution either, as it increases cell shear force, diminishing viability.

DBB, in particular, experiences the ejection of one droplet accompanied by several satellite droplets, diminishing bioprinting resolution [230]. Bioprinting process resolution is further influenced by the actuation mechanism, droplet-nozzle interactions, and droplet-substrate interactions. Notably, the hydrophilicity of nozzle inner walls and biomaterial surface tension affect print quality. Lowering nozzle inner wall hydrophilicity and biomaterial surface tension delay droplet disintegration and reduce ejection velocities. Similarly, the substrate's contact angle determines biomaterial spreading, impacting bioprinting process resolution.

In LBB, jet dynamics and the impact of ejected biomaterial are influenced by biomaterial rheology and the distance between the ribbon and collector. Ali et al. successfully bioprinted MSCs with minimal shear stress and high process resolution by modulating these forces [53]. Guillotin's study also highlighted the effect of biomaterial viscosity and laser parameters on bioprinting resolution [231]. Enhancing bioprinting resolution often comes at the cost of decreased cellular functionality parameters, necessitating optimization of process parameters like shear stress [232]. Generally, LBB tends to achieve higher bioprinting resolution than DBB and EBB. For EBB, improving bioprinting resolution can be pursued through a tapered nozzle, reducing exposure time to high shear stress, employing hyphenation with electrohydrodynamic effects [233, 234], or ultimately utilizing a nozzle-free extrusion system.

2.6.1.6 Crosslinking and Solidification

Many natural and synthetic biomaterials currently available undergo solidification through various methods, including physical, chemical, or enzymatic crosslinking. For instance, alginate undergoes ionotropic crosslinking using calcium chloride (CaCl2) solutions or calcium sulfate (CaSO4). Polymer solidification occurs as the polymer solution transitions to a gel at a specific temperature. When printed on a cooled stage, polymers like agarose, gelatin, and methylcellulose transform from a hot solution (40-80 °C) to a gel [235, 236]. Physically crosslinked hydrogels, however, tend to be mechanically weak, necessitating reinforcement with other materials to enhance stability. Photocurable hydrogels, on the other hand, can be printed on an illuminated stage by incorporating a suitable photo-initiator [237]. Several studies have reported the 3D printing of photocurable biomaterials with and without cell populations [200, 238, 239]. Printing photocurable polymers offers advantages such as rapid processing, minimal

detrimental effects on cells, and the ability to adjust crosslinking intensity easily by changing light intensity. Gelation of ionotropic polymers extruded in a reactive substance bath is another approach, and the advantage lies in the rapid solidification of polymers, with minimal impact on cell populations at physiological temperatures [236, 240]. Reactive printing and cell culture media have been applied to gellan gum solutions [241].

The dispensing rate of materials is influenced by the biomaterial's initial viscosity and the crosslinker's density. Generally, higher viscosity biomaterials can be bioprinted more rapidly, requiring less crosslinker, resulting in more stable constructs under physiological conditions. In extrusion-based bioprinting (EBB), where extrusion force is applied pneumatically or mechanically, highly viscous biomaterials can be used compared to drop-on-demand bioprinting (DBB) methods. Slower gelation kinetics can lead to cell death, and biomaterials like alginate and PEG-DA have shorter gelation times than collagen and chitosan [41]. A highly viscous solution requires less crosslinking time, allowing faster deposition rates. High crosslinker density can facilitate fast solidification, allowing for faster dispensing rates, but the toxicity of a high concentration of crosslinker should be considered. EBB, in particular, requires a rapid gelation process for desired fidelity, often achieved through ionic crosslinking [242]. Using supporting nanoclays in bioprinting can minimize the impact of gelation speed on print fidelity [243]. Another challenge in bioprinting is selecting the appropriate crosslinking density to achieve structural integrity without inducing cytotoxic responses [244]. Optimizing cellular density is also crucial for achieving optimum solidification, as high cell concentrations might occasionally interfere with the crosslinking mechanism of hydrogels [245].

2.6.1.7 Post-processing and Maturation

Tissue maturation following construct bioprinting is a time-dependent process; therefore, post-bioprinting needs to be done under well-regulated circumstances, particularly in bioreactors. These settings have a significant impact on cell-cell interactions, and post-bioprinting processes allow for the vast manipulation of stimuli to modify the kinetics of any differentiation process. By creating an environment that is similar to the in vivo environment, such as an ex-plant culture, these parameters can be further tuned to imitate the in vivo environment.

Conditioning

The failure to generate tissue constructs with clinically relevant thickness in vitro is often attributed to the lack of mass transfer of nutrients and metabolites, particularly due to the absence of an internal vascular network. This limitation affects both conventionally cultured and bioprinted tissue constructs despite efforts to incorporate vasculature. To address this challenge, perfusion in bioreactors becomes a necessary step, as they provide controlled conditions and stimulating environments for tissue maturation.

Bioreactors, serving as vessels for controlled biochemical processes, play a crucial role in tissue engineering. Various types, such as spinner flasks, rotating walls, compression, strain, hydrostatic pressure, and flow perfusion bioreactors, have been employed to engineer tissues. Flow perfusion bioreactors, for instance, employ a pump system and a chamber connected by tubes to enhance fluid transport through tissue constructs.

Bioreactors have proven effective in engineering different tissues, including bone, skin, cardiovascular, and cartilage. Examples include rotating wall vessel bioreactors to observe mature chondrocytes and cartilaginous tissues from

cartilage progenitor cells or bone marrow stromal cells. Spinner flask bioreactors have demonstrated cartilage and bone tissue formation within weeks of culture. Microfluidic perfusion bioreactors have been developed to accelerate the differentiation of bioprinted constructs into specific tissues, such as heart and bone.

While bioreactors have shown utility, improvements are needed for broader clinical translation, including enhanced user-friendliness, process consistency, and volume output. As exemplified by Aastrom Bioscience Inc.'s perfusion bioreactor, automation offers opportunities for improved scalability. Recent advances also include real-time monitoring and feedback control of vital parameters, such as temperature, oxygen levels, and pH, along with developing oxygen-imaging sensors for mapping oxygen distribution in 3D scaffolds.

In tissue engineering, the classical paradigm involved the triad of cells, scaffolds, and growth factors. However, recognizing that external stimuli can induce differentiation led to the incorporation of physiologically-mimetic mechanical and biochemical stimuli in bioreactors. Many bioreactors have been designed to apply mechanical stimuli like hydrostatic pressure, compression, shear, and tension, accelerating the maturation of tissue constructs. For instance, mechanical stimulation in cartilage tissue engineering, such as pulsatile hydrostatic pressure or compression, enhances chondrocyte differentiation and extracellular matrix synthesis. Similarly, mechanical or electrical stimulation has been applied in cardiac tissue engineering to improve tissue formation. The extent and values of stimuli in different studies for tissue maturation in bioreactors are extensively detailed in the literature. Recent reports highlight bioreactor systems designed explicitly for clinical heart valve tissue engineering.

2.6.1.8 Quality Control and Assessment

Quality control and assessment in bioprinting are essential for ensuring the printed constructs' accuracy, reproducibility, and reliability. This involves evaluating the resolution and fidelity of bioprinted structures compared to design specifications, ensuring the regular calibration of bioprinters, and verifying printer parameters. Characterization of material properties, including rheological aspects of biomaterials and assessment of cell viability and functionality, is crucial. Biomaterial composition, structural integrity, sterility, and crosslinking efficiency are key areas of scrutiny. Testing the in vitro and, if applicable, in vivo performance of bioprinted constructs provides insights into biocompatibility, tissue maturation, and regeneration - imaging techniques, such as microscopy or CT scans, aid in visualizing internal structures. Bioprinted constructs' compatibility with bioreactors and adherence to documentation practices contribute to maintaining quality standards. Continuous improvement and adaptation of quality control measures are imperative for the evolving field of bioprinting. Regular validation and standardization of protocols enhance the reliability and reproducibility of bioprinted products.

2.7 Printer Setup

Over the years, there have been many developments in the field of bioprinting, including material science, tissue engineering, biotechnology, regenerative medicine, robotics, and automation. However, there is limited access to bioprinters currently, which doesn’t comply with the rapidly expanding demand for bioprinting research. To increase availability, existing 3D printers are used and adjusted to the needed settings. There are many ways to change the printer setting to achieve the desired research outcome.

The low structural stability of the material throughout the printing process can severely affect the geometry and architecture of the desired structure design. It is one of the greatest issues that many additive manufacturing processes face, particularly those using soft materials such as hydrogels. Among the strategies used to get around this limitation is the use of sacrificial support materials. This printing style is referred to as Free Embedding of Suspended Hydrogels (FRESH). This enables a construct to be printed in one or more biomaterials of choice while also embedded in a structurally supportive scaffold material that is printed in parallel. The sacrificial material can be removed once the construct has been completed and stabilized using post-printing reactions or treatments. This method can also be utilized to incorporate design elements such as channels that aid in the perfusion of printed constructions [246, 247]. However, using sacrificial materials often requires a bioprinting platform capable of multi-material printing. FRESH is an innovative solution that doesn't require multimaterial printer functionality to achieve the desired results. However, developing a bioprinting platform that is compatible with FRESH bioprinting could be of interest to many researchers. Some attempts to make bioprinters more accessible have included repurposing low-cost fused filament fabrication (FFF) printers for bioprinting applications [248, 249].

One of the challenges in bioprinting is the requirement of multi-disciplinary collaboration. Recently, many researchers have taken it upon themselves to create an available and user-friendly solution to this problem. They are allowing other researchers to adopt the technology and advance in the field. An article by Enberg et al. created an open-source extrusion-based bioprinter that uses an E3D motion system and tool changer to achieve high-resolution multi-material printing [250]. They allowed their work to be easily adapted for different bioprinting applications as well as for any other additional tools to be incorporated for more outstanding system capabilities.

To test their concept, they printed multi-material constructs with distinct layers of laminin collagen using the FRESH bioprinting method. Then, they seeded these scaffolds with cells to demonstrate cell growth and included cells into the bioink before printing to examine the cell viability rate. Their bioprinter was designed to enable contamination-free printing by adding a transparent polycarbonate cabinet with an integrated HEPA filter and an intake fan for air circulation. They also added an automatic tool offset calibration and bed levelling for ease of switching between materials, especially since they created their bioprinter with the potential to use up to 4 syringe pump tools and biomaterials. To test the multi-material capability, the authors designed a square construct intersected by eight spokes that originated from the structure’s center, and they used cell-laden laminin bioink to create it. The extrusion of the cell-laden bioink has some adverse effects when trying to seed cells onto the printed construct.

The cells they used in their experiments were MDA-MB-231, which are breast cancer cells that are neoplastic and interact in an anchorage-independent growth [251]. They looked at the viability when they were added to the laminin before printing and, extruded using an 18G needle and manually deposited through a syringe. The assessed protocol of the cells was “live/dead,” and their viability was scored about 20 hours after printing and one week after. The results shown that the extrusion through the 18G needle had the highest viability the day after the printing process. However, it declined by around 10% one week later. For the cells deposited using a syringe, their viability after the first day was lower, but then received similar observation of cell viability a week later as the extrusion. Their results show how their

printing process did not negatively impact cell viability in their laminin constructs, as well as the possibility of long-term studies using the constructs [252].

When it comes to multi-material bioprinting, the important advantage in structure design comes from the capacity of the bioprinter to have the functionality to allow printing with multiple materials. An example of this is the printing of channels. A sacrificial material such as Pluronic F127 is used to print these channels and transform them into hydrogel constructs. The Pluronic has reversed effects with temperature when compared to hydrogel, making it easier to remove after printing. This technique can also be used to create perfusion channels in prints to increase cell viability and survival in larger constructs [253]. Then, there is also the idea of combining the different biomaterials in organized ratios to experiment with tissue culture environments to evaluate cell responses to different treatments and surrounding matrix compositions [253 – 257].

Another important challenge in bioprinting is in optimizing the resolution of the print. Recent advancements have improved the printing resolutions of individual filaments to below 100 μm. However, when it comes to printing in small filaments, an accurate extrusion of biomaterial is needed in a nano-litre volume. The commercially available bioprinters and extruders are very costly and use pneumatic controls. These controls limit the minimum extrusion of the biomaterial volume and prevent retractions that are required for high-resolution and complex internal geometry printing. A paper by Tashman et al. presents a syringe pump design for extrusion-based printers for soft materials, which they called the Replistruder 4. The authors took advantage of the geometry customizability and the comfort of 3D plastic printing while improving the performance by integrating high-precision linear motion parts. Their new syringe pump holder is compatible with a large range of syringes, is compact, and is lightweight, so it can be utilized for multi-material bioprinting [258]. To test their design, they used a 2.5 mL Hamilton gastight syringe to print collagen constructs using 3.35 nL individual filaments and 300 - 500 μm width patent channels extruded from a 100 µm needle. These channels were printed using the FRESH printing method. They examined the resolution of the printed channels by imaging the prints using optical coherence tomography (OCT) and infrared light-based optical imaging that obtain high-resolution 3D images using light-scattering samples. As well as they investigated the accuracy of the channel widths by means of image segmentation, which resulted in the mean widths of the channels being 489.1 ± 21.09 μm, 398.7 ± 26.83 μm and 354.3 ± 30.68 μm. These results suggest a need for the prints to be optimized. In the end, they validated that the Replistruder has high-fidelity capabilities. They also shown how precise control over extrusion and retraction implicated the print functionality in high-resolution constructs.

Another research shown how a fully assembled Prusa RepRap i3 Mk2 was converted to a bioprinter using firmware modifications via Marlin and by replacing the plastic extruder with Nydus One Syringe Extruder (NOSE). The NOSE approach has a lot of positive factors in its design. It allows for personal modification on a GPL license and RepRap basis. It also has a user-friendly calibration routine and reproducible prints, while the open-source software composer can set crucial parameters such as nozzle length, syringe diameter and container size. It has also been tested for cell-line and stem cell safety when using the FRESH printing method. All while being an economically feasible addition to an existing printer. While some improvements could be made to the NOSE concept, it overall can manage a safe transformation between a plastic 3D printer and a 3D bioprinter. The concept comes from a piston-driven hydrogel

extrusion and allows for the alteration of different syringe diameters and volumes. Using the following principle allows the control over the amount of hydrogel being deposited [259]:

i. Small diameter syringe + small amounts of hydrogel = slow printing of geometries in fine elements
ii. Large diameter syringe + large amounts of hydrogel = fast printing of geometries in bold elements

The paper by Bessler et al. optimized their approach to syringes by using the 10mL one with a 0.8cm diameter. They developed a path-planning software that allows the arrangement of the printing information inside containers such as six-well plates. This tool designs a trail for the nozzle to travel on without colliding with the container in which it will be printed. The software also adds security stops on the printer before the start of the print to allow the modular syringe holder to be mounted. When they tested their methodology, they saw a cellular survival rate of 81% for the HEK293 cells and 85% for the embryonic stem cells [259].

2.8 Desired Printer Design

The quality, effectiveness, and adaptability of bioprinted constructions are significantly influenced by the design and development of bioprinters. The increasing demand for bioprinted tissues makes it essential to improve bioprinters' capability to satisfy the various needs of tissue engineering applications. This chapter focuses on controlling the desired functionality for bioprinter design, encompassing aspects such as printing resolution, speed, versatility, and user-friendliness.

Replicating complex tissue architecture accurately and preserving cell viability requires great resolution. Another important consideration is printing speed since it can greatly cut down on fabrication time and boost the bioprinting process' overall effectiveness.

The capacity to print a variety of biomaterials with different viscosities and mechanical properties, such as hydrogels, biomaterials, and cell-filled structures, is referred to as versatility in bioprinter design. Bioprinters should also be made to accommodate various tissue sizes, geometries, and kinds so that bespoke tissue constructs can be made to meet the demands of individual patients.

Additionally, usability is crucial since bioprinters must be simple to operate and intuitive, especially for non-techies. This provides functions, including software interfaces for creating and managing prints, automated calibration, and simple-to-follow maintenance procedures.

In order to improve the capabilities and application of bioprinting technology in tissue engineering and regenerative medicine, this chapter emphasizes the significance of incorporating these desired functionalities into bioprinter design.

2.8.1 Compactness

For efficient clinical deployment, it's crucial for bioprinters to be compact, allowing them to be placed inside laminar flow units to maintain sterility and easily fit into operation theatres. Although most bioprinters are designed for fabricating tissue constructs on a centimetre scale, their hardware typically occupies a large space. Therefore,

compactness has been a key goal since the inception of bioprinter development, driving manufacturers to prioritize smaller designs.

For instance, the upgraded BioBots bioprinter occupies only 28,317 cm3, easily fitting inside a laminar-flow hood, while the previous Biobot2 model consumed 64,327 cm3. Similarly, the inkjet bioprinter Autodrop Compact by Microdrop Technologies GmbH measures 562 × 772 × 550 mm. Microfab Technologies offers the Jetlab 4 model with a footprint of 63 × 57 cm.

Compactness leads to smaller printable product dimensions, prompting manufacturers to offer larger models. For example, the Jetlab 4 substrate size is 160×120mm, while the advanced version has a working area of 200 × 200 mm. The Autodrop Compact model boasts a positional accuracy of 25 μm, a maximum speed of 75 mm/s, and a payload of 5 kg for the Y-axis, compared to 5 μm, 125 mm/s, and 10 kg, respectively, for the larger model [228].

Clinical translation necessitates a compact bioprinter with high accuracy, deposition velocity, and resolution. To achieve this, exploring miniaturized robotic arms with remote and wireless control possibilities and using lightweight materials with high specific strengths is crucial [260 - 262].

The choice of bioprinter is also influenced by the type of tissue to be printed. For scaffold-free printing, a more compact bioprinter may be ideal due to the small volume of biomaterial required [263]. However, scaffold-free bioprinting may demand higher resolutions to control cell-cell distances [264]. To meet these needs, robotics at the mesoscale level (1–4 μm) with multiple degrees of freedom are needed to enable printing on non-planar surfaces [265].

2.8.2 Degree of Freedom

Earlier bioprinting technologies were often adapted from commercial paper printers. Groups led by Boland and Nakamura were among the first to explore transforming printers like Epson or HP models into bioprinters [266, 267]. Unlike paper printers, which typically move in a single direction, bioprinters require additional axes to create 3D structures. As a result, various modifications, such as integrating a motorized table for vertical axis movement, have been attempted but with limited success.

However, most commercial bioprinters are limited to operating in three axes, which may not be sufficient for intra-operative bioprinting of irregular-shaped defects in clinical settings. Printing on non-planar surfaces and concavities requires more degrees of freedom [197, 268]. The BioAssemblyBot, featuring a 6-axis robotic arm based on pneumatic micro-extrusion, represents an advancement over traditional extrusion bioprinters with three axes. The robotic arm can adjust its spacing to match the porosity of designed constructs, and it offers additional options, such as rotation about the z-axis and the ability to interchange lateral or dual rotation axes.

2.8.3 Speed

Another crucial consideration for bioprinter selection is printing speed. Various bioprinting modalities have different average speeds, such as LIFT: 200–1,600 mm s−1, acoustic DBB: 1–10,000 droplets s−1, and EBB: 10 μm s−1–700 mm s−1 [197, 260]. Printing can take several hours, especially for multi-layer constructs. Direct writing methods offer high resolution but slow speed, such as less than 102 drops per second, while forward transfer methods have lower

resolutions but can print up to 5 × 103 drops per second [268]. Typical speeds for commercially available extrusion-based bioprinters are around 25 mm/s, determined by the stepper motor configuration and driver.

Efforts have been made to reduce bioprinting time, such as using multi-array laser-based stereolithography, multi-nozzle droplet or extrusion-based bioprinters, and a multi-arm robotic extrusion-based bioprinter [269 – 271].

Despite the ability of bioprinters to deposit cells at high rates, the composition of the biomaterial, especially cell-laden biomaterials, also affects the achievable speeds. Higher deposition speeds can reduce cell viability and cell division post-printing due to increased stresses. Additionally, prolonged standing time inside a reservoir due to slow printing rates can further reduce cell viability.

2.8.4 Affordability

The high cost of bioprinters represents a significant barrier to their widespread adoption for routine clinical applications. The stringent sterility requirements of bioprinting processes further compound the expense. However, it is well-established that as demand for a technology increases, its cost tends to decrease. Therefore, as the number of bioprinter users rises and proof-of-concept applications become more prevalent, it is anticipated that bioprinters will become more commercially viable, following a trend similar to that observed with plastic 3D printers.

Currently, most clinically relevant bioprinters are priced at $150,000 to $300,000. However, several startup companies strive to develop more affordable bioprinters accessible to a broader customer base. Despite this, many lower-cost bioprinters are based on extrusion principles and may exhibit inferior fabrication properties. Certain pneumatic extrusion bioprinters can also carry hefty price tags, with models like BioAssembly bots priced around $160,000 and nSrypt exceeding $200,000. In contrast, recently launched bioprinters in this category, such as BioBots and Inkredible, are available at a much lower cost, typically ranging from $10,000 to $100,000. Laser-based bioprinters, which can be built from scratch, tend to fall in the range of $100,000.

Alternatively, bi-axial droplet-based biomaterials without live-cell dispensing capabilities can be developed at a significantly lower cost using commercial paper-jet printers. However, the cost may increase for biological applications from $20,000 to $70,000. Generally, the automation level, resolution, and number of print heads are key cost determinants. For example, a dual-head bioprinter with photo-crosslinking capability can cost between $5,000 and $10,000, while a basic model excluding the biomaterial extruder may cost as little as $500. Conducting a component cost analysis is crucial to identifying strategies for cost reduction. Thus why Reid et al. developed an automated bioprinter using a low-cost Felix 3D printer and a protocal for human-induces pluripotent cell differentiator back in 2016. They were able to improve the resolution and convention of the extrusion process through the use of finite element modelling, designing a functioning and low cost bioprinter [272].

2.8.5 Versatility

Versatility is a critical property of bioprinters, referring to their ability to work with various types of biomaterials, including those with a wide range of viscosities and different gelation processes, as well as accommodating different bioprinting processes. Versatile bioprinters should also offer customization options for end-users to tailor the

instrument to specific applications. One example of such versatility is seen in the Biobot series of bioprinters, which are known for their adaptability to different biomaterial types and printing requirements. The open-source Fab@Home bioprinter also stands out for its remarkable versatility, allowing users to work with various biomaterials and printing processes.

In the droplet-based category, bioprinters like the Nordson Pico® series and MD series from Microdrop Technologies offer significant versatility for high-throughput applications. These printers provide enhanced control over the generation of droplets and their spatial deposition, accommodating a wide range of biomaterial properties and printing needs.

Extrusion-based bioprinters are often considered more versatile because they can dispense biomaterials with various viscosities. In contrast, laser-based bioprinters are limited by the types of biomaterials that can be irradiated by the laser or undergo photopolymerization. Droplet-based bioprinters can handle different biomaterials but are prone to nozzle clogging, especially with high-viscosity biomaterials, which can limit their versatility. For example, many bioprinters are designed for alginate or Pluronic biomaterials, which have limited clinical utility for tissue regeneration. Therefore, system automation based on these biomaterials may not be suitable for end-users seeking functional biomaterials with broader clinical applications [154].

2.8.6 Practicality

One crucial factor determining the success of bioprinting is the practicality of mass-scale tissue production. Current technologies often yield cell numbers suitable only for laboratory-scale studies, emphasizing the need for advancements to enable the production of clinically relevant volumes of tissues and organs. Achieving this scale requires the implementation of advanced, automated bioprocessing technologies that adhere to good manufacturing practices and rigorous quality monitoring standards [273].

The source of cells can also pose constraints on scalability. For instance, stem cells from younger patients may be passed up to 40 generations, while older patients may be limited to only 25 population cycles [274].

Organovo, a pioneering company in the field, has successfully produced liver tissue lines for drug toxicity testing and has progressed in bioprinting kidney and skin tissues [275]. Additionally, bioprinting-assisted fabrication of tumour-on-chip platforms is emerging as a practical solution for cancer research [276].

The development of scalable bioprinting technologies and the availability of suitable cell sources are crucial steps toward achieving the practicality of mass-scale tissue production for clinical applications.

2.8.7 User-friendliness

Given that a significant number of end-users are expected to come from medical and biotechnological fields, the user interface of bioprinters must be user-friendly. The usability of a bioprinter can be assessed based on the time and complexity of steps required to obtain functional outputs, as well as the minimal training time needed for a new user. End-users should be able to focus on clinical problems without being burdened by intricate instrumentation operations. Therefore, user-friendliness should be a key consideration in bioprinter development.

Many extrusion- and some droplet-based bioprinters are known for their user-friendly interfaces. Some bioprinters are shipped as separate parts, allowing users to assemble them. In addition to ease of installation, these printers offer user-friendly operation with interactive software. It's important to note that changing the biomaterial after dispensing an initial quantity loaded should be seamless during operation. Bioprinters equipped with attached peristaltic pumps are preferred for this purpose.

In addition to operation, troubleshooting is also crucial, and a manual with clear descriptions should be provided. Since bioprinters consist of several small electronic and mechanical components, such as microchips, microcontrollers, stepper motors, gears, and belts, it's essential to use components that comply with international standards.

Bioprinters like Inkredible and Biobots are renowned for their user-friendly interfaces. However, sophisticated models like Envisiontec and Gesim Bioscaffolder require professional training for operation and troubleshooting [184, 185]. Laser-based bioprinters are generally less user-friendly, as they require more time to learn and are more intricate to operate.

2.8.8 Automation

One of the challenges facing current bioprinting techniques is the lack of a fully automated workflow, a feat already achieved by some other 3D printing technologies. Most sub-operations of 3D printing, such as extrusion of raw materials, fusion of metal powder, and photopolymerization, have been successfully automated [277 - 279]. However, automating bioprinting poses a significant challenge due to the nature of biomaterials, which must undergo sol-gel transition in physiological conditions without the use of high temperatures. This transition can lead to shape distortions that make high-resolution deposition challenging. Additionally, inherent hydrogel swelling or dehydration processes can cause the nozzle or printed material to not contact the previous layer, resulting in structural deformations that often require manual intervention.

In many bioprinting applications, multiple biomaterials are co-printed, each with its own kinetics of swelling or shrinking, further complicating automation. Efforts to address these challenges include implementing real-time monitoring technologies, which use optical cameras to observe construct height and provide feedback signals for subsequent dispensation [280]. It's important to note that dispensing automation should be compatible with other liquid handling and cell culture protocols. Several automated protocols for cell culture have been reported and should be integrated with bioprinting modalities for in situ applications [281 – 283].

Recent advancements include an automated process for creating surface topographic cues using a robotic biomaterial dispensation system, demonstrating potential for tissue engineering applications [284]. These efforts aim to improve the automation and efficiency of bioprinting processes, bringing them closer to achieving the level of automation seen in other 3D printing technologies.

2.8.9 Resolution

The resolution of a bioprinter is a crucial factor to consider when selecting one, as it determines the fidelity with which constructs can be fabricated. However, the resolution of bioprinted constructs often falls short of the nominal

resolution of the bioprinter itself. This discrepancy is attributed to factors such as biomaterial stability, solidification, and nozzle clogging, which are commonly observed in most bioprinting modalities. Achieving higher resolutions requires motion stages with micrometre-scale resolution.

The size of the nozzle is another important consideration in bioprinting, as it directly influences the accuracy of the final bioprinted constructs [263]. Droplet-based bioprinters can provide droplet sizes ranging from 1 to 300 picoliters, achieving single-cell resolution (50 μm), with deposition rates of 1–10,000 droplets per second [197]. The droplet size depends on the mechanism used by the droplet-based bioprinters. For example, micro-valve print heads with a similar orifice diameter produce larger droplets, around 100 μm, compared to thermal or piezoelectric, around 50 μm, and acoustic droplet bioprinters, around 10 μm. An example of a micro-valve bioprinter is Biofactory, which produces droplets in the range of 5 to 10 nL corresponding to > 100 μm droplet diameter [229].

Extrusion-based bioprinters commonly have positional resolutions in the micrometre range. For example, Allevi has a positional resolution of 5 μm, Fab@Home has 15 μm, and Inkredible has a range of 10 μm. Recently, Suntornnoud et al. proposed a mathematical method to predict the resolution of extrusion-based bioprinters based on a function of printing velocity, nozzle diameter, and applied pressure [285].

Laser bioprinters can achieve very high instrumental resolutions in lateral planes such as 30–100 μm, depending on the wavelength of the laser. Generally, laser-based direct-write methods have higher instrument resolution than laser-induced forward transfer, otherwise referred to as LIFT [190, 212]. The final resolution of LIFT constructs is also influenced by factors such as fluence energy, surface properties, and air gap [286].

Improving the resolution of bioprinters often comes with increased costs and printing times, as it involves the deposition of larger biomaterial loads and a greater number of dots per square inch specified in the design.

2.8.10 Commercialization

There has been considerable interest in 3D bioprinters and their potential to address organ transplantation challenges. However, the commercialization of bioprinters has not kept pace with the enthusiasm for exploring new applications of bioprinting. Extrusion-based bioprinters have received more comprehensive investigation compared to laser- or droplet-based bioprinters. Laser bioprinters have been the slowest to undergo commercial transformation, primarily due to their system complexities and cumbersome operations, although some commercial bioprinters based on stereolithography apparatus are now available.

There is little difference between the working principles in the realm of extrusion-based bioprinters, with different manufacturers offering advanced functions such as automatic biomaterial cartridge filling and software control for robotic movement. While a wide range of droplet-based printers are commercially available, most cannot print mammalian cells due to the small nozzle diameters compared to cell diameters. Additionally, there are numerous open-source 3D printers that can be customized into bioprinters for early-stage researchers.

Some commercial bioprinters are shipped in parts, requiring end-users to assemble them, potentially necessitating skilled service engineers from manufacturers to work with clinical personnel for clinical deployment. It is anticipated

that well-defined industrial norms for bioprinters will be developed in the future to increase their acceptability in the medical community. Standardization of software for 3D printers is also underway, focusing on attributes such as error compensation, tolerance, temperature variations, and dimensional performance, which can be adapted for bioprinters. This standardization will facilitate compatibility among different bioprinters, enabling cross-communication and simplifying integration with design software. Ultimately, bioprinting instrumentation aims to develop bioprinters with a wide range of deposition speeds, high resolution, multiple dispensation capabilities, and compatibility with various types of biomaterials to benefit a diverse user base.

Chapter 3 Mechanical Characterization of Biomaterials

Summary: This chapter explains how each material was created for printing purposes. These include the support bath and the three biomaterials, alginate, nanofibre, and hybrid alginate, as well as the process for testing them. The focus is dedicated to the different material properties used to print a heart wall section. These materials include the support bath, which was tested for its microparticle distribution, size, and rheological properties, as well as the biomaterials used to create the printed structure. These biomaterial materials were tested pre- and post-crosslinked for their different rheological properties such as viscosity, shear stress, compressional stress and stiffness.

3.1 Methodologies

There are two types of support materials, both of which were invented by the creators of the FRESH Bioprinting method: FRESH v1.0 and FRESH v2.0. Since version one is the most widely adopted/used, it was selected for this study as the material used for examination and as support for printing.

To prepare the gelatin slurry, 150 mL of 4.5%(w/v) gelatin Type A was mixed with 11 mM of $CaCl_2$ in 500 mL of a glass mason jar attachment for the blender used for the experiment. The glass was then placed in the fridge at 4℃ overnight to allow the mixture to cool into a gel consistency. Subsequently, 350 mL of washing solution of 11 mM $CaCl_2$ at a temperature of 4℃ was added to the blender and pulsed for 120 s. Once the solution was blended, it was added into 15 mL conical tubes to be centrifuged at 4200 rpm for 2 minutes. Centrifuging lets the particles settle at the bottom, leaving only the washing solution mixture at the top.

The supernatant, the non-gel portion found in the tubes, was then removed, and more washing solution was added to fill the tube to 14 mL consistently. The tubes were then placed back in the centrifuging machine to run again at the exact dimensions. This process was repeated until there were no more bubbles at the top of the supernatant solutions in the tube, approximately 3 - 5 times. Once there were no bubbles found at the top, it indicated that most of the soluble gelatin was removed.

The remaining solid gelatin was scraped out of the tubes and placed in petri dishes to store for testing. Since it is impossible to remove all the liquid when removing the supernatant, Kim wipes by Kimberly-Clark can be used to remove excess fluid. This should only be done for immediate use. It was observed that keeping the support bath in the fridge for an extended period of time can dry out the material. For storing purposes, it is best to leave more liquid in the dish and only remove the excess prior to printing. The bath needs to be stored in the fridge at 4 °C and consumed within a month as the gelatin particles tend to combine into a more rigid and more conjunct material, which is shown in Figure 3.2.

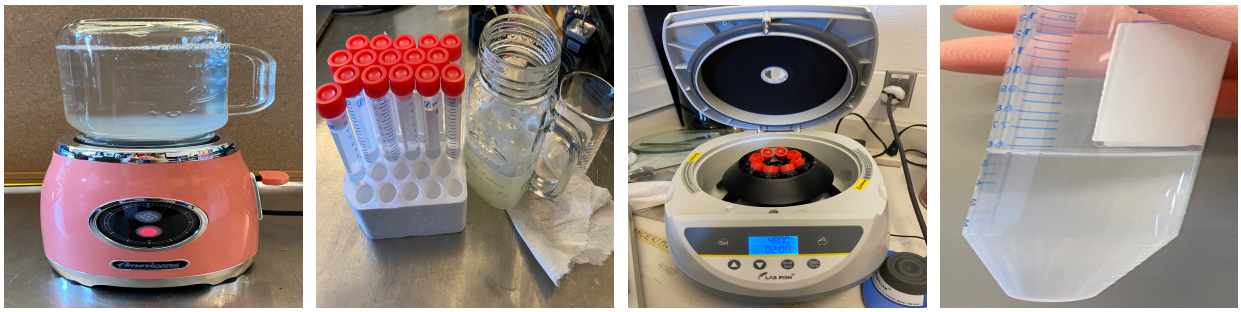

(a) (b) (c) (d)

Figure 3.1 Process of the making of gelatin slurry: (a) blending the solidified gelatin with calcium chloride, (b) transferring the solution to 15 ml syringes, (c) centrifuging the solution, and (d) resulting separation of the particles.

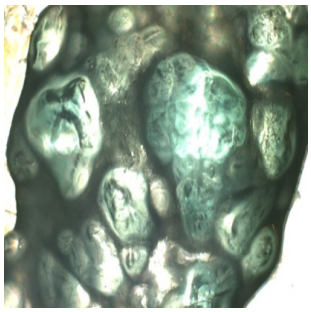

Figure 3. 3.2 Particles were found in the gelatin slurry bath after a month of storage, with the light source being from above.

3.1.1 Biomaterial Creation

Multiple materials were used in the experiments. Each of these biomaterials has a slightly different way of preparing them to receive the best results. The following steps were taken in preparation for the materials.

3.1.1.1 Alginate

Alginate biomaterial is derived from algae and is typically composed of alginate polymers, which can be crosslinked to form hydrogels. Alginate is a good, diverse biomaterial because of its biocompatibility, biodegradability, and printability. It is also a simple boink to create and can be easily altered for viscosity depending on the percentage of alginate used.

2% and 4% Concentration

Higher alginate concentrations need a different preparation style due to its high viscosity property. The following steps can be used for concentrations of 4%(w/v) alginate and lower.

PBS is added to a beaker with a couple of drops of red food colouring. The beaker is then placed on a stirring machine plate where it is heated to 60℃. Alginate in the desired percentage concentration is slowly added to the mixing beaker. Once the material is in the beaker, it can be sealed off with parafilm and left to mix until all clumps are removed. Once

done, they can be transferred to syringes, which will then be sealed from both ends and centrifuged at 3800 rpm for 2 minutes to remove all bubbles in the material.

The material can then be used for printing or placed in the fridge for storage. The material can then be stored for four weeks at a 4℃ temperature [287].

(a) (b)

Figure 3.3 The creation of alginate biomaterial: (a) semi-mixed (b) fully incorporated.

6% Alginate Concentrations

At 4% alginate concentration, the process of dissolving the alginate in the PBS is slightly difficult but still possible with a magnetic stirrer. However, any higher concentrations need an overhead magnetic stirrer to dissolve the alginate material in the PBS solution. All the other steps remain the same, including heating the magnetic plate. The only difference is the stirring aid used. The magnetic stirrer cannot mix the solution at high viscosities, even at the highest rpm available on the mixer machine, which is why the stirring stick is needed. Even then, there may need to be some manual mixing assistance to remove all the material clumps.

3.1.1.2 Nanofibre

The nanofibre biomaterial is the more complicated biomaterial when it comes to preparation. It starts with mixing 0.5% cellular nanofiber with PBS in a beaker for 15 minutes. Blue food dye is added to this material to distinguish it from others during printing. The beaker must be sealed with a parafilm to prevent the liquid from evaporating. From there, the material is taken to the ultrasonic machine and mixed for 30 seconds at 50% intensity. The beaker is then placed on the magnetic stirrer machine and heated to 60℃. Once a vortex has been created through the stirring, 6% of gelatin is slowly added to the mixture. The beaker is re-sealer and stirred for 30 minutes. The last material that is added is the alginate at a 6% ratio to the material. Then, it is mixed for another 15 minutes before the material is removed from the mixing plate and transferred into syringes. The syringes containing the materials were then sealed and centrifuged at 3800 rpm for 2 minutes to remove all bubbles in the material.

The material can then be used for printing or placed in the fridge for storage. Nanofiber has a shorter lifespan than the other materials. After a week in the refrigerator, the nanofibers slowly separate from the rest of the mixture. By the second week, the material's structural integrity during printing had slightly degraded. It is recommended that the material not be used in the past two weeks of storage.

3.1.1.3 Hybrid Biomaterial

The Hybrid biomaterial, as the name suggests, is a mix of alginate and gelatin, each at 2%(w/v) concentration. This biomaterial is simple to create and is noted by the colour green in the later experiments. To generate the biomaterial, 2%(w/v) of gelatin type B and 2%(w/v) of alginate were added to 40mL of 1xPBS. Green food colouring was also added to distinguish the biomaterial from the others. The beaker was then placed on a mixing plate heated to 60℃ with a magnetic stirrer and mixed until all clumps were removed. Once completed, the material was transferred to 10mL syringes, which were sealed off with syringe caps. The syringes containing the materials were then sealed and centrifuged at 3800 rpm for 2 minutes to remove all bubbles in the material.

The material can then be used for printing or placed in the fridge for storage. The material has a shelf life similar to the alginate; for that reason, it can be stored for four weeks at a 4℃ temperature.

3.1.2 Microscope Testing

Particle analysis was conducted for the gelatin slurry using an Optical and Fluorescence Microscope (Axiolab 5 by Zeiss). Two magnification sizes were used to examine the microparticle sizes and shape, and they are 10x and 40x.

The specimen used for analysis was created by adding a diluted food dye and distilled water to a small amount of gelatin slurry. This was done to make the particles visible as they are naturally clear in visibility, which would make it hard to see under the microscope on its own.

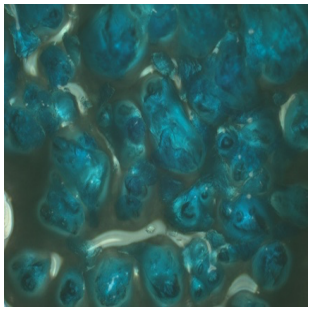

Figure 3.4 Particles found in the gelatin slurry bath, with a light source from above.

Two different light sources were used to evaluate the microparticles of the gelatin slurry: one light source from above the lens and one from below the microscope slide. The different light sources provide various aspects of the gelatin particles. The figure above shows the shape of the gelatin slurry when the light source is from above. It is observed that bulky portions of gelatin slurry looked slightly clumped together. It was used to see how they react to the other particles and to visualize their uniform distribution. However, the above light made it difficult to capture the particle sizes. For this reason, the light-transmitting below was used to analyze the particle sizes as it shown all aspects of the particles. As the light goes through the specimen, it visibly shows where the particles start and end.

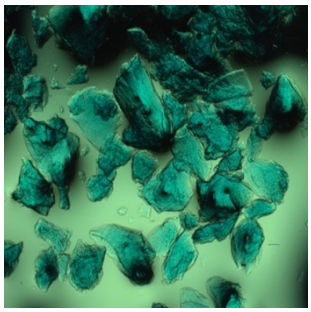

Figure 3.5 Particles found in the gelatin slurry bath, with the light source from below.

The cell visibility was because the dense areas (gelatin particles) were darker compared to the negative space between them, which was brighter and gave a more accurate description of the borders of each particle. This is depicted in Figure 3.6. In this light source, multiple images were taken to examine the typical widths and lengths of the gelatin particles.

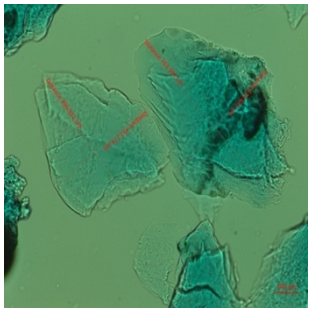

Figure 3.6 A particle measurement for isolated particles.

The particles were chosen randomly, using a mix of larger and smaller particles to achieve an accurate representation of the average particle size. Initially, the 4.5% gelatin slurry was examined as it was the percentage used by many researchers as well as by the founders of FRESH Bioprinting. Due to the large variance of particle sizes in the gelatin slurry and the varied results from other papers, it was necessary to test the gelatin slurry from 1% to 20% gelatin concentrations. In these tests, each gelatin slurry configuration was created in the same way and tested under the same procedures to eliminate any external interference that could cause a variance.

3.1.3 Rheological Testing

Rheological testing is vital for understanding and controlling the flow and deformation behaviour of materials. It plays a key role in quality control during manufacturing, aids in product development and process optimization, predicts material performance, ensures quality assurance, and helps troubleshoot issues. Rheological data is crucial for designing materials with specific properties, optimizing manufacturing processes, and gaining fundamental insights into material behaviour, making it an indispensable tool in various industries, including manufacturing, biomedicine, and materials science.

For these reasons, a rheometer apparatus (TA Discovery Model HR-30) was used to test both the gelatin slurry and the biomaterials, pre-crosslinked and post-crosslinked, for their mechanical properties.

Figure 3.7 Rheometer apparatus from TA Discovery Model HR-30.

3.1.3.1 Gelatin Slurry Testing

A sweep flow test was performed to test the gelatin slurry in terms of viscosity and shear rate. The machine utilized a concentric cylinder. This was done to eliminate the overflow of gelatin during the test cycle. There were three tests performed on the machine with the gelatin: one at 4℃, which is the needed temperature for the gelatin slurry to keep it's support material characteristics, another at 25℃ representing room temperature, and the last at 36℃ representing body temperature level. These tests were conducted to see how the gelatin slurry reacts at different temperature levels to understand the possible printing impact.

The tests were originally conducted for 4.5% gelatin concentration, which then pivoted to 1% to 20% gelatin concentration for all three temperatures.

3.1.3.2 Biomaterial Testing

The three different biomaterials used to print the different heart layers were tested in different states at different temperatures. These tests were conducted to check the material's characteristics for optimal printing and to determine if the characteristics match in mimicking the native tissue.

Pre-crosslinked

Testing biomaterials pre-crosslinking is crucial for assessing their mechanical, rheological, and biocompatible properties. This pre-crosslinking evaluation allows researchers to fine-tune formulations, predict material behaviour post-crosslinking, and ensure that the biomaterial meets specific performance criteria. Understanding the baseline characteristics is essential for optimizing crosslinking processes, predicting final material properties, and ultimately designing biomaterials tailored for specific biomedical applications.

Before the material crosslinked and set, it was examined for its properties, such as stress, viscosity and modulus at different temperatures. These properties were important for understanding how the materials react during the printing process. The stress in the material shows how much it can withstand, which impacts the cells that are added to biomaterial. Then, the viscosity shows how easily the material can be printed at different temperatures. This is crucial

to reduce the material's stress and understand the pressure needed to extrude it. Again, this step is useful for protecting live cells in biomaterials. The materials were tested at 4℃ to see the characteristics of the materials at the needed temperature for the gelatin slurry. Then, at 25℃ to see if we do not use special conditions (average room temperature) with the printer. Lastly, in the case of in-vivo printing, the materials were examined at 36℃.

Post-crosslinked

Post-crosslinking testing of biomaterials is essential to evaluate the final product's mechanical strength, stability, and biocompatibility. This phase ensures that the crosslinking process has achieved the desired properties, such as improved structural integrity and resistance to degradation. Post-crosslinking tests provide insights into the material's ability to withstand physiological conditions, ensuring its suitability for biomedical applications. Assessing the effectiveness of crosslinking aids in quality control, validates the material's performance, and informs further refinements in developing biomaterials for medical use.

For this reason, the materials were tested once they were printed and had adequate time to crosslink in the gelatin slurry. Once the materials set, they were washed and tested for compression and stiffness using the rheology machine.

Figure 3.8 Testing the rheological properties of the post-crosslinked alginate.

3.2 Importance of Material Characterization

Assessing materials for bioprinting is important for biocompatibility purposes. The materials utilized for 3D bioprinting must naturally be compatible with living tissues and cells. Due to the high sensitivity of the human body to foreign substances and the potential for adverse effects from any incompatibility, it is crucial to assess the suitability of materials carefully. The assessment ensures that the materials will not harm or interfere with the biological elements that are being printed, boosting the bioprinted structures' long-term viability and functionality [288].

Furthermore, the material characteristics significantly impact the viability of cells enclosed within the printed structures. Factors such as the material's porosity, surface chemistry, and mechanical properties can impact cell survival and growth. Insufficient material characterization can result in poor cell viability, making the bioprinted tissue useless or unsuitable for its intended use [289].

Another critical factor is how well bioprinted tissues function. Materials must be designed to mimic the mechanical stability, pliability, and biochemical cues of native tissues. In order to construct functional tissue constructs for

regenerative medicine, disease modelling, and drug testing, accurate material characterization is crucial. Accurate material characterization is required to achieve the desired tissue functionality.

A practical concern with 3D bioprinting is printability. To enable precise deposition and layering of biomaterials, various bioprinters and printing techniques require specific material properties. The materials' rheological behaviour, viscosity, and flow characteristics are crucial to the printing process. For successful printing, these properties must be thoroughly characterized so that the bioprinter can function properly and produce structures of the highest calibre.

The characteristics of the support material have a significant impact on the structural integrity of bioprinted structures. Support structure materials must maintain their shape and offer enough support during printing. When printing complex, drooping, or delicate structures, it is crucial to characterize the mechanical properties of the support material, such as its tensile strength and elasticity, to ensure that it can support the printed constructs.

Additionally, some applications call for materials that gradually deteriorate or resorb with time. For example, as the bioprinted tissue develops, gradual material degradation may be required for tissue scaffolds or drug delivery systems. To ensure that the material is biodegradable and resorbable when necessary, proper material characterization aids in defining the degradation kinetics [290].

Material characteristics affect resource use, cost-efficiency, and regulatory compliance, in addition to having an immediate impact on bioprinted structures. Regulatory bodies frequently demand thorough material characterization to guarantee the safety and effectiveness of bioprinted products for clinical use. Understanding material characteristics can also result in more effective resource use, less waste, and a more streamlined bioprinting procedure.

In conclusion, evaluating material properties in 3D bioprinting is complex and essential. Getting biocompatible, viable, useful, and structurally sound tissues from bioprinting is essential. Additionally, it helps bioprinting processes be more effective, cost-efficient, and compliant with regulations, ultimately promoting field development and its many applications.

3.2.1 Gelatin Support Bath Material Characterization

The success of the advancement of the 3D printing method in bioprinting applications depends heavily on the material characterization of the materials that are used in the printing process. For the FRESH bioprinting method, the gelatin slurry support bath is the basis of its printing capabilities. By encasing hydrogel-based biomaterials in a support bath, FRESH bioprinting is a cutting-edge technique that makes it possible to create intricate, high-resolution biological structures. During the printing process, the support bath, which is typically made of gelatin, is extremely important in preserving the structural integrity of the bioprinted object. In order to make sure the gelatin slurry support bath material it is necessary to characterize its particle and rheological properties.

3.2.1.1 Analysis of 4.5% (w/v) Gelatin Composition

According to the creators of the FRESH printing method, the support bath for bioprinting needs to contain 4.5%(w/v) of gelatin [67]. While this number is not justified or restricted, it was used as the initial interaction and testing of the

gelatin slurry for possible bioprinting applications. The material was tested similarly to the authors for its rheological and its microparticle properties.

Microparticle Analysis

The material characterization of a gelatin slurry support bath used in FRESH bioprinting includes microparticle analysis. Microparticles in this context may refer to tiny aggregates or solid particles present in the gelatin support bath. It is essential to comprehend and characterize these microparticles because they can impact the calibre and effectiveness of the support bath and, consequently, the bioprinted structures. The following factors were considered when conducting a microparticle analysis: size and distribution, concentration, composition, agglomeration, impact on print quality, removability, prevention and mitigation and quality control.

The purpose of examining the concentration of the bath is to quantify the concentration of microparticles in the gelatin slurry. High concentrations of microparticles can lead to clogging of the printer nozzle, affect print quality, and hinder the flow of the support bath.

In terms of the composition of the microparticles, it is important to analyze them for contaminants or aggregates of gelatin to find potential sources of interference in the printing process. Agglomeration refers to the formation of clusters of particles, which is an irreversible formation. There are two reasons for agglomeration in a material: either due to Brownian motion or gravitation. In most cases, the result is that the particles collide due to their random motion and stick together, forming clusters. The motions/movements are dependent on the particle sizes and terminal velocity. The cluster of particles has effects on the material's PH level, ionic strength, flow properties and homogeneity [291].

Another reason for the microparticle analysis is the impact on quality print. This refers to the influences of the presence of microparticles in the printing process and how they affect the surface of the printed structure. Microparticles may lead to irregularities or defects in the printed tissue constructs, making it essential to determine their impact on the final product. Additionally, once the printed material is set, the support material needs to be removed. This is why the removability of the support bath is also a factor to be considered. Evaluating the ease of removing the microparticles from the printed structure without damaging the structure itself can be difficult if the particles are not the right size and distribution. This can further impede the tissue fabrication process in the tissue culturing step, which is why the material needs quality control. Control protocols need to be used to monitor and minimize the presence of microparticles during the preparation and handling of the gelatin support bath.

Lastly, the most vital test factor, which is the size and distribution of the microparticles of the gelatin, is not only an important test as it contributes to all the other mentioned factors but also for the following several reasons:

- **Print Quality:** The quality and accuracy of structures created using bioprinting can be significantly impacted by the size and size distribution of the particles in the support bath. Large or unevenly distributed particles can lead to irregularities in the printed object, which can result in flaws or errors in the structure.
- **Nozzle Clogging:** Nozzle clogging in the bioprinter can result from large or irregularly sized particles. Clogged nozzles prevent the gelatin support bath from being extruded, which can halt printing and harm the nozzle. This compromises the integrity of the bioprinted structure and wastes time and resources.

- **Rheological Behaviour:** The presence of particles affects the support bath's rheological characteristics, such as viscosity and flow behaviour. The support bath's flow can be affected by the particle size and distribution, either making it too viscous or too thin. The material's capacity to offer structural support during bioprinting may be compromised as a result.
- **Tissue Viability:** Maintaining the viability of encapsulated cells and tissues is essential for bioprinting applications. Large particles may physically damage or stress cells while being printed, jeopardizing the bioprinted tissue's functionality and viability.
- **Material Homogeneity:** The homogeneity of the support bath is influenced by the narrow size distribution of the particles. The uniformity of the support during printing can be impacted by inconsistent particle sizes because they can cause variations in the behaviour of the material.
- **Structural Integrity:** During printing, the support bath is essential for preserving the structural integrity of bioprinted structures, especially those with complex geometries or overhanging features. The support bath can hold the bioprinted materials securely without collapsing due to the carefully managed particle size and distribution.
- **Post-Processing and Removal:** The support bath must be removed after bioprinting without causing damage to the structures. The right-sized particles are simpler to separate from the printed material. A bioprinted structure may become tangled with particles if they are too large or too small, causing it to be difficult to filter out.
- **Contamination and Purity:** Particles of different sizes could be a sign of contamination or inconsistent support bath preparation. To prevent unwanted elements from being added to the bioprinted structures, it is crucial to ensure the purity of the support bath.

All the mentioned factors were considered during tests to enhance the material's functionality. By checking and controlling the size and size distribution of particles in the gelatin support bath, researchers can enhance the reliability and repeatability of the bioprinting process. This leads to better print quality, reduced operational issues, and a higher likelihood of successfully creating bioprinted tissues and structures with the desired characteristics and functionality.

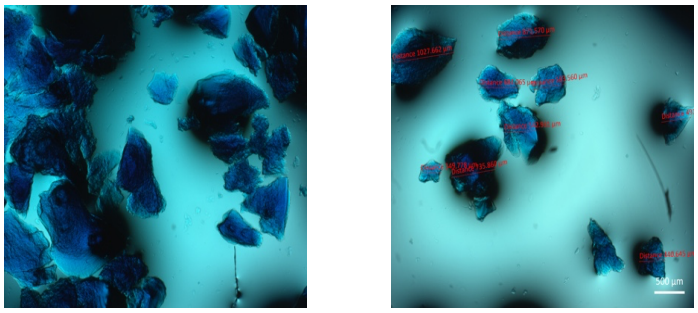

(a) (b)

Figure 3.9 The microscope pictures taken for the 4% gelatin slurry concentration: (a) a cluster of particles without numerical data, and (b) measurements taken to examine

Thus, why the support bath material was examined under a microscope to see the particle distribution, size of the particles and uniformity of the material; it was concluded that the material had non-uniform particle sizes and distribution; the lengths ranged from 385.11 μm to 1372.83 μm. Calculating the mean ferret diameter from these values resulted in a diameter of 878 μm. However, based on previous articles, the optimal mean ferret diameter should average 55.3 ± 2 μm [68].

Rheological Analysis

For the rheological test, a Discovery Hybrid Rheometer was used from TA Instruments. The machine utilized a concentric cylinder. This was done to eliminate the overflow of gelatin during the test cycle. Two tests were performed on the machine with the gelatin - one at the average room temperature and another at an average body temperature level.

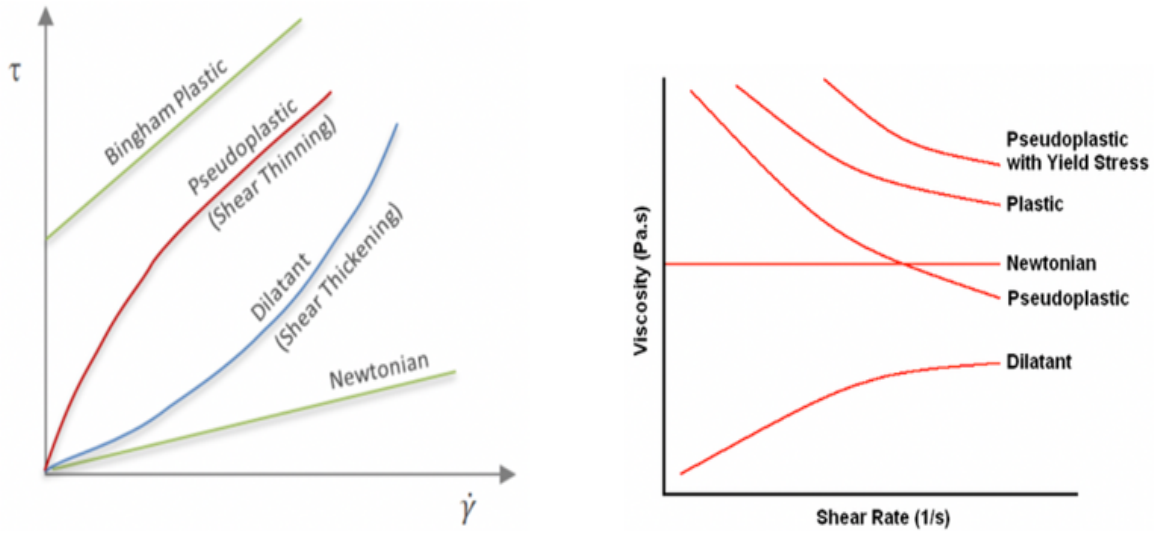

(a) (b)

Figure 3.10 (a) Shear stress vs shear rate, and (b) viscosity vs shear rate.

Figure 3.10 shows the graphs created from the results of the rheology tests as a form of patterning the different material outcomes as a comparison for further studies. These graphs were used to characterize the gelatin slurry based on the resulting curves.

The test performed at room temperature shows that the viscosity vs shear rate pattern is similar to the one found in 3.10 (b) for plastic. By comparing Figure 3.10 (a) and Figure 3.11 (b), the pattern found from the slurry does not resemble either of the patterns for typical liquid. It seems to be a hybrid of Bingham plastic and Pseudoplastic.

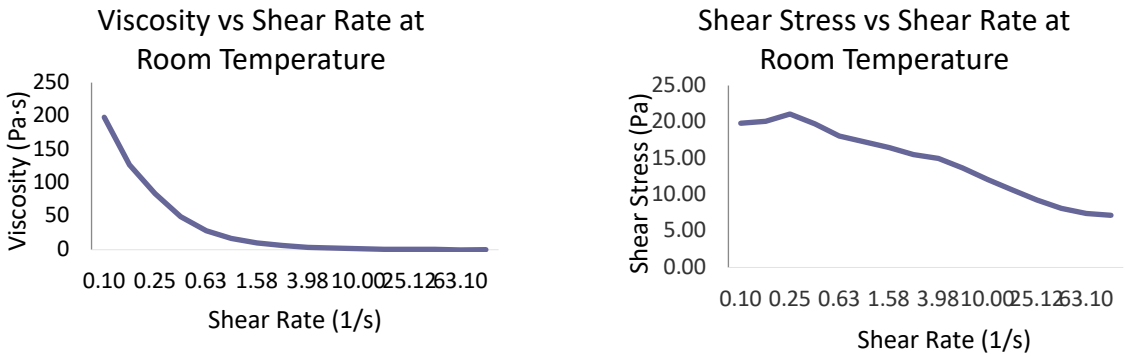

(a) (b)

Figure 3.11 Results from the rheology flow test at 25 ℃: (a) viscosity vs the shear rate, and (b) shear stress vs the shear rate.

The rheology test results for a temperature of 36 ℃ show a similar pattern to those found at room temperature. However, there appears to be more variation in the shear stress pattern. Additionally, the viscosity and the shear rate values seem lower. For viscosity, the maximum value is found at 198 Pa·s at room temperature and about 110 Pa·s at body temperature. This is similar to the shear stress values as well.

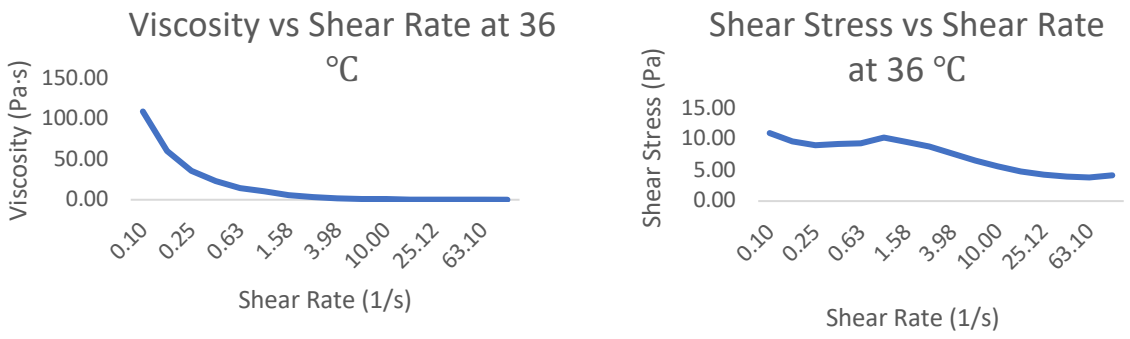

(a) (b)

Figure 3.12 Results from the rheology flow test at 36 ℃: (a) viscosity vs the shear rate, and (b) shear stress vs the shear rate.

While it is clear that the slurry contains a plastic-like consistency in forms of viscosity, the results of the shear stress are not clear on whether it can be characterized as a Bingham-Plastic as it should have been in theory.

Printing Test For Material Properties

Once the tests were done to characterize the slurry, a free hand printing test was conducted using alginate, which was dyed blue in colour, to assess the printing capabilities of the material. In the figure below, it is observed that, at first, a shape was in the form of a ball and a line before moving to more complex shapes to see if the material structure would stay intact.

This test concluded that the needle could easily slide through the gelatin slurry without any effort. When depositing the alginate, the material did not move or dissolve in the bath. The printed shape stayed in the embedded form until it solidified and could easily be removed. Once out of the support material, the printed object was washed in the washing solution prepared for the gelatin slurry to remove any remaining support bath particles.

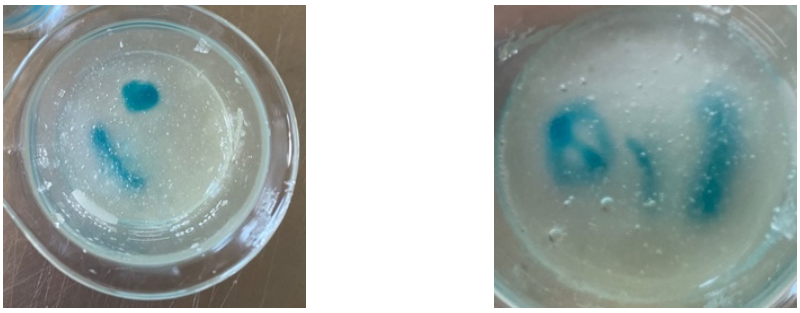

(a) (b)

Figure 3.13 Print testing of alginate in the gelatin slurry bath: (a) basic shapes, and (b) complex shapes.

Discussion on the Gelatin Slurry Performance

In conclusion, in this particular study, it was seen that the gelatin slurry reacts and performs in the needed way to print delicate and complex structures. This was concluded by the printing test. However, the slurry is not composed of uniform microparticles. Each particle has different sizes and shapes, which creates a setback in the finished product as the layers will not be as smooth as they would be from a more uniform and smaller particle-configured support bath. The bath should not be stored for long periods of time as it tends to decrease in volume, and the gelatin particles conjoin. This creates a problem with the pre-creation of the slurry bath for printing.

Additionally, the rheology tests confirmed that the slurry is plastic. In theory, it is known that the gelatin bath contains materials that should allow it to behave, such as Bingham plastic. The resulting curves did not show this phenomenon. Instead, it seemed to have combined results with Bingham plastic and Pseudoplastic. The results for the viscosity curves proved that the slurry behaved like plastic. This paper demonstrates that the slurry has plastic properties but does not characterize it as a perfect Bingham plastic.

Since the printing trial seemed to work in the intended matter, the shear stress results could be based on the bath containing more than the needed washing solution. Since the washing solution is deionized water-based calcium chloride, it can be assumed that it could have navigated the results to start out as a Bingham Plastic but, in turn, change into a shear-thinning material.

3.2.1.2 Gelatin Composition Study

Based on the information found for the 4.5%(w/v) gelatin support bath material. A composition test was conducted, where multiple batches of gelatin slurry were created and tested for their microparticles and rheological properties. The gelatin composition ranged from 1%(w/v) to 20%(w/v). All materials were created using the same steps and techniques to eliminate externally created variances in the materials.

The reasons behind the study was to create a uniform distribution and particle sizes for the material while not jeopardizing the rheological properties. Due to the limited data on the gelatin bath material, this test was also used as a reference to possibly increase the gelatin percentage in the bath, which can result in the increased amount of the support material created in the same amount of time as the recognized 4.5%(w/v) gelatin slurry.

Microparticle Analysis Results

Each batch of the gelatin slurry was tested for its microparticle size and uniformity. For each percentage, the average size was determined by evaluating the size of 13 particles in different size ranges. Then, these were added together to find each particle's average size in micrometres.

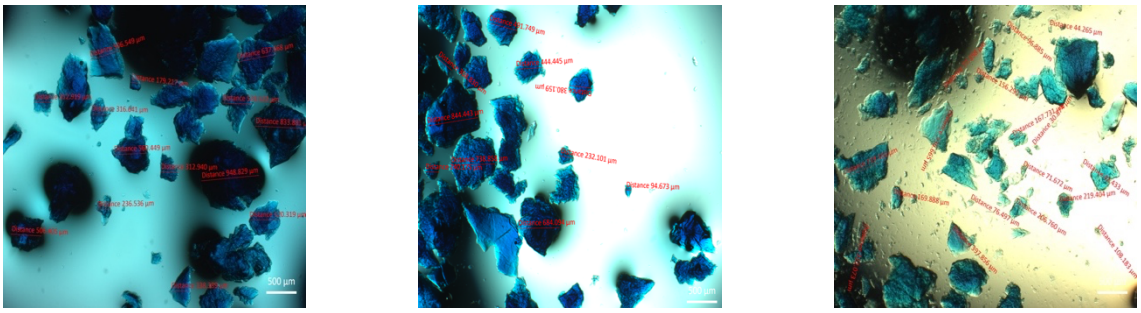

(a) (b) (c)

Figure 3.14 Example images of how the size was determined for the particles in: (a) 3%, (b) 8%, and (c) 13%.

Table 3.1 shows all the milestone results in increments of 5%, these being 1%, 5%, 10%, 15% and 20%, for the particle sizes. When looking at the results, it can be seen that there are no correlations between the gelatin percentage in the slurry and the particle size uniformity or distribution. It was the same for all the numbers that were examined. Since all the slurries were created using the same technique, there is no correlation between the amount of gelatin that can be added to the slurry versus the particle sizes.

Table 3.1 Milestones of the particle sizes tested from 1% to 20% gelatin composition.

% of Gelatin Composition	Size in Micrometers	Number of Particles
1	628.39	13
5	490.54	13
10	371.05	13
15	449.29	13
20	531.45	13

From this finding came the idea to test the material for different techniques. A gelatin percentage was chosen and created in multiple different ways to test if it affected the particle sizes and distribution. These were:

- Freezing the gelatin prior to blending.

- Blending technique changes:
    - Pulsating for 120 seconds
    - Continuous blending for 120 seconds.
    - Pulsating for 1 minute and continuous blending for the other minute.
    - Continuous blending first, then pulsating for equal amounts of time.
    - Pulsating for 30 seconds and continuous blending for 30 seconds, repeating this until 120 seconds are completed.

All of these techniques were used to create a batch of the gelatin slurry, which was examined under the microscope to see if it changed the results of the microparticle size, uniformity and distribution. However, the results shown the same as before. It was deeming the microparticles uncontrollable for FRESH 1.0 gelatin slurry. Thus, the rheological properties were examined for all the compositions to determine if there were any differences in terms of characteristics.

Rheology Analysis Results

The rheological properties of all the different compositions were examined to characterize the different compositions compared to the traditional 4.5% gelatin composition. The characteristics that were examined were viscosity, shear stress and modulus. The tests were also conducted at three temperatures.

The materials were tested at 4℃ to determine the characteristics of the materials at the needed temperature for the gelatin slurry. Then, at 25℃ to verify if we do not use special conditions (average room temperature) with the printer. Lastly, in the case of in-vivo printing, the materials were examined at 36℃. These results were compared to the 4.5% gelatin composition results to see how the higher or lower gelatin composition affects the different characteristics.

Viscosity

The viscosity of the support material is important as it will determine how easily the needle can cross the material to print. As well as it must be able to support the biomaterial to create the delicate and complex structures that are needed for bioprinting. Especially for medical use such as organ printing.

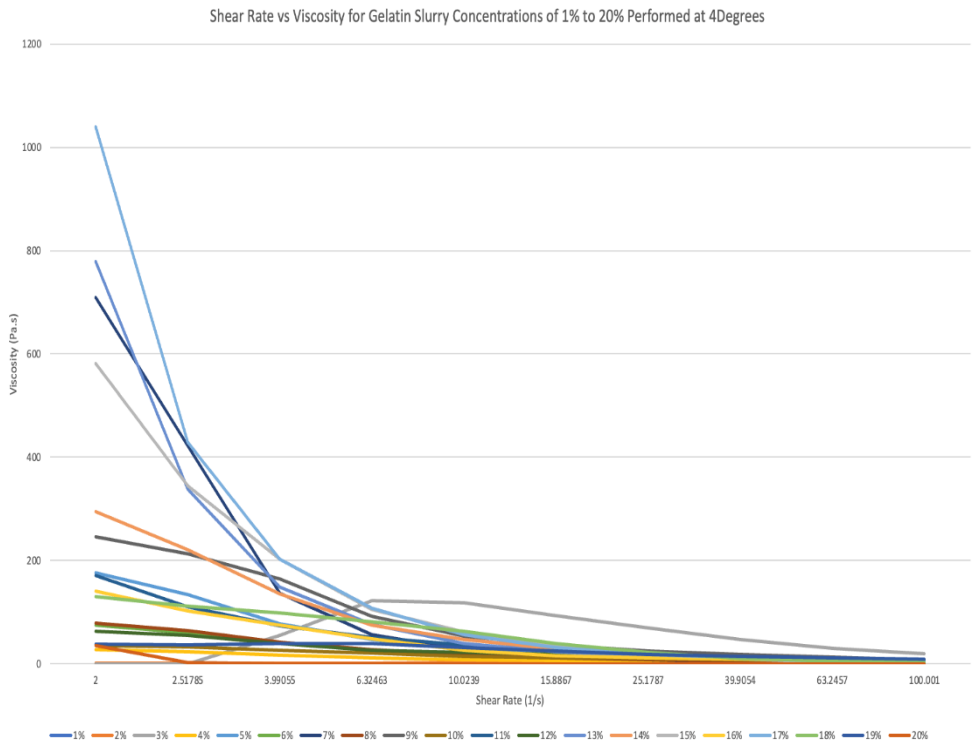

Figure 3.15 Viscosity results at 4℃ of the gelatin slurry tested from 1% to 20% gelatin composition.

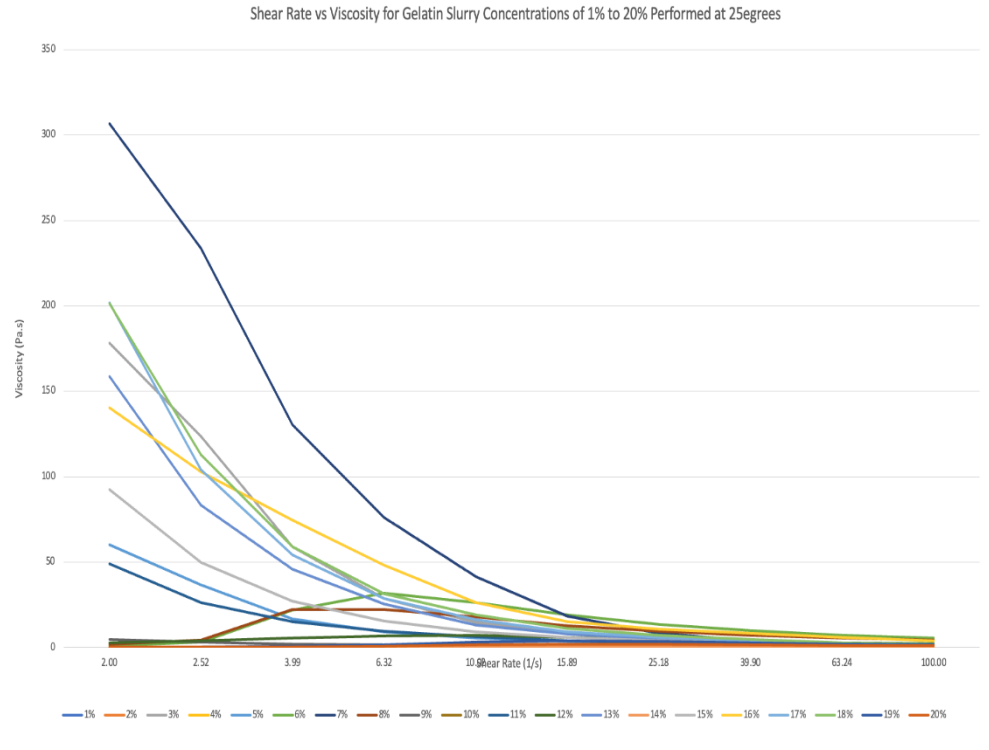

Figure 3.16 Viscosity results at 25℃ of the gelatin slurry tested from 1% to 20% gelatin composition.

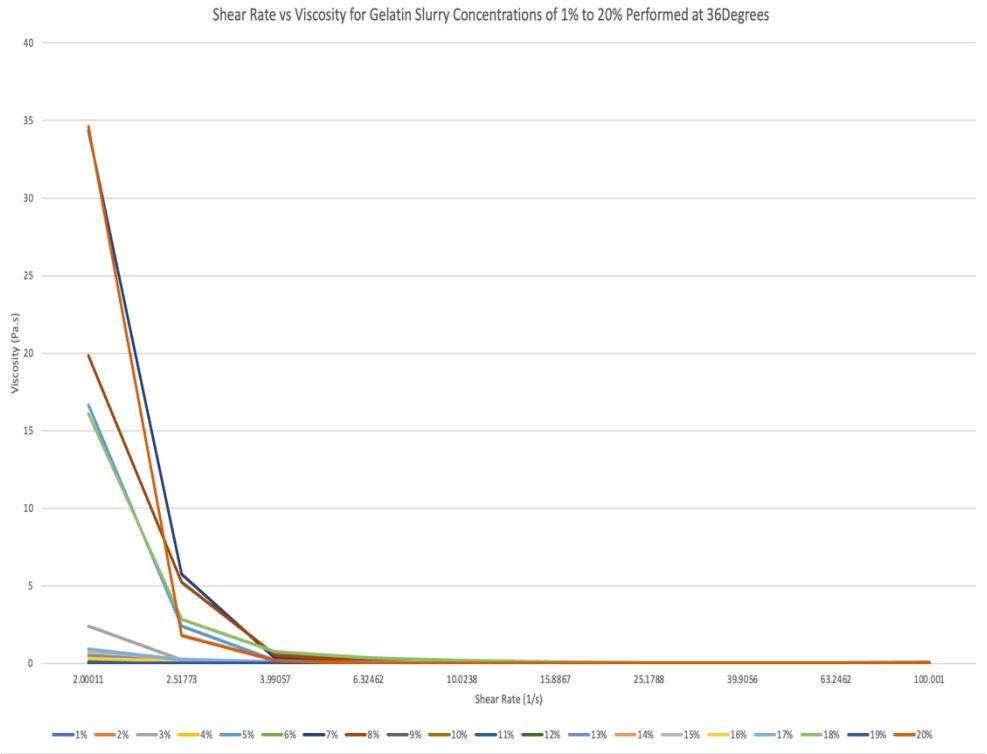

Figure 3.17 Viscosity results at 36°C of the gelatin slurry tested from 1% to 20% gelatin composition.

The viscosity test results at each temperature shown that the lower gelatin compositions had similar results. However, the higher concentrations had higher viscosities. However, one of the outliers in this trend was the 17% gelatin composition, which had similar properties to the 4.5% gelatin concentration. Since the typical temperature for printing is room temperature, we are looking for a material with around 200 Pa·s, which is consistent with peanut butter. This characteristic will allow it to hold up the weight of printer structures, which is where the particles come into play since it has to be able to have a needle pass through it without restriction. The viscosity at 200 Pa·s made up of particles allows the material to do just as intended. Since the viscosity is similar, 17% gelatin composition seems favourable, providing larger batches of the material to be made in the same process.

Shear Stress

The shear stress is a characteristic evaluated for the material to see how it reacts when the needle obstructs its shape. The gelatin slurry displays a liquid-like behaviour around the needle where the applied shear stress is higher than the yield stress. It needs to allow the needle to move through it easily while still upholding the shape that is needed for printing.

It is an essential characteristic since it is the primary advocate for the printed material's integrity. If the shear stress of the support bath is inadequate, it can cause deformation or damage to the printed structure. According to the 4.5% gelatin slurry results, the desired shear stress is around 20 pascals.

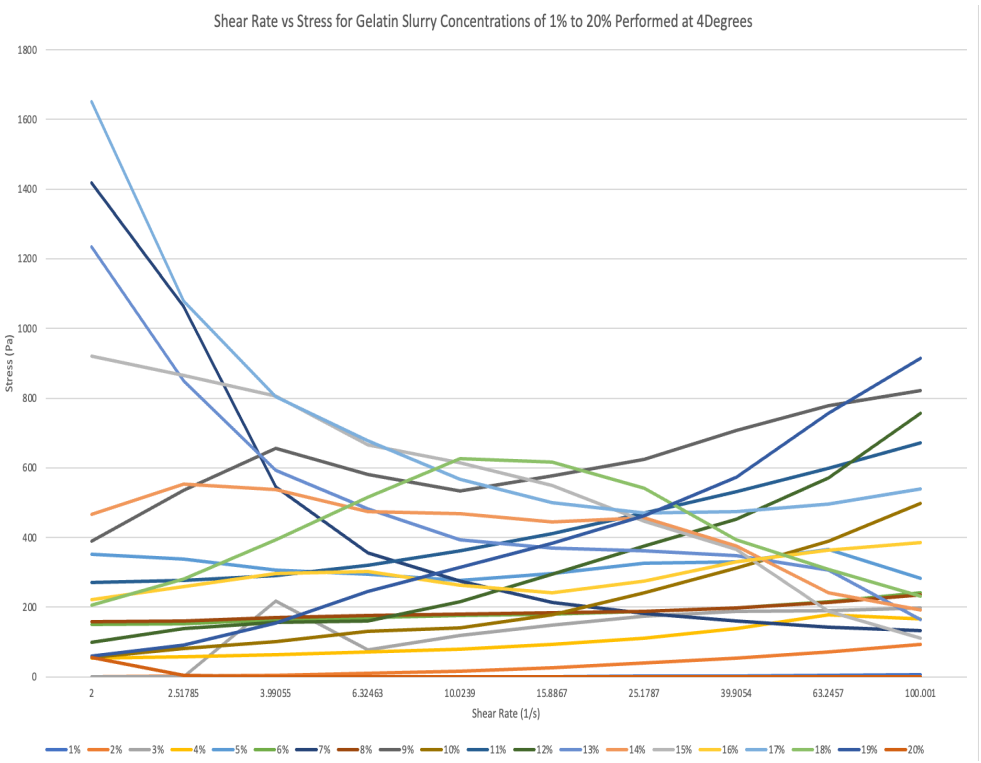

Figure 3.18 Stress results at 4℃ of the gelatin slurry tested from 1% to 20% gelatin composition.

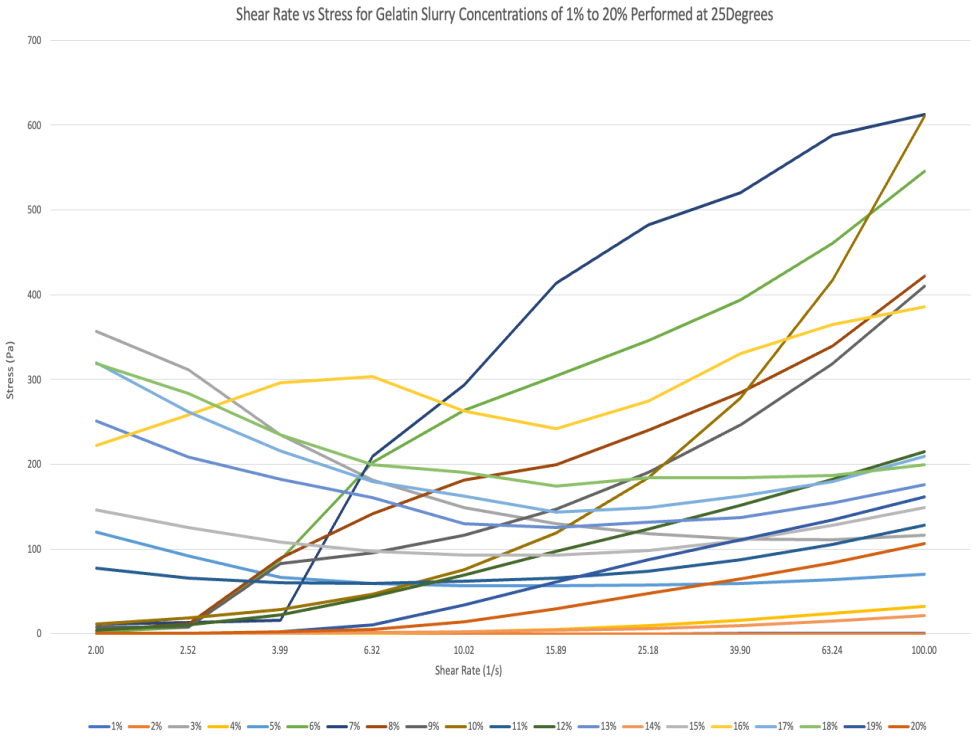

Figure 3.19 Stress results at 25℃ of the gelatin slurry tested from 1% to 20% gelatin composition.

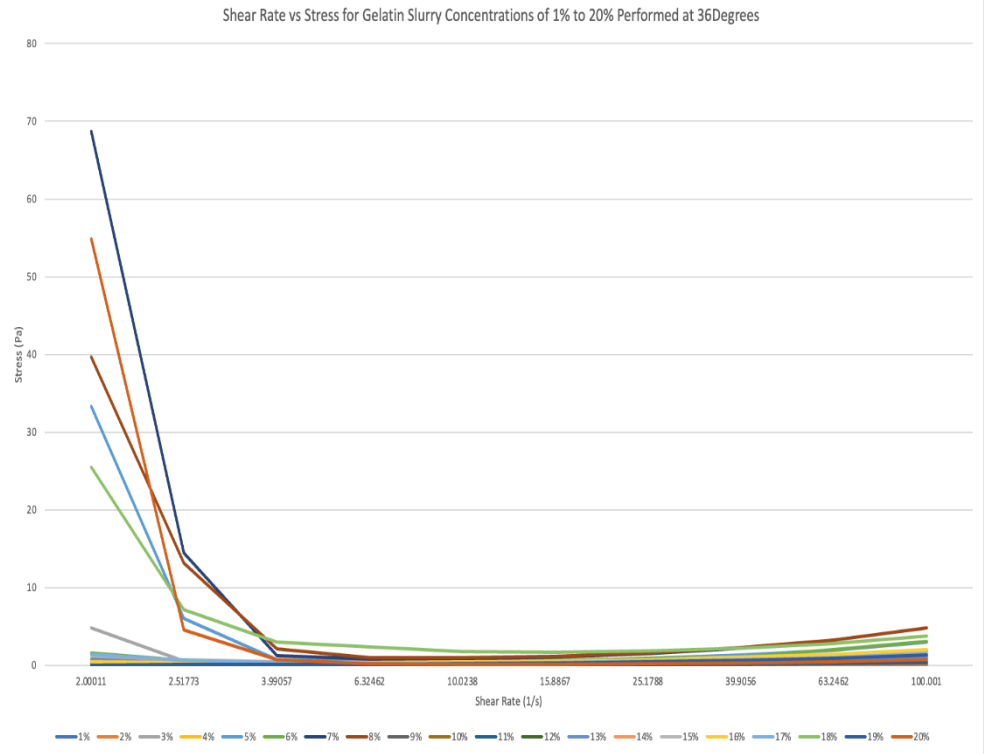

Figure 3.20 Stress results at 36℃ of the gelatin slurry tested from 1% to 20% gelatin composition.

The shear stress results are slightly different than those for the viscosity. This time, the gelatin slurry compositions only followed the same pattern at 36℃. There were some variances in the pattern for some of the compositions at 4℃ and 25℃. For this characteristic, the higher the gelatin percentage, the higher the shear stress for the material. Also, the higher percentages started from higher shear stress and either stayed the same/slightly increased or decreased. The lower percentages started at a low shear stress and increased significantly. An example is the 10% gelatin composition, which went from around 0 to 600 pascals.

The initial tests show a decrease in the 4.5% gelatin slurry pattern. Thus, when viewing the graph with the results of the geltain concentration tests, the 17% gelatin slurry composition follows a similar pattern to the recommended gelatin concentration of the 4.5%. Making it a viable alternative in terms of viscosity and stress. According to the literature, the FRESH support structure should be equal to or exceed 100 Pa, which, in this case, is done as the value is around 120 Pa [68].

Modulus

Examining the modulus of a material is crucial for understanding its mechanical characteristics, particularly the elastic modulus, which serves as a key indicator of a material's stiffness, deformation behaviour, and elasticity. High modulus values signify stiffness, while low values indicate flexibility. This information is vital for selecting materials tailored to specific applications requiring stiffness. Moreover, it is essential for predicting material behaviour under different loading conditions, facilitating the optimal design of components and structures. The modulus serves as a fundamental

parameter guiding material selection, supporting the compatibility of materials in composite structures, and ultimately influencing the overall performance and longevity of engineered systems.

The modulus of a support bath material in FRESH bioprinting is a critical parameter for several reasons. First and foremost, the support bath needs to provide sufficient mechanical support to the printed biomaterial during the bioprinting process. The modulus, which indicates the material's stiffness and elastic properties, influences its ability to uphold the printed structure without deformation or collapse.

A carefully chosen support bath modulus is essential to prevent damage to the delicate printed biomaterial and maintain the structural integrity of the 3D-printed construct. If the support bath is too rigid, it may impose excessive stresses on the printed material, leading to distortion or failure. On the other hand, if the support bath is too soft, it might not effectively hold the printed layers in place.

Additionally, the modulus of the support bath can impact the ease of removal after the bioprinting process. A support material with a suitable modulus facilitates the gentle extraction of the printed structure without causing damage or altering its shape.

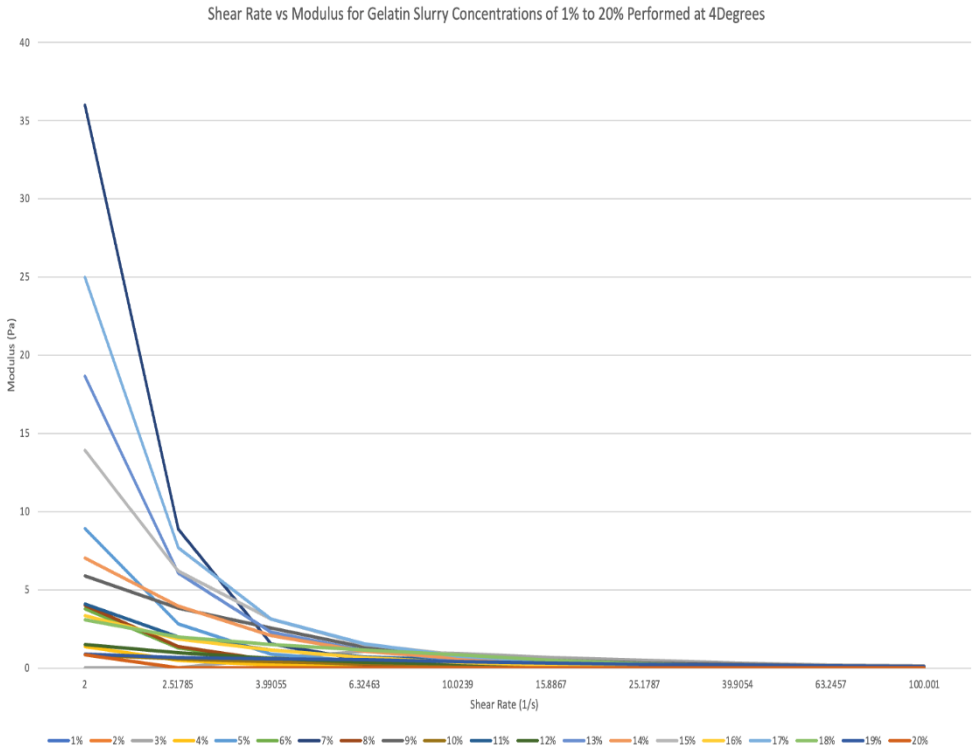

Figure 3.21 Modulus results at 4℃ of the gelatin slurry tested from 1% to 20% gelatin composition.

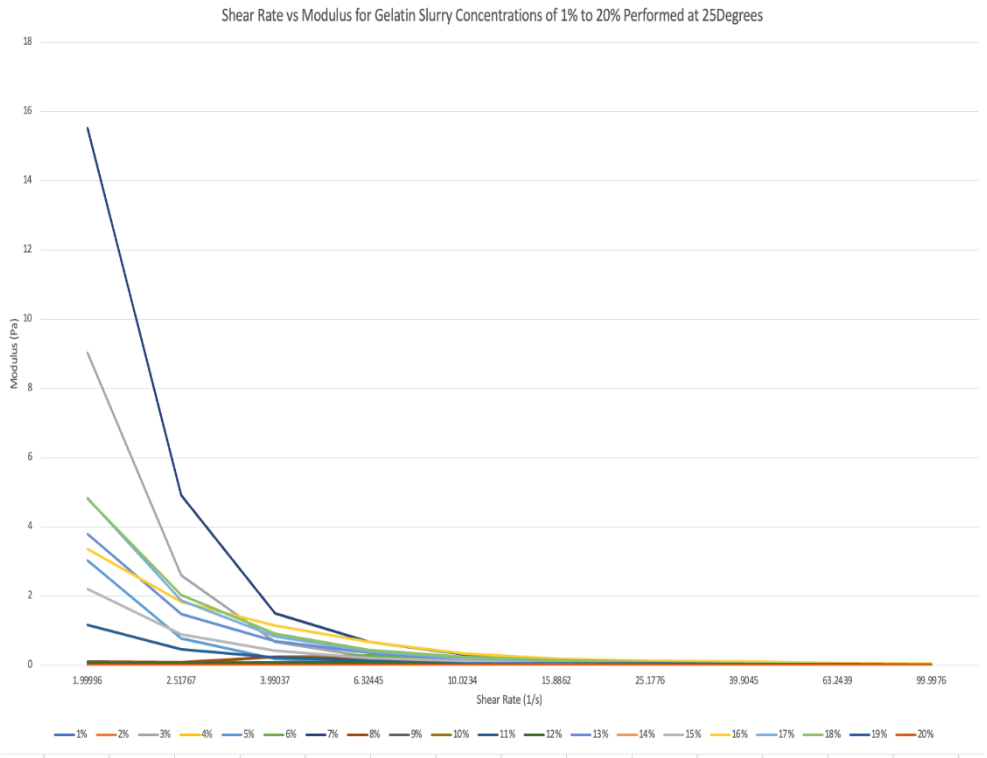

Figure 3.22 Modulus results at 25°C of the gelatin slurry tested from 1% to 20% gelatin composition.

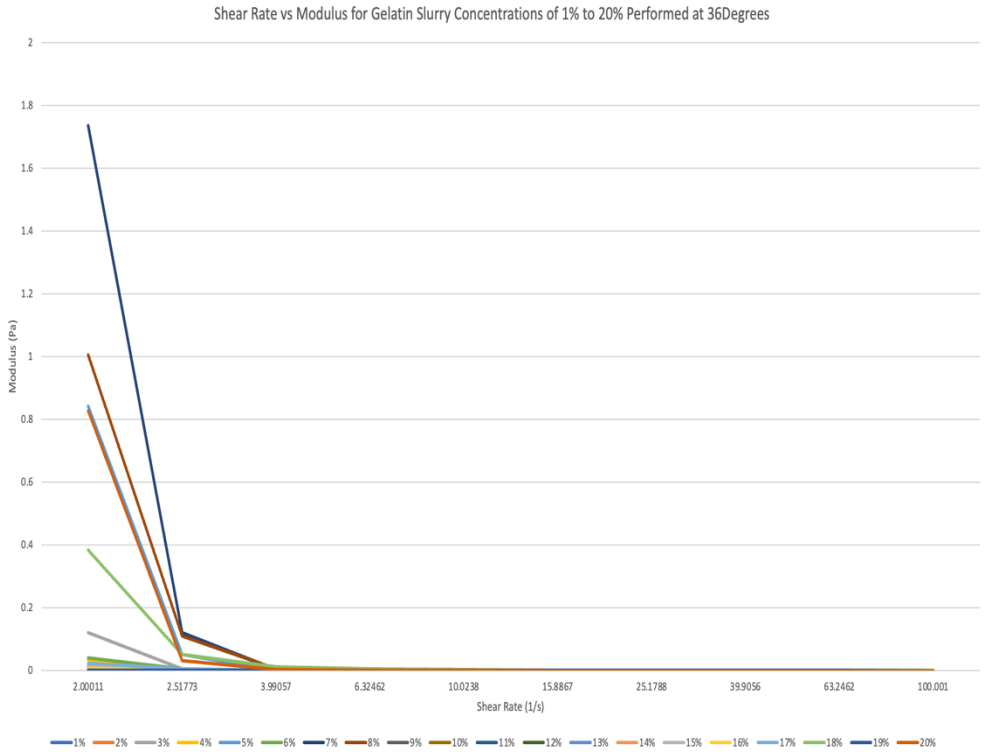

Figure 3.23 Modulus results at 36°C of the gelatin slurry tested from 1% to 20% gelatin composition.

Since the original material composition was not tested for modulus, no real pattern or numerical value comparison is needed. However, the FRESH support bath should stop any overflow from the printed biomaterial and rapidly recover to prevent the biomaterial dispersion. Doing this will ensure that the moving nozzle has no crevasses or air pockets trailing from it [292]. This can be monitored with the stiffness of the support bath, represented by the modulus. Previous studies suggest that the storage modulus G' of the material should be between 5 kPa and 10 kPa to allow suitable support for the low-viscosity biomaterials while allowing the needle to pass through [74, 293, 294]. These numbers seem high compared to the results received from the tests; however, based on a different study suggests that different support baths need different modulus amounts that vary significantly. Based on that study, the modulus can reach low amounts of up to 1 kPa [295]. This means that the modulus in this case is on the lower end but still acceptable for the needed use case.

3.2.1.3 Gelatin Preparation

The above-mentioned study is mainly brought to light when considering the quality control, prevention, and mitigation factors in a microparticle analysis. The importance of quality control is already mentioned above. However, prevention and mitigation are important due to the implementation of measures to prevent or reduce the presence of microparticles in the gelatin slurry. This may include optimizing the gelatin preparation process, using filtered or purified gelatin, and maintaining clean working environments. The preparation process was further explored in the later part of the study.

Different preparation forms were used to stabilize the gelatin slurry particle uniformity further. The different preparation tests were conducted on the 17% (w/v):

- Freeze the material during the gelling process to form a more solid block.
- Instead of pulsing the blender for 120s as the recommended process step, continuous blending was used at high speed for 120s.
- A mix blending approach was used: 60s mixing at high speed and 60s pulsing. For this step different make-up of the same approach was used. For example, pulsing first or second, or 30s blending and 30s pulsing, which was repeated for 120s.

In conclusion, it was seen that none of the different processes affected the results of the microparticles and rheology. Thus, the study concluded that the gelatin slurry cannot be controlled for its microparticle size and distribution. Since the size of the particles was in between too big (damage to the printed material surface) and too small (increased challenge of removability), and the material could hold the shape of delicate structures during printing, it did not require extreme changes for functionality.

3.2.1.4 Results Analysis of the Gelatin Slurry Study

The gelatin slurry cannot be controlled in terms of uniformity, particle sizes and distribution. The different gelatin percentages have similar rheological properties, and an increased percentage can be used for printing. This will cut down on preparation time for printing as larger batches of the support bath can be made using the same amount of

time. Since the creation process for the support bath is lengthy, this option can be very helpful for larger prints, such as the printing of a realistic human heart.

3.3 Material Selection

Material selection is a critical determinant of success in 3D bioprinting. The selected biomaterials must ensure biocompatibility, facilitate the printing process, and mimic the characteristics of natural tissues. The material selection for FRESH bioprinting, in terms of the biomaterial material, is a bit tricky as it has to mimic the organ or tissue it is creating and work with the support bath it is printed into. Selecting an appropriate biomaterial with characteristics such as crosslinking in the support bath is essential for the success of FRESH bioprinting projects. The choice of biomaterial will depend on the specific tissue being printed and the goals of the bioprinting project. Researchers often conduct extensive material characterization and testing to ensure the selected biomaterial meets these criteria.

3.3.1 Characteristics Needed for the Materials for Each of the Heart Wall's Layer

It is crucial to use biomaterials that replicate the mechanical and structural characteristics of native heart tissues when trying to bioprint structures resembling the heart wall's layers. There are three main layers that make up the heart wall: the endocardium, myocardium, and epicardium. To create functional cardiac tissues, it is essential to select the appropriate biomaterial for each layer, as each has unique properties.

3.3.1.1 Endocardium

The endocardium is the heart's innermost layer, made up of a smooth, thin layer of endothelial cells. For this layer, thin biomaterials with blood vessel-like properties are required. For this layer, hydrogels with good compatibility with endothelial cells are appropriate. Low-stiffness biomaterials based on collagen or gelatin can mimic the endocardial layer.

3.3.1.2 Myocardium

The myocardium is the heart's thick, muscular layer that causes contractions. Biomaterials with greater electrical conductivity and stiffness are needed to mimic the contractile properties. Materials that are frequently used are:

- Cardiomyocytes or cardiac stem cells are frequently combined with synthetic and natural materials, like hydrogels, to create engineered cardiac tissues.
- Biomaterials based on fibrin: Blood contains the protein fibrin, which can be used to build a matrix that supports cardiomyocytes. It offers an environment favourable for cell contraction, adhesion, and alignment.
- Conductive substances: Some conductive nanoparticles, such as carbon nanotubes or graphene, are incorporated into biomaterials to mimic the electrical characteristics of the myocardium.

3.3.1.3 Epicardium

The outermost layer of the heart, called the epicardium, is a slender membrane that serves as protection. Thin, flexible biomaterials with characteristics akin to those of the pericardium, the sac that envelops the heart, should be used for this layer. Biomaterials composed of low-stiffness materials or elastin can mimic the epicardial layer.

It is important to remember that careful integration of these various biomaterials is necessary to create a multi-layered structure that faithfully replicates the heart wall. An example of a conventional method would be printing the outer epicardial layer after printing the myocardial layer containing cardiomyocytes and the inner endocardial layer.

The field of cardiac tissue engineering is always changing, and scientists are trying to create increasingly complex biomaterials with characteristics similar to those of the various layers of the heart wall. These developments are essential for applications like disease modelling and cardiac tissue regeneration.

3.3.2 Chosen Materials

After carefully curating the materials based on their cost, biocompatibility, crosslinking capabilities and mimicking the natural tissue, the following three materials were chosen: Alginate, Nanofibre and a Hybrid biomaterial, which contains Alginate and Gelatin.

All three of these materials crosslink with the help of Calcium Chloride, the material found in the gelatin bath. This means the materials can be printed pre-crosslinked, reducing the pressure the printer needs to extrude the material.

The chosen materials were further examined for their pre-crosslinked and post-crosslinked properties to examine their characteristics and understand whether they were the right ones. As well as to test how the different materials react to each other and the gelatin slurry.

3.4 Pre-Crosslinked Biomaterial Material Characterization

The pre-crosslinked materials were tested for their characteristics in terms of viscosity and shear stress to evaluate their performance in terms of printing. For the process of adding cells to the biomaterials, the material needs to have low viscosity and shear stress. Low viscosity is needed for the material to flow easily through the extrusion point without much pressure from the printer. High amounts of pressure can harm the cells during the printing process. The recommended viscosity for the biomaterial is around 10 mPa·s [296]. The soft tissue biomaterials also require a low shear stress rate and an elastic modulus between 1 to 16 kPa, especially in cardiac tissues with notably high blood vessel density.

Figure 3.24 Three pre-crosslinked materials prior to being tested.

3.4.1 Alginate

Alginate was initially tested to determine the proper concentration for printing, which included the viscosity to test the appropriate temperature and percentage without causing harm to cells or increased pressure on the printer. Figure 3.25 shows the viscosity of the 4% biomaterial at different temperatures. It is shown that the higher the temperature is, the less viscous the material becomes. It is also seen that even at the low needed temperature of 4°C, which is the preferred temperature of the gelatin slurry, the material is still in the accepted range for viscosity.

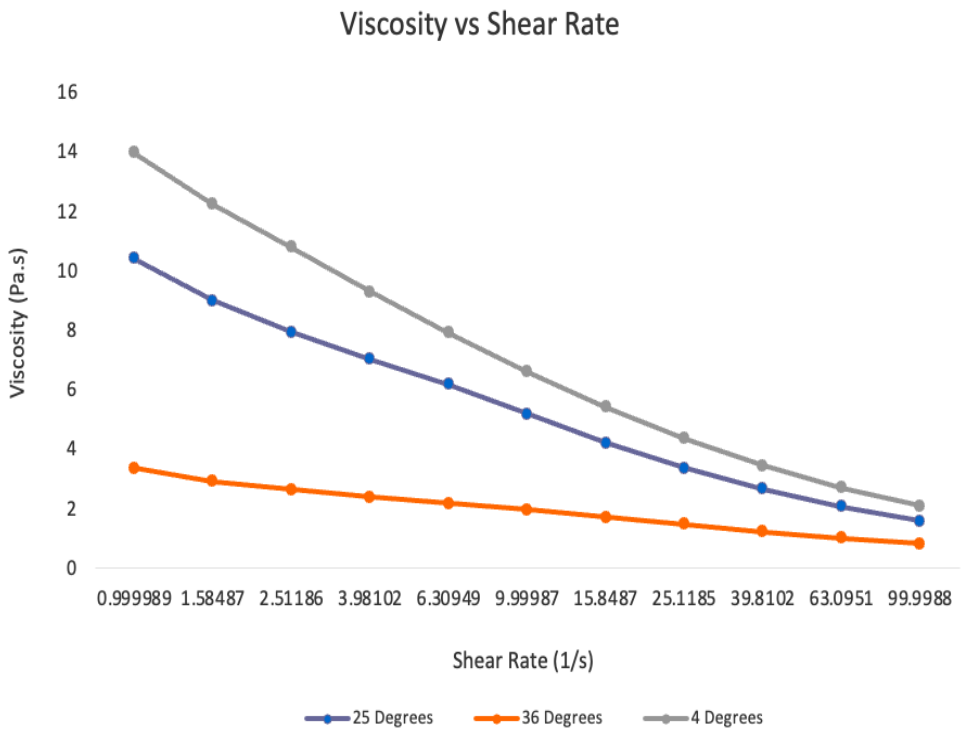

Figure 3.25 The pre-crosslinked alginate when tested for viscosity.

3.4.2 Nanofibre

Nanofibre is the unique biomaterial of the three identified biomaterials, as it is already slightly pre-crosslinked. Thus, it is a bit more viscous to start with than the other materials. It also follows the same pattern as the alginate, where the viscosity decreases as temperature increases. At 36°C, it has a similar viscosity to the alginate at around 3.5 Pa·s. However, at both room temperature and at 4°C, the material has exceeded the recommended viscosity rate by almost double.

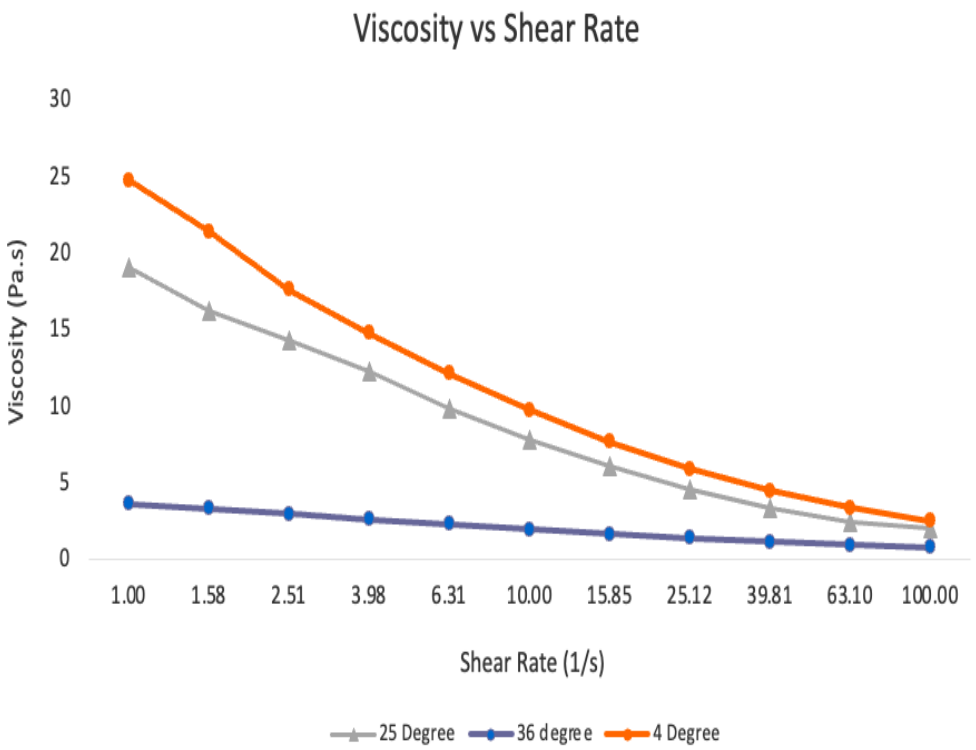

Figure 3.26 The pre-crosslinked Nanofibre when tested for viscosity.

3.4.3 Hybrid Biomaterial (Alginate 2% and Gelatin 2%)

The hybrid biomaterial has low concentrations of alginate and gelatin, making it the least viscous material of the three identified biomaterials. The lowest temperature, which is at 4℃, is at the recommended viscosity. Thus, it is the most successful material for printing at the gelatin slurry temperature. It follows the same viscosity pattern as its proceeding biomaterials and has the same viscosity as alginate at the highest temperature of 36℃.

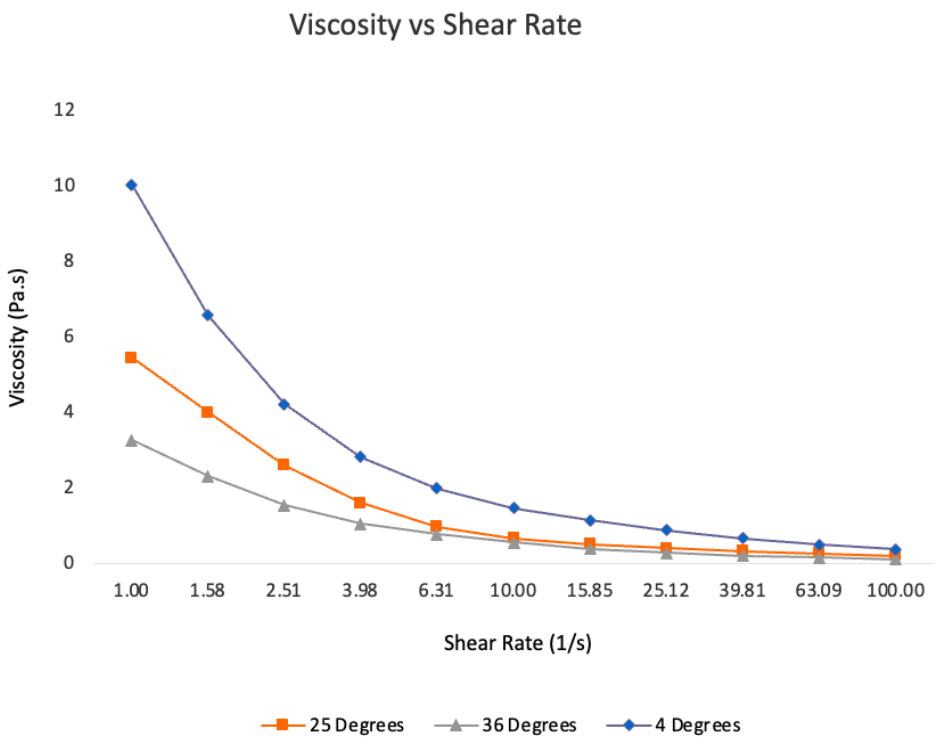

Figure 3.27 The pre-crosslinked hybrid biomaterial when tested for viscosity.

It can be noticed that while all three materials have different viscosity values, they follow the same pattern of viscosity versus temperature. While it would be favourable to print the material at the gelatin slurry temperature, the results show that the nanofibre biomaterial would have too high of viscosity for printing. Based on the results, the best temperature would be to print at 36℃. However, this temperature would melt the gelatin slurry particles needed to hold the material in place while it sets. Thus, the conclusion is that based on the viscosity results of the materials, it is recommended to have all the materials printed at room temperature.

3.4.4 Stress and Modulus

Based on the needed temperature for printing, three biomaterials were also tested for stress and modulus. Figures 3.28 and 3.29 show the results for both stress and modulus of the biomaterials, which were tested at 25℃.

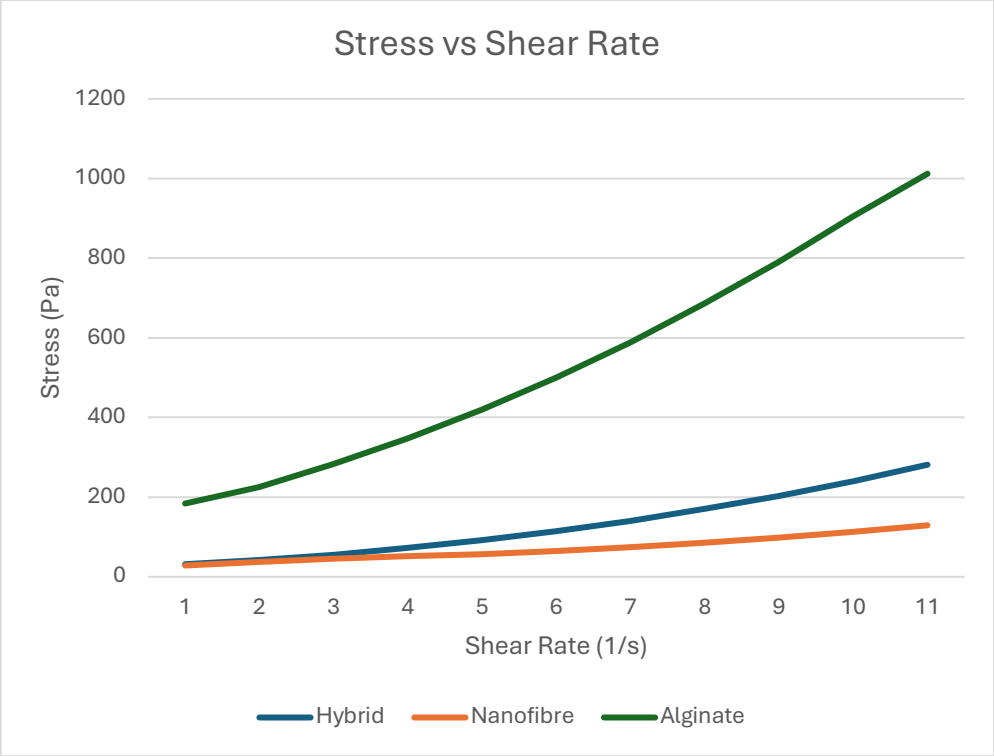

Figure 3.28 The stress results from the pre-crosslinked biomaterials.

The stress of the material needs to be low for the biomaterials. It is seen from the graph that the biomaterials start off at low-stress values, but they all increase with the shear rate.

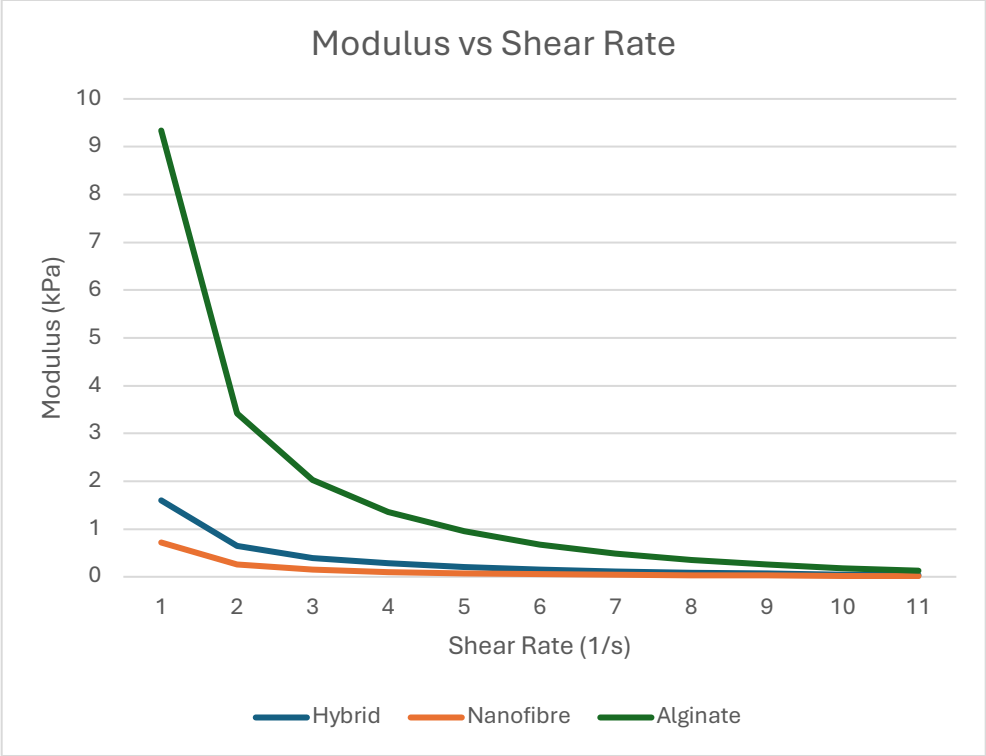

Figure 3.29 The modulus results from the pre-crosslinked biomaterials.

The recommended elastic modulus of the pre-crosslinked biomaterials is between 1 and 16 kPa. This range is chosen to replicate the compliance and elasticity of the heart muscle. Generally, the elastic modulus for cardiac tissues is in the range of 5 to 20 kPa. It is noticed that all three biomaterials fit the recommended range for modulus. However, alginate has the highest modulus, almost five times the amount of the other two materials, making it the most elastic material.

3.5 Post-Crosslinked Material Characterization

It is essential to characterize biomaterials after crosslinking in order to evaluate and comprehend the final characteristics of 3D-printed structures in bioprinting applications. Crosslinking is a frequently employed technique during and after the printing process to stabilize and solidify biomaterials, which are often made of biomaterials like hydrogels or polymers. Researchers frequently choose or create biomaterials with particular mixes of synthetic and natural polymers, cross-linking agents, and other additives to obtain the required mechanical qualities. By optimizing these formulations, mechanical characteristics can be tailored to closely resemble those of the intended tissue, which promotes productive tissue engineering and favourable functional results. For post-crosslinked material characteristics, it is important to look at the stiffness and compression, both depicted by a stress versus strain graph.

The way a material reacts to applied forces is shown graphically by the stress-strain curve. The stress-strain curve sheds light on the mechanical characteristics of post-crosslinked biomaterials when used to 3D print heart tissue. Predicting how the printed cardiac tissue construct will react to mechanical stresses, such as those encountered during

heart contraction and relaxation, requires an understanding of the stress-strain behaviour of post-crosslinked biomaterials. Using this data, scientists may fine-tune biomaterial compositions, cross-linking techniques, and printing conditions to produce mechanical qualities almost resembling real cardiac tissue.

3.5.1 Alginate

Alginate is the most elastic material of the three, based on the results from the pre-crosslinked evaluation. It is predicted that it will be able to withstand the most amount of compression.

(a) (b)

Figure 3.30 Crosslinked alginate tested for its rheological properties: (a) the coupon before tested, and (b) the coupon after a compression test.

Figure 3.31 shows that the alginate was able to withstand about 11 kPa of stress during the compression test. For the stress test, it was only able to withstand roughly 85 Pa.

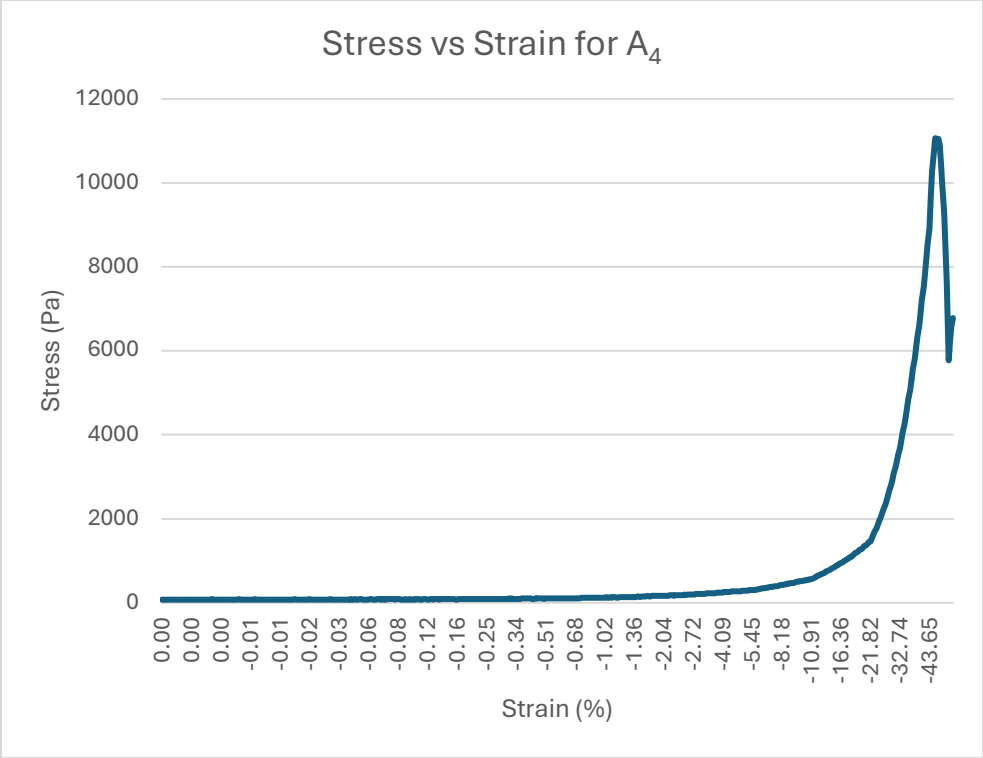

Figure 3.31 The results of the compression test for alginate.

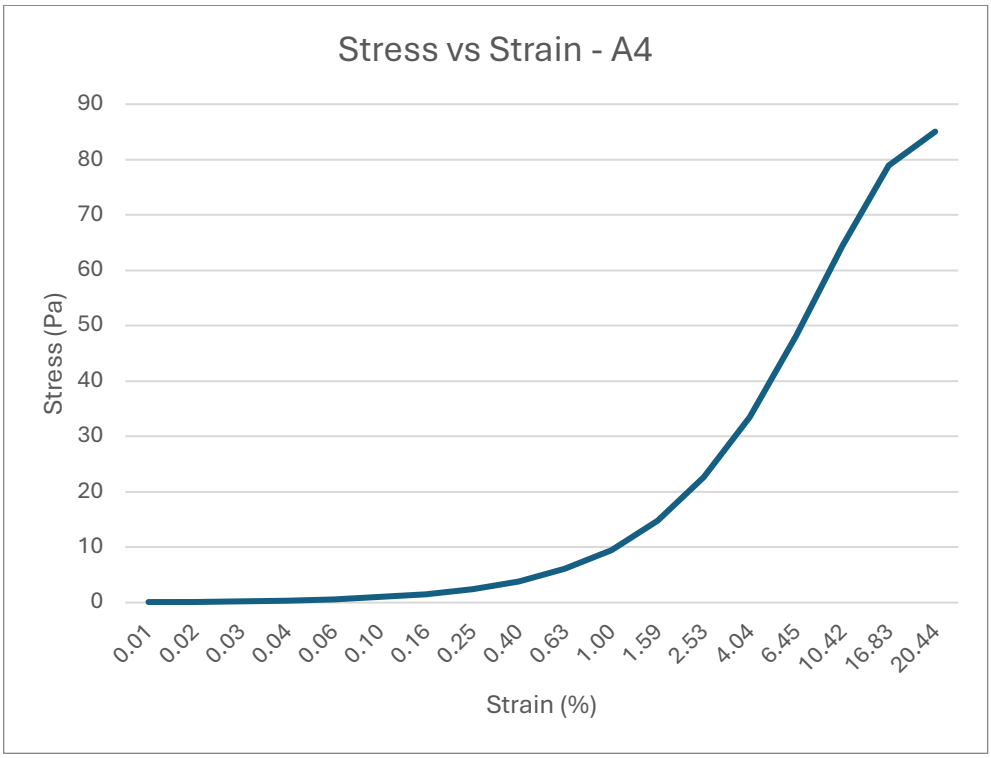

Figure 3.32 The results of the stiffness test for alginate.

3.5.2 Nanofibre

Nanofibre was expected to withstand the most compression from three materials but the least stress. This concept is based upon the fact that nanofibre had the highest viscosity of the three materials in pre-crosslinked form; this constitutes that it is most likely the stiffest material in both pre- and post-crosslinked. In theory, based on that reason, it could hold higher stress when being compressed than when tested for stiffness, where it sends pulsations through the material.

(a) (b)

Figure 3.33 Crosslinked nanofibre tested for its rheological properties: (a) the coupon before tested, and (b) the coupon after a compression test.

The nanofibre was able to withstand around 450 Pa of stress when it was being compressed. The results of the stiffness test shown that it could withstand almost 25 Pa of stress. This is much lower than both the alginate and the hybrid biomaterial. This suggests the opposite of what was expected: instead of the material being able to withstand more stress due to its high viscosity, it actually made it more inclined to rupturing in terms of the amount of stress that can be exerted on the printed material. However, since this material is the myocardium portion of the heart wall, there will not be a large amount of stress exerted onto this material specifically as it is encapsulated and protected by the two more elastic materials.

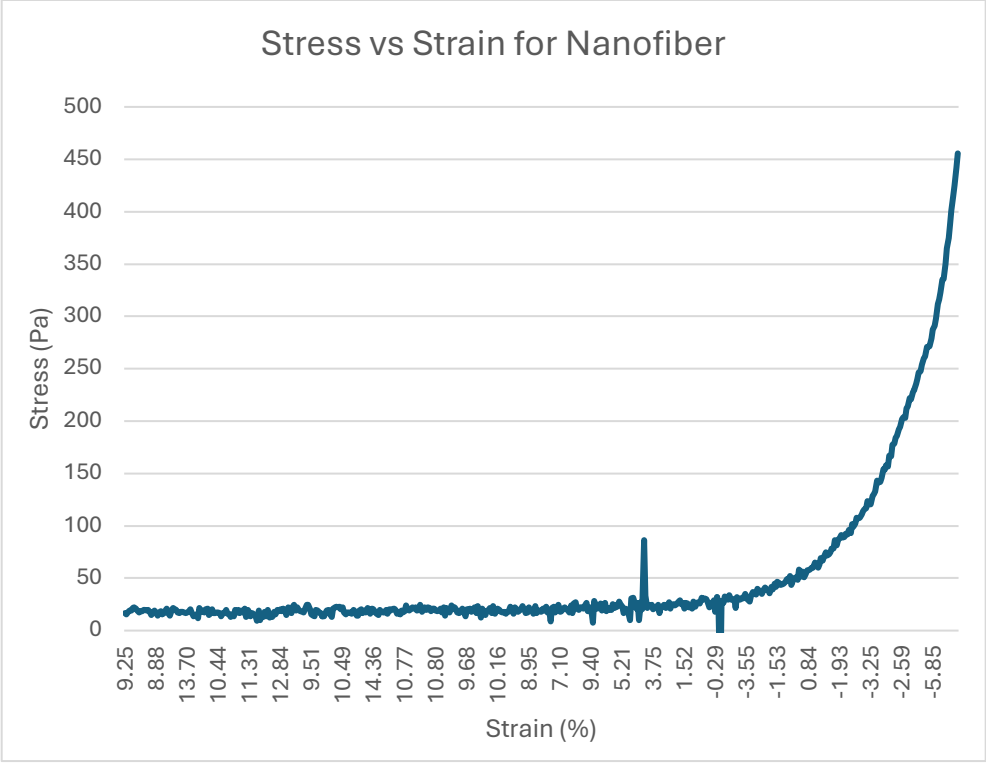

Figure 3.34 The results of the compression test for nanofiber.

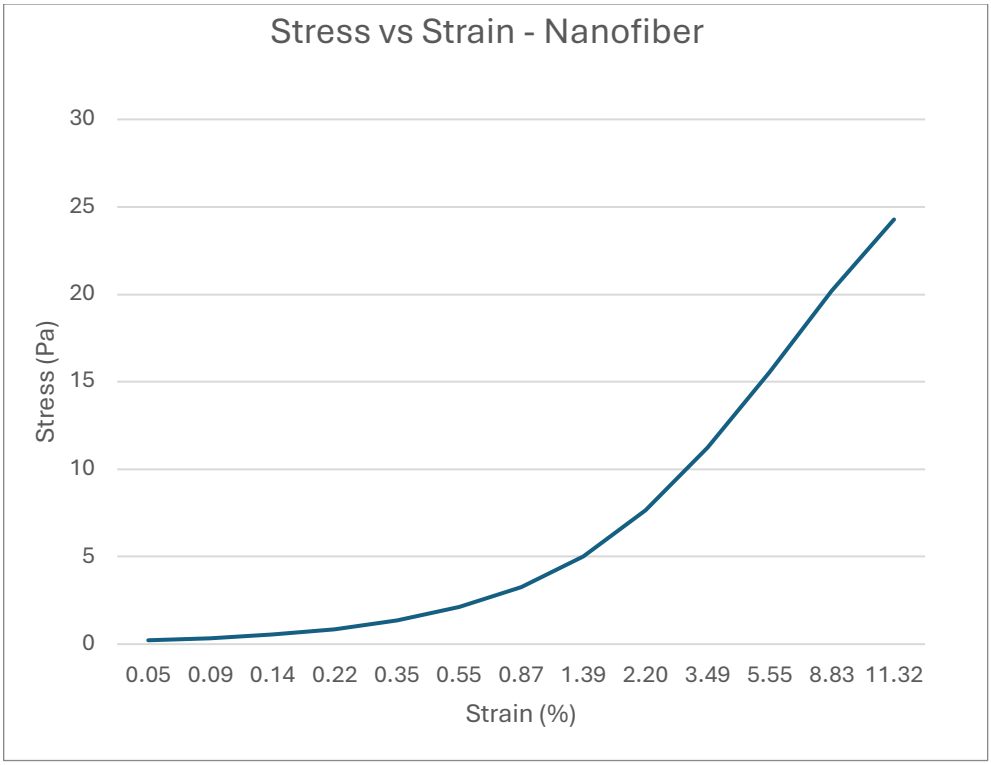

Figure 3.35 The results of the stiffness test for nanofiber.

3.5.3 Hybrid Biomaterial (Alginate 2% and Gelatin 2%)

Based on the results from both alginate and nanofibre, it was expected that the hybrid biomaterial would have similar results. Originally, the idea was that the material's low viscosity would not withstand as much force as the other two materials, especially compared to nanofibre. However, the results from nanofibre being much lower than that of the alginate predicted how the material would behave a bit harder.

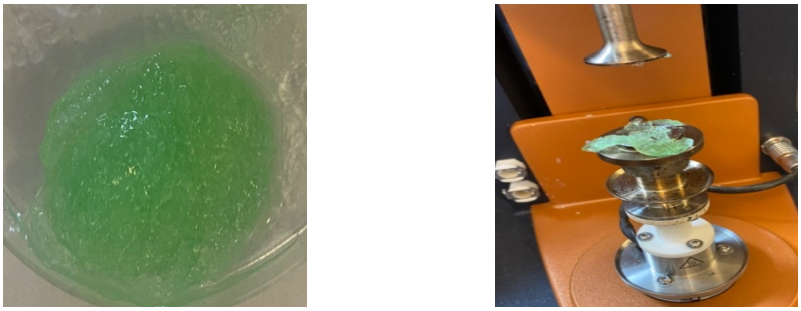

(a) (b)

Figure 3.36 Crosslinked hybrid biomaterial tested for its rheological properties: (a) the coupon before tested, and (b) the coupon after a compression test.

The results of the tests shown that the hybrid biomaterial was able to withstand a little bit over 8000 Pa of stress when tested for stiffness and about 60 Pa when tested for compression. It seemed to show that this material can withstand more stress than the nanofibre biomaterial but less than the alginate.

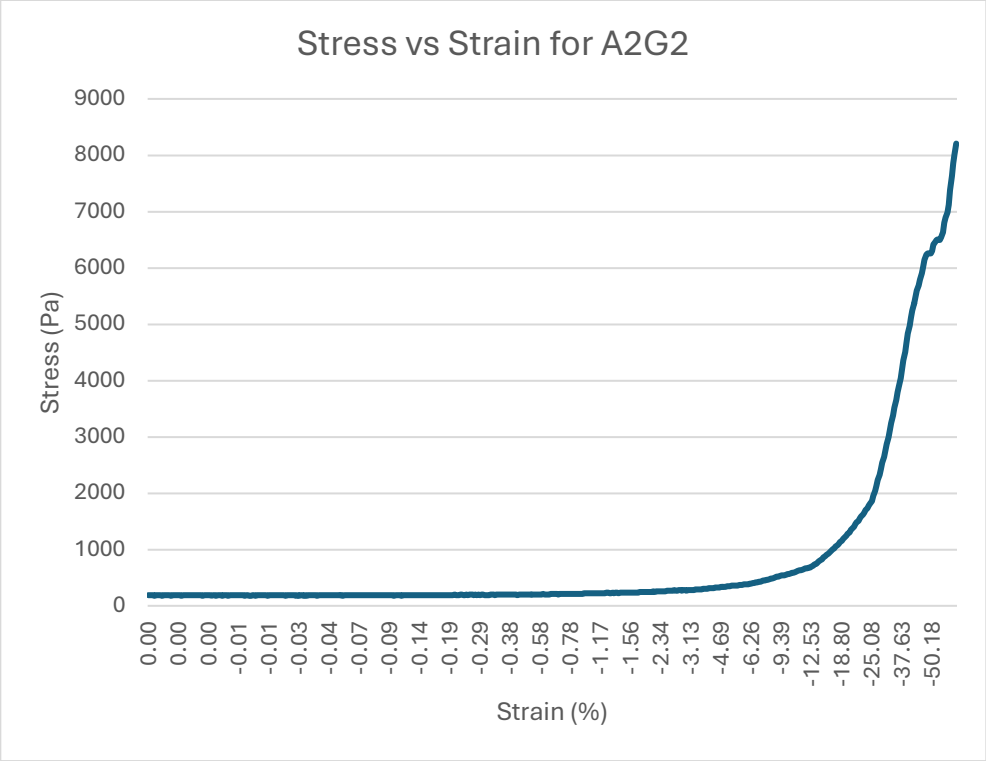

Figure 3.37 The results of the stiffness test for hybrid alginate-gelatin.

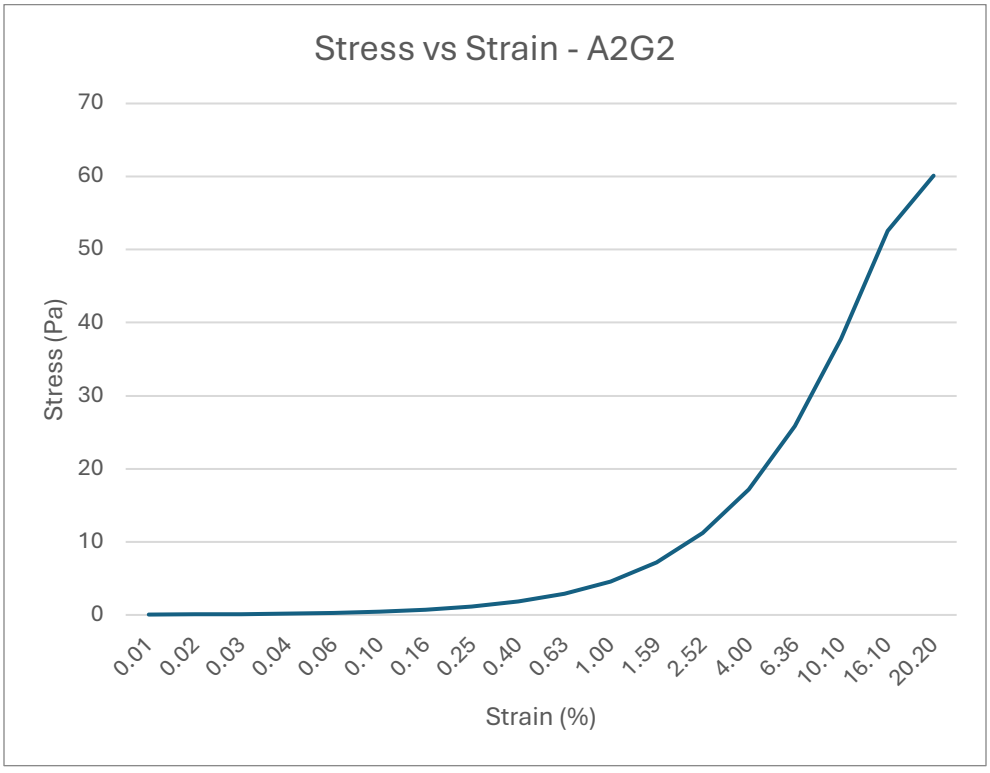

Figure 3.38 The results of the stiffness test for hybrid alginate-gelatin.

3.6 L-Shape Test

An L-shape test was conducted on the three biomaterial materials printed in air, water, and gelatin slurry to examine their resulting prints. This test was important in validating the need for the support bath.

The reason for the L shape came from the idea of structural integrity. The L shape will not appear in the final print if the material collapses. This is different than if a simple wall structure was used, which would still appear as the intended shape but in the wider proportion.

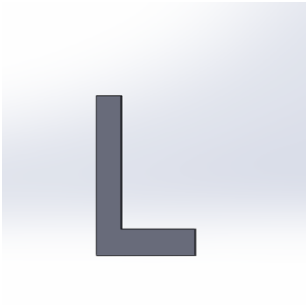

Figure 3.39 CAD model of the L-shape test.

3.6.1 Alginate

Alginate is expected to hold the printed shape slightly. It has a low viscosity, which will cause deformation to the printed structure without crosslinking or a supportive material; thus, why it is predicted that printing in either water or air will not result in the proper structure, unlike when it is printed with gelatin slurry as a support base.

3.6.1.1 Air

The first element that alginate was printed in was air. The material followed the required structure in terms of the L shape. Even once the print was done and the dish was removed, the L shape was prominent in the printed structure. However, the more the dish sat without adding the crosslinking agent, the more the material expanded and deteriorated, losing its intended printing shape. Figure 3.41 shows the printing results of when the material was originally removed from the printer as it completed printing.

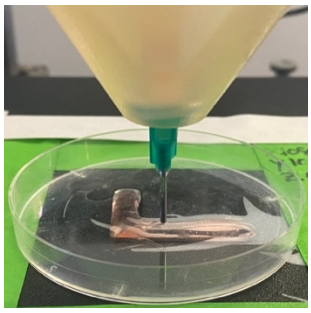

Figure 3.40 Printing of the L-shape in air using Alginate.

Figure 3.41 Printed results of the L-shape in air for Alginate.

3.6.1.2 Water

The following material that alginate was tested for in terms of base material for printing was water. In theory, water has a more significant density than air, making it a more acceptable base material, as it should hold the structure's shape more than the air. However, it would not be able to support the printing material because it does not have pronounced particles but rather a fluid base.

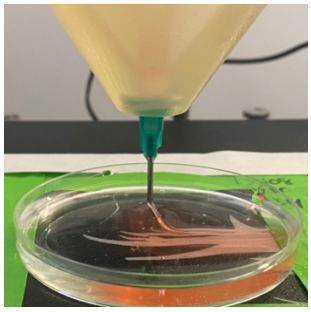

Figure 3.42 Printing of the L-shape in water using Alginate.

It is seen from Figure 3.43 that while the L shape is noticeable for the printed structure, it seems that the biomaterial is melting into the water. Thus, the printed shape is being washed out, causing a thinning of the material, creating an almost halo on the printed structure.

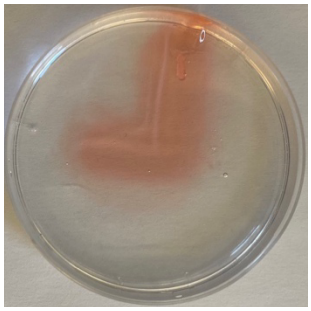

Figure 3.43 Printed results of the L-shape in water for Alginate.

5.6.1.3 Gelatin Slurry

The last material the alginate was printed in was the gelatin slurry. The use of gelatin slurry as the base material is expected to hold its desired shape and have a height higher than both water and air for the printed structure.

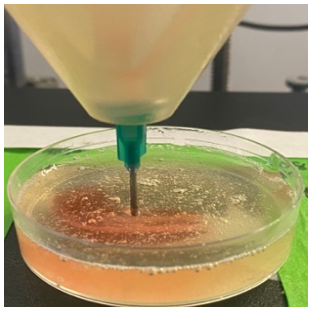

Figure 3.44 Printing of the L-shape in gelatin slurry using Alginate.

The results shown close to the expected outcome. The L shape was prominent in the printed structure, and there was no halo around it as with the water. The gelatin slurry particles also suspended the alginate, which created more layers, making it the tallest-standing structure of the three base materials. However, due to the calcium in the gelatin slurry, the printed structure started to swell and crosslink, making it a bit thicker than the main structure. This difference can be seen between Figure 3.41 and Figure 3.45.

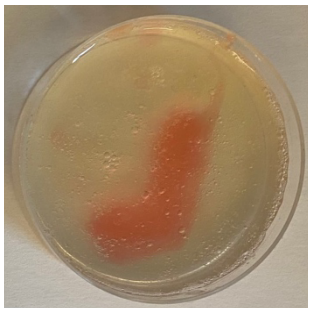

Figure 3.45 Printed results of the L-shape in gelatin slurry for Alginate.

3.6.2 Nanofibre

The following material that was tested for the three different base elements was nanofibre. Nanofibre is different from the other two materials because it is already semi-crosslinked. For this reason, the material is expected to hold the desired shape under all circumstances.

3.6.2.1 Air

Nanofibre is the most desirable material for printing in the air. It has a low viscosity, which allows it to hold up its own shape under all circumstances. Figure 3.47 shows that the L shape, which was printed with the nanofibre, was prominent and had the same height as the alginate printed in gelatin slurry. This proves that the nanofibre may not need a base material for printing complex and delicate shapes.

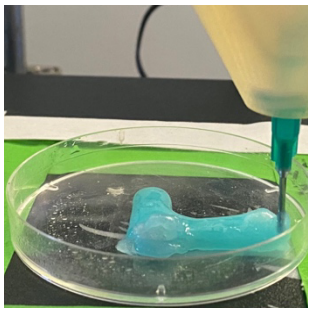

Figure 3.46 Printing of the L-shape in air using Nanofibre.

Figure 3.47 Printed results of the L-shape in air for Nanofibre.

3.6.2.2 Water

The gelatin slurry was tested for its printing properties in water. It had similar results to the alginate in terms of slightly dispersing material. Alginate resulted in a halo; the nanofibre shown more floating biomaterial strands, as shown in Figure 3.48.

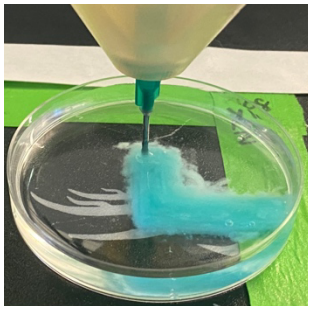

Figure 3.48 Printing of the L-shape in water using Nanofibre.

Nonetheless, the water seemed to help level the biomaterial slightly, creating a perfect L shape, which is visible in Figure 3.49. The water created straight lines and edges compared to the printed structure in the air, which seemed to lose the straight edges. However, there is a slight halo around the finished product. It is not as prominent as with the alginate, but it is detectable around the edges. In conclusion, the water assisted the material in forming straight edges and letting the material level itself out, resulting in an identical shape that was desired.

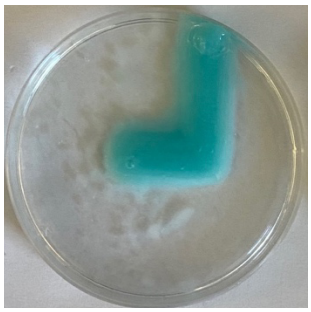

Figure 3.49 Printed results of the L-shape in water for Nanofibre.

3.6.2.3 Gelatin Slurry

The gelatin slurry was the last material tested as a base for the nanofibre biomaterial. Since the material does not need as much support as its other biomaterial counterparts, the expected results should be similar to the water but with cleaner edges in terms of the halo not appearing around the parameters.

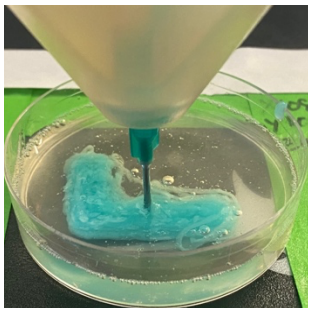

Figure 3.50 Printing of the L-shape in gelatin slurry using Nanofibre.

Figure 3.50 shows the printing process of the nanofibre in the gelatin slurry. Due to the gelatin slurry particles, any material strand that did not stick to the underneath layer floated in the slurry, which did not result in the exact shape. However, Figure 3.51 shows that while those strands are slightly visible, the shape and the edges of the L shape are exactly as designed. It does not look as perfect as in the water, as the density of the gelatin slurry is higher, which does not allow the material to level out as it did in the water. Overall, it can be concluded that the nanofibre does not need a base material for printing; however, adding a base material helps make the shape more prominent. It gave similar results as the alginate in terms of height and structure, but surprisingly, the nanofibre results of being printed in the water were unexpected. It seems that the dense material needs a less dense base to allow the material layers to even out in between additional layers being added.

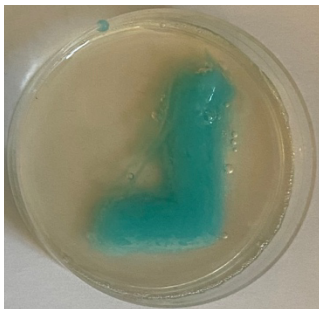

Figure 3.51 Printed results of the L-shape in gelatin slurry for Nanofibre.

3.6.3 Hybrid Biomaterial

The final biomaterial tested for different base materials was the hybrid biomaterial of 2% alginate and 2% gelatin. This material had the lowest viscosity, predicting that it would not be able to hold up its shape in either air or water. It will follow a similar pattern to alginate.

3.6.3.1 Air

Following the routine from the other two materials, the hybrid biomaterial was first tested in the air to see the printed results. Before reaching the final print, it was noticed that the material started to lose its shape and flatten out. It did not possess any of the needed characteristics of the L shape. The results resembled more of a bean shape than an L. This material is too thin to print without crosslinking between layers or support material. However, this was expected when looking at the pre-crosslinked material test results.

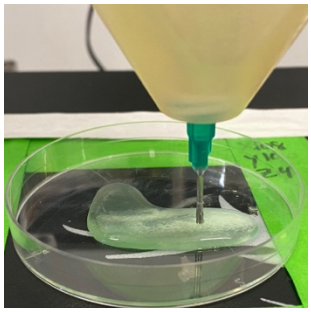

Figure 3.52 Printing of the L-shape in the air using the hybrid biomaterial.

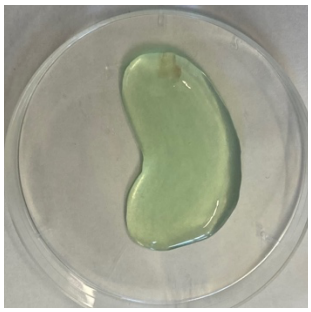

Figure 3.53 Printed results of the L-shape in the air for Hybrid biomaterial.

3.6.3.2 Water

The second material used as a support material was water. The expected result was to see something similar to the results of alginate in water. This means the L shape is visible with a washed-out halo around the edges.

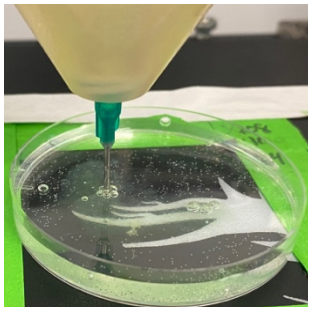

Figure 3.54 Printing of the L-shape in water using the Hybrid biomaterial.

The expected results did not match the finished print for this material. While the L shape is slightly visible, it is really hard to see the expected shape without knowing it. The water completely washed out the biomaterial, where it expanded in size, and the colour lightened to a very faint green. It is hard to tell if the results are better than the air as the L shape looks more prominent, but it is also hard to recognize in the dish.

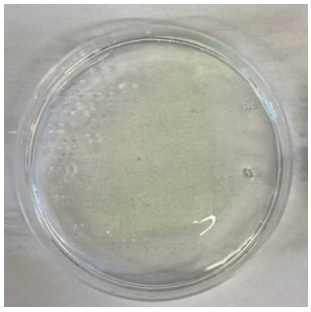

Figure 3.55 Printed results of the L-shape in water for hybrid biomaterial.

3.6.3.3 Gelatin Slurry

The final material for hybrid biomaterial testing was the gelatin slurry. The predicted results were that the gelatin slurry would hold up the material and allow it to build upward, where a visible L shape would occur, similar to both prior materials. However, with the results in water and air being different than the alginate, it is hard to predict what the final structure, which is printed in the gelatin slurry base, will look like.

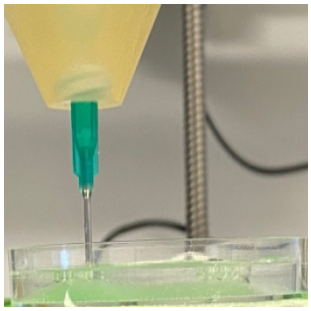

Figure 3.56 Printing of the L-shape in gelatin slurry using the hybrid biomaterial.

Once the print was finished and the dish was removed, the result shown a perfect L shape, as seen in the figure below. The hybrid biomaterial seems to need assistance from a high-viscosity material as a base to create the desired shape.

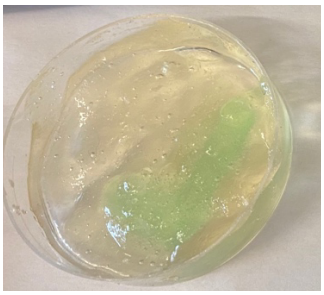

Figure 3.57 Printed results of the L-shape in gelatin slurry for hybrid biomaterial.

3.6.4 Conclusion on Base Material Selection

In conclusion, all three materials shown better structural integrity when printed into the gelatin slurry. The following table combines all the materials and their different printed results within the materials they were printed into.

Table 3.2 Results of the biomaterials printed in different mediums.

Mediums	Air	Water	Gelatin slurry

Alginate	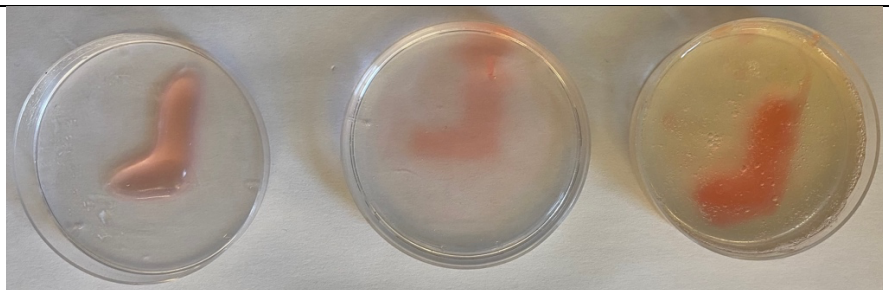
Nanofibre	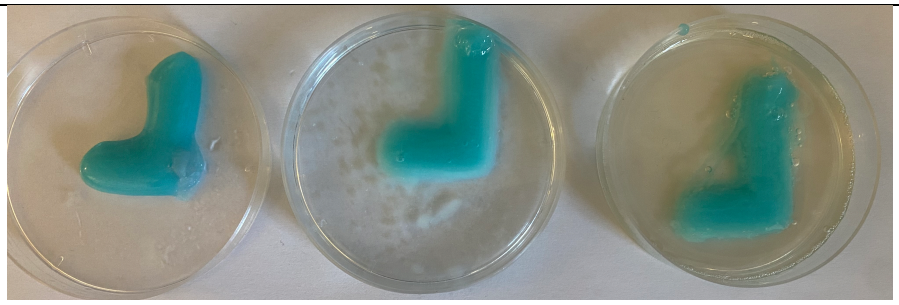
Hybrid	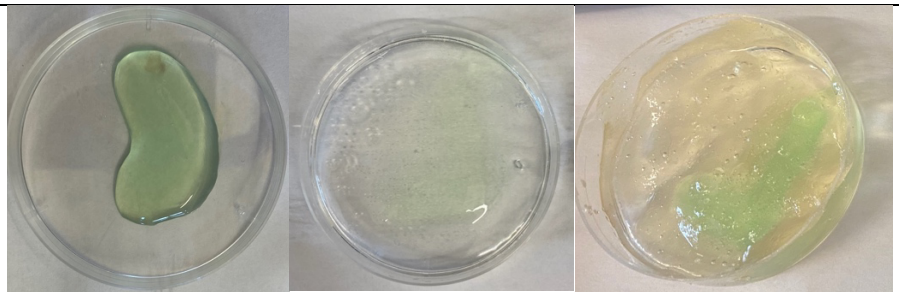

Overall, the nanofibre biomaterial held its shape the best in all three mediums. This was an expected outcome as the material was semi-crosslinked prior to printing. It can hold its shape during the printing process. However, there can be clearly seen a variance in the results for the material as even though all three forms show an L shape, it is most prominent in the gelatin slurry.

The hybrid biomaterial possesses the lowest viscosity and struggles to hold its shape without support. It can be seen that when printed in the air, it did not hold the structure but instead expanded, creating a non-recognizable chape. Then, when printed in water, the material almost disappeared. Finally, in the gelatin slurry, the material could construct a recognizable L-shape. This test proves the necessity of the gelatin slurry support bath for bioprinting. It can support the creation of structures for all materials, allowing the printing of delicate and complex structures.

3.7 Printed Material Weight Analysis

FRESH bioprinting is great for many reasons, especially for printing shapes and structures that were impossible before. However, when a hydrogel is printed in an aqueous culture media, such as the gelatin slurry, it has a tendency to increase in volume with the uptake of the fluid. There are multiple variations of this material swelling, but for FRESH bioprinting, it can be referred to as a polymer-solvent interaction [297]. The polymer-solvent interactions are important for material chemistry, volume fraction, and swelling behaviour, all affecting water intake [298].

Some of the reasons for this phenomenon. First is the hydrogel properties. Post-print swelling is largely determined by the intrinsic characteristics of the hydrogel used as the biomaterial. Hydrogels have the ability to expand when they take in water from the support bath. The osmotic pressure also plays a role. This fundamental concept refers to the movements of fluids passing through cell membranes. It is described as the pressure created when solvent molecules, usually water, move through a semipermeable membrane from a region with a lower solute concentration to one with a higher solute concentration. The printed material may absorb water due to variations in the osmotic pressure between the hydrogel and the support bath. Another factor could be the solvents in the support bath may diffuse into the printed hydrogel and cause it to swell, depending on the composition of the bath. The last factor that could cause the material to swell is the cross-linking degree, which is the extent to which a hydrogel can crosslink with the added material, which affects its ability to retain water.

Some implications from this swelling are dimensional changes, structural stability and cell viability. Excessive swelling can lead to mechanical stress on encapsulated cells, potentially affecting their viability and functionality. A coupon was printed using the alginate biomaterial to test the swelling capacity of the printed material. The coupon was tested when it was first printed and then every hour after that until the material reached a stable weight.

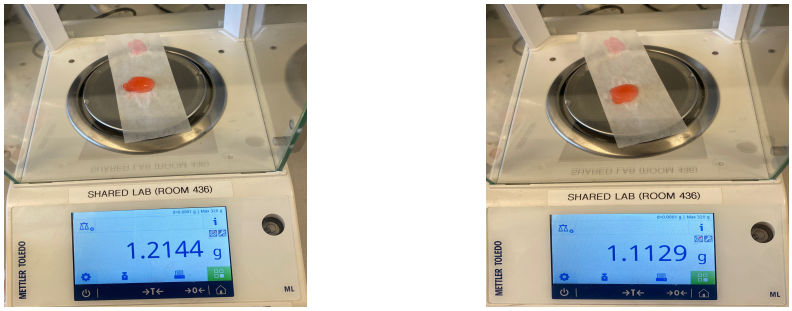

(a) (b)

Figure 3.58 The printed coupon as it was : (a) removed from the gelatin slurry, and (b) an hour later.

In the figure above, it can be seen that the starting weight of the material was roughly 1.2 grams. The results shown that the material decreased by about 0.1 grams every hour until it reached 0.28 grams. Alluding to the fact that almost 1 gram from the original printed material was liquid weight. The study was completed by allowing the material to sit in the air. However, if the material was in a closed specimen bag and left either in the fridge or at room temperature, it did not lose weight over time. The sealing of the product is really important for holding the initial structural integrity and water weight.

3.8 Conclusion

First, I undertook a thorough investigation to assess the characteristics of diverse biomaterials both before and after undergoing crosslinking, a pivotal stage in the bioprinting process due to their multifaceted impact on the development and application of bioprinted constructs. Firstly, thorough characterization ensures the biocompatibility of materials, guaranteeing that they do not provoke adverse immune responses or toxic reactions when introduced into living systems. By understanding how materials interact with biological environments, researchers can select suitable

candidates for bioprinting applications, thereby enhancing the safety and efficacy of bioprinted constructs. Moreover, the mechanical properties of bioprinted materials are critical for replicating the structural integrity and functionality of native tissues. Through characterization, researchers can assess parameters such as stiffness, elasticity, and tensile strength, tailoring material formulations to match the mechanical properties of target tissues. This ensures that bioprinted constructs can withstand physiological forces and maintain their structural integrity over time, facilitating successful tissue regeneration and integration. Additionally, material characterization informs the printability of materials, determining their suitability for use in specific bioprinting techniques and platforms. Rheological properties such as viscosity and shear thinning behaviour are essential considerations for achieving precise deposition and spatial resolution in bioprinted constructs. By evaluating these properties, researchers can optimize printing parameters and select materials that exhibit favourable extrusion behaviour, thus enhancing the fidelity and reproducibility of bioprinted structures. Furthermore, material characterization facilitates the functionalization of bioprinted constructs with bioactive molecules or growth factors, improving their capacity to promote cell adhesion, proliferation, and differentiation. By assessing the compatibility of materials with biomolecular cargoes, researchers can optimize delivery strategies and enhance the bioactivity of bioprinted constructs, thereby augmenting their therapeutic potential in regenerative medicine applications.

This analysis sought to comprehend the behaviour of these materials and the alterations in their traits post-crosslinking, which is crucial for successful bioprinting. By scrutinizing parameters such as shear stress, compressional stress, biocompatibility, and elastic modulus, I gained valuable insights into the appropriateness of each material for emulating specific layers of heart tissue. The findings of these analyses were utilized to align each biomaterial with the heart tissue layer it could most effectively replicate. The studies indicated that the nanofiber bioink closely resembled the characteristics of muscular tissue, making it an ideal candidate for replicating the myocardium layer. Its structural similarity to natural muscle tissue, combined with its mechanical properties like elasticity and tensile strength, render it well-suited for mimicking the contractile function of the myocardium. Moreover, the hybrid bioink, comprising alginate and gelatin, was chosen to emulate the endocardium segment of the heart wall. Gelatin, a component of the hybrid bioink, has been recognized for its ability to enhance cell retention rates, biodegradability and elastic properties, making it suitable for mimicking the compliant nature of the endocardium, which experiences stretching and deformation during the cardiac cycle. Lastly, the 4% alginate bioink was selected to represent the epicardium layer of the heart wall. Alginate's known biocompatibility and capacity to form stable hydrogels make it suitable for encapsulating cells and providing structural support. The 4% concentration of alginate was identified as the optimal choice for replicating the mechanical properties of the epicardium, which serves as the heart's outermost protective layer. This meticulous matching process ensures that the chosen biomaterials accurately mimic the distinct properties of each heart tissue layer. By selecting biomaterials that closely resemble native tissue characteristics, researchers can enhance the functionality and compatibility of bioprinted constructs, advancing the development of bioengineered heart tissues for applications in regenerative medicine and disease modelling.

3.8.1 Limitations

Various materials were investigated for use in bioprinting with the aim of identifying the optimal material for printing the cardiac wall, with consideration of the cost of materials in order to provide broader accessibility in organ printing for transplant purposes. The three materials identified due to their similar characteristics and mass creation possibilities were alginate 4%, 2% alginate and 2% gelatin hybrid biomaterial, and nanofibre.

Alginate biomaterial, while widely used in bioprinting due to its biocompatibility and gelation properties, has certain limitations. One significant drawback is its poor cell adhesion and mechanical stability, leading to low cell viability and limited structural integrity of printed constructs. Additionally, alginate lacks inherent bioactive cues necessary for promoting cell proliferation and differentiation, necessitating the incorporation of additional bioactive components. Also, when it comes to the alginate percentage in the biomaterial, lower percentages allow for easier printing due to their low viscosity; however, they do not have structural stability when printed outside of a support material. Higher percentages have better structural stability when printed, but due to their high viscosity, the pressure in the printing process increases, possibly harming the cells. For this reason, a 4% alginate solution, which is a middle-ground biomaterial, was used in terms of viscosity and structural integrity.

Similarly, alginate-gelatin biomaterial mixes attempt to address the imitations that alginate possesses by combining alginate's printability with gelatin's cell adhesion properties. However, achieving optimal ratios to balance printability, mechanical strength, and cell compatibility remains a challenge. Furthermore, gelatin's susceptibility to enzymatic degradation may compromise the long-term stability and functionality of printed constructs. Also, the low percentage material mix allows for easy printing as it has low viscosity, but similarly to alginate, it has low structural integrity while printing.

Lastly, Nanofiber biomaterials offer promising opportunities for enhancing mechanical properties and mimicking the natural extracellular matrix. Nevertheless, challenges persist in precisely controlling fibre alignment, diameter, and dispersion within the biomaterial, affecting printability and cell behaviour. Additionally, the scalability and reproducibility of nanofiber fabrication techniques present practical limitations that need to be addressed for widespread adoption in bioprinting applications. Nanofiber is also a high viscous biomaterial, which means that it had to be heated to 36℃ before printing to decrease the viscosity enough to print without problems in the printer as well as to create cell safety procedures by reducing the pressure outputted during printing.

Overall, all materials seemed to either lack structural integrity or have high viscosity, which increases the pressure needed for the printer to extrude the materials, causing harm to cells. In the case of the studies completed in this thesis, they were managed according to their limitations to allow for the necessary outcomes. However, when it comes to mass organ bioprinting, the materials may need to be fine-tuned for better-printed outcomes and cell retention.

3.8.2 Future Work

There is always the possibility of further improving the biomaterials to more closely resemble the cardiac wall layer characteristics. The current materials were chosen for the idea of mass organ printing, where low-cost materials are needed to complement the high costs of patient cell harvesting for personalized organ printing. Personalization is vital

for organ transplants to ensure that the patient's immune system does not reject the foreign organ. However, when price is not considered, new hybrid materials could be created that have similar characteristics but higher cell viability. The viscosity of the materials could also be optimized for easier printing to ensure a better cell survival rate and decreased internal pressure of the bioprinter. Furthermore, depending on the structure of the desired print, there could be materials explored as support materials in addition to the support bath to ensure the structure keeps the intended structure parameters. For example, Pluronic F-127 was slightly explored as an additional material due to its temperature characteristics of being liquid at low temperatures and gel-like at higher temperatures. While the material was not further explored in this study, it shown excellent capabilities for future researchers.

Chapter 4 Printer Design and Adaptation

Summary: This chapter focuses on the changes made to the printer to allow for the printing of multiple materials using the FRESH bioprinting method. The chapter also explores characteristics of what a printer should have for desirability and function for bioprinting purposes.

4.1 Introduction

The quality of the printed structure is only as good as the bioprinter. For this reason it is important to use the bioprinter which works best with the chosen printing method. For the case of FRESH bioprinting, there isn't a specific printer that can be used as it can be integrated with all bioprinters. However, printing multiple materials is a challenge especially using FRESH bioprinting due to the constant calibration need and the ease of changing printing parameters. Each time a new print size would be implemented, it has a new base dish for the support material which changes the printing axis and how the material gets switched. The focus in this chapter will be on solving the calibration which would be needed when there are material changes. This is done by designing a print head that can hold three materials at a time and can print them right after one another without the need for the printhead to leave the print site.

4.2 Print Head Design Process

A key component of bioprinting technology, the print head's design is essential to successfully creating intricate tissue architectures. Various factors must be considered during the design process, such as material selection, nozzle shape, and the biomaterial dispensing mechanism. Achieving the fine resolution required for bioprinting while guaranteeing the gentle handling of sensitive biological materials is one of the main problems in print head design. The precision and resolution of the printed constructions depend highly on the nozzle diameter and shape selection. To enable the printing of various tissue types, the print head must also be compatible with a wide variety of biomaterials, each of which has distinct rheological properties.

In order to regulate the deposition of biomaterial with high accuracy and repeatability, the dispensing mechanism must be optimized as part of the design process. Different levels of control over droplet size, velocity, and location are available with different dispensing technologies, including mechanical, piezoelectric, and pneumatic systems. Furthermore, scalability, ease of maintenance, and connection with other bioprinter components are critical design considerations. Improvements in print head design are essential for opening up new avenues in tissue engineering and regenerative medicine as bioprinting technology develops.

4.2.1 First Printhead Design

The printhead design was based on having three different materials printed out of a single merger point. This would allow the printing of multiple materials to be completed in one printing process rather than through a stop-and-change mechanism. The reason behind this is to eliminate any errors through calibration that could arise from switching the printhead and resuming the printing process.

Printing multiple materials back-to-back also allows the printing of organs such as the heart wall. Depositing the layers with the different biomaterials back-to-back also creates a mixed layer where the two materials merge. This phenomenon leads to better bonding between the layers as they are not separated and connected by different materials but instead transition from the base material to the next material.

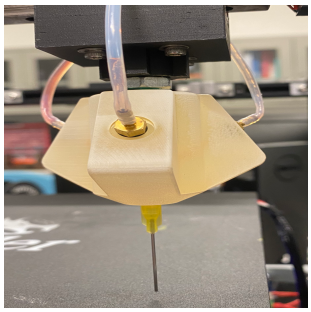

Figure 4.1 The first printhead design.

The first print head was printed with regular PBS filament and examined before moving to resin printing, which created the initial print head which was used for experiments. The high-resolution resin printer was chosen for creating the printhead due to its smooth finished surface, availability in terms of in-house fabrication and, lastly, because the material was clear enough to show if there were any leftover materials after the post-printing cleaning process. Since cell safety is the main concern when considering bioprinting, a see-through material was needed to ensure no material or contamination within printing batches. The resin material can easily be cleaned between printing processes. A monthly deep cleaning can also be done using an ultrasonic bath to release all clogs or material residue if there are any stuck in the chambers.

Figure 4.2 The broken syringe and syringe holder resulted from the pressure during the printing process.

While the printhead worked in terms of multi-material printing, it imposed some challenges, including the fact that it only worked seamlessly if all three materials were being printed at once. Even then, the flow of the extruded biomaterial preferred to travel towards the other biomaterial chambers rather than through the needle to be extruded. This caused increased pressure in the printhead and the syringe, causing both the syringe and the syringe holder to break under the needed force. Additionally, because the material wanted to flow backward into other chambers while printing, it created flow problems when printing two materials. It made it almost impossible to print a single material

structure. For these reasons, the properties of the printhead and the printhead itself were re-examined for further exploration.

4.2.2 Angle of Nozzle

To achieve the best printing results, an angle test was conducted to assess the flow through the printhead. The angles that were considered in the printhead design were 30°, 45°, 60°, and 90°. Prototypes were created to try the different angles and assess the flow differences. It was concluded that the angle of the print head channels was not as important as the merger point where all the inks collided.

For the first design, a 45° angle was chosen. This caused a very narrow merger point between the three channels. The narrow merger point led to a pressure increase when all three materials were printed during the printing process. Especially since to deposit the secondary material, it first had to push the previous material out of the narrow channel. Thus, the 60° angle was chosen for the final printhead design because it allowed for a better merger point between the biomaterials. Also, the channel between the merger point and the needle was shortened, which also increased the pressure in the printhead.

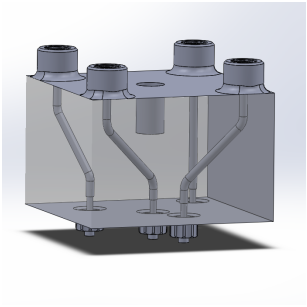

Figure 4.3 CAD model of a printhead to measure the possible angles for the printhead.

4.2.3 Finalized Print Head Design

The finalized printhead design not only addressed but also eliminated all the challenges in the initial printhead design. By reconfiguring the connection of the pipes and the printhead to incorporate a one-way valve, the issue of the backflow of materials was effectively resolved. This modification enabled the printer to handle a single material as well as up to 3 different biomaterials without any cross-contamination or flow disruptions. Moreover, the pipes' diameters and the printhead's internal shafts were increased, which had the dual benefit of reducing the pressure required for extrusion and minimizing the occurrence of clogs. This adjustment also led to a smoother extrusion process, as the changes in diameters along the setup decreased the step-ups and downs, further aiding in pressure reduction and ensuring a more consistent printing outcome. Overall, these enhancements significantly improved the bioprinter's reliability, versatility, and efficiency, making it an invaluable tool for advanced tissue engineering and regenerative medicine applications.

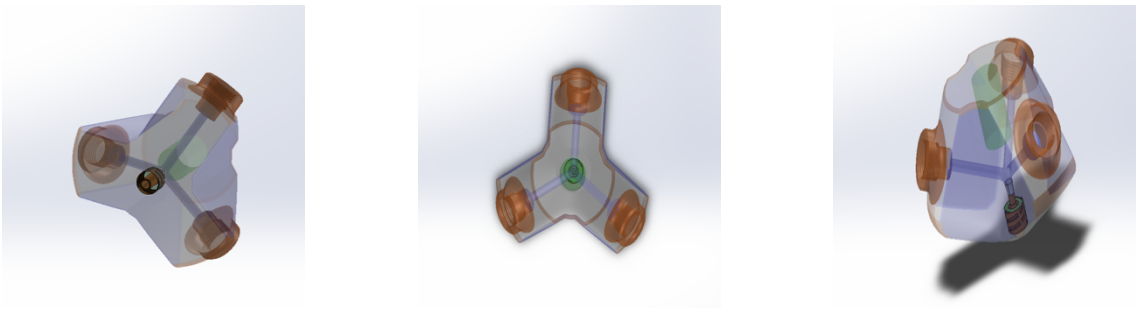

(a) (b) (c)

Figure 4.4 CAD model of the finalized printhead from different angles: (a) angled below, (b) completely below, and (c) from the side.

The picture below depicts the finished product of the printhead made in-house by the custom resin 3D printer. The material is clear enough to show all the details of the printhead, which are visible in the CAD model. Also, the chambers can also be seen clearly, same as with the initial printhead, which is an important factor in keeping the item clean so there is no contamination of the prints.

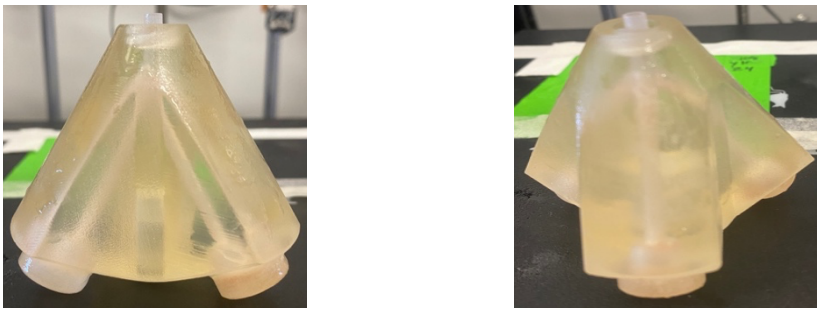

(a) (b)

Figure 4.5 Finalized printhead made out of resin (a) side view where channel connection is visible, and (b) single channel view.

Lastly, the final print was fitted to the printer to test the connection. As with any printer, there are necessary offsets to add to the dimensions to ensure all the sizing will fit with the connecting pieces, even if the calibration is slightly off. In this case, the printhead came out well with the connections and was ready to be assembled and used for trials with the biomaterials.

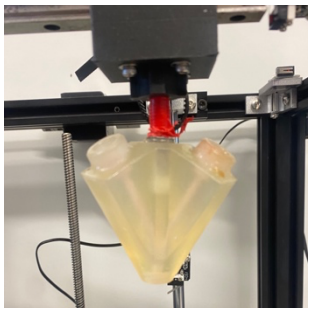

Figure 4.6 Printhead connected to the printer.

Adding the one-way valves and the increased dimensions of the chambers and the pipes reduced pressure during the printing process. This meant more seamless printing without breaking the components. It also meant less extrusion force was needed during printing, which increased the printer's value when live cells were added to the printing process. Thus, this printhead design was used for all experiments with a single material, two materials, and three-material printing.

4.3 Finalized Printer Setup

FRESH bioprinting poses unique challenges, particularly in managing the different material properties and temperatures required for optimal printing. Thus showcasing the need to design a bioprinter setup tailored specifically for FRESH bioprinting of multiple materials. This setup not only overcomes the challenges associated with FRESH bioprinting but also allows for the continuous printing of multiple materials without stopping the printing process from changing materials. While there are many different bioprinters out there which have this type of function, they differ in 2 ways. For one, they have multiple extrusion points, which could still disrupt the calibration points; this model is shown in Figure 4.7. The specific model in the figure is by Aether, a start-up company in San Francisco. The second difference is the cost. Bioprinters typically range higher than a regular 3D printer such as the ender. Adapting a 3D printer for bioprinting purposes which is affordable, accessible and open source is important in terms of research as more researchers can use it and adjust it to fit the research needs.

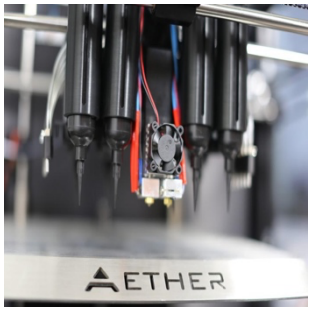

Figure 4.7 Aether multi-material printer [300]

The current figure shows the final print setup and the changes made to the Ender 3D printer. The setup includes three stationary linear extruders on the left side of the printer. These linear extruders received custom syringe holder parts that were designed for a 10 mL syringe native to the lab. The custom parts were 3D printed in the lab using Prussia printers and regular PBS filament. Each syringe is equipped with plastic pipe connectors, which are meant to be tight to ensure no material is escaping from the section. The pipes run over the printer's top and are connected to the custom printhead via a plastic one-way valve. The current one-way valve is a bit bulky for the printer setup. However, no other valves on the market were available with the needed dimensions, which were for an 8/32-inch pipe diameter. The custom printhead is connected to the printer, which is the only moving portion. Finally, the bottom of the printhead has the connection to allow the screw on of a printing needle.

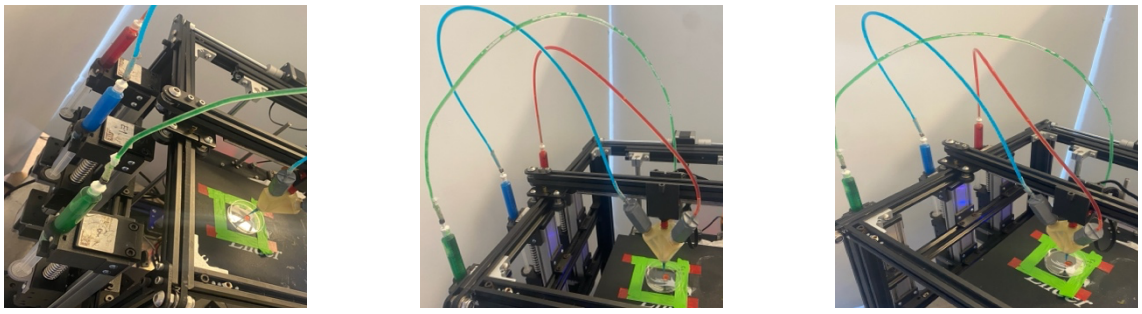

(a) (b) (c)

Figure 4.8 The finalized printer design from different angles: (a) syringes on the left, (b) top view down and (c) from the right top angle.

4.4 Importance of the Designed Printer

Designing a 3D bioprinter specifically for FRESH bioprinting without the need to leave the print site when changing materials offers several significant advantages. One key benefit is the ability to maintain the structural integrity and fidelity of the printed construct. FRESH bioprinting relies on the precise layer-by-layer deposition of bio-inks within a supportive hydrogel bath. Suppose the print head must move away from the print site to change materials. In that case, it can disrupt the delicate hydrogel matrix, leading to structural deformation or collapse of the printed structure. As well as, by eliminating the need to move the print head, a bioprinter designed for continuous FRESH printing can significantly reduce the risk of contamination. Each time the print head moves away from the print site, contaminants can be introduced into the printing environment, which can compromise the integrity and safety of the printed tissues or organs. Maintaining a closed-loop printing process minimizes these risks, ensuring the printed constructs remain sterile and suitable for biomedical applications.

A dedicated FRESH bioprinter can also streamline the printing process and improve overall efficiency. By eliminating the time-consuming steps involved in moving the print head and recalibrating the printing parameters, researchers can achieve higher throughput and produce more complex structures in less time. This increased efficiency is particularly valuable for large-scale tissue engineering projects or when printing multiple constructs with different bio-inks or cell types. While those are the main reasons for custom designing and adapting a 3D bioprinter, there are a couple more reasons to include.

4.4.1 Preservation of Microstructural Integrity

FRESH bioprinting relies on precisely placing bio-inks within a supportive hydrogel bath to create complex, high-resolution structures. Moving the print head away from the print site can disrupt the hydrogel matrix, leading to structural deformation or collapse of the printed construct. By designing a bioprinter that can change materials without leaving the print site, researchers can maintain the microstructural integrity of the printed tissues or organs, ensuring that they closely resemble native tissues in terms of organization and function.

4.4.2 Enhanced Cell Viability and Functionality

The ability to change materials without disrupting the printing process is crucial for ensuring the viability and functionality of the printed cells. Cells are sensitive to environmental changes, and any disruptions during the printing process can affect their viability and function. By minimizing disturbances and maintaining a stable printing environment, a dedicated FRESH bioprinter can improve cell survival rates and enhance the functionality of the printed tissues or organs.

4.4.3 Improved Printing Precision and Accuracy

Continuously printing without leaving the print site increases printing precision and accuracy. It eliminates the need to reposition the print head, which can introduce errors and inconsistencies in the printed structures. A bioprinter designed for continuous FRESH printing can achieve higher printing resolutions and produce more intricate structures with greater fidelity, advancing the development of complex tissues and organs.

4.4.4 Reduced Material Waste and Cost

Minimizing the need to purge or waste materials when changing bio-inks can lead to cost savings and reduced material waste. Traditional bioprinters often require purging the print head with excess material to ensure a clean transition between bio-inks, which can be inefficient and wasteful. A bioprinter designed for FRESH bioprinting can eliminate excessive purging, allowing for more efficient use of materials and reducing costs associated with material waste.

4.4.5 Facilitation of Multi-Material and Multi-Cell Type Printing

FRESH bioprinting is particularly suited for printing complex tissues and organs composed of multiple cell types and bio-inks. A bioprinter that can change materials without leaving the print site enables researchers to seamlessly switch between different bio-inks and cell types during printing, facilitating the fabrication of heterogeneous tissues with controlled spatial distribution of cells and materials.

4.5 Conclusion

Printer adaptation and design are pivotal in bioprinting, serving multiple critical functions. They enable the customization of conventional 3D printers to accommodate the unique properties of biological materials, ensuring that bioprinting processes can optimize the deposition of living cells and biomaterials while minimizing damage. This adaptation facilitates controlled deposition through specialized extrusion systems and nozzle configurations, which are crucial for creating intricate tissue architectures. Additionally, it supports the integration of multiple materials, enabling the fabrication of heterogeneous tissue constructs with diverse cell types and extracellular matrix components. Furthermore, adapted printers support novel bioprinting techniques by providing specialized hardware and software features tailored to specific methods. Moreover, these adaptations ensure scalability and reproducibility, which are essential for advancing bioprinting toward clinical applications. Overall, printer adaptation and design play a fundamental role in advancing bioprinting technologies for tissue engineering, regenerative medicine, and other biomedical applications.

FRESH bioprinting is a unique printing method as it is a process of printing inside a supportive material that is usually kept in a dish throughout the printing process. This means that to allow the changing of material using a printhead change, it would have to go up and over the dish and then back down into it once the change is complete. This allows for errors in the printing process, as any movement could cause discrepancies in the building process. The other method for multi-material printing is through multiple nozzles on one printhead. The changing of materials during the printing process is more accessible, but if the dish is small, then the double or triple nozzle printhead will not be able to access the print site; thus, why the current multi-material bioprinters are not suitable for the FRESH bioprinting method. This research gap was solved by creating a multi-material printhead using a single extrusion point. Allowing for the capabilities of a single material printing all the way to three materials with the ability to mix the materials by extruding two or more materials at once. This design was created using a 3D printer that was adapted for bioprinting capabilities. This process allows for a lower-cost 3D printer alternative for bioprinting while keeping it open source.

4.5.1 Limitations

Creating an open-source bioprinter has its positive outcomes. However, there are also some limitations when the material changes from plastic 3D printing to biomaterial printing for bioprinting purposes. First of all, the materials have different characteristics and behaviour. For instance, the materials for 3D printing are solid, while for bioprinting, they are liquid, which means that the extrusion percentage of the materials needs to be changed and optimized for the bioprinting method chosen. In this case, the material swells from the support material as it intakes the calcium chloride for cross-linking purposes. So, not only does it have to have a lower extrusion percentage, but there also needs to be more significant gaps between layers to ensure that the subsequent layer is printed above the previously deposited layer.

Then, when it comes to multi-material extrusion, the concept holds promise for creating complex tissue structures with multiple cell types and biomaterials, but technical challenges persist in achieving precise control over the deposition of different materials. One of the main challenges was clogging due to one material having higher viscosity over the other, as well as over extrusion of one material over the other, again due to their viscosity properties. There is also the limitation of ensuring compatibility between different materials when layering them. If the materials are not compatible, they will not stick together, and the layers can fall apart once removed from the support material. Lastly, the current cleaning processes used for the print head did not leave a residue. If researchers neglect the cleaning process, there could be biomaterials stuck in the printhead canals, which could contaminate and block future printing processes.

4.5.2 Future Adjustments on the Printer Design

While the current printer setup functions as intended, there is room for further improvement. A significant challenge in FRESH bioprinting lies in the temperature requirements of the biomaterials and support materials. Biomaterials often perform optimally at higher temperatures due to their lower viscosity, facilitating smoother extrusion and deposition. In contrast, the gelatin slurry base, crucial for providing structural support, must be maintained at cold temperatures to maintain consistency. While this issue did not arise in the printing process performed for a section of the heart wall, during long printing sessions, for example, printing a full-sized heart, the gelatin slurry may begin to

lose its desired characteristics as it adjusts to the external temperature, potentially compromising print quality and structural integrity. To address this challenge without compromising the low-pressure extrusion necessary for delicate tissues, one proposed enhancement is the integration of a heated biomaterial chamber within the printer. This chamber would allow the biomaterials to be heated to their optimal temperatures during printing, ensuring easy flow while maintaining a low overall printing temperature. By implementing this solution, researchers can mitigate issues related to temperature differentials, thereby improving the reliability and consistency of FRESH bioprinting for a wide range of tissue engineering applications.

Further enhancements can be made by improving the calibration process to transition a non-bioprinter into a bioprinter. This involves accounting for the differences in material extrusion between traditional printing and bioprinting, ensuring more accurate and precise structures. Additionally, accounting for the swelling of materials between layers is essential for maintaining the integrity and dimensional accuracy of the printed constructs. While these adjustments primarily involve software modifications, they also require some calibration of the hardware components to ensure optimal performance. By refining the calibration process, researchers can enhance the functionality and reliability of the bioprinter, ultimately advancing the field of tissue engineering and regenerative medicine.

Lastly, an additional mixing chamber could be added to the extrusion point for materials, allowing for even more material opportunities within the current printing setup. While the setup is currently three biomaterials maximum, adding the mixing chamber can allow these biomaterials to be used on their own or by mixing them together during printing. Adjusting the ratios opens up an opportunity for multiple material possibilities in a single printing process. For example, the current biomaterials used were alginate, nanofibre and a hybrid biomaterial made from 2% gelatin and 2% alginate concentration. By adding the mixing chamber, the hybrid biomaterial could be eliminated and replaced with gelatin. Then the hybrid biomaterial could be created during the printing process by sending a certain amount of each biomaterial (alginate and gelatin) to the mixing chamber. So, while there are only three material inputs, the example shown the possibility of printing four different materials without leaving the print site.

The only limitation that currently can be foreseen is the addition of cells may have to be after the printing process is completed as different cells have different jobs that they do, and if the biomaterials are mixed with the intended cells, combining the materials could actually harm them or change their job tasks. However, overcoming this limitation could create an ultimate multi-material bioprinter that could increase use cases and be incorporated with other bioprinting methods.

Chapter 5 Optimization of Bioprinting Process

Summary: This chapter discusses and compares the printing processes for bioprinting. The focus is on the changes made to optimize the current printing process for the development of heart wall tissue.

5.1 Introduction

FRESH bioprinting makes it possible to create intricate, multi-material structures with high resolution. There are several crucial steps in the FRESH bioprinting process, such as preparation of the support bath, biomaterial formulation, printing process, crosslinking, printed structure removal and post-processing. At the same time, the format is the same for the printing process, no matter the amount of biomaterial used or the structure being printed. Some complex steps behind the scenes need a little more attention.

5.2 Printer Setup

The printer setup is explained in detail in Chapter 4 – printer design- however, the printer setup and G-codes to set up printing using a single biomaterial versus multiple biomaterials are slightly different and require manual adjusting. One thing that both prints have in common is the initial step of the printing needly needs to be positioned at a height above the dish, which has the gelatin slurry support material to ensure it will go past the sides of the dish before descending to the base portion of the dish where it will start printing. The height of the petri dish will depend on the amount being printed and the structure of the desired print. Then, the base where the material will be printed also needs calibration. This is because all dishes have different material thicknesses, which will all be above the print bed's position. If the needle is calibrated to the print bed, it could break the needle during the printing process as it will be pushed into the base of the dish. It could also break the dish depending on the material's strength. Lastly, it could not extrude any material since it is closed off at the base of the dish, and as the needle moves, the dish moves with it. If the gap is too big between the needle and the base of the dish, there is no traction for the material to hold onto. If the material is not deposited in the correct position, it could stick to the flow of material from the needle following the needle’s movements. This means that the extruded material will not follow the desired structure shape. Each calibration is mandatory for any printing process to ensure a positive printing outcome.

5.2.1 Single Material Printing

The current layout design allows multiple materials to be printed from the same nozzle. While the first printhead design did not allow for printing a single material, the final printhead with the one-way valved allowed the possibility of a single material being printed. When printing with a single biomaterial, there were no necessary changes that need to be made to the printer or the G-code besides ensuring the needle goes over the edge of the petri dish before descending to the bed level and the settings of which the extruder needs to be selected for printing. The printer does not have a sensor to automatically choose the extruder with the material input.

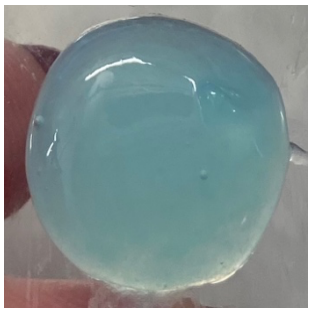

Figure 5.1 Coupon created from 3D printing with nanofiber.

To show the ability of the 3D printer with a single material, a coupon was created using nanofiber biomaterial. Since the nanofiber has good structural integrity, it was the best material to use when testing the capabilities and reproductivity of the printer since it can hold its shape during the printing process. The material was sprayed with a calcium chloride concentration of 20% to ensure the printed material crosslinked post-printing and thus can be used for tests on printed material characteristics. This coupon was repeated for all materials and multiple printing processes to ensure that the printing process could recreate the intended shapes and sizes. Concluding that the printing process and the print setup were correct for a single material opened up the possibility of two materials, as there would only be a couple of adjustments that need to be added to a single material printing setting.

5.2.2 Multi-material Printing

Printing with multiple boinks has its challenges and processes. When it comes to printing numerous materials, it is imperative that the materials be added where the material being printed first gets added last. This is because if the other materials are in the end channel of the print head and the needle, it will be the first material pushed out during the material extrusion portion of the printing.

Figure 5.2 CAD model for multi-material printing.

Once the materials are added, the printing can be completed the same way as a single material. However, the extruders need to be assigned in order of printing and to the layers it will be printing. Due to the current capacity of the printer, these adjustments are done manually prior to printing.

5.2.3 Material Transitioning for Multi-material Printing

For this printing style, the G-code was manually adjusted to change the material earlier than when the next phase of the structure was created. This was to ensure that when the material crosses over to the next layer of the heart wall sample, it will use the material chosen to have properties similar to the native layer.

The figure below shows that when the code is not correctly set up, the next wall layer is printed with the material used for the prior layer. The trial print was conducted without the gelatin slurry base to assess the precise impact of the changing layers. Once the materials were printed as needed, the test was performed in the gelatin slurry to evaluate if the crosslinking changed the parameters of the printing process.

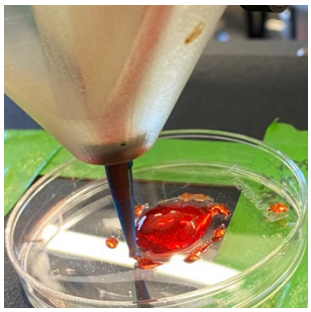

Figure 5.3 Depiction of incorrect G-code for material switch within hybrid tissue printing.

Using a trial-and-error evaluation, it was seen that the material that was being extruded needed to be changed two printing layers earlier to change materials for the next printed shape. It also means there would be a slight layer where the material mixes before it fully transfers to the following material to create the next shape in the layout.

5.3 G-code Setup

The G-code collection for the prints is the same. The model was created initially in Solidworks and saved as an STL file, which can be imported into slicer software. The slicer used in all the experiments is the Prusa Slicer. Since Prusa is meant for 3D printing plastics, there were some necessary modifications to the software to allow for 3D FRESH bioprinting. The G-code was downloaded and uploaded to the printer control site once the slicer was adjusted for the material and printing outcome. There were slight modifications made to the G-code manually to allow the printing of multiple materials.

5.3.1 Slicer Adjustments for Bioprinting

Since the slicer program is associated with the 3D printer, it is set to extrusion of filament material. Filament has a high viscosity compared to biomaterial, especially since the filament is heated at the extrusion point for deposition, while biomaterial is liquid throughout. For this reason, if the slicer program is not correctly adjusted, it extrudes materials. This phenomenon is depicted in the image below.

Figure 5.4 Finished printing product without the proper extrusion parameters set.

The three materials were printed using the vertical printing style to print a multi-material coupon. Since the extrusion parameters were not set, the materials were over-excited. Since there was no time for the materials to be set before the subsequent material was printed, they all combined. The different biomaterial colours can be spotted in small sections,

but overall, the printed shape did not hold its intended shape, nor were the different layers distinguishable. However, once the proper extrusion rate was set, the material did not over-extrude.

5.4 Material Preparation & Sterilization

Sterilization of materials and parts in bioprinting is a multifaceted process with far-reaching implications for research, clinical applications, and patient safety. At its core, sterilization is a critical barrier against contamination, safeguarding the integrity and reliability of bioprinted tissues or organs. Contamination with microorganisms, including bacteria, fungi, and viruses, can introduce variables that compromise experimental outcomes, leading to inaccurate or unreliable data in research settings. By eliminating these contaminants, sterilization helps maintain the purity and consistency of bioprinted constructs, ensuring the validity and reproducibility of experimental results.

Beyond its role in research integrity, sterilization is paramount for ensuring the viability and functionality of the cells used in bioprinting. The sterilization process must effectively eliminate microorganisms while preserving the integrity of the biomaterials and cells. Proper sterilization methods help maintain cell viability, ensuring the printed tissues possess the desired properties and functions. This is essential for successfully creating tissues with specific characteristics and functionalities, such as mimicking the structure and function of native tissues. Moreover, sterilization contributes to the biocompatibility of bioprinted constructs by removing harmful chemicals or residues that could trigger immune responses or rejection in the body. This aspect is particularly critical for bioprinted products intended for clinical use, where patient safety is paramount. Adherence to sterilization standards is essential to ensure compliance with regulatory guidelines and facilitate the approval process for clinical applications.

5.4.1 Sterilization procedures for Bioprinting

Sterilization methods must effectively eliminate possible contaminants while ensuring that the biomaterials and cells remain viable and functional. Some potential methods could be used for this purpose. One of them is autoclaving, which is a widely used sterilization method in bioprinting, involving the exposure of materials to high-pressure steam at temperatures around 121°C for a specified period, which is typically between 15 and 20 minutes. This method is highly effective in killing many microorganisms, including bacteria, viruses, and spores.

Another method is ethylene oxide sterilization, which is used for materials and parts that cannot withstand high temperatures or moisture. While effective against various microorganisms, ethylene oxide sterilization requires specialized equipment and careful handling due to the toxic nature of ethylene oxide. Gamma irradiation is a sterilization method that uses high-energy gamma rays to sterilize materials, often used for sterilizing disposable items such as syringes and packaging materials. Although effective, gamma irradiation can alter the properties of some materials. UV-C sterilization utilizes UV-C light to kill microorganisms by damaging their DNA, commonly used for surface sterilization of materials and equipment in a laboratory setting. Sterile filtration is used to sterilize liquids or gases by passing them through a sterile filter with pore sizes small enough to trap microorganisms. This method is frequently used for sterilizing cell culture media and other liquid solutions used in bioprinting.

The last sterilization method is a chemical method, such as hydrogen peroxide or peracetic acid, which can be used to sterilize materials that cannot be autoclaved or irradiated. However, these methods require careful handling and proper ventilation due to the use of toxic chemicals. Plasma sterilization is a low-temperature method that uses ionized gas to sterilize materials. It is effective against a wide range of microorganisms and is often used for sterilizing heat-sensitive materials. In bioprinting, selecting a sterilization method that is compatible with the materials and cells being used is essential. Establishing and following proper sterilization protocols are critical to ensure the safety and quality of the bioprinted tissues or organs.

5.4.2 Sterilization Practices for Current Experiment

Since no live cells were used in the experiments, sterilization for cell safety was not an essential factor. However, creating a routine for safe printing procedures was important to prepare for future experiments, including those with live cells. For this reason, all biomaterials were created using PBS as the base material to ensure cell safety and cultivation. Before printing, the parts the biomaterial goes through are flushed with PBS.

After each printing, the pipes and the printhead are flushed through with warmed-up PBS until clear. The process was then repeated with 95% ethanol to ensure no residue was left behind before completing a final flush with room-temperature PBS. These steps ensure there is no residue left in the printer, which can cause contamination.

5.5 Printing Process

The above sub-chapters discuss the behind-the-scenes steps to prepare for the printing of a heart wall layer and the needed adjustments for an open-source bioprinter. However, it is crucial to understand what is unique about FRESH bioprinting and how it revolutionizes bioprinting.

5.5.1 FRESH Bioprinting Process

FRESH bioprinting is a specific technique within the broader field of bioprinting. The key distinction lies in the approach to printing complex structures with soft materials, particularly hydrogels. In conventional bioprinting methods, layers of biomaterial are deposited and crosslinked or solidified to create the desired structure. This can be challenging when dealing with soft, delicate materials, as the layers may collapse or deform during the printing process. FRESH bioprinting, on the other hand, utilizes a support bath of gelatin or other sacrificial materials. The biomaterial is deposited into this bath, which holds the shape of the printed structure in a gel-like support medium. The support bath prevents the collapse of softer structures during the printing process. After the printing is complete, the support bath is easily melted or washed away, leaving behind the intricate, three-dimensional bioprinted structure.

Figure 5.6 represents the printing steps for FRESH bioprinting. The diagram skipped the initial prep steps with the cell cultivation and the material preparations, such as the biomaterials and gelatin slurry base. However, it shows the step-by-step process from extrusion printing to removing the printed structure.

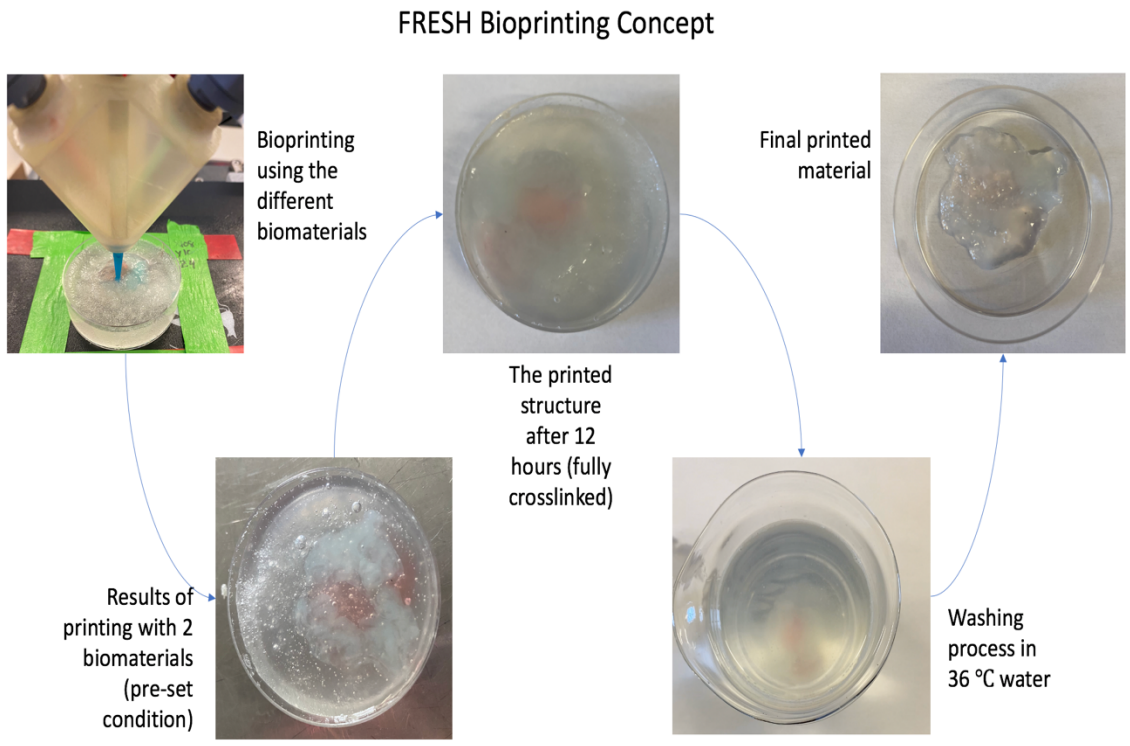

Figure 5.5 Printing process for FRESH bioprinting.

5.6 Cell Safety

In bioengineering, the safety of cells is a critical aspect, especially in the realms of tissue engineering, regenerative medicine, and bioprinting. The success of these endeavours hinges on ensuring that the cells employed survive and maintain their intended functionality within the engineered tissues. Achieving this involves several crucial considerations. First and foremost is the biocompatibility of materials, ensuring that they do not elicit adverse reactions from the cells. Careful selection and rigorous quality assessment of cell sources are imperative, guaranteeing that only healthy and viable cells are utilized in the engineering process. Maintaining a sterile environment during cell handling and tissue fabrication is essential to prevent contamination.

Optimizing cell viability involves creating conditions that support the cells' survival and metabolic activities. This includes controlling parameters such as temperature, humidity, and nutrient supply. Adherence to ethical guidelines in cell sourcing and handling is paramount, aligning with established standards and regulations. Long-term safety post-implantation is also a significant concern, requiring ongoing research to understand the behaviour of bioengineered tissues within the living organism.

The dynamic nature of bioengineering means that continuous advancements in cell culture techniques, scaffold design, and bioprinting technologies enhance bioengineered tissues' overall safety and efficacy. The goal is to ensure that the cells not only endure the fabrication process but also thrive and function optimally within the host environment after

transplantation. This multidimensional approach to cell safety underscores bioengineering practices' complex and interdisciplinary nature.

5.6.1 Cell Death

The vitality of cells in bioprinting is subject to various factors, encompassing cell storage in the printer, thermal impacts during the printing procedure, and mechanical forces applied throughout bioprinting. Cell storage conditions and processes during printing can potentially impact cell viability, requiring stability in a medium that aids recovery from cell-detaching solutions and the associated stresses. These detachment methods, including trypsin, TrypLE, and collagenase, along with centrifugation and washing, are known to affect cell survival, phenotype, and differentiation potential [301, 302]. Thermal injury is another concern, where studies reveal that inkjet printing, with temperatures exceeding 200°C, results in a minimal increase of 4–10°C in biomaterial temperatures, minimally affecting mammalian cell viability [303, 304]. Mechanical stress is also a crucial consideration as cells respond to it by altering gene expression and function. Extrusion pressure has been linked to cellular viability, with high-pressure extremes showing as little as 40% viability [305]. Mechanical pressure in inkjet printing encourages MSC differentiation into bone and cartilage, while shear stress in extrusion techniques promotes differentiation into endothelial and bone tissues [306, 307]. The choice of 3D technology, such as laser-assisted and inkjet bioprinting, depends on resolution requirements, target tissue, and other factors [308]. Extrusion bioprinting may be essential for high-viscosity biomaterials, and the effects of shear stress can be mitigated by modifying biomaterial composition and controlling back pressure [309].

5.7 Conclusion

Optimizing the printing process, particularly for FRESH bioprinting, is essential for a multitude of reasons. It enables precise control over material deposition and interfacial interactions, which is crucial for fabricating complex tissue architectures with high fidelity and resolution. By minimizing shear stress and mechanical damage to cells during extrusion and deposition, optimized printing processes preserve cell viability and functionality, which is essential for fabricating bioprinted constructs with viable cells capable of proliferating and remodelling within the engineered tissue. Fine-tuning printing parameters such as extrusion pressure, nozzle diameter, and printing speed ensure high spatial resolution and the creation of intricate tissue structures. Moreover, optimized printing conditions lead to enhanced structural integrity and mechanical stability of bioprinted constructs, facilitating their validation and translation to clinical applications. Overall, optimization of the printing process for FRESH bioprinting is paramount for advancing tissue engineering and regenerative medicine, enabling reproducibility, scalability, and the development of patient-specific treatments.

5.7.1 Limitations

Notably, the limitations of FRESH bioprinting lie in the complexity of optimizing the printing process. While FRESH offers advantages like the ability to print complex structures and support delicate biomaterials, achieving optimal printing parameters presents challenges. Fine-tuning variables such as hydrogel composition, printing speed, temperature control, and support bath properties is essential for ensuring precise structure deposition and maintaining

biomaterial integrity. However, the interplay between these parameters can be intricate, leading to difficulties in achieving consistent print quality and structural fidelity. Moreover, the need for thorough experimentation and iterative adjustments prolongs the optimization process, delaying research progress and potentially limiting the scalability of FRESH bioprinting for clinical applications.

Furthermore, the current support material does not have consistent outcomes in terms of gelatin particle sizes and shapes. Different creation processes and gelatin compositions were explored to find a process where the particles were consistent in size. As well as the compositions were investigated to see if the amount of gelatin in the material would play a role in the particle sizes and shape. However, the results of the study were inconclusive as there was no correlation, and pre-producibility was not achieved. The results, however, shown that increasing the gelatin composition created larger batches of support material, which sped up the printing prep times. Nonetheless, with the different particle sizes and shapes, the surface of the printed structure is not as smooth as it would need to be for the heart wall. The rough surface of the printed organ can affect the fluid properties of blood and other liquids that the organ would come in contact with.

The last limitation found in the printing process was the crosslinking properties of the chosen biomaterials. The printed structure had to be kept in the support material overnight to ensure that the structure was fully set. A study was completed to analyze how the different calcium percentages inside the support material react with the biomaterials. The results shown that the biomaterials set faster in higher calcium percentages, but the increased crosslinking speed negatively affected the extrusion process of the biomaterials as they crosslinked and stuck to the needle.

Addressing the above-mentioned limitations through enhanced process control, material optimization, and automation strategies is crucial for advancing the reliability and efficiency of FRESH bioprinting technology.

5.7.2 Future Work

The current printing process is optimized for the intended outcomes of this thesis as well as to ensure all parts work together to achieve the printing of hybrid tissues. However, the printing process could be further optimized by decreasing the crosslinking time of the biomaterials, as currently, they need to sit in the support bath for a minimum of 12 hours to achieve the desired state for removal from the support bath.

Chapter 6 Evaluation of Hybrid Tissue Fabrication

Summary: This chapter explores the fabrication of hybrid tissue. Each of the previously examined biomaterials is matched to a corresponding heart wall layer due to the matching characteristics discussed in this chapter. Then, different printing techniques for 3D bioprinting are discussed. Finally, the printing of three materials and the corresponding layout are explored according to the current printing technology possibilities.

6.1 Introduction

Tissue engineering has emerged as a transformative field in regenerative medicine, offering the potential to create functional tissue substitutes for damaged or diseased organs. Central to the advancements in tissue engineering is the development of bioprinting technologies, which allow for the precise deposition of cells and biomaterials to fabricate complex tissue constructs. One particularly promising area within bioprinting is the creation of hybrid tissues, which combine multiple cell types and biomaterials to replicate the intricate architecture and functionality of native tissues.

Fabricating hybrid tissues requires careful consideration of several key factors, including selecting appropriate cell types and biomaterials. Cell selection is critical to ensure the printed tissues exhibit the desired functionality and biological responses. Biomaterials play a crucial role in providing the necessary structural support and biochemical cues for cell growth and differentiation. The design of biomaterials, which are used to encapsulate cells and biomaterials during printing, must also be optimized to ensure proper extrusion and crosslinking properties. One of the main challenges in bioprinting hybrid tissues is achieving precise control over the spatial organization of different cell types and biomaterials. This requires developing advanced printing techniques that can deposit multiple materials with high resolution and fidelity. Despite these challenges, bioprinting hybrid tissues hold immense promise for a wide range of applications in regenerative medicine, disease modeling, and drug discovery. The ability to engineer tissues with complex architectures and functionalities opens new possibilities for personalized medicine and tissue replacement therapies. By advancing the understanding of tissue development and regeneration, bioprinting hybrid tissues have the potential to revolutionize healthcare and reshape the future of medicine.

While there are many steps before creating life-size organs using hybrid bioprinting, creating a small section of the heart wall with individual layers made of different biomaterials is a start. In creating the small section, the materials needed to be allocated to the corresponding heart wall layer first, and then a trial of two materials was examined before confidently moving to three materials for printing. One of the biggest challenges was the printing or placement of biomaterials, which dictated the outcome of the hybrid tissue.

6.2 Material Correlation to Layers

In Chapter 3, a comprehensive analysis was conducted to evaluate the properties of various biomaterials before and after crosslinking. This examination aimed to understand how these materials behave and how their characteristics

change once they are crosslinked, which is a crucial step in the bioprinting process. By examining parameters such as shear stress, compressional stress, biocompatibility, and elastic modulus, researchers were able to gain insights into the suitability of each material for mimicking specific layers of the heart tissue.

The results of these analyses were then used to match each biomaterial to the heart tissue layer it could best mimic. For example, biomaterials with high elasticity and tensile strength might be suitable for mimicking the myocardium, the muscular middle layer of the heart responsible for its pumping action. On the other hand, biomaterials with excellent biodegradability and cell adhesion properties could be more suitable for mimicking the endocardium, the inner lining of the heart chambers.

This meticulous matching process ensures that the selected biomaterials are tailored to mimic each heart tissue layer's specific properties accurately. By choosing biomaterials that closely resemble the native tissue characteristics, researchers can improve the functionality and compatibility of the bioprinted constructs, bringing us closer to the development of bioengineered heart tissues for regenerative medicine and disease modeling applications.

The analysis revealed that the nanofiber biomaterial exhibited characteristics that closely resembled a muscular tissue layer, making it an ideal candidate for representing the myocardium layer in the heart wall. The nanofiber biomaterial's structural similarity to natural muscle tissue and its mechanical properties, such as elasticity and tensile strength, make it well-suited for replicating the contractile function of the myocardium.

The hybrid biomaterial, which combines alginate and gelatin, was selected to mimic the endocardium portion of the heart wall. Gelatin, a component of the hybrid biomaterial, has been shown to enhance cell retention rates in biomaterials and printer constructs [310]. Additionally, gelatin's elastic properties make it suitable for mimicking the compliant nature of the endocardium, which experiences stretching and deformation during the cardiac cycle.

Lastly, the 4% alginate biomaterial was chosen to represent the epicardium layer of the heart wall. Alginate is known for its biocompatibility and ability to form stable hydrogels, making it a suitable material for encapsulating cells and providing structural support. The 4% alginate concentration best replicates the epicardium's mechanical properties, which is the outermost layer of the heart wall responsible for protecting the heart and maintaining its shape.

6.3 Two-material Printing Capabilities

Perfecting the printing process for coupons of different biomaterials marked a significant milestone, paving the way for the next phase of the research: hybrid tissue bioprinting. This transition was not just a leap from one material to three; rather, it involved a careful and systematic approach. Before delving into the complexities of multi-material bioprinting, it was crucial to conduct tests using two materials to better understand the capabilities and challenges of hybrid tissue engineering. These initial tests served as a foundation for exploring the potential of combining multiple materials in a single construct.

To assess the capabilities of hybrid tissue engineering, various printing methods were examined. Vertical printing, which involves layer-by-layer deposition of materials to build up the desired structure, was one of the methods

evaluated. This approach allows for precise control over the spatial arrangement of the materials and is well-suited for creating complex, multi-layered tissues.

Horizontal printing, in the form of rings, was another technique explored. This method involves printing concentric circles of different materials to create ring-shaped constructs. Horizontal printing offers a different perspective on multi-material bioprinting, allowing researchers to study the interactions between materials in a planar configuration.

Lastly, mixing the materials was investigated as a potential method for creating hybrid tissues. By blending and extruding two materials simultaneously, researchers aimed to achieve a homogenous blend that could exhibit the properties of both materials. This approach offers simplicity and efficiency but requires careful consideration of material compatibility and mixing ratios.

Overall, these tests provided valuable insights into the challenges and opportunities of hybrid tissue bioprinting. Systematically exploring different printing methods and material combinations leads to a deeper understanding of the complexities of creating functional, multi-material tissues for regenerative medicine and tissue engineering applications.

6.3.1 Vertical Placement

Vertical printing of hybrid tissue is a promising bioprinting technique that allows for the creating of complex, multi-layered structures with precise control over the spatial arrangement of different materials. This method involves depositing layers of biomaterials vertically, one on top of the other, to build up a three-dimensional tissue construct. Vertical printing is particularly well-suited for creating tissues with distinct layers, such as the heart wall, which has multiple layers with different thicknesses.

One of the key advantages of vertical printing is its ability to create tissues with spatially defined regions of different materials. This is essential for mimicking the heterogeneous nature of native tissues, where different cell types and biomaterials are arranged in specific patterns. Controlling the deposition of materials at each layer can create tissues with precise architecture and functionality. Another advantage of vertical printing is its compatibility with a wide range of biomaterial formulations. Different biomaterials can be used for each layer, allowing the mechanical and biochemical properties of the tissue to be tailored to meet specific requirements. For example, a stiff biomaterial may be used for the myocardium to mimic the contractile properties of muscle tissue. In contrast, a more compliant biomaterial may be used to replicate the endocardium's elastic nature. Vertical printing also offers scalability, making it suitable for producing tissues of varying sizes and complexities. This scalability is essential for drug screening and disease modeling applications, where tissues need to be reproducible and consistent across different experiments.

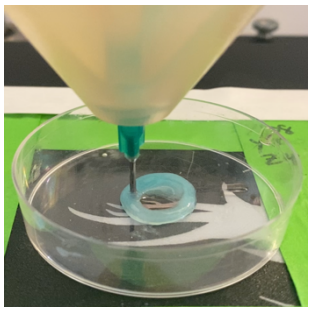

Figure 6.1 Vertical 3D printing where nanofiber (blue) is printed on top of the alginate biomaterial (red).

Despite its advantages, vertical printing of hybrid tissue also presents challenges. One of the main challenges is ensuring proper adhesion between layers to prevent delamination. This requires optimizing the printing parameters, such as the extrusion pressure and speed, as well as the choice of biomaterials and support materials.

6.3.2 Horizontal Placement

Horizontal printing of hybrid tissue is an alternative bioprinting technique that offers unique advantages and challenges compared to vertical printing. In horizontal printing, concentric circles or layers of different materials are deposited on a flat surface to create a planar, multi-material construct. This method allows for the creating of tissues with different material compositions in a single plane, offering a different approach to creating complex tissue structures.

One of the key advantages of horizontal printing is its simplicity and efficiency. Unlike vertical printing, which requires precise control over the vertical deposition of materials, horizontal printing involves depositing materials in a single plane, making it easier to control and manipulate. This simplicity allows rapid prototyping and testing of different material combinations and designs. Horizontal printing also offers flexibility in terms of material selection. Since materials are deposited in a single plane, a wider range of biomaterials with varying viscosities and properties can be used. This flexibility allows researchers to create tissues with diverse mechanical and biochemical properties, mimicking the complex nature of native tissues more accurately. Another advantage of horizontal printing is its suitability for creating tissues with gradient properties. By varying the composition of the biomaterials across the plane, researchers can create tissues with smooth transitions between different material compositions. This is particularly useful for creating tissues with heterogeneous properties, such as the transition zone between different tissue types.

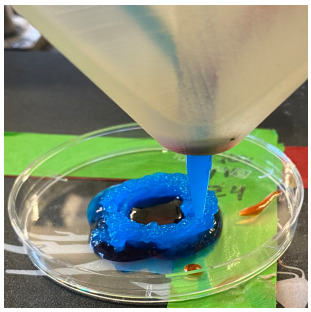

Figure 6.2 Horizontal 3D printing of alginate (red) as the first layer and nanofibre (blue) as the encompassing second layer.

However, horizontal printing also presents challenges. One of the main challenges is achieving proper adhesion between layers. Since materials are deposited in a single plane, there is a risk of delamination between layers if the adhesion is insufficient. This requires careful selection of biomaterials and optimization of printing parameters to ensure proper bonding between layers.

Another challenge is maintaining the structural integrity of the tissue during and after printing. Since materials are deposited in a planar configuration, there is a risk of sagging or deformation of the tissue structure. This requires using support materials or strategies to reinforce the structure and maintain its shape.

6.3.3 Mixing of Materials

Mixing biomaterials is a technique used in bioprinting to create hybrid tissues with properties that are intermediate between those of the individual biomaterials. This approach involves blending two or more biomaterials together during the extrusion process, resulting in a unique mixture that combines the desirable characteristics of each biomaterial. One of the key advantages of mixing biomaterials is the ability to create tissues with tailored properties. By carefully selecting and blending biomaterials with different viscosities, mechanical strengths, and biocompatibilities, we can create hybrid tissues with properties that closely match native tissues. It also extends the material capabilities in a single printing process. For example, blending a stiff biomaterial with a more compliant biomaterial can result in a hybrid tissue with mechanical properties that are optimized for a specific application.

Mixing biomaterials also allows for the creation of tissues with gradient properties. By varying the composition of the biomaterial mixture along a single axis, researchers can create tissues with smooth transitions between different material properties. This gradient approach is particularly useful for creating tissues with complex architectures, such as vascularized tissues or tissues with heterogeneous cell populations.

In terms of the hybrid tissue creation, mixing the materials could be important for the transitional layer portion of the tissue. For example, when the alginate layer is complete and the nanofiber is printed, there is a chance that the two materials do not stick to each other due to their different properties. However, a transitional layer of the two materials allows the mixed biomaterial to connect to the alginate and act as a connector glue for the nanofiber.

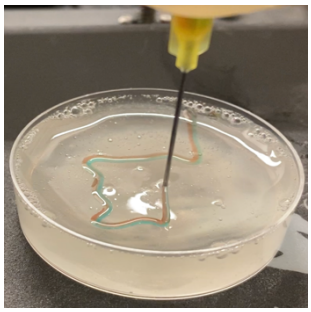

Figure 6.3 Mixing of nanofiber and alginate during the extrusion phase of printing.

However, mixing biomaterials presents several challenges. One of the main challenges is achieving a homogenous mixture of biomaterials with different viscosities and properties. Ensuring that the biomaterials are thoroughly mixed before extrusion is crucial for achieving consistent and predictable printing outcomes. This requires careful selection of mixing techniques and optimization of mixing parameters, such as mixing speed and duration.

Another challenge is maintaining the stability of the biomaterial mixture during and after printing. Since biomaterials with different properties may have different crosslinking or gelation kinetics, there is a risk of phase separation or gelation issues. This requires careful control of printing parameters, such as extrusion rate and temperature, to ensure that the biomaterial mixture remains stable throughout the printing process.

6.4 Layout

When considering 3D printing of the heart wall, replicating its complex structure poses several challenges. The heart wall consists of multiple layers, each with distinct properties and functions, making it difficult to mimic using traditional 3D printing techniques. One challenge is replicating the myocardium's intricate architecture, consisting of densely packed muscle fibers arranged in a helical pattern. Achieving this level of detail and organization in a 3D-printed construct requires advanced printing methods and materials that can replicate cardiac muscle tissue's mechanical properties and alignment. Another challenge is recreating the heart wall's heterogeneity, consisting of different layers with varying cell types and extracellular matrix composition. 3D printing techniques must be able to deposit multiple biomaterials or materials with different properties to mimic each layer's composition and function accurately.

Ensuring proper vascularization of the 3D-printed heart wall is crucial for its long-term viability and function. Replicating the intricate network of blood vessels within the heart wall presents a significant challenge, as current 3D printing techniques struggle to create vascular structures with the necessary complexity and perfusion capabilities. If all these challenges weren’t enough, the heart wall also has a very tricky chape in terms of curvature as well as different thicknesses throughout the different sections of the heart wall. Figure 6.4 shows a depiction of a section of the heart wall at the bottom curvature of the heart, where the thickness is typically 1mm for the endocardium and the epicardium and about 8mm for the myocardium.

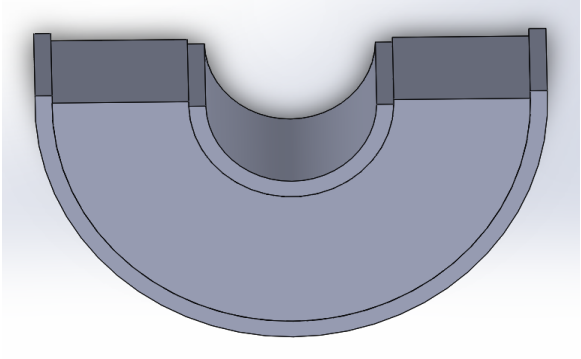

Figure 6.4 CAD model of realistic heart wall position.

Achieving the shown model is difficult with current 3D printing techniques. Especially when printing upward, there is a higher chance of printing this model style from a side view. However, even then, there are issues with the curvatures as the materials are not printed simultaneously but one after the other. For this reason, different layouts and printing placements were tested to address how the hybrid tissue could be printed.

6.4.1 Vertical Placement

As mentioned above, vertical printing of hybrid biomaterials presents challenges, particularly regarding the setting of each layer before the next is applied. Suppose the base layer is not fully set before printing the next material. In that case, the subsequent material can sink into the previous one rather than sitting on top, leading to unintended mixing and spreading. This also meant a deformation to the intended shape it was meant to print. To address this issue, the base material must be fully crosslinked before adding the next layer. However, this poses a challenge as the material typically takes a minimum of 6 hours; based on previous tests on attempts to remove the printed structure from the gelatin slurry to crosslink to a point where it can withstand added weight, making it seemingly impossible to print multiple layers in a single print job.

One approach to overcome this challenge was to increase the calcium content in the gelatin slurry, aiming to accelerate the material's setting process. While this seemed promising, the increased calcium content resulted in a different swelling rate for the materials. Consequently, the layer calibration was affected, causing the material to harden around the printing needle. The following material was printed into a hardened shell, resulting in a final product with a crosslinked exterior and a liquid interior. Additionally, with the material crosslinked to the needle, it did not follow the intended shape. Although this approach introduced a new concept of multi-material printing, it did not fulfill the original goal of creating a tissue with three distinct layers.

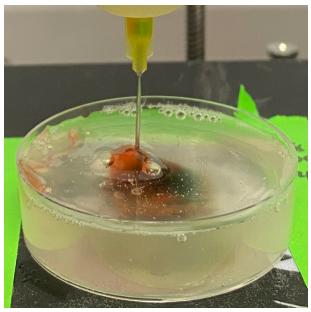

Figure 6.5 Printing a vertical structure using two materials in a gelatin slurry with increased calcium levels of 15%.

Figure 6.5 shows the results of the increased calcium in the gelatin slurry when printing a vertical structure with two materials. The observed behavior indicates a significant challenge in the 3D printing process, where the materials are not behaving as intended. The material deposition does not follow a predictable pattern, and there are distinct differences in the distribution of materials within the structure. The red material, which was intended to form the base part of the structure, instead adhered to the needle and solidified around it. This resulted in the red material acting as a barrier or "sack" that constrained the movement of the subsequent material, which was the blue nanofiber seen mixed in the print. As the needle moved during the printing process, the red material moved along, creating an unintended effect where the red material dictated the shape and placement of the blue nanofiber.

6.4.1.1 Increased Calcium Concentration in the Gelatin Slurry Base

The recomended calcium concentration is 11mM, which translates roughly to 1% calcium concentration. To test the different crosslinking rates of the materials, the calcium concentration was increased to 10%, 15% and 20% to see the rapid crosslinking times with the material. The photos below show the printing of the least viscous material, which is the hybrid biomaterial in the 20% calcium concentration. The hybrid biomaterial was used because it needed the most time to set due to its low viscosity. This made it a perfect material to test the capabilities of express crosslinking. The test results were that the material was completely set as it was extruded from the needle, causing a barrier where it printed upward around the needle rather than downward. The resulting print was also fully crosslinked throughout.

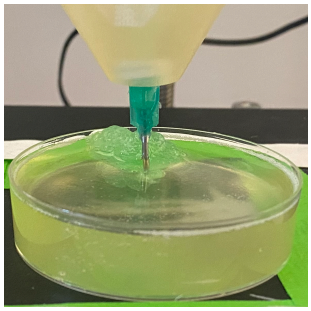

Figure 6.6 Printing the hybrid biomaterial into the gelatin slurry base with an increased calcium concentration of 20%.

The 15% concentration also showed similar results to the 20% concentration; however, in this case, the material created a sack for the material to sit into and extruded the material inside of it, causing a crosslinked exterior and a liquid interior.

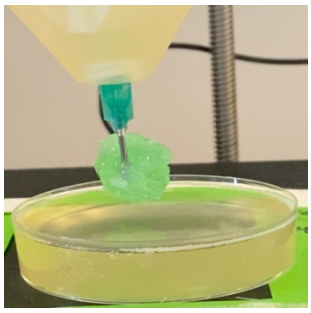

Figure 6.7 Printing the hybrid biomaterial into the gelatin slurry base with an increased calcium concentration of 15%.

Lastly, the 10% concentration also followed the same pattern as the other concentration, but this time, it had a bit more structural integrity, where it expanded outwards but not enough to form around and attach to the needle. It still did not stay in one place while the printhead was extruding; rather, it followed it as with the other concentrations.

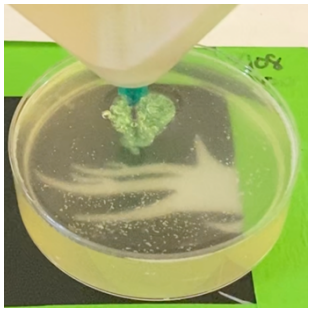

Figure 6.8 Printing the hybrid biomaterial into the gelatin slurry base with an increased calcium concentration of 10%.

High calcium concentrations proved to be effective in accelerating the material's crosslinking and hardening process, enabling the printed objects to be removed shortly after printing. However, this rapid setting also caused the material to deviate from its intended printed structure shape, indicating that a balance between setting time and structural integrity needs to be achieved. Lower concentrations of calcium were found to be more suitable for maintaining the intended structural shape of the printed object.

To explore the potential benefits of both rapid setting and structural integrity, further studies could be conducted to investigate the possibility of adding a higher calcium concentration in liquid form post-printing to the dish with the printed product. This approach could potentially reduce the material's setting time. However, one of the unknowns that needs to be evaluated is whether the post-printing addition of substances compromises the printed structure. However, this idea was not pursued further due to the primary objective of creating hybrid tissue. Instead, the bioprinting process resumed using the original 11mM calcium concentration, and the printed products were allowed

to set overnight to ensure complete crosslinking. This decision was made to prioritize the printed tissues' structural integrity and functionality over the printing process's speed.

6.4.2 Horizontal Placement

Based on the tests with vertical printing, it became evident that this approach was not ideal for printing hybrid tissues. The current state of printing technologies is not yet ready to effectively handle the complexities of curved hybrid tissue printing. As a result, the most logical and feasible printing style remained horizontal. However, the printed tissue structure must follow a pattern similar to the heart wall. For this reason, the idea of encompassing circles was depicted in the figure below.

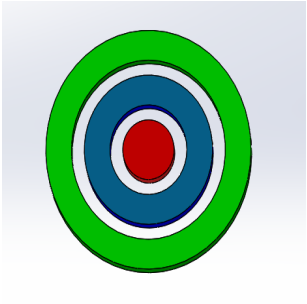

Figure 6.9 CAD model of the printing of three tissue layers.

The idea is to have the materials encompassing each other moving outward in circles, with a section of a combined material layer between the transitioning material. The transition layer will allow the materials to adhere to each other better than if it was a material switch method of multi-material printing.

This approach offers several advantages. First, it does not require designing or implementing a completely new printing style, leveraging the existing horizontal printing setup. Second, it allows for the creating of complex structures resembling the natural patterns found in biological tissues, such as the heart wall. Third, incorporating a combined material layer between transitioning materials ensures a smooth and cohesive integration of different materials, promoting structural integrity and functionality in the printed tissues.

Overall, the encompassing circles technique represents a practical and effective method for achieving the desired structural pattern in hybrid tissues, demonstrating the adaptability and innovation possible within the realm of 3D bioprinting.

6.5 Printing a Section of the Heart Wall

Bioprinting of a section of the heart wall involves a complex and precise process to replicate the structure and function of native cardiac tissue. The heart wall comprises three main layers (endocardium, myocardium, and epicardium), for which the selection of biomaterials that serve as the scaffold for the cells has already been examined and chosen in response to the characteristics they will mimic. The cells that correspond to the ones in the heart wall include cardiomyocytes, endothelial cells, and fibroblasts. These cells can be added to the biomaterial prior to the printing

process. Since research around the bioprinting of the heart wall is still a new phenomenon, the focus was on the technique of the printing process rather than the testing of cell adhesion. However, the entire printing process was examined and optimized with an understanding of cell safety, meaning further research can be conducted using the process outcomes with the cells without needing adjustments in terms of cell livelihood through printing.

The printing process consisted of first printing the epicardium using the alginate biomaterial, and then the nanofiber was printed second as the myocardium layer and hybrid biomaterial was printed last as the endocardium layer. The printed outcome with these allocations is shown in the picture below.

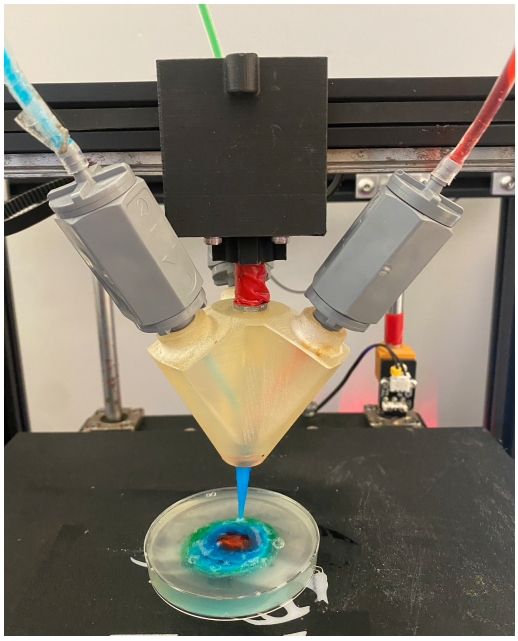

Figure 6.10 Printing of the final layer of the fabricated heart wall tissue.

The printing process of the hybrid tissue was the same as the FRESH printing process, with the printing of the gelatin support material. Once the print was complete, it was allowed to be set and crosslinked in the gelatin slurry overnight. To remove the printed structure, the dish with the gelatin slurry and the print were submerged in 36℃ PBS. The temperature of the wash fluid is important to quickly dissipate the gelatin slurry without compromising the structural integrity of the printed structure. Figure 6.11 shows the printed structure at different steps in the printing process.

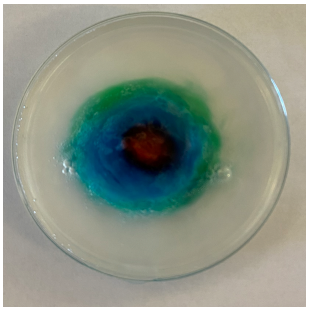

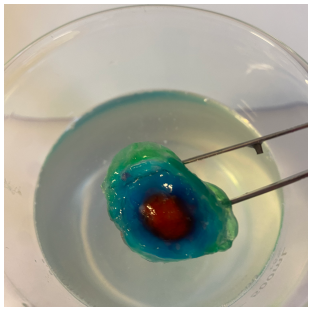

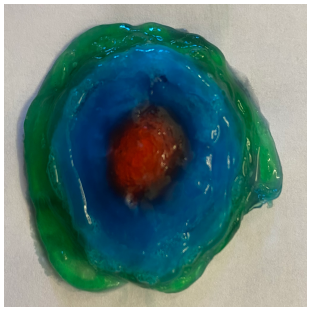

(a) (b) (c)

Figure 6.11 Printing process of hybrid tissue: (a) printed structure after crosslinking, (b) printed structure after washing, and (c) final finished product.

One of the key observations during the setting process of the biomaterial was the gradual loss of color intensity over time when the biomaterial was immersed in the gelatin slurry. This phenomenon was highlighted in a trial run using a single drop of food colouring is shown in figure 6.12, where it was noted that by the end of the printing cycle, both biomaterials appeared almost identical in colour. While this colour change may not be a critical issue for the primary purpose of bioprinting, which is the creation of organs for transplants, it presents a challenge when attempting to differentiate between different tissue sections and evaluate the feasibility of hybrid tissue creation. To address this issue, a recommendation was made to add six or more drops of food coloring to the various biomaterials. This approach ensures that the colours remain distinct within the biomaterial throughout the printing process, facilitating the evaluation of different tissue sections and enhancing the ability to create hybrid tissues.

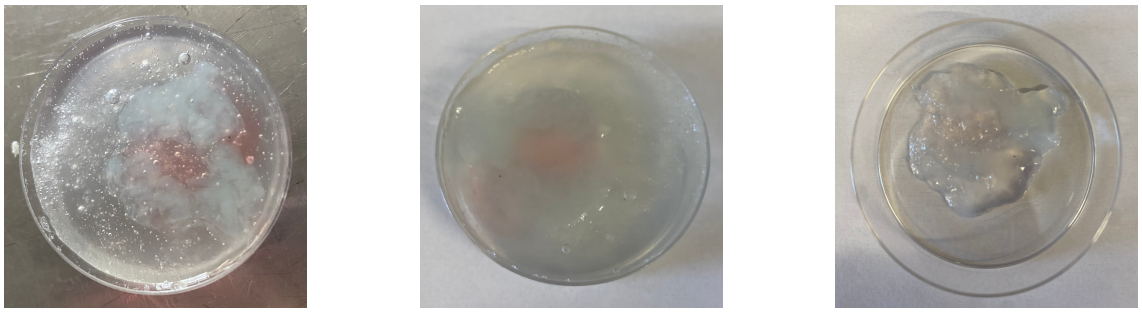

(a) (b) (c)

Figure 6.12 Printing process of hybrid tissue: (a) printed structure after the printing process, (b) printed structure after crosslinking, and (c) final finished product.

One of the challenges encountered during horizontal printing was exemplified in the third layer, where the hybrid biomaterial exhibited sagging and deformation compared to the other two material printing. Interestingly, this issue was not observed when testing with only two materials, suggesting that adding the third material contributed to this outcome. The sagging and deformation of the hybrid biomaterial could be attributed to its lower viscosity, which may have hindered its ability to maintain its shape as effectively as the other materials when setting in the support material. The properties of the biomaterial, such as its viscosity and gelation kinetics, play a crucial role in determining its behaviour during printing and post-printing. In this case, the lower viscosity of the hybrid biomaterial may have resulted in insufficient structural support, leading to sagging and deformation. This highlights the importance of carefully selecting and optimizing the properties of each biomaterial to ensure compatibility and prevent issues, especially when creating hybrid tissue constructs.

To address this challenge, several strategies can be employed. One approach is to modify the composition of the hybrid biomaterial to increase its viscosity and improve its structural integrity. This can be achieved by adjusting the concentration of the biomaterial components or incorporating additives that enhance viscosity and gelation properties.

Additionally, optimizing the printing parameters, such as the extrusion rate and temperature, can help minimize sagging and deformation by ensuring proper deposition and support of the biomaterial during printing.

Overall, the sagging and deformation of the hybrid biomaterial serve as a valuable learning experience, highlighting the importance of understanding and optimizing the properties of each biomaterial in multi-material printing. By addressing these challenges, the precision and reliability of horizontal printing for creating complex, multi-material tissues with tailored properties for various tissue engineering applications can be enhanced.

6.6 Cell Integration

To test for the cell distribution during the hybrid tissue bioprinting process, fluorescent microbeads were added to biomaterial. The use of fluorescent beads represents dead cells since they are similar in size. These beads can accurately represent how the cells would be distributed in the different materials post printing. As well as it could give feedback on how the pressure from the printer can affect the cells. This is an important factor for cell viability.

6.6.1 Material Consistency Changes

To accommodate for the cell integration, the biomaterial was made with Dulbecco's Modified Eagle's Medium. The medium supports the growth of mammalian cells. It has a variety of nutrients that supports all cell types making the cells grow faster, increase their productivity, increase their consistency and lastly it also creates easier purification.

Figure 6.13 Medium and fluorescent microbeads used for cell representation.

However, the use of the two materials changed the consistency of the biomaterial as well as the original colour scheme. The colours changed due to the pink colour of the medium. The biomaterials were created with the same steps as outlined in the methodologies section with the exception of the alginate receiving food colouring as the medium already creates a pinkish-red colour for the biomaterial. The consistency was similar to the biomaterial made using PBS but once the material came to a room temperature setting had a thicker gel consistency. The materials, including the hybrid biomaterial were able to hold their own weight during the printing process much better than the in the showcased results of the support material tests without the materials having cell integration.

6.6.2 Printed Tissue Construct

The materials were then used to fabricate the hybrid tissue layout created previously. However, with the biomaterial differences, the finished product had better material distribution and shape than previously. Showcasing that the addition of the cells and the medium benefited the printing process while not adding pressure to the procedure.

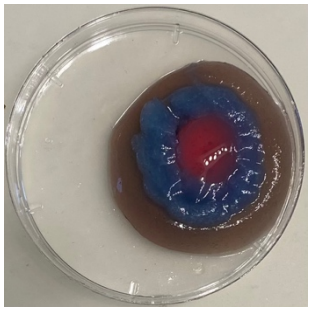

Figure 6.14 Printed hybrid tissue using cell viable medium and fluorescent microbeads.

The hybrid and alginate biomaterial had a smooth layer finish. However, the nanofiber material was not able to distribute as the other materials and as previously printed without the cell viable medium and microbeads. Thus, the material will need to be further developed to have the similar finish and levelling of the other two materials with cell addition.

6.6.3 Distribution of Cells

The three material was tested pre and post printing to see the distribution differences between crosslinking. A microscope from Echo was used to conduct the tests at a 2x magnification. The results showcased that the crosslinking did not affect the distribution of the materials.

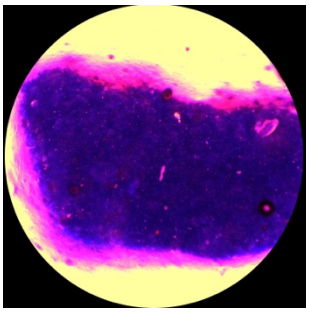

a)

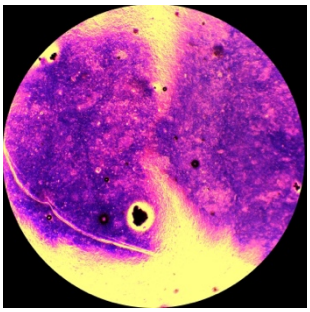

b)

Figure 6.15 The distribution of the microbeads in alginate a) pre-crosslinked and b) post-crosslinked.

The next step was to see the distribution differences between the three materials post-crosslinked using a fluorescent microscope to better highlight the fluorescent beads in the material. Using a fluorescent microscope by Zeiss, the particles were analyzed at three settings, 2x, 10x and 20x magnification to see the different distributions in the material and as well as the distances between the particles.

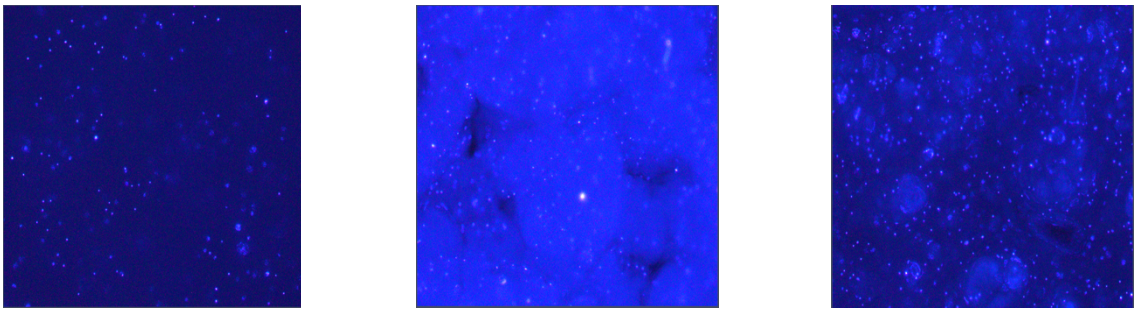

a) b) c)

Figure 6.16Biomaterials with fluorescent beads at 2x magnification a) alginate, b) nanofiber, and c) hybrid biomaterial.

At 2x magnification it was showcased the density of the beads inside of the biomaterials. The results showed that the alginate had the least amount of cell retention while the hybrid biomaterial had the highest cell retention after printing. This could be result of the material having better cell retention characteristics. Materials with gelatin have higher cell retention rates, which can be seen for both the nanofiber and the hybrid material.

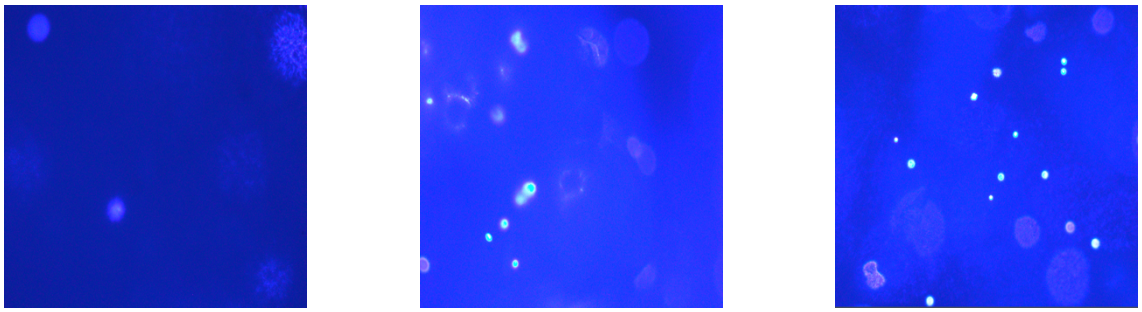

a) b) c)

Figure 6.17 Biomaterials with fluorescent beads at 10x magnification a) alginate, b) nanofiber, and c) hybrid biomaterial.

At the 10x magnification, the clusters of the beads were examined to see how they act inside of the different materials. Alginate have less particles in clusters, and less clusters around the printed structure. Nanofiber had more clusters located around with visibly more particles. Lastly, the hybrid biomaterial had the most amount of beads in a cluster and had multiple clusters around.

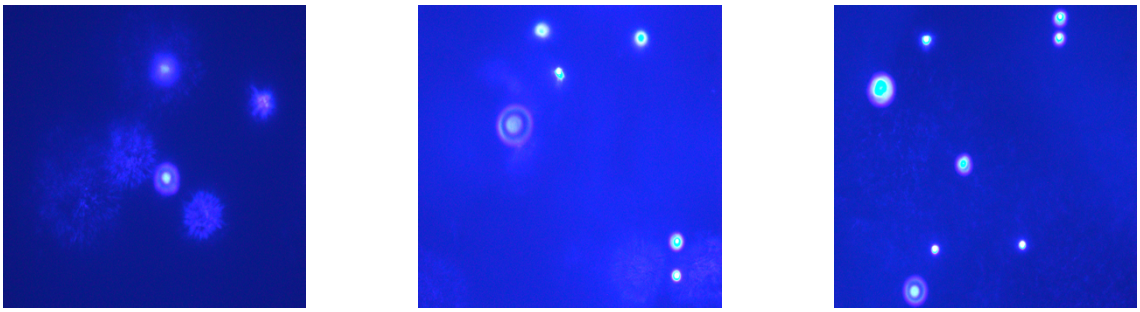

a) b) c)

Figure 6.18 Biomaterials with fluorescent beads at 20x magnification a) alginate, b) nanofiber, and c) hybrid biomaterial.

A 20x magnification was used to see the distances of the beads to predict the reactions and distances between cells in a small parameter. The distances between the beads varied however, it was common to have a minimum of two beads close to each other. The beads for alginate were less spread out and had a less number of cells than the other material.

a) b)

Figure 6.19 Cell retention at the material boarders, a) alginate with nanofiber and b) nanofiber with the hybrid biomaterial.

The cell retention at the different material boarders were also examined using the fluorescent beads. The results show how the cells react to the different materials mixing. For the boarder with alginate and nanofiber, majority of the cells from the alginate migrated towards the boarder with the nanofiber biomaterial. The hybrid biomaterial and nanofiber boarder also had the same reaction where the beads representing the cells had a higher concentrations at the boarder.

6.7 Conclusion

Hybrid tissue fabrication using 3D bioprinting holds profound significance in the context of organ transplantation for several compelling reasons. Firstly, it addresses the critical shortage of donor organs, a persistent challenge in transplantation medicine. Harnessing bioprinting technology to fabricate hybrid tissues composed of biomaterials and patient-derived cells offers a promising solution to overcome the limitations of organ availability, potentially reducing transplant waiting lists and saving countless lives. Secondly, hybrid tissue fabrication enables the customization of tissue constructs to match the specific anatomical and immunological needs of individual patients. Traditional organ transplantation often necessitates immunosuppressive therapy to prevent rejection, which poses risks of complications and compromises the patient's overall health. With bioprinting, personalized tissue constructs can be engineered using the patient's own cells, mitigating the risk of rejection and obviating the need for lifelong immunosuppression. This customized approach enhances transplant success rates and improves long-term patient outcomes. Additionally, hybrid tissue fabrication using 3D bioprinting enables the development of alternative transplant options for patients ineligible for conventional organ transplantation. For individuals with complex medical conditions, congenital abnormalities, or previous transplant failures, bioprinted tissue constructs offer a viable therapeutic alternative that circumvents the limitations of traditional transplantation. By providing tailored solutions to meet the unique needs of each patient, hybrid tissue fabrication expands the scope of transplantation medicine and offers hope to those in need of life-saving

interventions. Moreover, hybrid tissue fabrication provides the possibility of creating functional tissue constructs with enhanced physiological properties and organ-specific functionalities. Bioprinting techniques allow for the precise deposition of multiple cell types, growth factors, and biomaterials to replicate the intricate structure and function of native tissues and organs. By mimicking the microarchitecture and cellular composition of natural tissues, bioprinted hybrid constructs exhibit improved integration, vascularization, and functionality, leading to more successful organ transplants and better patient outcomes. Furthermore, bioprinted cardiac tissue constructs exhibit enhanced physiological properties and functionalities compared to conventional synthetic materials. By precisely arranging multiple cell types, extracellular matrix components, and biomaterials, bioprinting enables the recreation of the complex microenvironment of the heart. These bioprinted constructs can exhibit electrical conductivity, contractility, and vascularization, which are crucial for supporting cardiac function and integration post-transplantation. Additionally, bioprinted cardiac tissues can serve as in vitro models for drug screening, disease modelling, and cardiac regenerative therapies, accelerating research and innovation in the field of cardiology.

The study was able to address these issues by evaluating different biomaterial characteristics to select the one that matches the different cardiac wall layers.

6.7.1 Limitations

Hybrid tissue bioprinting, particularly when employing three or fewer materials and utilizing the FRESH bioprinting method, faces several limitations. One major constraint lies in achieving precise spatial control and integration of multiple cell types and biomaterials within the printed construct. Coordinating the deposition of different biomaterials while maintaining structural integrity and cell viability poses significant challenges, particularly given the need for optimal printing parameters for each material. Additionally, ensuring proper crosslinking and compatibility among the various components during the printing process is crucial yet intricate. There is also the limitation in available compatible biomaterials for FRESH bioprinting, which has suitable rheological properties and biocompatibility for hybrid tissue bioprinting, further restricting the versatility and applicability of this approach. Overcoming these limitations demands advancements in biomaterial formulation, printing techniques, and process optimization strategies to enhance the precision, reproducibility, and functionality of hybrid tissue constructs.

6.7.2 Future Work

While the section of the cardiac wall was successfully printed, there could be further improvements in terms of printing layout. For example, the horizontal circular printing layout was chosen due to the printer's capabilities while also looking for a pattern that is similar to the heart wall layout. However, if possible, a vertical layered layout would better suit the fabrication of heart wall tissue. To accomplish that, the printer needs to be optimized for the material’s swelling as well as the crosslinking speed to ensure it does not swell around the needle encompassing it and/or solidify around the needle where the following material instead of extruded above gets extruded inside of the first material.

Furthermore, if the vertical printing properties are examined successfully, they can be further explored by creating a semi-circular layout where the materials are layered vertically, as shown in Figure 6.4. When looking at an anatomical heart, all three printing styles are needed to print the structure.

Chapter 7 Conclusions and Future Works

This thesis has embarked on an in-depth investigation into the potential of 3D bioprinting for the fabrication of hybrid cardiac tissues, employing the FRESH bioprinting technique. The research has been guided by the objective of replicating the complex structure and function of the cardiac wall, aiming to contribute to the advancements in regenerative medicine and organ transplantation. Herein, we summarize our findings, discuss the implications, acknowledge the limitations, and propose directions for future research.

7.1 Summary of Research Findings

In the first objective of biomaterial selection and characterization, the study successfully identified specific biomaterials for replicating the distinct layers of the heart wall. The materials for the layers are the following: alginate for the epicardium, nanofiber for the myocardium, and a hybrid of alginate and gelatin for the endocardium. These materials were chosen based on their rheological properties, biocompatibility, and mechanical characteristics pre- and post-crosslinking, aligning closely with the native properties of each cardiac layer. As well as the material characteristic need for the different live cells native in each heart wall layer.

Then in terms of the second objective of printer adaptation, significant strides were made in modifying a conventional 3D printer to support the FRESH bioprinting technique, with a focus on printing hybrid cardiac tissues using multiple materials. An original printhead capable of handling three biomaterials simultaneously was developed, enabling seamless material switching without leaving the print site, thus addressing calibration challenges and improving printing efficiency. The integration of one-way valves into the printhead design effectively prevented backflow, allowing for the flexible printing of individual or multiple materials. Adjustments to the printer setup, including custom syringe holders and optimized pipe diameters, were critical in reducing printing pressure to maintain cell viability. Sterilization and maintenance protocols were established to ensure cell viability. Despite facing challenges such as ensuring layer adhesion and maintaining structural integrity, solutions such as printhead design modifications and printing parameter optimizations were identified.

Then for the third objective on the printing process, revealed critical insights into optimizing bioprinting for hybrid cardiac tissue fabrication. Key advancements included the development of tailored G-code setups and slicer adjustments to accommodate the unique rheological properties of biomaterials, ensuring precise control over the deposition process. The chapter highlighted the crucial role of sterilization practices in maintaining cell safety and viability, underscoring the importance of a sterile printing environment. Challenges such as the need for rapid material crosslinking without compromising structural integrity were addressed through innovative approaches like adjusting calcium concentrations in the gelatin slurry. However, the balance between crosslinking speed and maintaining the intended structure proved complex, leading to the adoption of the original calcium concentration for overnight setting.

Lastly, the fourth objective of hybrid tissue fabrication utilizing 3D bioprinting techniques offered promising advancements in the replication of cardiac wall structures, emphasizing the selection of biomaterials to match distinct

heart layers and the incorporation of multiple materials for improved mimicry of tissue layers. This chapter demonstrated the ability to fabricate sections of the heart wall, achieving a structured composition that closely resembles the natural cardiac tissue through careful material selection and innovative printing strategies, such as horizontal printing and material encompassing techniques. Despite facing challenges such as achieving precise spatial control, maintaining structural integrity, and ensuring cell viability, the research identified viable solutions, including optimizing printing layouts and material properties.

7.2 Impact

The research described in the thesis holds a significant impact due to its multifaceted contributions to the field of bioprinting. By targeting existing research gaps in areas such as material selection, hybrid tissue formation, bioprinter capabilities, and process optimization, the study addresses several existing research gaps within the field of bioprinting, contributing novel insights that aim to bridge these disparities, furthering the advancement of tissue engineering and regenerative medicine. Through the introduction of novel findings and innovative approaches, such as the evaluation of new biomaterials for cardiac tissue engineering and the adaptation of bioprinting technology for FRESH bioprinting, the research pushes the boundaries of bioprinting technology and expands the possibilities for creating complex tissue architectures with enhanced functionalities.

Firstly, the research focuses on material selection for cardiac wall tissue engineering, an area where a comprehensive understanding of suitable biomaterials is crucial for successful tissue regeneration. By systematically evaluating various biomaterials, including alginate, nanofibers, and hybrid bioinks, the study offers valuable insights into the properties and characteristics required for mimicking the complex structure and functionality of the cardiac wall. Secondly, the thesis explores the formation of hybrid tissues, an innovative approach that combines different biomaterials to create constructs with enhanced properties and functionalities. This novel concept not only expands the repertoire of available biomaterials for bioprinting but also opens new avenues for creating tissue constructs with tailored properties, such as improved mechanical strength, biocompatibility, and cell adhesion.

Furthermore, the study introduces a bioprinter with hybrid tissue fabrication capabilities using the FRESH bioprinting method. This adaptation of existing bioprinting technology allows for the simultaneous extrusion of multiple materials from a single extrusion point, enabling the fabrication of complex tissue architectures with high precision and resolution. The integration of FRESH bioprinting methods into the bioprinter enhances its versatility and applicability for tissue engineering applications, particularly in the context of cardiac tissue regeneration.

Lastly, the thesis focuses on optimizing the bioprinting process with a specific emphasis on ensuring the structural stability of the printed materials. This optimization involves fine-tuning printing parameters, such as extrusion pressure, nozzle diameter, and printing speed, to achieve optimal printing outcomes while maintaining the structural integrity of the printed constructs. By addressing this critical aspect of bioprinting, the study enhances the reliability and reproducibility of bioprinted tissue constructs, paving the way for their potential translation into clinical applications.

With direct implications for clinical practice, the study offers potential solutions to pressing healthcare challenges, including the shortage of donor organs and the need for personalized tissue constructs. Moreover, its translational potential is underscored by its implications for the development of bioengineered tissues for transplantation, disease modelling, and drug screening. Finally, the research contributes to the scientific knowledge base in the field of bioprinting, generating new insights, methodologies, and techniques that can inform future research endeavours and accelerate the translation of tissue engineering innovations from the laboratory to the clinic, ultimately benefiting patients in need of regenerative therapies.

7.3 Limitations and Future Directions

The study faced limitations related to the optimization of the bioprinting process for multi-material applications, the need for controlled yet accelerated crosslinking methods, and achieving the dynamic mechanical properties of the cardiac wall. One significant drawback is the accuracy with which different biomaterials and cell types can be integrated and controlled in space within a printed structure. This is further complicated by the requirement that components work well together during the printing process. Furthermore, choosing biomaterials that work with the FRESH bioprinting method is difficult and limits how versatile the process can be. Progress in biomaterial science, the creation of more advanced bioprinting technologies, and improved process optimization techniques are required to overcome these constraints. These limitations present opportunities for further research, especially towards the development of innovative biomaterials, refining bioprinting techniques, and incorporating cellular components into bioprinted constructs for in vivo functionality evaluation.

The thesis also outlines avenues for further investigation, some future directions for research include improving the printer's design to allow for vertical, layered printing that more closely resembles the structure of the heart wall, investigating materials that can solidify faster without sacrificing structural integrity, and maybe implementing a heated biomaterial chamber to control temperature-sensitive bioprinting processes. These paths not only hold the potential to surmount the existing obstacles but also to enhance the potential applications of bioprinting in cardiac tissue engineering and regenerative medicine.

7.4 Concluding Remarks

In conclusion, the research effectively accomplished all originally established goals by seamlessly combining various elements to create a portion of the heart wall through the utilization of a modified 3D bioprinter. This section of the heart wall consisted of three separate layers of tissue. The seamless creation of complex tissue structures was made possible by this printer's unique ability to extrude multiple materials through a single nozzle. All areas of the study have room for improvement, but the limitations that have been noted and the directions that have been suggested for further research offer a clear path for future investigations.

The materials selected were proven compatible with the FRESH bioprinting technique, accurately representing the various layers of the cardiac wall. The bioprinter, designed for this particular use, demonstrated promising functionality; however, additional improvements are required to support a wider range of materials and to attain higher printing precision. The FRESH printing process was optimized to the unique requirements of the materials and the

printer, and different printing and material formulation strategies were investigated to determine the best course of action. At the end of the project, a cardiac wall section was successfully bioprinted using a circular pattern to mimic the layered structure of the heart. This approach was determined by the need to replicate the heart's natural wall resemblance while also taking into account the printing technology's limitations.

This thesis establishes a strong basis for further research and constitutes a significant advancement in the field of 3D bioprinting for cardiac tissue engineering. Even though there are still difficulties, the potential shown by this study highlights the fascinating opportunities that lie ahead. The dream of bioprinted cardiac tissues for individualized medical applications and treating heart diseases is getting closer to reality as our understanding and technological capabilities grow, ushering in a new era in regenerative medicine.

References

[1] Denolin, H., Kuhn, H., Krayenbuehl, H., Loogen, F., & Reale, A. (1983). The definition of heart failure. European Heart Journal, 4(7), 445–448. https://doi.org/10.1093/oxfordjournals.eurheartj.a061500

[2] Ponikowski, P., Voors, A. A., Anker, S. D., Bueno, H., Cleland, J. G., Coats, A. J., ... Filippatos, G. (2016). 2016 ESC Guidelines for the diagnosis and treatment of acute and chronic heart failure: The Task Force for the diagnosis and treatment of acute and chronic heart failure of the European Society of Cardiology (ESC). European Journal of Heart Failure, 18(8), 891–975.

[3] Braunwald, E. (2019). Heart failure. JACC: Heart Failure, 7(8), 692–693.

[4] Masenga, S. K., & Kirabo, A. (2023). Hypertensive heart disease: Risk factors, complications and mechanisms. Frontiers in Cardiovascular Medicine, 10. https://doi.org/10.3389/fcvm.2023.1205475

[5] Cowie, M. R., et al. (1997). The epidemiology of heart failure. European Heart Journal, 18(2), 208–225. https://doi.org/10.1093/oxfordjournals.eurheartj.a015223

[6] Lister, Z., Rayner, K. J., & Suuronen, E. J. (2016). How biomaterials can influence various cell types in the repair and regeneration of the heart after myocardial infarction. Frontiers in Bioengineering and Biotechnology, https://doi.org/10.3389/fbioe.2016.00062

[7] National Heart, Lung, and Blood Institute. (2020). Heart failure. Retrieved from https://www.nhlbi.nih.gov/health-topics/heart-failure

[8] Allbrook, D. (1981). Skeletal muscle regeneration. Muscle & Nerve, 4(3), 234–245. https://doi.org/10.1002/mus.880040311

[9] Mercola, M., Ruiz-Lozano, P., & Schneider, M. D. (2011). Cardiac muscle regeneration: Lessons from development. Genes & Development, 25(4), 299–309. https://doi.org/10.1101/gad.2018411

[10] Bowen, R. E. S., Graetz, T. J., Emmert, D. A., & Avidan, M. S. (2020). Statistics of heart failure and mechanical circulatory support in 2020. Annals of Translational Medicine, 8(13). https://doi.org/10.21037/atm-20-1127

[11] Public Health Agency of Canada. (2017). Heart disease in Canada: Highlights from the Canadian Chronic Disease Surveillance System, 2017. Retrieved from https://www.canada.ca/en/public-health/services/publications/diseases-conditions/heart-disease-canada-fact-sheet.html

[12] National Heart, Lung, and Blood Institute. (2020). Heart failure. Retrieved from https://www.nhlbi.nih.gov/health-topics/heart-failure

[13] Morris, J. H., & Chen, L. (2019). Exercise training and heart failure: A review of the literature. Cardiac Failure Review, 5(1), 57–61. https://doi.org/10.15420/cfr.2018.31.1

[14] O'Connor, C. M., et al. (2009). Efficacy and safety of exercise training in patients with chronic heart failure: HF-ACTION randomized controlled trial. JAMA: Journal of the American Medical Association, 301(14), 1439–1450. https://doi.org/10.1001/jama.2009.454

[15] Ambrosy, A. P., et al. (2014). The global health and economic burden of hospitalizations for heart failure: Lessons learned from hospitalized heart failure registries. Journal of the American College of Cardiology, 63(12), 1123–1133. https://doi.org/10.1016/j.jacc.2013.11.053

[16] Mohammadi, S., Hedjazi, A., Sajjadian, M., Ghoroubi, N., Mohammadi, M., & Erfani, S. (2016). Study of the normal heart size in northwest part of Iranian population: A cadaveric study. Journal of Cardiovascular and Thoracic Research, 8(3), 119–125. https://doi.org/10.15171/jcvtr.2016.25

[17] Gray, H. (2005). Gray's Anatomy (39th ed.). London: Churchill; pg 997-1003.

[18] U.S. Department of Health and Human Services. (n.d.). Structure of the heart. Structure of the Heart | SEER Training. Retrieved February 24, 2023, from https://training.seer.cancer.gov/anatomy/cardiovascular/heart/structure.html

[19] Quijada, P., Trembley, M. A., & Small, E. M. (2020). The role of the epicardium during heart development and repair. Circulation Research, 126(3), 377–394. https://doi.org/10.1161/circresaha.119.315857

[20] Gun, L. (2023). Epicardium: What is it, functions, and more. Epicardium: What Is It, Functions, and More. Retrieved February 25, 2023, from https://www.osmosis.org/answers/epicardium

[21] Gray, G., Toor, I., Castellan, R., Crisan, M., & Meloni, M. (2018). Resident cells of the myocardium: More than spectators in cardiac injury, repair and Regeneration. Current Opinion in Physiology, 1, 46–51. https://doi.org/10.1016/j.cophys.2017.08.001

[22] Kowalczyk, A. P., & Green, K. J. (2013). Structure, function, and regulation of desmosomes. Progress in Molecular Biology and Translational Science. Retrieved February 24, 2023, from https://www.ncbi.nlm.nih.gov/pmc/articles/PMC4336551/

[23] MediLexicon International. (n.d.). Cardiac muscle tissue: Definition, function, and structure. Medical News Today. Retrieved February 24, 2023, from https://www.medicalnewstoday.com/articles/325530

[24] Bionity. (n.d.). Endocardium. Retrieved February 24, 2023, from https://www.bionity.com/en/encyclopedia/Endocardium.html

[25] Khan, S., Fakhouri, F., Majeed, W., & Kolipaka, A. (2017). Cardiovascular magnetic resonance elastography: A review. NMR in Biomedicine, 31(10). https://doi.org/10.1002/nbm.3853

[26] Arani A, Glaser KL, Arunachalam SP, et al. (2017). In vivo, high-frequency three-dimensional cardiac MR elastography: Feasibility in normal volunteers. Magnetic Resonance in Medicine, 77, 351–360. https://doi.org/10.1002/mrm.26101

[27] Feiner, R., Shapira, A., & Dvir, T. (2019). Scaffolds for tissue engineering of functional cardiac muscle. In M. Mozafari, F. Sefat, & A. Atala (Eds.), Handbook of Tissue Engineering Scaffolds: Volume One (pp. 685–703). Woodhead Publishing. https://doi.org/10.1016/B978-0-08-102563-5.00032-0

[28] Jett, S., Laurence, D., Kunkel, R., Babu, A. R., Kramer, K., Baumwart, R., Towner, R., Wu, Y., & Lee, C.-H. (2018). An investigation of the anisotropic mechanical properties and anatomical structure of porcine atrioventricular heart valves. Journal of the Mechanical Behavior of Biomedical Materials, 87, 155–171. https://doi.org/10.1016/j.jmbbm.2018.07.024

[29] Thomas. (2018). 3D printed jellyfish robots created to monitor fragile coral reefs. 3D Printer and 3D Printing News. Retrieved from http://www.3ders.org/articles/20181003-3d-printed-jellyfish-robots-created-to-monitor-fragile-coral-reefs.html

[30] Shahrubudin, N., Lee, T. C., & Ramlan, R. (2019). An overview on 3D printing technology: Technological, materials, and applications. Procedia Manufacturing, 35, 1286–1296. https://doi.org/10.1016/j.promfg.2019.06.089

[31] Syed, A. M. T., Elias, P. K., Amit, B., Susmita, O., Lisa, O., & Charitidis, C. (2017). Additive manufacturing: Scientific and technological challenges, market uptake and opportunities. Materials Today, 1, 1-16.

[32] He, Y., Gu, Z., Xie, M., Fu, J., & Lin, H. (2020). Why choose 3D bioprinting? part II: Methods and bioprinters. Bio-Design and Manufacturing, 3(1), 1–4. https://doi.org/10.1007/s42242-020-00064-w

[33] He, Y., Xie, M., Gao, Q., & Fu, J. (2019). Why choose 3D bioprinting? Part I: A brief introduction of 3D bioprinting for the beginners. Bio-Design and Manufacturing, 2(4), 221–224. https://link.springer.com/article/10.1007/s42242-019-00053-8

[34] Zhu, W., Ma, X., Gou, M., Mei, D., Zhang, K., & Chen, S. (2016). 3D printing of functional biomaterials for tissue engineering. Current Opinion in Biotechnology, 40, 103-112. doi:10.1016/j.copbio.2016.03.014

[35] Li, J., Chen, M., Fan, X., & Zhou, H. (2016). Recent advances in bioprinting techniques: [35] Approaches, applications and future prospects. Journal of Translational Medicine, 14(1). https://doi.org/10.1186/s12967-016-1028-0

[36] Hoehne, J. L., Carlstron, R., Dernorwsek, J., Cristovam, P. C., Bachiega, H. L., Abensur, S. I., & Schor, P. (2020). Piezoelectric 3D bioprinting for ophthalmological applications: Process development and viability analysis of the technology. Biomedical Physics & Engineering Express, 6(3), 035021. https://doi.org/10.1088/2057-1976/ab7bf9

[37] Chan, W. W., Yeo, D. C. H., Tan, V., Singh, S., Choudhury, D., & Naing, M. W. (2020). Additive biomanufacturing with collagen inks. Bioengineering, 7(3), 1-23. doi:10.3390/bioengineering7030066

[38] Das, S., & Basu, B. (2019). An overview of hydrogel-based biomaterials for 3D bioprinting of soft tissues. Journal of the Indian Institute of Science, 99(3), 405-428.

[39] Jones, N. (2012). Science in three dimensions: The print revolution. Nature, 487(7405), 22–23.

[40] Li, J., Chen, M., Fan, X., & Zhou, H. (2016). Recent advances in bioprinting techniques: Approaches, applications and future prospects. Journal of Translational Medicine, 14(1). https://doi.org/10.1186/s12967-016-1028-0

[41] Jana, S., & Lerman, A. (2015). Bioprinting a cardiac valve. Biotechnology Advances, 33, 1503–1521. doi: 10.1016/j.biotechadv.2015.07.006.

[42] Okamoto, T., Suzuki, T., & Yamamoto, N. (2000). Microarray fabrication with covalent attachment of DNA using bubble jet technology. Nature Biotechnology, 18, 438–441. doi: 10.1038/74507.

[43] Xu, T., Jin, J., Gregory, C., Hickman, J. J., & Boland, T. (2005). Inkjet printing of viable mammalian cells. Biomaterials, 26, 93–99. doi: 10.1016/j.biomaterials.2004.04.011.

[44] Hockaday, L. A., Kang, K. H., Colangelo, N. W., Cheung, P. Y., Duan, B., Malone, E., ... & Bonassar, L. J. (2012). Rapid 3D printing of anatomically accurate and mechanically heterogeneous aortic valve hydrogel scaffolds. Biofabrication, 4(3), 035005. doi: 10.1088/1758-5082/4/3/035005.

[45] Duan, B., Hockaday, L. A., Kang, K. H., & Butcher, J. T. (2013). 3D bioprinting of heterogeneous aortic valve conduits with alginate/gelatin hydrogels. Journal of Biomedical Materials Research Part A, 101(5), 1255-1264. doi: 10.1002/jbm.a.34420.

[46] Chien, K. B., & Shah, R. N. (2013). Three-dimensional printing of soy protein scaffolds for tissue regeneration. Tissue Engineering Part C: Methods, 19(6), 417-426. doi: 10.1089/ten.tec.2012.0383.

[47] Chien, K. B., Aguado, B. A., Bryce, P. J., & Shah, R. N. (2013). In vivo acute and humoral response to three-dimensional porous soy protein scaffolds. Acta Biomaterialia, 9(9), 8983-8990. doi: 10.1016/j.actbio.2013.07.005.

[48] Haberstroh, K., Ritter, K., Kuschnierz, J., Bormann, K. H., Kaps, C., Carvalho, C., ... & Gellrich, N. C. (2010). Bone repair by cell-seeded 3D-bioplotted composite scaffolds made of collagen treated tricalciumphosphate or tricalciumphosphate-chitosan-collagen hydrogel or PLGA in ovine critical-sized calvarial defects. Journal of [47] Biomedical Materials Research Part B: Applied Biomaterials, 93(2), 520-530. doi: 10.1002/jbm.b.31611.

[49] Lim, T. C., Chian, K. S., & Leong, K. F. (2010). Cryogenic prototyping of chitosan scaffolds with controlled micro and macro architecture and their effect on in vivo neo-vascularization and cellular infiltration. Journal of Biomedical Materials Research Part A, 94, 1303–1311.

[50] Guillemot, F., Souquet, A., Catros, S., Guillotin, B., Lopez, J., & Faucon, M. (2010). High-throughput laser printing of cells and biomaterials for tissue engineering. Acta Biomaterialia, 6, 2494–2500. doi:10.1016/j.actbio.2009.09.029

[51] Barron, J. A., Wu, P., Ladouceur, H. D., & Ringeisen, B. R. (2004). Biological laser printing: A novel technique for creating heterogeneous 3-dimensional cell patterns. Biomedical Microdevices, 6, 139–147. doi:10.1023/B:BMMD.0000031751.67267.9f

[52] Ringeisen, B. R., Kim, H., Barron, J. A., Krizman, D. B., Chrisey, D. B., Jackman, S., ... & Spargo, B. J. (2004). Laser printing of pluripotent embryonal carcinoma cells. Tissue Engineering, 10, 483–491. doi:10.1089/107632704323061843

[53] Ali, M., Pages, E., Ducom, A., Fontaine, A., & Guillemot, F. (2014). Controlling laser-induced jet formation for bioprinting mesenchymal stem cells with high viability and high resolution. Biofabrication, 6, 045001. doi:10.1088/1758-5082/6/4/045001

[54] Klebe, R. (1988). Cytoscribing: A method for micropositioning cells and the construction of two- and three-dimensional synthetic tissues. Experimental Cell Research, 179(2), 362–373. https://doi.org/10.1016/0014-4827(88)90275-3

[55] Wilson, W. C., Jr., & Boland, T. (2003). Cell and organ printing 1: Protein and cell printers. Anatomical Record. Part A, Discoveries in Molecular, Cellular, and Evolutionary Biology, 272, 491–496.

[56] Mironov, V., Boland, T., Trusk, T., Forgacs, G., & Markwald, R. R. (2003). Organ printing: Computer-aided jet-based 3D tissue engineering. Trends in Biotechnology, 21(4), 157–161.

[57] Gao, Q., He, Y., Fu, J. Z., Liu, A., & Ma, L. (2015). Coaxial nozzle-assisted 3D bioprinting with built-in microchannels for nutrients delivery. Biomaterials, 61, 203–215.

[58] Hinton, T. J., Jallerat, Q., Palchesko, R. N., Park, J. H., Grodzicki, M. S., Shue, H. J., ... & Feinberg, A. W. (2015). Three-dimensional printing of complex biological structures by freeform reversible embedding of suspended hydrogels. Science Advances, 1(9).

[59] Highley, C. B., Rodell, C. B., & Burdick, J. A. (2015). Direct 3D printing of shear-thinning hydrogels into self-healing hydrogels. Advanced Materials, 27(34), 5075–5079.

[60] Bhattacharjee, T., Zehnder, S. M., Rowe, K. G., Jain, S., Nixon, R. M., Sawyer, W. G., & Angelini, T. E. (2015). Writing in the granular gel medium. Science Advances, 1(8), e1500655.

[61] Pyo, S. H., Wang, P., Hwang, H. H., Zhu, W., Warner, J., & Chen, S. (2017). Continuous optical 3D printing of green aliphatic polyurethanes. ACS Applied Materials & Interfaces, 9(1), 836–844.

[62] Huang, H. W., et al. (2019). Advances in biomimetic stimuli responsive soft grippers. Nano Convergence, 6(1), 494–503.

[63] Sapoznik, E., Niu, G., Nomi, M., Wang, Z., & Soker, S. (2015). Regeneration of the vascular system. Translational Regenerative Medicine.

[64] Gao, B., Yang, Q., Zhao, X., Jin, G., Ma, Y., & Xu, F. (2016). 4D bioprinting for biomedical applications. Trends in Biotechnology, 34(12), 746–756. http://dx.doi.org/10.1016/J. TIBTECH.2016.03.004.

[65] Kakisis, J.D., Liapis, C.D., Breuer, C., & Sumpio, B.E. (2005). Artificial blood vessel: the Holy Grail of peripheral vascular surgery. Journal of Vascular Surgery, 41(2), 349–354.

[66] Kang, H.W., et al. (2016). A 3D bioprinting system to produce human-scale tissue constructs with structural integrity. Nature Biotechnology, 34(3), 312–319.

[67] Samfors, S., Karlsson, K., Sundberg, J., Markstedt, K., & Gatenholm, P. (2014). Regeneration of the vascular system. Circulation Journal, 78, 323–350.

[68] Shiwarski, D.J., Hudson, A.R., Tashman, J.W., & Feinberg, A.W. (2021). Emergence of FRESH 3D printing as a platform for advanced tissue biofabrication. APL Bioengineering, 5(1), Article 011504. doi:10.1063/5.0032777

[69] Vaezi, M., & Yang, S. (2015). Extrusion-based additive manufacturing of PEEK for biomedical applications. Virtual and Physical Prototyping, 10(2), 123–135.

[70] Vaezi, M., Seitz, H., & Yang, S. (2013). A review on 3D micro-additive manufacturing technologies. International Journal of Advanced Manufacturing Technology, 67(5-8), 1721–1754.

[71] Corbett, D.C., Olszewski, E., & Stevens, K. (2019). A FRESH take on resolution in 3D bioprinting. Trends in Biotechnology, 37(11), 1153–1155. https://doi.org/10.1016/j.tibtech.2019.09.003

[72] Bahram, M., Mohseni, N., & Moghtader, M. (2016). An Introduction to Hydrogels and Some Recent Applications. IntechOpen. doi:10.5772/64301

[73] Fedorovich, N.E., Alblas, J., de Wijn, J.R., Hennink, W.E., Verbout, A.J., & Dher, W.J.A. (2007). Hydrogels as Extracellular Matrices for Skeletal Tissue Engineering: State-of-the-Art and Novel Application in Organ Printing. Tissue Engineering, 13(8), 1905–1925. doi:10.1089/ten.2006.0175

[74] Lee, A., Hudson, A.R., Shiwarski, D.J., Tashman, J.W., Hinton, T.J., Yerneni, S., ... Feinberg, A.W. (2019). 3D bioprinting of collagen to rebuild components of the human heart. Science, 365(6452), 482−487.

[75] Dasgupta, Q., & Black, L.D., 3rd. (2019). A FRESH SLATE for 3D bioprinting. Science, 365, 446–447.

[76] Gregorian, B., et al. (2019). Multivascular networks and functional intravascular topologies within biocompatible hydrogels. Science, 364, 458–464.

[77] Kelly, B.E., et al. (2019). Volumetric additive manufacturing via tomographic reconstruction. Science, 363, 1075–1079.

[78] Madden, L.R., et al. (2010). Proangiogenic scaffolds as functional templates for cardiac tissue engineering. Proceedings of the National Academy of Sciences of the United States of America, 107(34), 15211–15216.

[79] Olsson, A.K., et al. (2006). VEGF receptor signalling – in control of vascular function. Nature Reviews Molecular Cell Biology, 7(5), 359–371.

[80] Benning, L., Gutzweiler, L., Tröndle, K., Riba, J., Zengerle, R., Koltay, P., ... Finkenzeller, G. (2018). Assessment of hydrogels for bioprinting of endothelial cells. Journal of Biomedical Materials Research Part A, 106(4), 935-947. doi:10.1002/jbm.a.36291

[81] Gungor-Ozkerim, P.S., Inci, I., Zhang, Y.S., Khademhosseini, A., & Dokmeci, M.R. (2018). Biomaterials for 3D bioprinting: An overview. Biomaterials Science, 6(5), 915-946. doi:10.1039/c7bm00765e

[82] Antich, C., de Vicente, J., Jimenez, G., Chocarro, C., Carrillo, E., Montanez, E., Galvez-Martin, P., & Marchal, J.A. (2020). Bio-inspired hydrogel composed of hyaluronic acid and alginate as a potential biomaterial for 3D bioprinting of articular cartilage engineering constructs. Acta Biomaterialia, 106, 114-123. doi:10.1016/j.actbio.2020.01.046

[83] Krishnakumar, G.S., Sampath, S., Muthusamy, S., & John, M.A. (2019). Importance of crosslinking strategies in designing smart biomaterials for Bone Tissue Engineering: A systematic review. Materials Science and Engineering: C, 96, 941–954. https://doi.org/10.1016/j.msec.2018.11.081

[84] Haugh, M.G., Jaasma, M.J., & O'Brien, F.J. (2009). The effect of dehydrothermal treatment on the mechanical and structural properties of collagen-GAG scaffolds. Journal of Biomedical Materials Research Part A, 89(2), 363–369.

[85] Gomes, S.R., Rodrigues, G., Martins, G.G., Henriques, C.M., & Silva, J.C. (2013). In vitro evaluation of crosslinked electrospun fish gelatin scaffolds. Materials Science and Engineering: C Materials for Biological Applications, 33(3), 1219–1227.

[86] Ratanavaraporn, J., Rangkupan, R., Jeeratawatchai, H., Kanokpanont, S., & Damrongsakkul, S. (2010). Influences of physical and chemical crosslinking techniques on electrospun type A and B gelatin fiber mats. International Journal of Biological Macromolecules, 47(4), 431–438.

[87] Nitzsche, H., Lochmann, A., Metz, H., Hauser, A., Syrowatka, F., Hempel, E., ... Müller, T. (2010). Fabrication and characterization of a biomimetic composite scaffold for bone defect repair. Journal of Biomedical Materials Research Part A, 94(1), 298–307.

[88] Tierney, C.M., Haugh, M.G., Liedl, J., Mulcahy, F., Hayes, B., & O'Brien, F.J. (2009). The effects of collagen concentration and crosslink density on the biological, structural and mechanical properties of collagen-GAG scaffolds for bone tissue engineering. Journal of the Mechanical Behavior of Biomedical Materials, 2(2), 202–209.

[89] Kamakura, S., Sasaki, K., Honda, Y., Anada, T., Matsui, K., Echigo, S., & Suzuki, O. (2007). Dehydrothermal treatment of collagen influences on bone regeneration by octa-calcium phosphate (OCP) collagen composites. Journal of Tissue Engineering and Regenerative Medicine, 1(6), 450–456.

[90] Wahl, D.A., Sachlos, E., Liu, C., & Czernuszka, J.T. (2007). Controlling the processing of collagen-hydroxyapatite scaffolds for bone tissue engineering. Journal of Materials Science: Materials in Medicine, 18(2), 201–209.

[91] Davidenko, N., Bax, D.V., Schuster, C.F., Farndale, R.W., Hamaia, S.W., & Best, S.M. (2016). Optimization of UV irradiation as a binding site conserving method for crosslinking collagen-based scaffolds. Journal of Materials Science: Materials in Medicine, 27(1), 14.

[92] Kubyshkina, G., Zupančič, B., Štukelj, M., Grošelj, D., Marion, L., & Emri, I. (2011). The influence of different sterilization techniques on the time-dependent behaviour of polyamides. Journal of Biomedical Nanotechnology, 2, 361–368.

[93] Lew, D.H., Liu, P.H., & Orgill, D.P. (2007). Optimization of UV cross-linking density for durable and nontoxic collagen GAG dermal substitute. Journal of Biomedical Materials Research Part B: Applied Biomaterials, 82(1), 51–56.

[94] Poldervaart, M.T., Goversen, B., de Ruijter, M., Abbadessa, A., Melchels, F.P.W., Öner, F.C., ... Alblas, J. (2017). 3D bioprinting of methacrylated hyaluronic acid (MeHA) hydrogel with intrinsic osteogenicity. PLoS One, 12(6), e0177628.

[95] Tsai, W.B., Chen, Y.R., Li, W.T., Lai, J.Y., Liu, H.L. (2012). RGD-conjugated UV-crosslinked chitosan scaffolds inoculated with mesenchymal stem cells for bone tissue engineering. Carbohydrate Polymers, 89(2), 379–387.

[96] Shimojo, A.A., de Souza Brissac, I.C., Pina, L.M., Lambert, C.S., Santana, M.H. (2015). Sterilization of auto-crosslinked hyaluronic acid scaffolds structured in microparticles and sponges. Biomedical Materials Engineering, 26(3–4), 183–191.

[97] George, J., Kuboki, Y., Miyata, T. (2006). Differentiation of mesenchymal stem cells into osteoblasts on honeycomb collagen scaffolds. Biotechnology and Bioengineering, 95(3), 404–411.

[98] Lin, W.H., Yu, J., Chen, G., Tsai, W.B. (2016). Fabrication of multi-biofunctional gelatin-based electrospun fibrous scaffolds for enhancement of osteogenesis of mesenchymal stem cells. Colloids and Surfaces B: Biointerfaces, 138, 26–31.

[99] Parenteau Bareil, R., Gauvin, R., Berthod, F. (2010). Collagen-based biomaterials for tissue engineering applications. Materials, 3(3), 1863–1887.

[100] Bigi, A., Cojazzi, G., Panzavolta, S., Rubini, K., Roveri, N. (2001). Mechanical and thermal properties of gelatin films at different degrees of glutaraldehyde crosslinking. Biomaterials, (8), 763–768.

[101] Bigi, A., Cojazzi, G., Panzavolta, S., Roveri, N., Rubini, K. (2002). Stabilization of gelatin films by crosslinking with genipin. Biomaterials, (24), 4827–4832.

[102] Reddy, N., Reddy, R., Jiang, Q. (2015). Crosslinking biopolymers for biomedical applications. Trends in Biotechnology, 33(6), 362–369.

[103] Nicoletti, A., Fiorini, M., Paolillo, J., Dolcini, L., Sandri, M., Pressato, D. (2013). Effects of different crosslinking conditions on the chemical-physical properties of a novel bio-inspired composite scaffold stabilized with 1,4-butanediol diglycidyl ether (BDDGE). Journal of Materials Science: Materials in Medicine, 24(1), 17–35.

[104] Bock, N., Riminucci, A., Dionigi, C., Russo, A., Tampieri, A., Landi, E., ... Marcacci, M. (2010). A novel route in bone tissue engineering: magnetic biomimetic scaffolds. Acta Biomaterialia, 6(3), 786–796.

[105] Tampieri, A., Iafisco, M., Sandri, M., Panseri, S., Cunha, C., Sprio, S., ... Herrmannsdörfer, T. (2014). Magnetic bioinspired hybrid nanostructured collagen-hydroxyapatite scaffolds supporting cell proliferation and tuning regenerative process. ACS Applied Materials & Interfaces, 6(18), 15697–15707.

[106] Minardi, S., Corradetti, B., Taraballi, F., Sandri, M., Van Eps, J., Cabrera, F.J., ... Tasciotti, E. (2015). Evaluation of the osteoinductive potential of a bio-inspired scaffold mimicking the osteogenic niche for bone augmentation. Biomaterials, 62, 128–137.

[107] Calabrese, G., Giuffrida, R., Fabbi, C., Figallo, E., Lo Furno, D., Gulino, R., ... Forte, S. (2016). Collagen-hydroxyapatite scaffolds induce human adipose-derived stem cells osteogenic differentiation in vitro. PLoS One, 11(3), e0151181.

[108] Bang, S., Das, D., Yu, J., Noh, I. (2017). Evaluation of MC3T3 cells proliferation and drug release study from sodium hyaluronate-1,4-butanediol diglycidyl ether patterned gel. Nanomaterials, 7(10).

[109] Michael, F. Butler, Yiu-Fai Ng, D.A. Paul. (2003). Mechanism and kinetics of the crosslinking reaction between biopolymers containing primary amine groups and genipin. Journal of Polymer Science Part A: Polymer Chemistry, 41(24), 3941–3953.

[110] Tonda-Turo, C., Gentile, P., Saracino, S., Chiono, V., Nandagiri, V.K., Muzio, G., Canuto, R.A., Ciardelli, G. (2011). Comparative analysis of gelatin scaffolds crosslinked by genipin and silane coupling agent. International Journal of Biological Macromolecules, 49(4), 700–706.

[111] Madhavan, K., Belchenko, D., Motta, A., Tan, W. (2010). Evaluation of composition and crosslinking effects on collagen-based composite constructs. Acta Biomaterialia, 6(4), 1413–1422.

[112] Fessel, G., Cadby, J., Wunderli, S., Weeren, R., Snedeker, J.G. (2014). Dose- and time-dependent effects of genipin crosslinking on cell viability and tissue mechanics – toward clinical application for tendon repair. Acta Biomaterialia, 10(5), 1897–1906.

[113] Wang, C., Lau, T.T., Loh, W.L., Su, K., Wang, D.A. (2011). Cytocompatibility study of a natural biomaterial crosslinker-Genipin with therapeutic model cells. Journal of Biomedical Materials Research Part B: Applied Biomaterials, 97(1), 58–65.

[114] Nam, K., Kimura, T., Kishida, A. (2008). Controlling coupling reaction of EDC and NHS for preparation of collagen gels using ethanol/water co-solvents. Macromolecular Bioscience, 8, 32–37.

[115] Cammarata, C.R., Hughes, M.E., Ofner, C.M. (2015). Carbodiimide induced cross-linking, ligand addition, and degradation in gelatin. Molecular Pharmaceutics, 12(3), 783–793.

[116] Bax, D.V., Davidenko, N., Gullberg, D., Hamaia, S.W., Farndale, R.W., Best, S.M., Cameron, R.E. (2017). Fundamental insight into the effect of carbodiimide crosslinking on cellular recognition of collagen-based scaffolds. Acta Biomaterialia, 49, 218–234.

[117] OldeDamink, L.H.H., Dijkstra, P.J., Luyn, M.J.A., Wachem, P.B., Nieuwenhuis, P., Feijen, J. (1995). Cross-linking of dermal sheep collagen using a water-soluble carbodiimide. Journal of Materials Science: Materials in Medicine, 6(8), 460–472.

[118] Pieper, J.S., Hafmans, T.J., Veerkamp, H., Van Kuppevelt, T.H. (2000). Development of tailor-made collagen–glycosaminoglycan matrices: EDC/NHS crosslinking, and ultrastructural aspects. Biomaterials, 21, 581–593.

[119] Davidenko, N., Schuster, C.F., Bax, D.V., Raynal, N., Farndale, R.W., Best, S.M., Cameron, R.E. (2015). Control of crosslinking for tailoring collagen-based scaffolds stability and mechanics. Acta Biomaterialia, 25, 131–142.

[120] Li, C.Q., Huang, B., Luo, G., Zhang, C.Z., Zhuang, Y., Zhou, Y. (2010). Construction of collagen II/hyaluronate/chondroitin-6-sulfate tri-copolymer scaffold for nucleus pulposus tissue engineering and preliminary analysis of its physico-chemical properties and biocompatibility. Journal of Materials Science: Materials in Medicine, 21(2), 741–751.

[121] Teixeira, S., Fernandes, M.H., Ferraz, M.P., Monteiro, F.J. (2010). Proliferation and mineralization of bone marrow cells cultured on macroporous hydroxyapatite scaffolds functionalized with collagen type I for bone tissue regeneration. Journal of Biomedical Materials Research Part A, 95(1), 1–8.

[122] Sun, H., Zhu, F., Hu, Q., Krebsbach, P.H. (2014). Controlling stem cell-mediated bone regeneration through tailored mechanical properties of collagen scaffolds. Biomaterials, 35(4), 1176–1184.

[123] Vorrapakdee, R., Kanokpanont, S., Ratanavaraporn, J., Waikakul, S., Charoenlap, C., Damrongsakkul, S. (2013). Modification of human cancellous bone using Thai silk fibroin and gelatin for enhanced osteoconductive potential. Journal of Materials Science: Materials in Medicine, 24(3), 735–744.

[124] Rodriguez, I.A., Sell, S.A., McCool, J.M., Saxena, G., Spence, A.J., Bowlin, G.L. (2013). A preliminary evaluation of lyophilized gelatin sponges, enhanced with platelet-rich plasma, hydroxyapatite and chitin whiskers for bone regeneration. Cell, 2(2), 244–265.

[125] Rodriguez, I., Saxena, G., Sell, S., Bowlin, G. (2014). Mineralization and characterization of composite lyophilized gelatin sponges intended for early bone regeneration. Bioengineering (Basel), 1, 62–84.

[126] Rodriguez, I.A., Saxena, G., Hixon, K.R., Sell, S.A., Bowlin, G.L. (2016). In vitro characterization of MG-63 osteoblast-like cells cultured on organic-inorganic lyophilized gelatin sponges for early bone healing. Journal of Biomedical Materials Research Part A, 104(8), 2011–2019.

[127] Goudouri, O.M., Vogel, C., Grünewald, A., Detsch, R., Kontonasaki, E., Boccaccini, A.R. (2016). Sol-gel processing of novel bioactive Mg-containing silicate scaffolds for alveolar bone regeneration. Journal of Biomaterials Applications, 30(6), 740–749.

[128] Lode, A., Meyer, M., Brüggemeier, S., Paul, B., Baltzer, H., Schröpfer, M., Winkelmann, C., Sonntag, F., Gelinsky, M. (2016). Additive manufacturing of collagen scaffolds by three-dimensional plotting of highly viscous dispersions. Biofabrication, 8(1), 015015.

[129] Jaligama, S., Po-Jung, H., Kameoka, J. (2016). Novel 3D coaxial flow-focusing nozzle device for the production of monodispersed collagen microspheres. Proceedings of the Annual International Conference of the IEEE Engineering in Medicine and Biology Society, EMBS, 2016, 4220–4223.

[130] Das, A., Fishero, B.A., Christophel, J.J., Li, C.J., Kohli, N., Lin, Y., Dighe, A.S., Cui, Q. (2016). Poly(lactic-co-glycolide) polymer constructs cross-linked with human BMP-6 and VEGF protein significantly enhance rat mandible defect repair. Cell and Tissue Research, 364(1), 125–135.

[131] Kaczmarek, B., Sionkowska, A., Kozlowska, J., Osyczka, A.M. (2018). New composite materials prepared by calcium phosphate precipitation in chitosan/collagen/hyaluronic acid sponge cross-linked by EDC/NHS. International Journal of Biological Macromolecules, 107, 247–253.

[132] Kumar, A., Nune, K.C., Misra, R.D.K. (2017). Design and biological functionality of a novel hybrid Ti-6Al-4V/hydrogel system for reconstruction of bone defects. Journal of Tissue Engineering and Regenerative Medicine, 12(4), 1133–1144.

[133] Carpena, N.T., Abueva, C.D.G., Padalhin, A.R., Lee, B.T. (2017). Evaluation of egg white ovomucin-based porous scaffold as an implantable biomaterial for tissue engineering. Journal of Biomedical Materials Research Part B: Applied Biomaterials, 105(7), 2107–2117.

[134] Greenberg, C.S., Birckbichler, P.J., Rice, R.H. (1991). Transglutaminases: multifunctional cross-linking enzymes that stabilize tissues. The FASEB Journal, 5, 3071–3077.

[135] Aeschlimann, D., Paulsson, M. (1994). Transglutaminases: protein cross-linking enzymes in tissues and body fluids. Thrombosis and Haemostasis, 71, 402–415.

[136] Orban, J.M., Wilson, L.B., Kofroth, J.A., El-Kurdi, M.S., Maul, T.M., Vorp, D.A. (2004). Crosslinking of collagen gels by transglutaminase. Journal of Biomedical Materials Research Part A, 68(4), 756–762.

[137] Halloran, D.M., Collighan, R.J., Griffin, M., Pandit, A.S. (2006). Characterization of a microbial transglutaminase cross-linked type II collagen scaffold. Tissue Engineering, 12(6), 1467–1474.

[138] Motoki, M., & Seguro, K. (1998). Transglutaminase and its use for food processing. Trends in Food Science & Technology, 9(5), 204–210.

[139] Collighan, R., Cortez, J., & Griffin, M. (2002). The biotechnological applications of transglutaminases. Minerva Biotechnology, 14, 143–148.

[140] Szondy, Z., Korponay-Szabó, I., Király, R., Sarang, Z., & Tsay, G.J. (2017). Transglutaminase 2 in human diseases. Biomedicine (Taipei), 7(3), 1–13.

[141] Oh, H.H., U, T., Isamu, Y., Toshiyuki, I.T., & Junzo. (2015). Effect of enzymatically cross-linked tilapia scale collagen for osteoblastic differentiation of human mesenchymal stem cells. Journal of Bioactive and Compatible Polymers, 31(1), 31–41.

[142] Ciardelli, G., Gentile, P., Chiono, V., Mattioli-Belmonte, M., Vozzi, G., Barbani, N., & Giusti, P. (2010). Enzymatically crosslinked porous composite matrices for bone tissue regeneration. Journal of Biomedical Materials Research Part A, 92(1), 137–151.

[143] Mentink, C.J., Hendriks, M., Levels, A.A., & Wolffenbuttel, B.H. (2002). Glucose-mediated cross-linking of collagen in rat tendon and skin. Clinical Chimica Acta, 321, 69–76.

[144] Willems, N.M., Langenbach, G.E., Stoop, R., Toonder, J.M., Mulder, L., Zentner, A., & Everts, V. (2014). Higher number of pentosidine cross-links induced by ribose does not alter tissue stiffness of cancellous bone. Materials Science and Engineering: C Materials for Biological Applications, 42, 15–21.

[145] Francis-Sedlak, M.E., Moya, M.L., Huang, J.J., Lucas, S.A., Chandrasekharan, N., Larson, J.C., Cheng, M.H., & Brey, E.M. (2010). Collagen glycation alters neovascularization in vitro and in vivo. Microvascular Research, 80(1), 3–9.

[146] Siimon, K., Reemann, P., Põder, A., Pook, M., Kangur, T., Kingo, K., Jaks, V., Mäeorg, U., & Järvekülg, M. (2014). Effect of glucose content on thermally cross-linked fibrous gelatin scaffolds for tissue engineering. Materials Science and Engineering: C Materials for Biological Applications, 42, 538–545.

[147] Francis-Sedlak, M.E., Uriel, S., Larson, J.C., Greisler, H.P., Venerus, D.C., & Brey, E.M. (2009). Characterization of type I collagen gels modified by glycation. Biomaterials, 30(9), 1851–1856.

[148] Krishnakumar, G.S., Gostynska, N., Campodoni, E., Dapporto, M., Montesi, M., Panseri, S., Tampieri, A., Kon, E., Marcacci, M., Sprio, S., & Sandri, M. (2017). Ribose-mediated crosslinking of collagen-hydroxyapatite hybrid scaffolds for bone tissue regeneration using biomimetic strategies. Materials Science and Engineering: C Materials for Biological Applications, 77, 594–605.

[149] Lam, P.L., Kok, S.H., Bian, Z.X., Lam, K.H., Tang, J.C., Lee, K.K., Gambari, R., & Chui, C.H. (2014). D-Glucose as a modifying agent in gelatin/collagen matrix and reservoir nanoparticles for Calendula officinalis delivery. Colloids and Surfaces B: Biointerfaces, 117, 277–283.

[150] Baskin, J.Z., Vasanji, A., McMasters, J., Soenjaya, Y., Barbu, A.M., & Eppell, S.J. (2012). Nanophase bone substitute in vivo response to subcutaneous implantation. Journal of Biomedical Materials Research Part A, 100(9), 2462–2473.

[151] Chiue, H., Yamazoye, T., & Matsumura, S. (2015). Localization of the dominant non-enzymatic intermolecular cross-linking sites on fibrous collagen. Biochemical and Biophysical Research Communications, 461, 445–449.

[152] Vicens-Zygmunt, V., Estany, S., Colom, A., Montes-Worboys, A., Machahua, C., Sanabria, A.J., Llatjos, R., Escobar, I., Manresa, F., Dorca, J., Navajas, D., Alcaraz, J., & Molina-Molina, M. (2015). Fibroblast viability and phenotypic changes within glycated stiffened three-dimensional collagen matrices. Respiratory Research, 16(82), 1–15.

[153] Fulden, U.-K. (2021). 3D bioprinting in medicine. Global Journal of Biotechnology and Biomaterial Science, 1–5. https://doi.org/10.17352/gjbbs.000015.

[154] Datta, P., Barui, A., Wu, Y., Ozbolat, V., Moncal, K. K., & Ozbolat, I. T. (2018). Essential steps in bioprinting: From pre- to post-bioprinting. Biotechnology Advances, 36(5), 1481–1504. https://doi.org/10.1016/j.biotechadv.2018.06.003.

[155] Appel, A. A., Anastasio, M. A., Larson, J. C., & Brey, E. M. (2013). Imaging challenges in biomaterials and tissue engineering. Biomaterials, 34, 6615–6630. https://doi.org/10.1016/j.biomaterials.2013.05.033.

[156] Nam, S. Y., Ricles, L. M., Suggs, L. J., & Emelianov, S. Y. (2014). Imaging strategies for tissue engineering applications. Tissue Engineering Part B: Reviews, 21, 1–44. https://doi.org/10.1089/ten.TEB.2014.0180.

[157] Teodori, L., Crupi, A., Costa, A., Diaspro, A., Melzer, S., & Tarnok, A. (2017). Three-dimensional imaging technologies: a priority for the advancement of tissue engineering and a challenge for the imaging community. Journal of Biophotonics, 10, 24–45. https://doi.org/10.1002/jbio.201600049.

[158] Ballyns, J. J., & Bonassar, L. J. (2009). Image-guided tissue engineering. Journal of Cellular and Molecular Medicine, 13, 1428–1436. https://doi.org/10.1111/j.1582-4934.2009.00836.x.

[159] Reiffel, A. J., Kafka, C., Hernandez, K. A., Popa, S., Perez, J. L., Zhou, S., ... Spector, J. A. (2013). High-fidelity tissue engineering of patient-specific auricles for reconstruction of pediatric microtia and other auricular deformities. PLoS One, 8(2), e56506. https://doi.org/10.1371/journal.pone.0056506.

[160] Iyer, S. R., Xu, S., Stains, J. P., Bennett, C. H., & Lovering, R. M. (2016). Superparamagnetic iron oxide nanoparticles in musculoskeletal biology. Tissue Engineering Part B: Reviews, 23, 373–385. https://doi.org/10.1089/ten.teb.2016.0437.

[161] Park, S. H., Kang, B. K., Lee, J. E., Chun, S. W., Jang, K., Kim, Y. H., ... Kim, H. J. (2017). Design and fabrication of a thin-walled free-form scaffold on the basis of medical image data and a 3D printed template: its potential use in bile duct regeneration. ACS Applied Materials & Interfaces, 9(14), 12290–12298. https://doi.org/10.1021/acsami.7b00849.

[162] Mycek, M.-A. (2015). Clinical translation of optical molecular imaging to tissue engineering: opportunities & challenges. In Optics in the Life Sciences, OSA Technical Digest. Optical Society of America. https://doi.org/10.1364/OTA.2015.OT1C.1.

[163] McCormick, M., Liu, X., Jomier, J., Marion, C., & Ibanez, L. (2014). ITK: enabling reproducible research and open science. Frontiers in Neuroinformatics, 8, 13. https://doi.org/10.3389/fninf.2014.00013.

[164] Sun, W., Starly, B., & Darling, A., Gomez, C. (2004). Computer-aided tissue engineering: application to biomimetic modelling and design of tissue scaffolds. Biotechnology and Applied Biochemistry, 39, 49. https://doi.org/10.1042/BA20030109.

[165] Larobina, M., & Murino, L. (2014). Medical image file formats. Journal of Digital Imaging, 27, 200–206. https://doi.org/10.1007/s10278-013-9657-9.

[166] Shen, H., Goldstein, A.S., & Wang, G. (2011). Biomedical imaging and image processing in tissue engineering. In N. Pallua & C.V. Suscheck (Eds.), Tissue Engineering (pp. 155–178). Springer Berlin Heidelberg. https://doi.org/10.1007/978-3-642-02824-3_9.

[167] Xu, S., Mundra, P.A., Li, H., Zhu, S., Welsch, R.E., & Rajapakse, J.C. (2013a). Image analysis for cellular and tissue engineering. In H. Yu & N.A.A. Rahim (Eds.), Imaging in Cellular and Tissue Engineering (pp. 223). CRC Press.

[168] Xu, T., Zhao, W., Zhu, J., Albanna, M.Z., Yoo, J.J., & Atala, A. (2013b). Complex heterogeneous tissue constructs containing multiple cell types prepared by inkjet printing technology. Biomaterials, 34, 130–139. https://doi.org/10.1016/j.biomaterials.2012.09.035.

[169] Lin, L., Zhang, H., Yao, Y., Tong, A., & Hu, Q. (2007). Application of image processing and finite element analysis in bionic scaffolds' design optimizing and fabrication. In K. Li, X. Li, G.W. Irwin, & G. He (Eds.), Life System Modeling and Simulation: International Conference, LSMS 2007 (pp. 136–145). Springer Berlin Heidelberg. https://doi.org/10.1007/978-3-540-74771-0_16.

[170] Mahmoud, S., Eldeib, A., & Samy, S. (2015). The design of 3D scaffold for tissue engineering using automated scaffold design algorithm. Australasian Physical & Engineering Sciences in Medicine, 38, 223–228. https://doi.org/10.1007/s13246-015-0339-4.

[171] Sudarmadji, N., Chua, C.K., & Leong, K.F. (2012). The development of computer-aided system for tissue scaffolds (CASTS) system for functionally graded tissue-engineering scaffolds. In M.A.K. Liebschner (Ed.), Computer-Aided Tissue Engineering (pp. 111–123). Humana Press. https://doi.org/10.1007/978-1-61779-764-4_7.

[172] Khoda, A.K.M., Ozbolat, I.T., & Koc, B. (2013). Designing heterogeneous porous tissue scaffolds for additive manufacturing processes. Computer-Aided Design, 45, 1507–1523. https://doi.org/10.1016/J.CAD.2013.07.003.

[173] Bücking, T.M., Hill, E.R., Robertson, J.L., Maneas, E., Plumb, A.A., & Nikitichev, D.I. (2017). From medical imaging data to 3D printed anatomical models. PLOS ONE, 12(5), e0178540. https://doi.org/10.1371/journal.pone.0178540.

[174] Coakley, M.F., Hurt, D.E., Weber, N., Mtingwa, M., Fincher, E.C., Alekseyev, V., ... Huyen, Y. (2014). The NIH 3D print exchange: a public resource for bioscientific and biomedical 3D prints. 3D Printing and Additive Manufacturing, 1, 137–140. https://doi.org/10.1089/3dp.2014.1503.

[175] Ozbolat, I.T., & Gudapati, H. (2016). A review on design for bioprinting. Bioprinting, 3–4, 1–14. https://doi.org/10.1016/j.bprint.2016.11.001.

[176] Requicha, A.G. (1980). Representations for rigid solids: theory, methods, and systems. ACM Computing Surveys, 12, 437–464. https://doi.org/10.1145/356827.356833.

[177] Ozbolat, I.T., & Koc, B. (2012a). 3D hybrid wound devices for spatiotemporally controlled release kinetics. Computer Methods and Programs in Biomedicine, 108, 922–931. https://doi.org/10.1016/j.cmpb.2012.05.004.

[178] Ozbolat, I.T., & Koc, B. (2012b). 3D hybrid wound devices for spatiotemporally controlled release kinetics. Computer Methods and Programs in Biomedicine, 108, 922–931. https://doi.org/10.1016/j.cmpb.2012.05.004.

[179] Afshar, M., Anaraki, A.P., Montazerian, H., & Kadkhodapour, J. (2016). Additive manufacturing and mechanical characterization of graded porosity scaffolds designed based on triply periodic minimal surface architectures. Journal of the Mechanical Behavior of Biomedical Materials, 62, 481–494. https://doi.org/10.1016/j.jmbbm.2016.05.027.

[180] Elomaa, L., Teixeira, S., Hakala, R., Korhonen, H., Grijpma, D.W., & Seppälä, J.V. (2011). Preparation of poly(ε-caprolactone)-based tissue engineering scaffolds by stereolithography. Acta Biomaterialia, 7, 3850–3856. https://doi.org/10.1016/j.actbio.2011.06.039.

[181] Melchels, F.P.W., Feijen, J., & Grijpma, D.W. (2009). A poly(d,l-lactide) resin for the preparation of tissue engineering scaffolds by stereolithography. Biomaterials, 30, 3801–3809. https://doi.org/10.1016/j.biomaterials.2009.03.055.

[182] Ćwikła, G., Grabowik, C., Kalinowski, K., Paprocka, I., & Ociepka, P. (2017). The influence of printing parameters on selected mechanical properties of FDM/FFF 3D-printed parts. IOP Conference Series: Materials Science and Engineering, 227, 012033. https://doi.org/10.1088/1757-899X/227/1/012033.

[183] Li, J.P., de Wijn, J.R., van Blitterswijk, C.A., & de Groot, K. (2010). The effect of scaffold architecture on properties of direct 3D fiber deposition of porous Ti6Al4V for orthopedic implants. Journal of Biomedical Materials Research Part A, 92, 33–42. https://doi.org/10.1002/jbm.a.32330.

[184] Lee, H., Koo, Y., Yeo, M., & Kim, G. H. (2017). Recent Cell printing systems for tissue engineering. International Journal of Bioprinting, 3, 27–41. https://doi.org/10.18063/IJB.2017.01.004.

[185] Lee, J., Kim, K. E., Bang, S., Noh, I., & Lee, C. (2017). A desktop multi-material 3D bioprinting system with open-source hardware and software. International Journal of Precision Engineering and Manufacturing, 18, 605–612. https://doi.org/10.1007/s12541-017-0072-x.

[186] Hinton, T.J., & Feinberg, A. (2016). 3D printing hydrogel and elastomer scaffolds in a fugitive support. In Frontiers in Bioengineering and Biotechnology Conference Abstract: 10th World Biomaterials Congress (p. 3031). https://doi.org/10.3389/conf.FBIOE.2016.01.03031.

[187] Akkouch, A., Yu, Y., & Ozbolat, I.T. (2015). Microfabrication of scaffold-free tissue strands for three-dimensional tissue engineering. Biofabrication, 7(3), 031002. https://doi.org/10.1088/1758-5090/7/3/031002.

[188] Jia, J., Richards, D.J., Pollard, S., Tan, Y., Rodriguez, J., Visconti, R.P., ... Mei, Y. (2014). Engineering alginate as biomaterial for bioprinting. Acta Biomaterialia, 10, 4323–4331. https://doi.org/10.1016/j.actbio.2014.06.034.

[189] Nicodemus, G.D., & Bryant, S.J. (2008). Cell encapsulation in biodegradable hydrogels for tissue engineering applications. Tissue Engineering Part B: Reviews, 14, 149–165. https://doi.org/10.1089/ten.teb.2007.0332.

[190] Jin, Y., Compaan, A., Bhattacharjee, T., & Huang, Y. (2016). Granular gel support-enabled extrusion of three-dimensional alginate and cellular structures. Biofabrication, 8(2), 025016.

[191] Derakhshanfar, S., Mbeleck, R., Xu, K., Zhang, X., Zhong, W., & Xing, M. (2018). 3D bioprinting for biomedical devices and tissue engineering: A review of recent trends and advances. Bioactive Materials, 3, 144–156. https://doi.org/10.1016/J.BIOACTMAT.2017.11.008.

[192] Yu, Y., Moncal, K.K., Li, J., Peng, W., Rivero, I., Martin, J.A., & Ozbolat, I.T. (2016). Three-dimensional bioprinting using self-assembling scalable scaffold-free “tissue strands” as a new biomaterial. Scientific Reports, 6, 28714. https://doi.org/10.1038/srep28714.

[193] Lee, H.-Y., Kim, H.-W., Lee, J.H., & Oh, S.H. (2015). Controlling oxygen release from hollow microparticles for prolonged cell survival under hypoxic environment. Biomaterials, 53, 583–591. https://doi.org/10.1016/J.BIOMATERIALS.2015.02.117.

[194] Rutz, A.L., Lewis, P.L., & Shah, R.N. (2017). Toward next-generation biomaterials: Tuning material properties pre- and post-printing to optimize cell viability. MRS Bulletin, 42, 563–570. https://doi.org/10.1557/mrs.2017.162.

[195] Matthew, J.E., Nazario, Y.L., Roberts, S.C., & Bhatia, S.R. (2002). Effect of mammalian cell culture medium on the gelation properties of Pluronic® F127. Biomaterials, 23, 4615–4619. https://doi.org/10.1016/S0142-9612(02)00208-9.

[196] Khattak, S.F., & Bhatia, S.R. (2005). Pluronic F127 as a cell encapsulation material: Utilization of membrane-stabilizing agents. Tissue Engineering, 11, 974–983. https://doi.org/10.1089/ten.2005.11.974.

[197] Murphy, S. V., & Atala, A. (2014). 3D bioprinting of tissues and organs. Nature Biotechnology, 32, 773–785. https://doi.org/10.1038/nbt.2958.

[198] Ouyang, L., Yao, R., Zhao, Y., & Sun, W. (2016). Effect of biomaterial properties on printability and cell viability for 3D bioplotting of embryonic stem cells. Biofabrication, 8, 035020. https://doi.org/10.1088/1758-5090/8/3/035020.

[199] Catros, S., Guillotin, B., Bacakova, M., Fricain, J.-C., & Guillemot, F. (2011). Effect of laser energy, substrate film thickness and biomaterial viscosity on viability of endothelial cells printed by laser-assisted bioprinting. Applied Surface Science, 257, 5142–5147. https://doi.org/10.1016/j.apsusc.2010.11.049.

[200] Dhariwala, B., Hunt, E., & Boland, T. (2004). Rapid prototyping of tissue-engineering constructs, using photopolymerizable hydrogels and stereolithography. Tissue Engineering, 10(9–10), 1316–1322.

[201] Fedorovich, N.E., Oudshoorn, M.H., van Geemen, D., Hennink, W.E., Alblas, J., & Dhert, W.J. (2009). The effect of photopolymerization on stem cells embedded in hydrogels. Biomaterials, 30, 344–353. https://doi.org/10.1016/j.biomaterials.2008.09.037.

[202] Wang, Z., Abdulla, R., Parker, B., Samanipour, R., Ghosh, S., & Kim, K. (2015). A simple and high-resolution stereolithography-based 3D bioprinting system using visible light crosslinkable biomaterials. Biofabrication, 7, 045009. https://doi.org/10.1088/1758-5090/7/4/045009.

[203] Obeng-Gyasi, S., Grimm, L.J., Hwang, E.S., & Klimberg, V.S. (2018). Indications and Techniques for Biopsy. In The Breast (5th ed., pp. 377–385). Elsevier. https://doi.org/10.1016/B978-0-323-35955-9.00028-3.

[204] Collins, S.F. (2014). Bioprinting is changing regenerative medicine forever. Stem Cells and Development, 23, 79–82. https://doi.org/10.1089/scd.2014.0322.

[205] Gruene, M., Pflaum, M., Deiwick, A., Koch, L., Schlie, S., Unger, C., ... Chichkov, B.N. (2011). Adipogenic differentiation of laser-printed 3D tissue grafts consisting of human adipose-derived stem cells. Biofabrication, 3. https://doi.org/10.1088/1758-5082/3/1/015005.

[206] Gruene, M., Deiwick, A., Koch, L., Schlie, S., Unger, C., Hofmann, N., ... Chichkov, B. (2011). Laser printing of stem cells for biofabrication of scaffold-free autologous grafts. Tissue Engineering Part C: Methods, 17(1), 79–87. http://dx.doi.org/10.1089/ten.TEC.2010.0359.

[207] Xu, F., Sridharan, B., Wang, S., Gurkan, U.A., Syverud, B., & Demirci, U. (2011). Embryonic stem cell bioprinting for uniform and controlled size embryoid body formation. Biomicrofluidics, 5(2), 22207. http://dx.doi.org/10.1063/1.3580752.

[208] Kurosawa, H. (2007). Methods for inducing embryoid body formation: In vitro differentiation system of embryonic stem cells. Journal of Bioscience and Bioengineering, 103(5), 389–398. http://dx.doi.org/10.1263/jbb.103.389.

[209] Tasoglu, S., & Demirci, U. (2013). Bioprinting for stem cell research. Trends in Biotechnology, 31(1), 10–19. http://dx.doi.org/10.1016/j.tibtech.2012.10.005.

[210] Youssef, A.A., Ross, E.G., Bolli, R., Pepine, C.J., & Leeper, N.J. (2016). The promise and challenge of induced pluripotent stem cells for cardiovascular applications. JACC: Basic to Translational Science, 1(6), 510–523. http://dx.doi.org/10.1016/j.jacbts.2016.06.010.

[211] Gao, F., Chiu, S.M., Motan, D.A.L., Zhang, Z., Chen, L., Ji, H.-L., … Lian, Q. (2016). Mesenchymal stem cells and immunomodulation: Current status and future prospects. Cell Death & Disease, 7, e2062. http://dx.doi.org/10.1038/cddis.2015.327.

[212] Irvine, S.A., & Venkatraman, S.S. (2016). Bioprinting and differentiation of stem cells. Molecules, 21(9), E1188.

[213] Madrigal, M., Rao, K.S., & Riordan, N.H. (2014). A review of therapeutic effects of mesenchymal stem cell secretions and induction of secretory modification by different culture methods. Journal of Translational Medicine, 12, 260. http://dx.doi.org/10.1186/s12967-014-0260-8.

[214] Cohen, D.E., & Melton, D. (2011). Turning straw into gold: Directing cell fate for regenerative medicine. Nature Reviews Genetics, 12(4), 243–252.

[215] Huang, P., Zhang, L., Gao, Y., He, Z., Yao, D., Wu, Z., ... Hui, L. (2014). Direct reprogramming of human fibroblasts to functional and expandable hepatocytes. Cell Stem Cell, 14(3), 370–384. http://dx.doi.org/10.1016/j.stem.2014.01.003.

[216] Ieda, M., Fu, J.-D., Delgado-Olguin, P., Vedantham, V., Hayashi, Y., ... Srivastava, D. (2010). Direct reprogramming of fibroblasts into functional cardiomyocytes by defined factors. Cell, 142(3), 375–386. http://dx.doi.org/10.1016/j.cell.2010.07.002.

[217] Darabi, R., Arpke, R.W., Irion, S., Dimos, J.T., Grskovic, M., ... Perlingeiro, R.C.R. (2012). Human ES- and iPS-derived myogenic progenitors restore DYSTROPHIN and improve contractility upon transplantation in dystrophic mice. Cell Stem Cell, 10(6), 610–619. http://dx.doi.org/10.1016/j.stem.2012.02.015.

[218] Pawlowski, M., Ortmann, D., Bertero, A., Tavares, J.M., Pedersen, R.A., & Vallier, L. (2017). Inducible and deterministic forward programming of human pluripotent stem cells into neurons, skeletal myocytes, and oligodendrocytes. Stem Cell Reports, 8(4), 803–812. http://dx.doi.org/10.1016/j.stemcr.2017.02.016.

[219] Sadelain, M., Papapetrou, E.P., & Bushman, F.D. (2011). Safe harbours for the integration of new DNA in the human genome. Nature Reviews Cancer, 12(1), 51–58. http://dx.doi.org/10.1038/nrc3179.

[220] Lukovic, D., Diez Lloret, A., Stojkovic, P., Rodríguez-Martínez, D., Perez Arago, M.A., Rodriguez-Jimenez, F.J., … Bhattacharya, S.S. (2017). Highly efficient neural conversion of human pluripotent stem cells in adherent and animal-free conditions. Stem Cells Translational Medicine, 6(4), 1217–1226. http://dx.doi.org/10.1002/sctm.16-0371.

[221] Nawroth, J.C., & Parker, K.K. (2013). Design standards for engineered tissues. Biotechnology Advances, 31(4), 632–637. http://dx.doi.org/10.1016/j.biotechadv.2012.12.005.

[222] Salih, V. (2013). Introduction. In S. Salih (Ed.), Standardisation in Cell and Tissue Engineering (pp. xxiii–xxvi). Woodhead Publishing. http://dx.doi.org/10.1016/B978-0-85709-419-3.50017-0.

[223] Dougherty, J., Schaefer, E., Nair, K., Kelly, J., & Masi, A. (2013). Repeatability, reproducibility, and calibration of the MyotonPro® on tissue mimicking phantoms. In SME 2013 Summer Bioengineering Conference, SBC 2013 (p. V01AT20A026). Sunriver, OR, United States. http://dx.doi.org/10.1115/SBC2013-14622.

[224] Cadena-Herrera, D., Esparza-De Lara, J.E., Ramírez-Ibañez, N.D., López-Morales, C.A., Pérez, N.O., Flores-Ortiz, L.F., & Medina-Rivero, E. (2015). Validation of three viable-cell counting methods: Manual, semi-automated, and automated. Biotechnology Reports, 7, 9–16. http://dx.doi.org/10.1016/j.btre.2015.04.004.

[225] Ke, N., Wang, X., Xu, X., & Abassi, Y.A. (2011). The xCELLigence system for real-time and label-free monitoring of cell viability. In M.J. Stoddart (Ed.), Mammalian Cell Viability: Methods and Protocols (pp. 33–43). Humana Press. http://dx.doi.org/10.1007/978-1-61779-108-6_6.

[226] Louis, K.S., & Siegel, A.C. (2011). Cell viability analysis using trypan blue: Manual and automated methods. In M.J. Stoddart (Ed.), Mammalian Cell Viability: Methods and Protocols (pp. 7–12). Humana Press. http://dx.doi.org/10.1007/978-1-61779-108-6_2.

[227] He, Y., Yang, F., Zhao, H., Gao, Q., Xia, B., & Fu, J. (2016). Research on the printability of hydrogels in 3D bioprinting. Scientific Reports, 6, 29977. http://dx.doi.org/10.1038/srep29977.

[228] Ozbolat, I. T., Moncal, K. K., & Gudapati, H. (2017). Evaluation of bioprinter technologies. Additive Manufacturing, 13, 179–200. http://dx.doi.org/10.1016/j.addma.2016.10.003

[229] Gudapati, H., Dey, M., & Ozbolat, I. (2016). A comprehensive review on droplet-based bioprinting: past, present and future. Biomaterials, 102, 20–42. https://doi.org/10.1016/j.biomaterials.2016.06.012.

[230] Li, J., Rossignol, F., & Macdonald, J. (2015). Inkjet printing for biosensor fabrication: Combining chemistry and technology for advanced manufacturing. Lab on a Chip, 15(13), 2538–2558. http://dx.doi.org/10.1039/C5LC00235D.

[231] Guillotin, B., Souquet, A., Catros, S., Duocastella, M., Pippenger, B., Bellance, S., ... Guillemot, F. (2010). Laser assisted bioprinting of engineered tissue with high cell density and microscale organization. Biomaterials, 31(28), 7250–7256. http://dx.doi.org/10.1016/j.biomaterials.2010.05.055.

[232] Blaeser, A., Duarte Campos, D.F., Puster, U., Richtering, W., Stevens, M.M., & Fischer, H. (2016). Controlling shear stress in 3D bioprinting is a key factor to balance printing resolution and stem cell integrity. Advanced Healthcare Materials, 5(3), 326–333. http://dx.doi.org/10.1002/adhm.201500677.

[233] Eagles, P.M., Qureshi, A., & Jayasinghe, S. (2006). Electrohydrodynamic jetting of mouse neuronal cells. Biochemical Journal, 394(2), 375–378. http://dx.doi.org/10.1042/BJ20051838.

[234] Gasperini, L., Maniglio, D., Motta, A., & Migliaresi, C. (2014). An electrohydrodynamic bioprinter for alginate hydrogels containing living cells. Tissue Engineering. Part C, Methods, 21(1-2), 123–132. http://dx.doi.org/10.1089/ten.tec.2014.0149.

[235] Landers, R., Hübner, U., Schmelzeisen, R., & Mülhaupt, R. (2002a). Rapid prototyping of scaffolds derived from thermoreversible hydrogels and tailored for applications in tissue engineering. Biomaterials, 23(20), 4437–4447. http://dx.doi.org/10.1016/S0142-9612(02)00139-4.

[236] Landers, R., Pfister, A., Hübner, U., John, H., Schmelzeisen, R., & Mülhaupt, R. (2002b). Fabrication of soft tissue engineering scaffolds by means of rapid prototyping techniques. Journal of Materials Science, 37(15), 3107–3116. http://dx.doi.org/10.1023/A:1016189724389.

[237] Skardal, A., Zhang, J., McCoard, L., Xu, X., Oottamasathien, S., & Prestwich, G.D. (2010a). Photocrosslinkable hyaluronan-gelatin hydrogels for two-step bioprinting. Tissue Engineering. Part A, 16(8), 2675–2685. http://dx.doi.org/10.1089/ten.tea.2009.0798.

[238] Billiet, T., Gevaert, E., De Schryver, T., Cornelissen, M., & Dubruel, P. (2014). The 3D printing of gelatin methacrylamide cell-laden tissue-engineered constructs with high cell viability. Biomaterials, 35, 49–62. http://dx.doi.org/10.1016/j.biomaterials.2013.09.078.

[239] Di Biase, M., Saunders, R.E., Tirelli, N., & Derby, B. (2011). Inkjet printing and cell seeding thermoreversible photocurable gel structures. Soft Matter, 7(6), 2639–2646. http://dx.doi.org/10.1039/C0SM00996B.

[240] Khalil, S., Nam, J., & Sun, W. (2005). Multi-nozzle deposition for construction of 3D biopolymer tissue scafFOLDS. RAPID PROTOTYPING JOURNAL, 11(1), 9–17. HTTP://DX.DOI.ORG/10.1108/13552540510573347.

[241] Ferris, C.J., Gilmore, K.J., Beirne, S., McCallum, D., Wallace, G.G., & in het Panhuis, M. (2013). Bio-ink for on-demand printing of living cells. Biomaterials Science, 1(2), 224–230. http://dx.doi.org/10.1039/C2BM00114D.

[242] Axpe, E., & Oyen, M.L. (2016). Applications of alginate-based biomaterials in 3D bioprinting. International Journal of Molecular Sciences, 17(12), 1976. http://dx.doi.org/10.3390/ijms17121976.

[243] Jin, Y., Liu, C., Chai, W., Compaan, A., & Huang, Y. (2017). Self-supporting nanoclay as internal scaffold material for direct printing of soft hydrogel composite structures in air. ACS Applied Materials & Interfaces, 9(20), 17456–17465. http://dx.doi.org/10.1021/acsami.7b03613.

[244] Jose, R. R., Rodriguez, M. J., Dixon, T. A., Omenetto, F., & Kaplan, D. L. (2016). Evolution of biomaterials and additive manufacturing technologies for 3D bioprinting. ACS Biomaterials Science & Engineering, 2, 1662–1668. https://doi.org/10.1021/acsbiomaterials.6b00088.

[245] Skardal, A., Zhang, J., & Prestwich, G.D. (2010b). Bioprinting vessel-like constructs using hyaluronan hydrogels crosslinked with tetrahedral polyethylene glycol tetracrylates. Biomaterials, 31(23), 6173–6184. http://dx.doi.org/10.1016/j.biomaterials.2010.04.045.

[246] Fitzsimmons, R. E. B., et al. (2018). Generating vascular channels within hydrogel constructs using an economical open-source 3D bio-printer and thermoreversible gels. Bioprinting, 9, 7–18. https://doi.org/10.1016/j.bprint.2018.02.001

[247] Thomas, A., et al. (2020). Vascular bioprinting with enzymatically degradable biomaterials via multi-material projection-based stereolithography. Acta Biomaterialia, 117, 121–132. https://doi.org/10.1016/j.actbio.2020.09.033

[248] Kahl, M., Gertig, M., Hoyer, P., FRIEDRICH, O., & GILBERT, D. F. (2019). ULTRA-LOW-COST 3D BIOPRINTING: MODIFICATION AND APPLICATION OF AN OFF-THE-SHELF DESKTOP 3D-PRINTER FOR BIOFABRICATION. FRONTIERS IN BIOENGINEERING AND BIOTECHNOLOGY. HTTPS://DOI.ORG/10.3389/FBIOE.2019.00184

[249] Krige, A., Haluška, J., Rova, U., & Christakopoulos, P. (2021). Design and implementation of a low cost bio-printer modification, allowing for switching between plastic and gel extrusion. HardwareX, 9, e00186. https://doi.org/10.1016/j.ohx.2021.e00186

[250] Engberg, A., Stelzl, C., Eriksson, O., O'Callaghan, P., & Kreuger, J. (2021). An open source extrusion bioprinter based on the E3D motion system and Tool Changer to enable fresh and multimaterial bioprinting. Scientific Reports, 11(1). https://doi.org/10.1038/s41598-021-00931-1

[251] Bharadwaj, S., Thanawala, R., Bon, G., Falcioni, R., & Prasad, G. L. (2005). Resensitization of breast cancer cells to anoikis by Tropomyosin-1: Role of Rho kinase-dependent cytoskeleton and adhesion. Oncogene, 24, 8291–8303. https://doi.org/10.1038/sj.onc.1208993

[252] Engberg, A., Stelzl, C., Eriksson, O., O'Callaghan, P., & Kreuger, J. (Year). An open-source extrusion bioprinter based on the E3D motion system and tool changer to enable FRESH and multimaterial bioprinting. Journal Name, Volume(Issue), Page range.

[253] Kolesky, D. B., Homan, K. A., Skylar-Scott, M. A., & Lewis, J. A. (2016). Three-dimensional bioprinting of thick vascularized tissues. Proceedings of the National Academy of Sciences, 113, 3179–3184. https://doi.org/10.1073/pnas.1521342113

[254] Liu, Y., et al. (2021). The stiffness of hydrogel based biomaterial impacts mesenchymal stem cells differentiation toward sweat glands in 3D-bioprinted matrix. Materials Science and Engineering: C, 118, 111387. https://doi.org/10.1016/j.msec.2020.111387

[255] DING, H., ILLSLEY, N. P., & CHANG, R. C. (2019). 3D BIOPRINTED GELMA BASED MODELS FOR THE STUDY OF TROPHOBLAST CELL INVASION. SCIENTIFIC REPORTS, 9, 18854. HTTPS://DOI.ORG/10.1038/S41598-019-55052-7

[256] FREEMAN, F. E., & KELLY, D. J. (2017). TUNING ALGINATE BIOMATERIAL STIFFNESS AND COMPOSITION FOR CONTROLLED GROWTH FACTOR DELIVERY AND TO SPATIALLY DIRECT MSC FATE WITHIN BIOPRINTED TISSUES. SCIENTIFIC REPORTS, 7, 17042. HTTPS://DOI.ORG/10.1038/S41598-017-17286-1

[257] Hamid, O. A., Eltaher, H. M., Sottile, V., & Yang, J. (2021). 3D bioprinting of a stem cell-laden, multi-material tubular composite: An approach for spinal cord repair. Materials Science and Engineering: C, 120, 111707. https://doi.org/10.1016/j.msec.2020.111707

[258] Tashman, J. W., Shiwarski, D. J., & Feinberg, A. W. (2021). A high performance open-source syringe extruder optimized for extrusion and retraction during fresh 3D bioprinting. HardwareX, 9. https://doi.org/10.1016/j.ohx.2020.e00170

[259] Engberg, A., et al. (Year). A high performance open-source syringe extruder optimized for extrusion and retraction during FRESH 3D bioprinting Nydus One Syringe Extruder (NOSE): A Prusa i3 3D printer conversion for bioprinting applications utilizing the FRESH-method. Journal Name, Volume(Issue), Page range.

[260] Huda, M. N., Yu, H., & Cang, S. (2016). Robots for minimally invasive diagnosis and intervention. Robotics and Computer-Integrated Manufacturing, 41, 127–144. http://dx.doi.org/10.1016/j.rcim.2016.03.003

[261] Jokic, S., Novikov, P., Maggs, S., Sadan, D., Jin, S., & Nan, C. (2014). Robotic positioning device for three-dimensional printing. CoRR, abs/1406.3400. arXiv:1406.3400.

[262] Susilo, E., Valdastri, P., Menciassi, A., & Dario, P. (2009). A miniaturized wireless control platform for robotic capsular endoscopy using advanced pseudokernel approach. Sensors and Actuators A: Physical, 156, 49–58. https://doi.org/10.1016/j.sna.2009.03.036.

[263] Ozbolat, I. T. (2017). 3D Bioprinting: Fundamentals, Principles and Applications. Academic Press.

[264] Moldovan, L., Babbey, C., Murphy, M., & Moldovan, N. I. (2017). Comparison of biomaterial-dependent and -independent bioprinting methods for cardiovascular medicine. Current Opinion in Biomedical Engineering, 2, 124–131. https://doi.org/10.1016/j.cobme.2017.05.009.

[265] Grames, C. L., Jensen, B. D., Magleby, S. P., & Howell, L. L. (2016). A Compact 2 Degree of Freedom Wrist for Robot-actuated Surgery and Other Applications, 1–12. https://doi.org/10.1115/DETC2016-60070.

[266] Nishiyama, Y., Nakamura, M., Henmi, C., Yamaguchi, K., Mochizuki, S., Nakagawa, H., & Takiura, K. (2009). Development of a three-dimensional bioprinter: construction of cell supporting structures using hydrogel and state-of-the-art inkjet technology. Journal of Biomechanical Engineering, 131. https://doi.org/10.1115/1.3002759.

[267] Wilson, W. C., & Boland, T. (2003). Cell and organ printing 1: protein and cell printers. Anatomy and Record Part A: Discoveries in Molecular, Cellular, and Evolutionary Biology, 272A, 491–496. https://doi.org/10.1002/ar.a.10057.

[268] Gazeau, J.-P., & Zeghloul, S. (2013). Design and operation of two service robot arms: a wide surface printing robot and an artist robot. In Information Resources Management Association (Ed.), Robotics: Concepts, Methodologies, Tools, and Applications (pp. 474–500). IGI Global.

[269] Tan, Y. S. E., & Yeong, W. Y. (2014). Direct Bioprinting of alginate-based tubular constructs using multi-nozzle extrusion-based technique. In Kai, C. C., Yee, Y. W., Jen, T. M., & Erjia, L. (Eds.), 1st International Conference on Progress in Additive Manufacturing (p. 93). https://doi.org/10.3850/978-981-09-0446-3_093.

[270] Bakhshinejad, A., & D'souza, R. M. (2015). A brief comparison between available bio-printing methods. In 2015 IEEE Great Lakes Biomedical Conference. https://doi.org/10.1109/GLBC.2015.7158294.

[271] Beke, S., Anjum, F., Tsushima, H., Ceseracciu, L., Chieregatti, E., Diaspro, A., & Athanassiou, A. (2012). Towards excimer-laser-based stereolithography: a rapid process to fabricate rigid biodegradable photopolymer scaffolds. Journal of the Royal Society Interface, 9, 3017–3026. https://doi.org/10.1098/rsif.2012.0300.

[272] Zhang, A. P., Qu, X., Soman, P., Hribar, K. C., Lee, J. W., Chen, S., & He, S. (2012). Rapid fabrication of complex 3D extracellular microenvironments by dynamic optical projection stereolithography. Advanced Materials, 24, 4266–4270. https://doi.org/10.1002/adma.201202024.

[273] Park, S., Kim, S., & Choi, J. (2015). Development of a multi-nozzle bioprinting system for 3D tissue structure fabrication. In 2015 15th International Conference on Control, Automation and Systems. https://doi.org/10.1109/ICCAS.2015.7364668.

[274] Reid, J. A., Mollica, P. A., Johnson, G. D., Ogle, R. C., Bruno, R. D., & Sachs, P. C. (2016). Accessible bioprinting: adaptation of a low-cost 3D-printer for precise cell placement and stem cell differentiation. Biofabrication, 8(2), 025017. https://doi.org/10.1088/1758-5090/8/2/025017.

[275] Placzek, M. R., Chung, I. M., Macedo, H. M., Ismail, S., Mortera Blanco, T., Lim, M., ... Mantalaris, A. (2009). Stem cell bioprocessing: fundamentals and principles. Journal of the Royal Society Interface, 6, 209–232. https://doi.org/10.1098/rsif.2008.0442.

[276] Stenderup, K., Justesen, J., Clausen, C., & Kassem, M. (2003). Aging is associated with decreased maximal life span and accelerated senescence of bone marrow stromal cells. Bone, 33, 919–926. https://doi.org/10.1016/j.bone.2003.07.005.

[277] Nguyen, D. G., Funk, J., Robbins, J. B., Crogan-Grundy, C., Presnell, S. C., Singer, T., & Roth, A. B. (2016). Bioprinted 3D primary liver tissues allow assessment of organ-level response to clinical drug induced toxicity in vitro. PLoS One, 11(7), e0158674.

[278] Knowlton, S., Joshi, A., Yenilmez, B., Ozbolat, I. T., Chua, C. K., & Khademhosseini, A. (2016). Advancing cancer research using bioprinting for tumor-on-a-chip platforms. International Journal of Bioprinting, 2, 3–8. https://doi.org/10.18063/IJB.2016.02.003.

[279] Bidare, P., Maier, R. R. J., Beck, R. J., Shephard, J. D., & Moore, A. J. (2017). An open-architecture metal powder bed fusion system for in-situ process measurements. Additive Manufacturing, 16, 177–185. https://doi.org/10.1016/j.addma.2017.06.007.

[280] Frketic, J., Dickens, T., & Ramakrishnan, S. (2017). Automated manufacturing and processing of fiber-reinforced polymer (FRP) composites: An additive review of contemporary and modern techniques for advanced materials manufacturing. Additive Manufacturing, 14, 69–86. https://doi.org/10.1016/j.addma.2017.01.003.

[281] Ren, L., Zhou, X., Song, Z., Zhao, C., Liu, Q., Xue, J., & Li, X. (2017). Process parameter optimization of extrusion-based 3D metal printing utilizing PW–LDPE–SA binder system. Materials, 10, 305. https://doi.org/10.3390/ma10030305.

[282] Wang, T., Kwok, T.-H., & Zhou, C. (2017). In-situ droplet inspection and control system for liquid metal jet 3D printing process. Procedia Manufacturing, 10, 968–981. https://doi.org/10.1016/j.promfg.2017.07.088.

[283] Kato, R., Iejima, D., Agata, H., Asahina, I., Okada, K., Ueda, M., & Honda, H. (2009). A compact, automated cell culture system for clinical scale cell expansion from primary tissues. Tissue Engineering Part C: Methods, 16, 947–956. https://doi.org/10.1089/ten.tec.2009.0305.

[284] Thomas, R., & Ratcliffe, E. (2012). Automated adherent human cell culture (mesenchymal stem cells). In R. R. Mitry & R. D. Hughes (Eds.), Human Cell Culture Protocols (pp. 393–406). Humana Press. https://doi.org/10.1007/978-1-61779-367-7_26.

[285] Triaud, F., Clenet, D.-H., Cariou, Y., Le Neel, T., Morin, D., & Truchaud, A. (2003). Evaluation of automated cell culture incubators. Journal of the Association for Laboratory Automation, 8(1), 82–86. https://doi.org/10.1016/s1535-5535(03)00018-2.

[286] Bhuthalingam, R., Lim, P. Q., Irvine, S. A., & Venkatraman, S. S. (2016). Automated robotic dispensing technique for surface guidance and bioprinting of cells. Journal of Visualized Experiments, 117. https://doi.org/10.3791/54604.

[287] Suntornnond, R., Tan, E. Y. S., An, J., & Chua, C. K. (2016). A mathematical model on the resolution of extrusion bioprinting for the development of new biomaterials. Materials, 9. https://doi.org/10.3390/ma9090756.

[288] Ozler, S. B., Kucukgul, C., & Koc, B. (2015). Bioprinting with live cells. In K. Turksen (Ed.), Bioprinting in Regenerative Medicine (pp. 67–88). Springer International Publishing. https://doi.org/10.1007/978-3-319-21386-6_3.

[289] Hondrum, S. O., & Fernandez, R. (1997). Effects of long-term storage on properties of an alginate impression material. The Journal of Prosthetic Dentistry, 77(6), 601–606. https://doi.org/10.1016/s0022-3913(97)70102-1

[290] Kim, J. (2023). Characterization of biocompatibility of functional Biomaterials for 3D bioprinting. Bioengineering, 10(4), 457. https://doi.org/10.3390/bioengineering10040457

[291] Schwab, A., Levato, R., D'Este, M., Piluso, S., Eglin, D., & Malda, J. (2020). Printability and shape fidelity of Biomaterials in 3D bioprinting. Chemical Reviews, 120(19), 11028–11055. https://doi.org/10.1021/acs.chemrev.0c00084

[292] Zhang, L., Yang, G., Johnson, B. N., & Jia, X. (2019). Three-dimensional (3D) printed scaffold and material selection for Bone Repair. Acta Biomaterialia, 84, 16–33. https://doi.org/10.1016/j.actbio.2018.11.039

[293] Singer, A., Barakat, Z., Mohapatra, S., & Mohapatra, S. S. (2018). Nanoscale Drug-Delivery Systems. In Nanocarriers for Drug Delivery, Nanoscience and Nanotechnology in Drug Delivery (pp. 395–419). https://doi.org/10.1016/b978-0-12-814033-8.00013-8

[294] Townsend, J. M., Beck, E. C., Gehrke, S. H., Berkland, C. J., & Detamore, M. S. (2019). Flow behavior prior to crosslinking: The need for precursor rheology for placement of hydrogels in medical applications and for 3D bioprinting. Progress in Polymer Science, 91, 126–140. https://doi.org/10.1016/j.progpolymsci.2019.01.003

[295] Compaan, A. M., Song, K., & Huang, Y. (2019). Gellan fluid gel as a versatile support bath material for fluid extrusion bioprinting. ACS Applied Materials & Interfaces, 11(6), 5714–5726. https://doi.org/10.1021/acsami.8b13792

[296] Basu, A., Saha, A., Goodman, C., Shafranek, R. T., & Nelson, A. (2017). Catalytically initiated gel-in-gel printing of Composite Hydrogels. ACS Applied Materials & Interfaces, 9(46), 40898–40904. https://doi.org/10.1021/acsami.7b14177

[297] Brunel, L. G., Hull, S. M., & Heilshorn, S. C. (2022). Engineered assistive materials for 3D bioprinting: Support baths and sacrificial inks. Biofabrication, 14(3), 032001. https://doi.org/10.1088/1758-5090/ac6bbe

[298] Theus, A. S., Ning, L., Hwang, B., Gil, C., Chen, S., Wombwell, A., Mehta, R., & Serpooshan, V. (2020). Bioprintability: Physiomechanical and biological requirements of materials for 3D bioprinting processes. Polymers, 12(10), 2262. https://doi.org/10.3390/polym12102262

[299] Cooke, M. E., & Rosenzweig, D. H. (2021). The rheology of direct and suspended extrusion bioprinting. APL Bioengineering, 5(1). https://doi.org/10.1063/5.0031475

[300] O'Neal, B. (2021, October 19). *Aether 1 bioprinter beta units to be involved in Massive Research Project Collaboration, released later in year at $9K - 3dprint.com: The Voice of 3D printing / additive manufacturing*. 3DPrint.com | The Voice of 3D Printing / Additive Manufacturing. https://3dprint.com/149410/aether-1-bioprinter-beta-units/

[301] Dimitriyev, M. S., Chang, Y. W., Goldbart, P. M., & Fernández-Nieves, A. (2019). Swelling thermodynamics and phase transitions of polymer gels. Nano Futures, 3, 042001–042043. https://doi.org/10.1088/2399-1984/ab45d5

[302] Parvin, S., Noorjahan, B. A., Abdul, M. A., Abdul, R. O., Maryam, M., Ehsan, J., et al. (2012). Comparison of different methods for the isolation of mesenchymal stem cells from human umbilical cord Wharton's jelly. In Vitro Cellular & Developmental Biology. Animal, 48(1), 75–83. https://doi.org/10.1007/s11626-011-9480-x

[303] Tsuji, K., Ojima, M., Otabe, K., Horie, M., Koga, H., Sekiya, I., et al. (2017). Effects of different cell-detaching methods on the viability and cell surface antigen expression of synovial mesenchymal stem cells. Cell Transplantation, 26(6), 1089–1102. https://doi.org/10.3727/096368917X694831

[304] Cui, X., Dean, D., Ruggeri, Z. M., & Boland, T. (2010). Cell damage evaluation of thermal inkjet printed Chinese hamster ovary cells. Biotechnology and Bioengineering, 106(6), 963–969. https://doi.org/10.1002/bit.22762

[305] Suzuki, K., Sun, R., Origuchi, M., Kanehira, M., Takahata, T., Itoh, J., et al. (2011). Mesenchymal stromal cells promote tumor growth through the enhancement of neovascularization. Molecular Medicine, 17(9-10), 579–587. https://doi.org/10.2119/molmed.2010.00157

[306] Chang, R., Nam, J., & Sun, W. (2008). Effects of dispensing pressure and nozzle diameter on cell survival from solid freeform fabrication–based direct cell writing. Tissue Engineering. Part A, 14(1), 41–48. https://doi.org/10.1089/ten.2007.0004

[307] Shav, D., & Einav, S. (2010). The effect of mechanical loads in the differentiation of precursor cells into mature cells. Annals of the New York Academy of Sciences, 1188(1), 25–31. https://doi.org/10.1111/j.1749-6632.2009.05079.x

[308] Stolberg, S., & McCloskey, K. E. (2009). Can shear stress direct stem cell fate? Biotechnology Progress, 25(1), 10–19. https://doi.org/10.1002/btpr.124

[309] Lee, H. J., Kim, Y. B., Ahn, S. H., Lee, J., Jang, C. H., Yoon, H., et al. (2015). A new approach for fabricating collagen/ECM-based biomaterials using preosteoblasts and human adipose stem cells. Advanced Healthcare Materials, 4(9), 1359–1368. https://doi.org/10.1002/adhm.201500193

[310] Tang-Quan, K. R., Xi, Y., Hochman-Mendez, C., Xiang, Q., Lee, P.-F., Sampaio, L. C., & Taylor, D. A. (2020). Gelatin promotes cell retention within decellularized heart extracellular matrix vasculature and parenchyma. Cellular and Molecular Bioengineering, 13(6), 633–645. https://doi.org/10.1007/s12195-020-00634-z